

1997

Design, synthesis, characterization and study of novel conjugated polymers

Wu Chen

Iowa State University

Follow this and additional works at: <https://lib.dr.iastate.edu/rtd>

 Part of the [Organic Chemistry Commons](#), and the [Polymer Chemistry Commons](#)

Recommended Citation

Chen, Wu, "Design, synthesis, characterization and study of novel conjugated polymers " (1997). *Retrospective Theses and Dissertations*. 11450.

<https://lib.dr.iastate.edu/rtd/11450>

This Dissertation is brought to you for free and open access by the Iowa State University Capstones, Theses and Dissertations at Iowa State University Digital Repository. It has been accepted for inclusion in Retrospective Theses and Dissertations by an authorized administrator of Iowa State University Digital Repository. For more information, please contact digirep@iastate.edu.

INFORMATION TO USERS

This manuscript has been reproduced from the microfilm master. UMI films the text directly from the original or copy submitted. Thus, some thesis and dissertation copies are in typewriter face, while others may be from any type of computer printer.

The quality of this reproduction is dependent upon the quality of the copy submitted. Broken or indistinct print, colored or poor quality illustrations and photographs, print bleedthrough, substandard margins, and improper alignment can adversely affect reproduction.

In the unlikely event that the author did not send UMI a complete manuscript and there are missing pages, these will be noted. Also, if unauthorized copyright material had to be removed, a note will indicate the deletion.

Oversize materials (e.g., maps, drawings, charts) are reproduced by sectioning the original, beginning at the upper left-hand corner and continuing from left to right in equal sections with small overlaps. Each original is also photographed in one exposure and is included in reduced form at the back of the book.

Photographs included in the original manuscript have been reproduced xerographically in this copy. Higher quality 6" x 9" black and white photographic prints are available for any photographs or illustrations appearing in this copy for an additional charge. Contact UMI directly to order.

UMI

A Bell & Howell Information Company
300 North Zeeb Road, Ann Arbor MI 48106-1346 USA
313/761-4700 800/521-0600

Design, synthesis, characterization and study of novel conjugated polymers

by

Wu Chen

**A dissertation submitted to the graduate faculty
in partial fulfillment of the requirements for the degree of
DOCTOR OF PHILOSOPHY**

Major: Organic Chemistry

Major Professor: Thomas J. Barton

Iowa State University

Ames, Iowa

1997

UMI Number: 9725401

UMI Microform 9725401
Copyright 1997, by UMI Company. All rights reserved.

**This microform edition is protected against unauthorized
copying under Title 17, United States Code.**

UMI
300 North Zeeb Road
Ann Arbor, MI 48103

**Graduate College
Iowa State University**

**This is to certify that the doctoral dissertation of
Wu Chen
has met the dissertation requirements of Iowa State University**

Signature was redacted for privacy.

Major Professor

Signature was redacted for privacy.

For the Major Program

Signature was redacted for privacy.

For the Graduate College

DEDICATION

TO MY PARENTS,
TO MY WIFE, HONGLING LI

TABLE OF CONTENTS

INTRODUCTION	1
I: SYNTHESIS, CHARACTERIZATION OF ELECTROLUMINESCENT POLYMERS CONTAINING CONJUGATED ARYL, OLEFINIC, THIOPHENE AND ACETYLENIC UNITS AND THEIR STUDIES FOR USE IN LIGHT-EMITTING DIODES (LED)	8
Literature Survey	8
Results and Discussions	12
Preparation and Characterization of the Polymers	12
Properties of the Polymers	21
The Polymer-Based LEDs	32
Conclusions	35
Experimental	36
II: SYNTHESIS, CHARACTERIZATION AND STUDY OF CONJUGATED POLYMERS CONTAINING SILOLE UNIT IN THE MAIN CHAIN	46
Literature Survey	46
Results and Discussions	61
Synthesis and Study of Poly(2,5-thiophene-2,5-silole)	61
Synthesis and Study of Poly(2,5-silole-ethynylene) and Poly(2,5-silole-butadiynylene)	67
Synthesis and Study of Poly(2,5-silole-ethynylene-paraphenylene-ethynylene)	73
Synthesis and Study of Poly(2,5-silole-ethynylene-dimethylsilylene-ethynylene)	82
Attempted Synthesis of Poly(2,5-silole-1,2,3-butatriene)	85
Attempted Synthesis of Poly(2,5-silole-1,2-vinylene)	91
Conclusions	92
Experimental	92

Experimental	92
III: SYNTHESIS, CHARACTERIZATION AND STUDY OF SILICON-BRIDGED AND BUTADIENE-LINKED POLYTHIOPHENES	100
Literature Survey	100
Results and Discussions	104
<u>Synthesis and Study of Silicon-Bridged Polythiophenes</u>	104
<u>Synthesis and Study of Butadiene-Linked Polythiophenes</u>	119
Conclusions	128
Experimental	128
FUTURE WORK	135
REFERENCES	138
ACKNOWLEDGEMENTS	148

INTRODUCTION

Conjugated organic polymers are polymers which contain overlapping p-orbitals throughout the polymer main chains. Three types of p-orbital units used to construct conjugated polymers are aromatic segments like phenyl, thiophene and other hetero-aromatic rings, non-aromatic C-C double bonds or triple bonds or C-N double bonds, and hetero atoms having nonbonding electron pairs like sulfur or nitrogen. The different combinations of these units can form a wide variety of conjugated polymers. The conjugated polymers which have been most studied are polyacetylene (PA),^{1,2} polydiacetylene (PDA),^{1(d),3} polyparaphenylene (PPP),^{1(b),4} polythiophene (PT),^{1(a),1(b),1(d),5} polyparaphenylenevinylene (PPV),^{1,6} polyparaphenyleneethynylene (PPE),⁷ polyaniline (PANI),¹ polyphenylenesulfide (PPS)^{1(b)} and polyacenes.⁸ The structures of these polymers are shown in Figure 1.

Conjugated polymers have been attracting attention for more than two decades because some can exhibit high electroconductivity (after doping),⁹ photoconductivity,⁴⁷ strong non-linear optical response¹⁰ or intense fluorescence. Conjugated polymers were first studied as conducting polymers. They are often capable of being doped, through chemical or electrochemical oxidation or reduction, to states of moderate to high electrical conductivity.^{1,2} Twenty years ago, the idea of a conducting polymer was purely a subject of theoretical debate; however, a fortunate coincidence of events in the late 1970s led to the first reports of polymeric materials with semiconductor properties. Since then, electrically conducting polymers have been a center of scientific interest and active multidisciplinary research. These materials have attracted academic and industrial research groups not only because of their theoretically interesting properties but also because of their technologically promising future.

A number of applications have been proposed for conducting polymers. They include field-effect transistors, light weight rechargeable batteries, electrochromic displays, erasable compact discs and photovoltaic devices. During the last twenty years, many attempts have been made to produce polymers with a high level of electrical conduction and much of this effort has been directed towards polyacetylenes. Oxidatively doped and stretch oriented

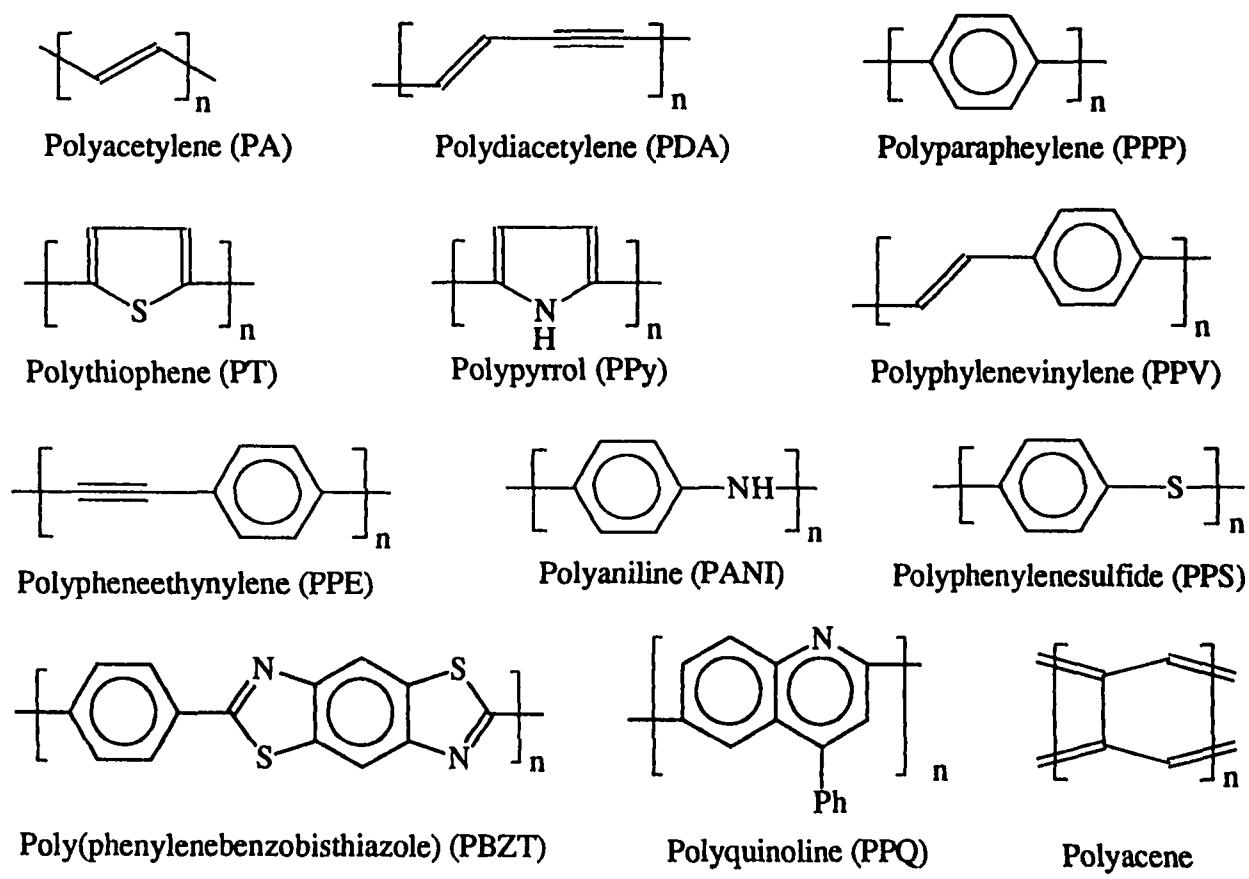


Figure 1: The structures of conjugated polymers

Table 1: Conductivities of conducting polymers

Polymer	Doping materials	Conductivities (Scm ⁻¹)
Polyacetylene	I ₂ , Br ₂ , Li, Na, AsF ₅	10,000
Polypyrrole	BF ₄ ⁻ , ClO ₄ ⁻	500-7500
Poly(3-alkylthiophene)	BF ₄ ⁻ , ClO ₄ ⁻ , FeCl ₄ ⁻	1000-10,000
Polyphenylenevinylene	AsF ₅	10,000
Polyphylene sulfide	AsF ₅	500
Polyphenylene	AsF ₅ , Li, K	1000
Polyaniline	HCl	200

trans-PA is the most conductive ($\sigma=10^3$ - 10^5 S/cm)¹¹ among conducting polymers. Table 1 gives the examples of the conductivities of these polymers.

Conjugated polymers can also exhibit photoconductive properties.⁴⁷ In the absence of light most polymers are fairly insulators. The lowest excited state in conjugated polymers is a band-to-band transition leading to the formation of free electron-hole pairs.⁴⁸ In this picture photoluminescence is interpreted in terms of radiative recombination of charge carriers after relaxing into polaronic states of the polymeric backbone. After being exposed to light (usually laser pulse), the conjugated polymers can generate electron-hole pairs. These pairs must dissociate to produce separated electrons and positive holes in such way that the electrons end up in the conducting states. Poly(2-phenyl-1,4-phenylenevinylene) (PPPV) has been studied as photoconductive polymer.^{47(a)}

Even though only doped conjugated polymers are conducting polymers, presently the underlying chemistry and physics of these materials in their undoped states may be more interesting. These undoped polymers have photoluminescent and electroluminescent properties. Although electroluminescence in organic materials has been known since the

1960s, the first observation of electroluminescence from polymeric devices was reported by physicists and chemists from the University of Cambridge in 1990.¹¹ This organic light-emitting device (LED) was constructed from undoped PPV sandwiched between indium tin oxide (ITO) and aluminum electrodes. Figure 2 shows the construction of an LED.

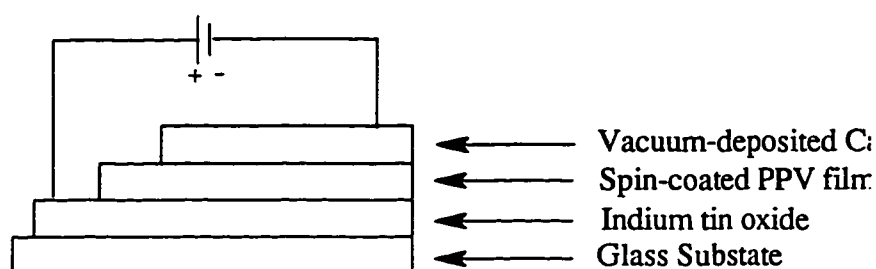


Figure 2: Schematic of an LED device

There are at least four steps involved in the operating mechanism of these devices: charge injection, charge transport, charge recombination and light emission. When a voltage is applied across the polymer film, the cathode injects electrons (in the form of radical anions) into the polymer film, while the anode injects holes (as radical cations). The electrical field makes these electrons and holes migrate toward each other through the film. When they meet in the middle, the energetic electrons can drop into the holes to form triplet or singlet excitons, which give up their excess energy as photons of light (Figure 3(a)).

In most conjugated polymers including PPV, the mobility of holes is faster than that of electrons.⁶ The differences in mobilities cause unbalanced charges in the polymer film and the charge recombination occurs close to or inside the negative electrode, which results in diminishing the electroluminescence (EL) quantum efficiency by the self-absorption. In order to achieve a high recombination efficiency, various types of cell structures have been proposed. One of the most common is a double-layer-type cell that has a layered structure composed of materials with different carrier transport properties, one transporting holes and the other electrons (Figure 3(b)). In this system, electrons and holes are injected from electrodes into the corresponding organic (carrier transporting) layers. Eventually, the recombination of the carriers takes place at or near the interface between the two organic

layers. Since the hole transport layer blocks electrons, and the electron transport layer blocks holes, the carriers are confined to the organic layer, thus maximizing the recombination efficiency. An improvement of EL quantum efficiency was also observed when PPV as replaced by a partially conjugated PPV.^{24(e)}

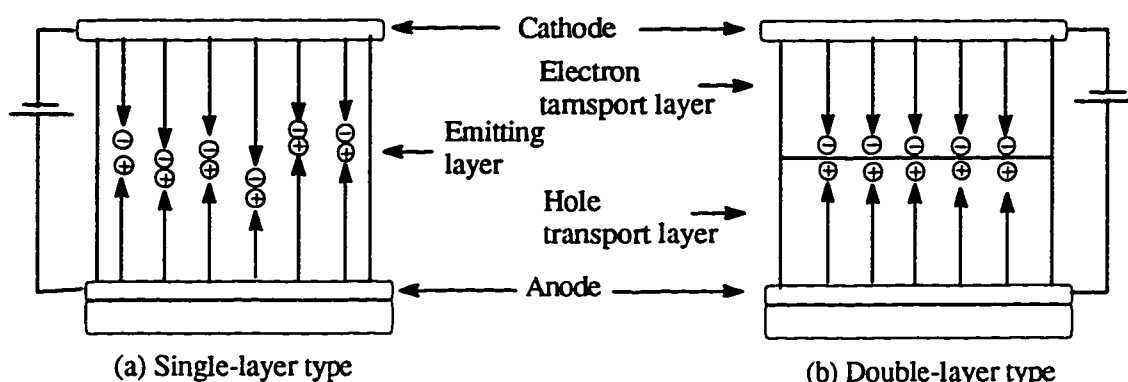


Figure 3: Configuration of typical LED

Since the first report of a PPV-based LED, there has been a rapidly increasing number of publications demonstrating the applications of these conjugated polymers in LED devices.¹² Other conjugated polymers used for EL application include PPE,^{25(b, c)} polyalkylthiophenes (PATs),¹³ polyalkylfluorenes (PAFs),¹⁴ PPP¹⁵ and poly(1,4-naphthalene vinylene) (PNV).¹⁶

Polymeric LEDs are likely to replace the inorganic LEDs in the future because of their advantages. The polymer-based light-emitting materials are light, inexpensive, flexible and efficient. They can be used for everything from lightweight backlights for computer displays to TVs that can be hanged flat on the wall or rolled up.

Conjugated polymers are emerging as an important class of third-order nonlinear optical (NLO) materials.¹⁷ NLO materials in devices allow light (photons) to be used instead of electrons for the representation, manipulation and transmission of information. Devices such as optical switches and modulators will perform the same functions as their electronic counterparts but with increased speed. As mentioned before, the devices are light, flexible and inexpensive.

The equations describing the polarization of a material as a function of applied field on both molecular level and the bulk level are shown in Figure 4.

Conjugated polymers such as polyacetylene,¹⁸ poly(phenylene vinylene) (PPV),¹⁹ polythiophene,²⁰ polydiacetylene²¹ and some other polymers have been shown to exhibit very large nonlinear optical response (Table 2).^{10, 17(b), 22}

Molecular Level	Bulk Level
$p = \alpha E + \beta E \cdot E + \gamma E \cdot E \cdot E + \dots$	$p = \chi^{(1)} E + \chi^{(2)} E \cdot E + \chi^{(3)} E \cdot E \cdot E + \dots$
p = polarization of individual molecule	p = polarization of bulk material
α = molecular polarizability	$\chi^{(1)}$ = linear susceptibility tensor
β = 1st hyperpolarizability	$\chi^{(2)}$ = 1st nonlinear susceptibility tensor
γ = 2nd hyperpolarizability	$\chi^{(3)}$ = 2nd nonlinear susceptibility tensor

Figure 4: Polarization of a medium induced by an external electric field

Table 2: Selected polymers that exhibit third-order nonlinearities^{17(b)}

Polymers	Nonresonant $\chi^{(3)}$ (esu) [wavelength]	Resonant $\chi^{(3)}$ (esu) [wavelength]	Measurement method
Polyacetylene	1.0×10^{-10} [950nm]	1.1×10^{-9} [620nm]	THG * spectroscopy
Polydiacetylene	4.0×10^{-10} [602nm]		DFWM **
Polythiophene		4.0×10^{-10} [602nm]	DFWM **
Poly(phenylbenzobisthiazole)	4.5×10^{-10} [602nm]		DFWM **
Polyquinoline	2.3×10^{-12} [2.38 μ m]	1.1×10^{-11} [1.2 μ m]	THG * spectroscopy
Polyphenylenevinylene		4.0×10^{-10} [602nm]	DFWM **
Polyaniline (emeraldine base)		3.7×10^{-11} [1.83 μ m]	THG * spectroscopy

* THG, third harmonic generation; ** DFWM, degenerate four-wave mixing

I: SYNTHESSES OF ELECTROLUMINESCENT POLYMERS CONTAINING CONJUGATED ARYL, OLEFINIC, THIOPHENE AND ACETYLENIC UNITS AND THEIR STUDIES FOR USE IN LIGHT-EMITTING DIODES (LED)

Literature Survey

Conjugated polymers today are most widely used in emitters. The first conjugated polymer applied to an electroluminescent (EL) device was PPV.¹¹ Since then, PPV-based LEDs have been extensively studied. PPVs usually have two identical, long side chains to increase their solubilities and processabilities (Figure 5).²⁶ These polymers, used as hole-transporting layers, have low quantum efficiencies. To improve their quantum efficiencies, several adjustments have been made. The unsymmetric MEH-PPV was employed in a LED device with a lower work function (ionization potential) metal, such as calcium, as the cathode.²³ The quantum efficiency can be high as 1%. Recently, electron-accepting cyano (-CN) groups have been introduced into PPV derivatives so that the polymer (CN-PPV) can transport electrons and have a lower HOMO-LUMO gap energy. A cell with double layers of PPV (as the hole transport layer) and CN-PPV (as electron transport layer) exhibits a higher quantum efficiency of 4%- one of the highest efficiencies ever reported.^{24(c, d)}

In contrast to the PPV, poly(*p*-phenyleneethynylene) (PPE) type polymers having structures similar to those of the PPV type polymers have received much less attention due to synthetic inaccessibility of processable PPE polymers.^{7, 25} Principal interest in much of this work has focused on the liquid crystalline properties of PPEs due to their rigid-rod structures. However, due to their highly fluorescent nature,⁴⁹ PPEs and their similar structures have been examined as potential materials in LED devices recently.^{11, 15} Electron delocalizations through a triple bond in phenyleneethynylene (PE) and a double bond in phenylenevinylene (PV) have been compared theoretically and experimentally.^{27(b)} Some evidence indicates that the double bond allows better electron delocalization than the triple bond. The direct observation is that the wavelength of electronic absorption maxima (λ_{\max}) of the PE compounds are shorter than those of the PV analogues. Figure 6 shows the examples of λ_{\max} of UV/Vis absorption.

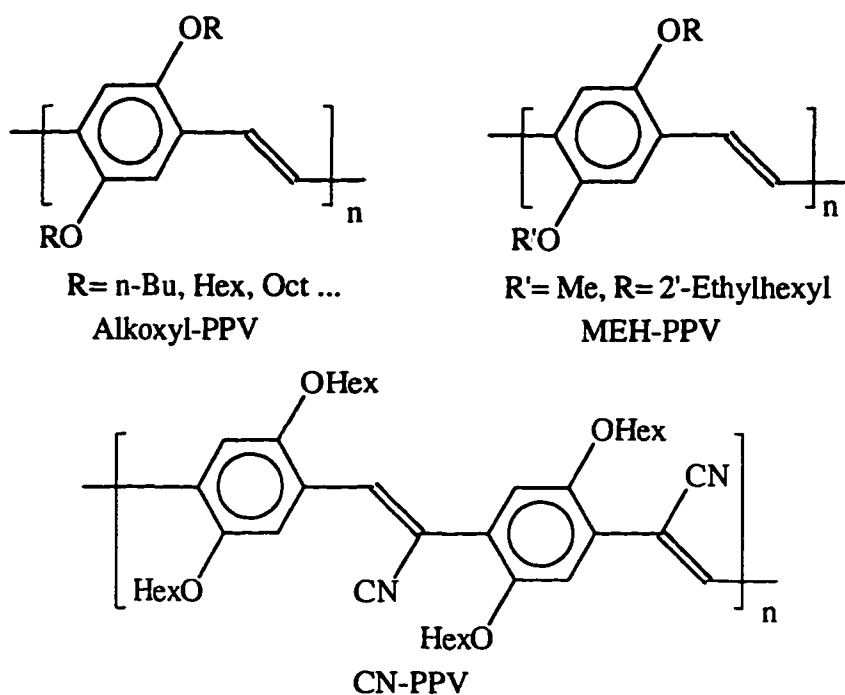


Figure 5: Molecular structures of PPV

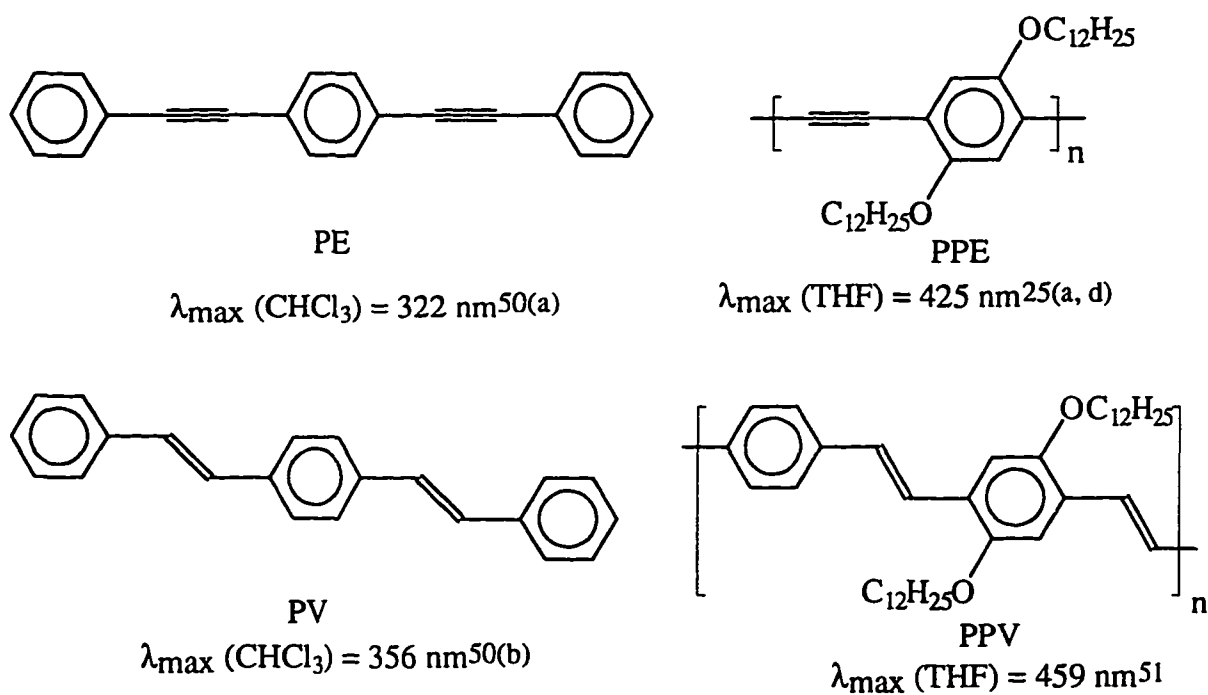
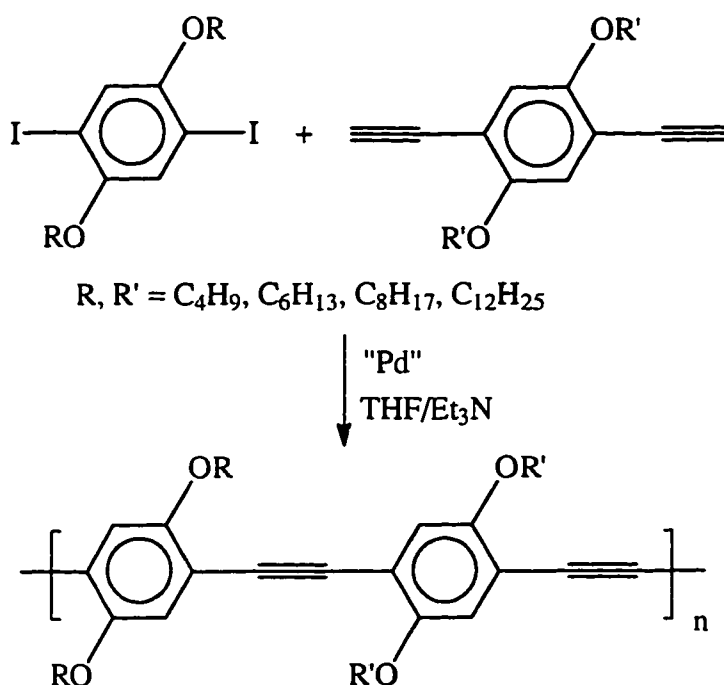


Figure 6: Electronic absorptions of PE, PV, PPE and PPV

Photoluminescent properties of PE derivatives and PV derivatives have been studied.²⁸ The reported quantum yields of photoluminescence of many of the PE derivatives are comparable to those of the PV analogues. The quantum yield of alkoxy PPE in toluene was reported to be as high as 50%,²⁹ which is about two times higher than that of PPV. Despite being highly fluorescent, studies of electroluminescence of the PPE system have not shown satisfactory results compared to the PPV system.

The syntheses of PPE and its derivatives were recently reviewed.^{25(a, b, d)} Recently, our group^{25(b, c)} and another group^{25(g)} synthesized soluble PPE with high molecular weight using the Heck-type coupling reaction (Scheme 1) and studied their use in LED. However the yellow-greenish light from the PPE-based LED's was of low intensity and the device was short-lived.



Scheme 1: Synthesis of soluble PPE

By similar Heck-type coupling, other PPE type polymers have been synthesized and studied (Figure 7).

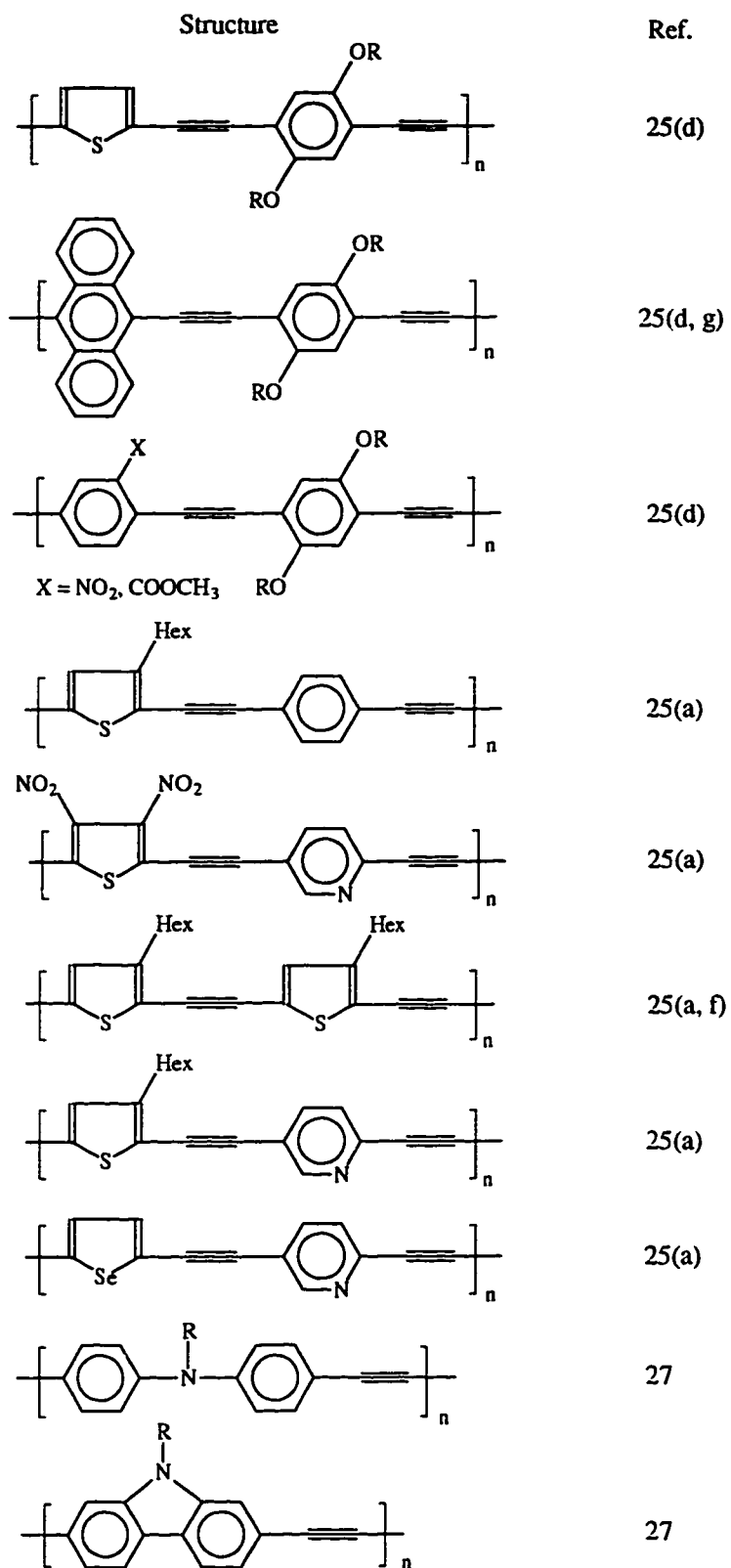


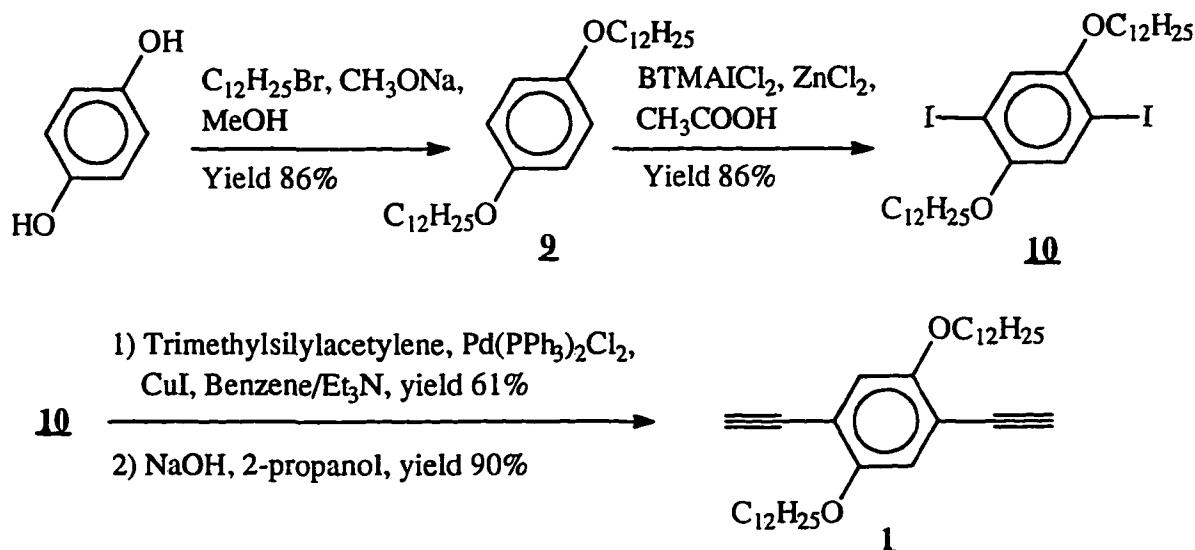
Figure 7: Other PPE type polymers

In our continuing effort to find more efficient PPE type polymers for LED application, we have synthesized a series of conjugated polymers and copolymers with combination of repeating units of PPV, PPE, and PPP and have begun to examine the effects of electronegative substituents on their optical properties.

Results and Discussions

Preparation and Characterization of Polymers

Monomer Preparation. The key monomers with which to synthesize PPE-type polymers via Heck-type coupling are diethynyl-arylenes and arylene dihalides. The diethynylarylene unit used in all the polymers is 1,4-diethynyl-2,5-didodecyloxybenzene **1**, which was synthesized as described in Scheme 2.^{25(b)}



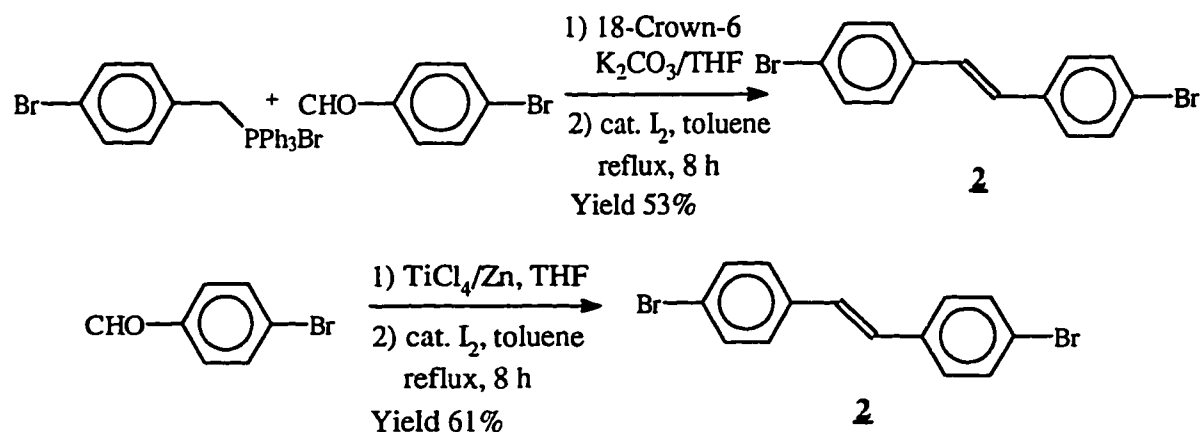
Scheme 2: Synthesis of monomer **1**^{25(b)}

Hydroquinone was reacted with 1-bromo-dodecane and CH_3ONa in CH_3OH , giving 1,4-didodecyloxy-benzene **2** in 86% yield. Iodination of **2** by excess ZnCl_2 and benzyltrimethylammonium dichloroiodate (BTMAICl_2) in acetic acid at $50\text{-}60^\circ\text{C}$ for 1 day gave 1,4-didodecyloxy-2,5-diiodobenzene **10** in 77% yield. The white diiodo product **10**

could be easily purified by recrystallization of the crude product in isopropanol or precipitation by adding the saturated crude product in THF into methanol. The palladium-coupling reaction between **10** and trimethylsilylacetylene in benzene/triethylamine, followed by desilylation, gave monomer **1**. Monomer **1** is a greenish crystalline material which is stable in the air.

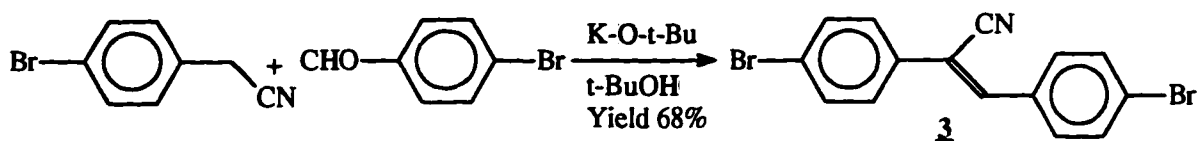
A PPV unit was put into the other monomer in order to form PPE and PPV copolymers, which may exhibit properties of both PPV and PPE. The double bond in the monomers was formed via a Wittig reaction,³¹ a McMurry Reaction³² or a Knoevenagel condensation.^{24(a)}

4,4'-Dibromostilbene **2** was synthesized by either a Wittig reaction or a McMurry reaction in moderate yields (Scheme 3). The conditions of this modified Wittig reaction³¹ were to use K_2CO_3 as a base and 18-crown-6 as a catalyst for a solid/liquid transfer process compared with the usual conditions of a McMurry reaction, which requires an absolute moisture- and air-free environment. The *cis*-isomer was converted to *trans*-isomer by refluxing in benzene with a catalytic amount of iodine for 8 hours.³³



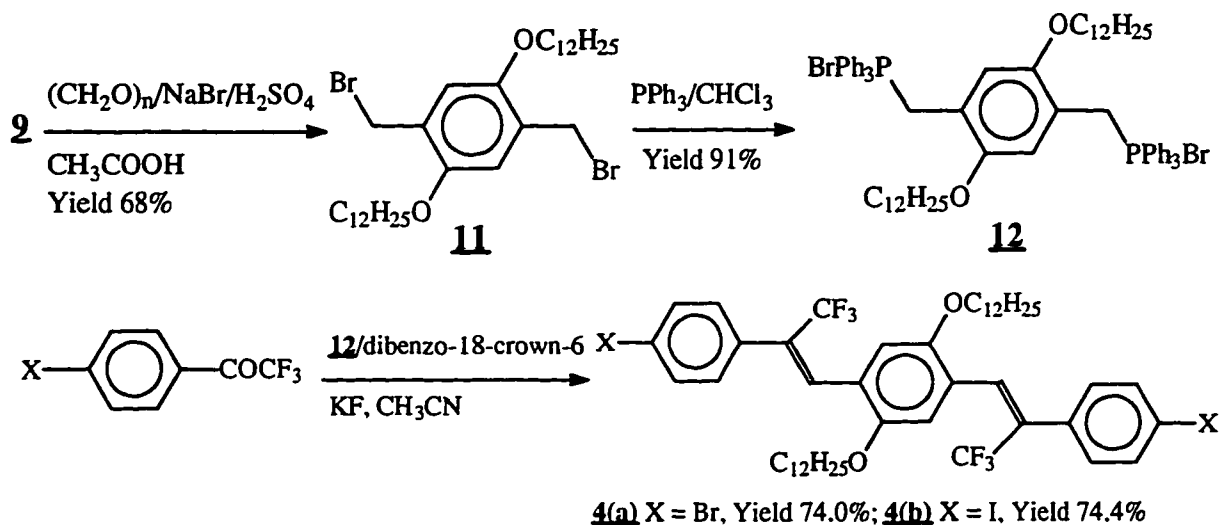
Scheme 3: Synthesis of 4,4'-dibromostilbene **2**

1,2-Di-(4-bromo-phenyl)-1-cyano-ethene **3** was synthesized by a Knoevenagel reaction^{24(a)} (Scheme 4). Stirring of a mixture of 4-bromobenzaldehyde and 4-bromophenyl-acetonitrile in KO-t-Bu/t-BuOH at 55⁰C for 3 hours gave monomer **3** in 68% yield.



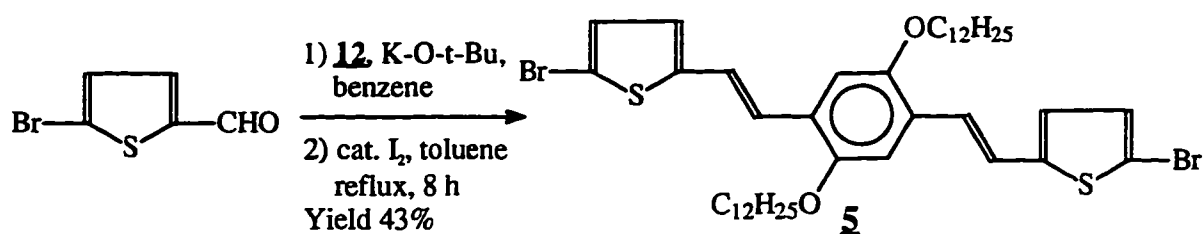
Scheme 4: Synthesis of 1,2-di-(4-bromo-phenyl)-1-cyano-ethene **3**

A trifluoromethyl group was introduced into monomer **4** for comparison with monomer **3** with regard to the effect of substituents on the luminescence properties of the polymers. Halomethylation of compound **9** with paraformaldehyde and HBr (generated from reaction of NaBr and H₂SO₄) in acetic acid gave compound **11**³⁴ in 68% yield, which was reacted with PPh₃ in CHCl₃ to generate phosphonium salt **12**³³ in 91% yield. A Wittig reaction between halophenyl trifluoromethyl ketone³⁵ and phosphonium salt **12** in CH₃CN produced monomer **4** (Scheme 5).³⁶



Scheme 5: Synthesis of monomer **4**

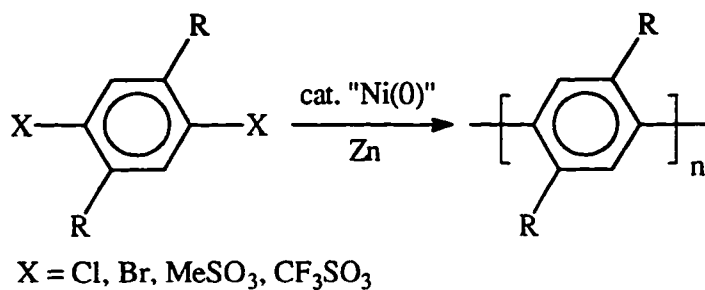
Monomer **6** was synthesized by a Wittig reaction using KO-t-Bu as a base in benzene³³ in 43% yield (Scheme 6). The pure *trans* product was obtained after the *cis* product was isomerized to its *trans* form as earlier described.



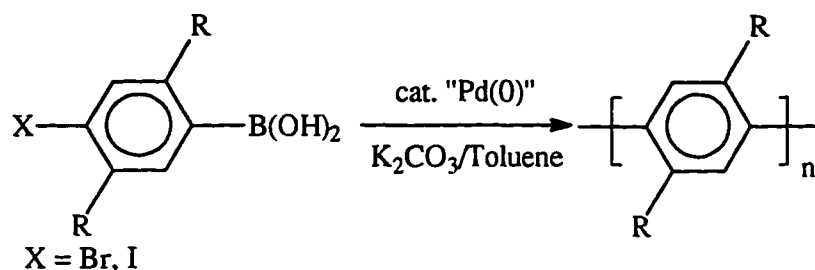
Scheme 6: Synthesis of monomer **5**

PPP, which contains only phenyl units in the main chain, has also been studied for use in LED devices.¹⁵ The PPP-based LED gives bright blue light. The syntheses of PPP are usually based on the nickel(0) catalyzed homocoupling of di(methylsulfonyl)-,³⁸ di(trifluoromethanesulfonyl)-³⁷ and dihalo-benzenes³⁷ in the presence of excess zinc or by palladium-(0) catalyzed heterocoupling (Suzuki coupling)³⁹ in toluene and aqueous K₂CO₃ solution (Scheme 7).

Homocoupling reaction

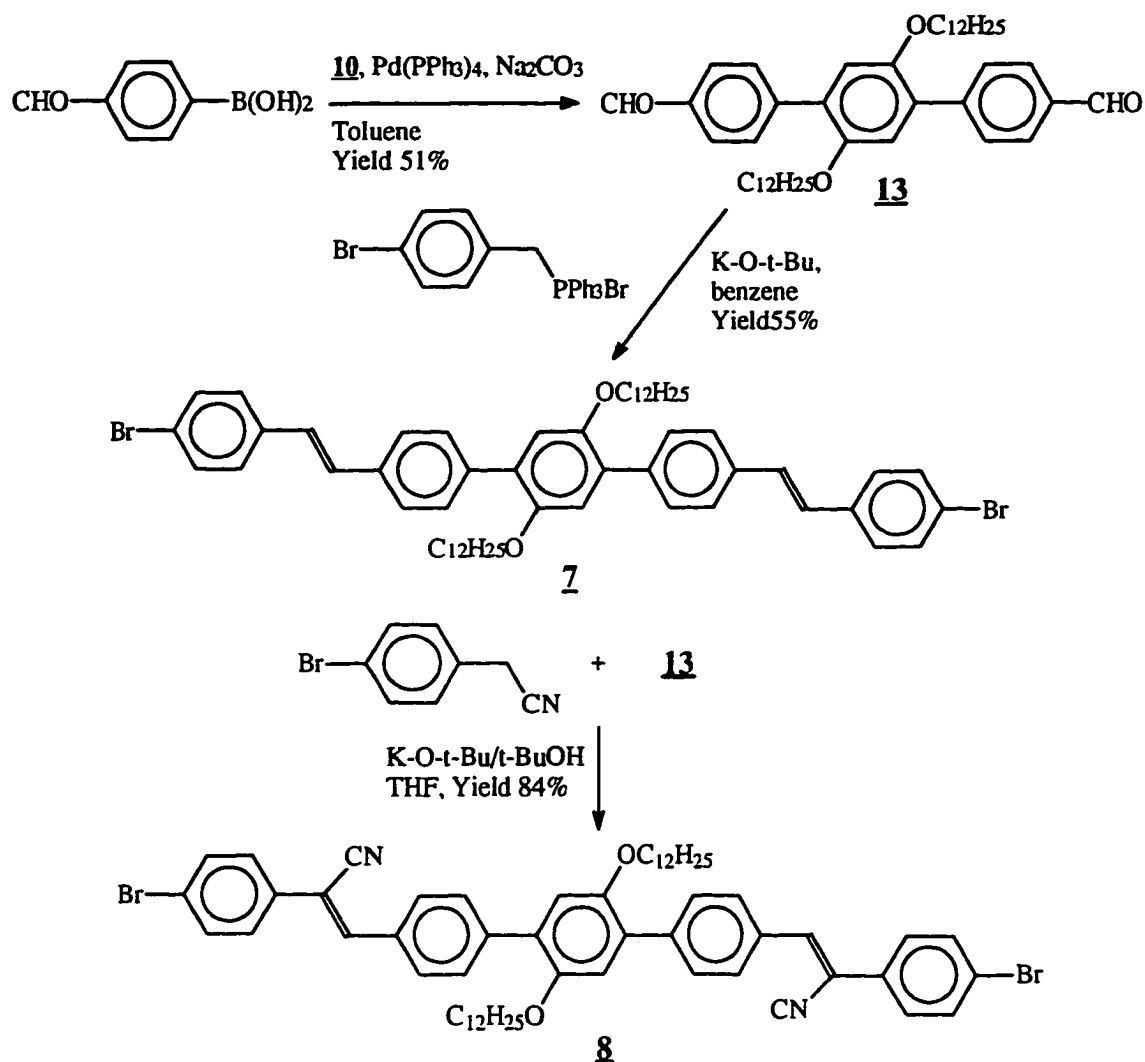


Heterocoupling reaction (Suzuki coupling)



Scheme 7: Synthesis of poly(paraphenylene) (PPP)

In order to obtain special optical properties, the PPP unit was added into the polymer main chains. The PPP unit was synthesized by a Suzuki reaction as shown in Scheme 8.



Scheme 8: Synthesis of monomer **7** and **8**

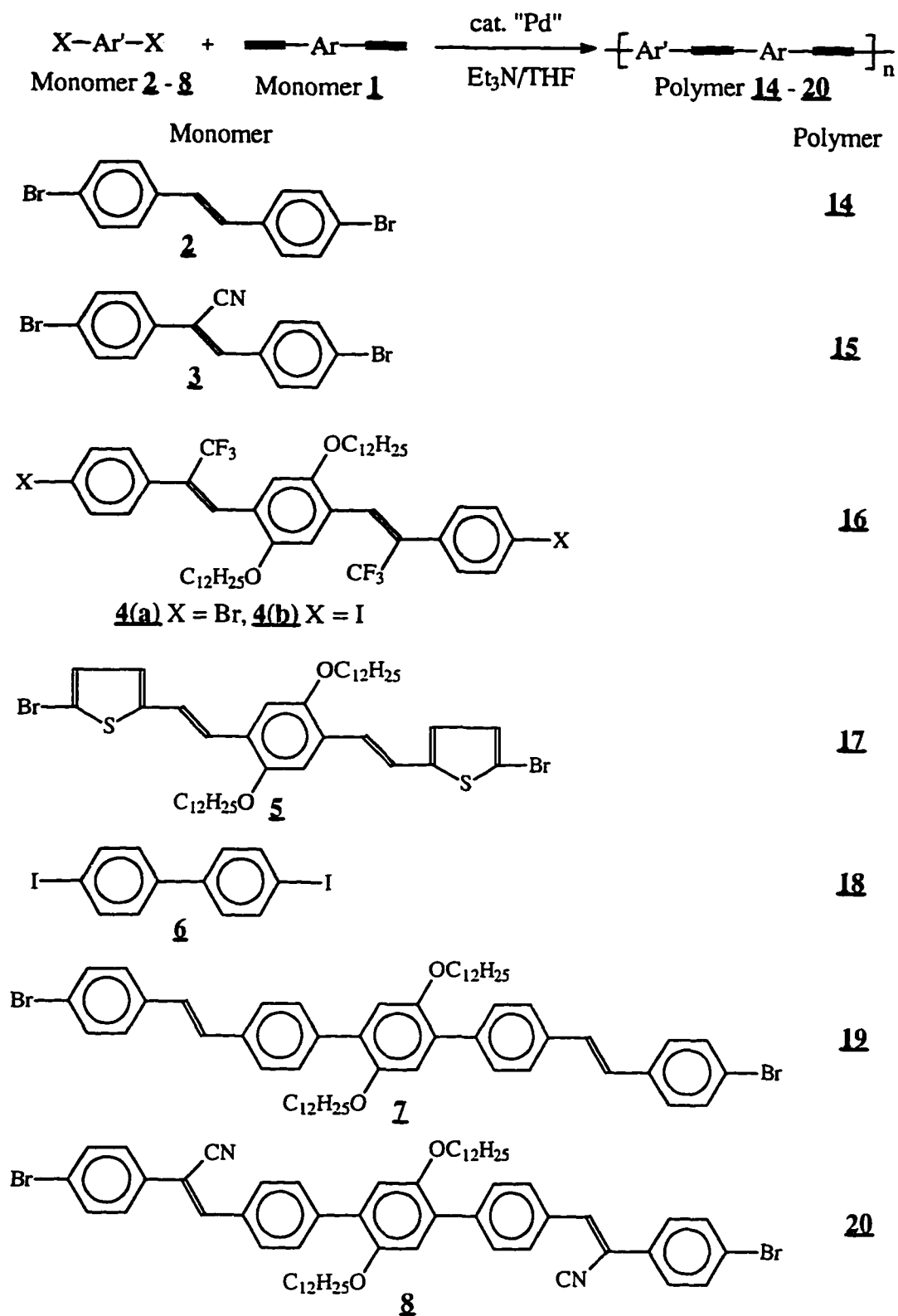
o-Formylphenylboronic acid⁴⁰ and Na_2CO_3 were allowed to react with compound **10** in refluxing DME solution for 2 days, according the Suzuki reaction, to give dialdehyde **13** in 51% yield. Compound **13** is a yellow solid, which emits blue luminescence in THF solution. A Wittig reaction of dialdehyde **13** and phosphonium salt in benzene gave monomer **7** in 55% yield. A Knoevenagel condensation²⁴ between dialdehyde **13** and 4-bromophenylacetonitrile

in *t*-BuOH/THF solution gave monomer **8** in 85% yield. Both monomers **7** and **8** are yellow solids and have strong blue luminescence in THF solution.

All the monomers were characterized by mass spectroscopy, ¹H- and ¹³C-NMR.

Polymer Preparation. Preparation of the polymers was based on Heck-type coupling as in Scheme 9. Several palladium catalyst systems have been used to synthesized a variety of polymers⁵² by this coupling reaction. It is well known that when X = I, high molecular weights can be obtained while when X = Br, the reactions usually require high temperature, long reaction time and give low molecular weights. In 1994, Moigne developed a catalyst system PdCl₂/CuAc₂/PPh₃ to obtain high molecular weight polymers when X = Br.^{25(d)} Thus, our polymerizations were carried out using this catalyst system in Et₃N/THF solution. The exclusion of oxygen is necessary to prevent catalyst deactivation and to minimize the copper-catalyzed coupling of acetylenes to diacetylenes which can compete with the desired reaction. The solutions of two monomers in Et₃N/THF in the presence of the catalysts were refluxed for three days. After work up, the polymers were simply purified by adding their saturated THF solutions into methanol to precipitate them several times. Most monomers were dibromo- compounds, while the others were diiodo- compounds. The yields of polymerizations were high as 90%, except polymers **19** and **20** (about 65%).

Polymer Characterization. The polymers were characterized by GPC, ¹H- and ¹³C-NMR. Molecular weight measurements were performed by gel permeation chromatography (GPC) calibrated by standard polystyrene using THF as an eluent. The weight average molecular weights (M_w) of the polymers range from 5 x 10³ to 8 x 10⁴ depending on the molecular weights of the monomers (Table 3). Polymer **14** has a molecular weight of 8.53 x 10³ which is close to that of polymer **15** (8.7 x 10³). The higher yield and higher molecular weight of polymer **16** (M_w = 2.47 x 10⁴, yield 90.2%) were obtained when diiodo-monomer **4(b)** were used instead of dibromo-monomer **4(a)** (M_w = 9.84 x 10³, yield 75.4%). The molecular weight of polymer **18** (M_w = 4.58 x 10³) is low compared with the other polymers. This is because of the impurity of 4,4'-diiodobiphenyl (only 95%, Aldrich). The higher molecular weight monomers gave the higher molecular weight polymers but the yields were



Scheme 9: Synthesis of the polymers

low (polymer **19** with $M_w = 3.21 \times 10^4$ and yield 65.5%, Polymer **20** with $M_w = 7.74 \times 10^4$ and yield 66.0%). However the degree of polymerization (DP) are about 10 for polymers **14-18** and 25 for polymer **19**, and 60 for polymer **20**. Polydispersities (PD) of these polymers were 1.45-2.57, which are typical for step growth polymerizations, except polymer **20** (PD = 5.71) due to the large monomer. Table 3 summarizes the results of polymerization.

Table 3: The yields, weight average molecular weights (M_w), polydispersities (PD) and degrees of polymerization (DP) of the polymers

Polymer	Yield (%)	M_w	PD (M_w/M_n)	DP
14	92.5	8.53×10^3	2.44	13.7
15	89.0	8.70×10^3	2.14	13.4
16	75.4 (X=Br)	9.84×10^3	2.12	8.0
	90.2 (X=I)	2.47×10^4	1.98	20.0
17	90.0	8.92×10^3	1.38	13.6
18	91.1	4.58×10^3	1.45	7.7
19	65.5	3.21×10^4	2.57	25.6
20	66.0	7.74×10^4	5.71	59.4

The $^1\text{H-NMR}$ spectra of the polymers are slightly different from those of the respective monomers. All the resonances are broader, and no signal was detected in the 3.3 ppm region for the acetylenic proton in any case. The protons of $-\text{CH}_2-$ groups attached by the oxygen in the side chain are at ~ 4.00 - 3.20 ppm. The $^{13}\text{C-NMR}$ spectra show two signals between 100 and 84 ppm, which represent two unsymmetric acetylenic carbons. The carbons of aromatic ring with alkoxy side groups and acetylene groups are detected at about 150, 115, and 113 ppm. The carbons belonging to the alkoxy side chains appear as very strong signals

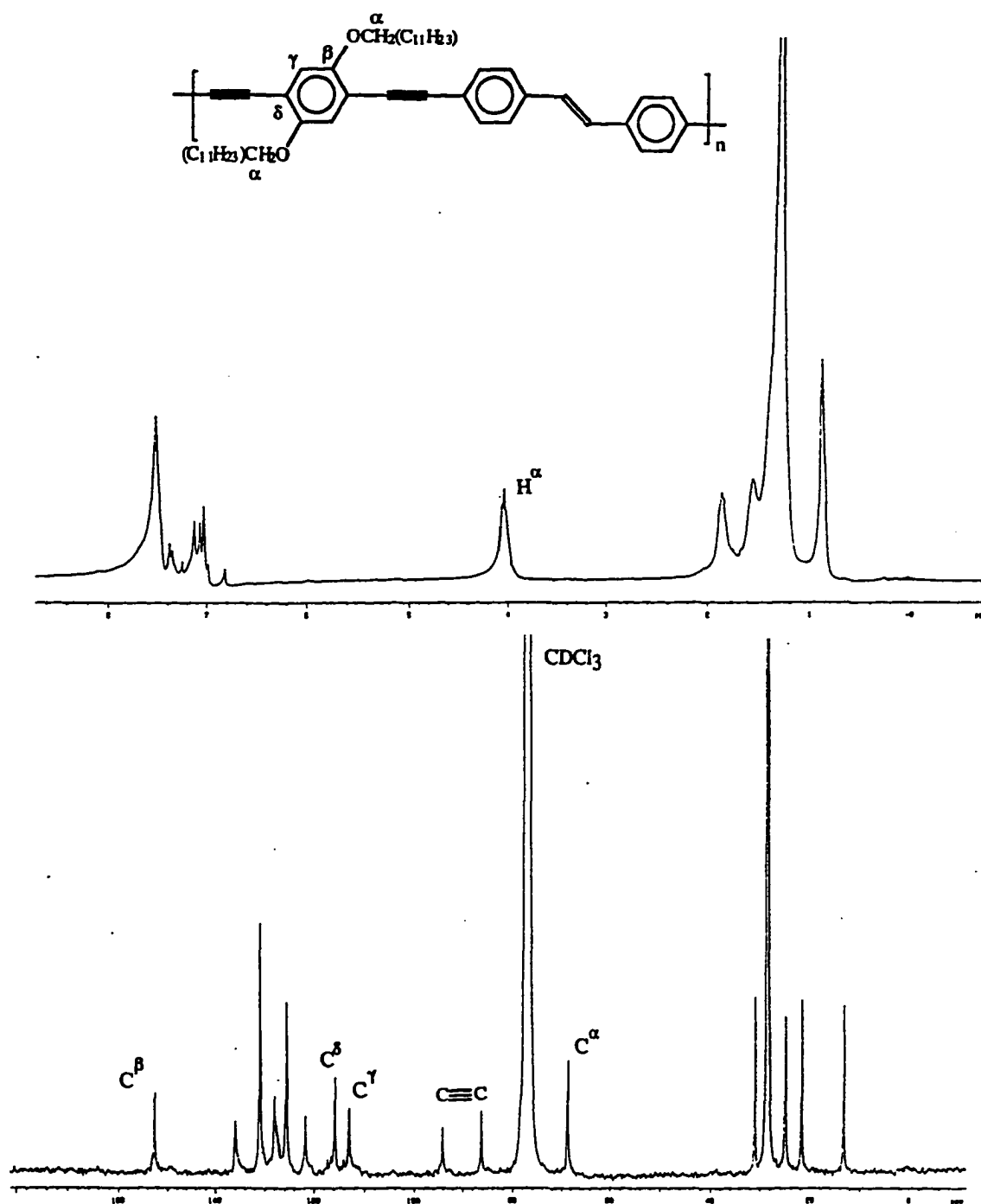


Figure 8: The ^1H -NMR and ^{13}C -NMR spectra of polymer **14**

at 70 ppm and from 32 to 13 ppm. A specific example of the $^1\text{H-NMR}$ and $^{13}\text{C-NMR}$ spectra of polymer **14** is shown in Figure 8. In the $^{13}\text{C-NMR}$ spectrum, the acetylenic carbons are at 94.07 and 86.15 ppm. The aromatic ring with side chains are at 152.58, 115.78 and 112.93 ppm. There are a total of 8 carbon signals between 153 to 112 ppm corresponded to the aromatic and vinyl carbons. There is only one vinyl carbon signal due to the symmetry of the polymer chain.

As for the polymers which contain two phenyl rings with alkoxy side groups in the main chain, the $^1\text{H-NMR}$ spectra show two kinds of $-\text{CH}_2-$ groups attached by the oxygen in the side chains. The $^{13}\text{C-NMR}$ spectra show these two kinds of methylene signals at ~ 70 ppm and the two kinds of aromatic carbons attached by alkoxy groups at ~ 150 ppm respectively (see Figure 9 for an example). The $^{13}\text{C-NMR}$ spectrum shows that polymer **16** has two acetylenic carbons at 93.38 and 86.65 ppm, two aromatic carbons of two phenyl rings attached by side chains at 152.96 and 150.06 ppm, two methylene carbons attached by oxygen in the side chains at 68.75 and 67.95 ppm. These methylene protons also can be seen clearly in the $^1\text{H-NMR}$ spectrum at 4.00 and 3.26 ppm.

Properties of the Polymers

Solubilities. All the polymers are yellow in the solid states except polymer **17** which is reddish. They are all quite soluble in organic solvents such as THF, CHCl_3 , CH_2Cl_2 and toluene due to the long alkoxy side group. They are green-yellow in THF and have green luminescence, except polymer **17**, which is red, and has strong green-blue luminescence.

Thermal Behaviors. Thermal behaviors of these polymers were studied by thermogravimetric analysis (TGA) and differential scanning calorimetric analysis (DSC) under nitrogen atmosphere. The TGA was performed from room temperature to 600°C with a ramp of $20^\circ\text{C}/\text{min}$. From the TGA spectra, these polymers have similar thermal stabilities. They start to lose weight rapidly at about $350\text{--}390^\circ\text{C}$ (about 5% weight loss) and after 450°C they slowly lose weight. At 600°C , char yields are about 45%, except polymer **17** (29%). For example, polymer **14** starts weight loss at 395°C (3% weight loss), and after 474°C (48%

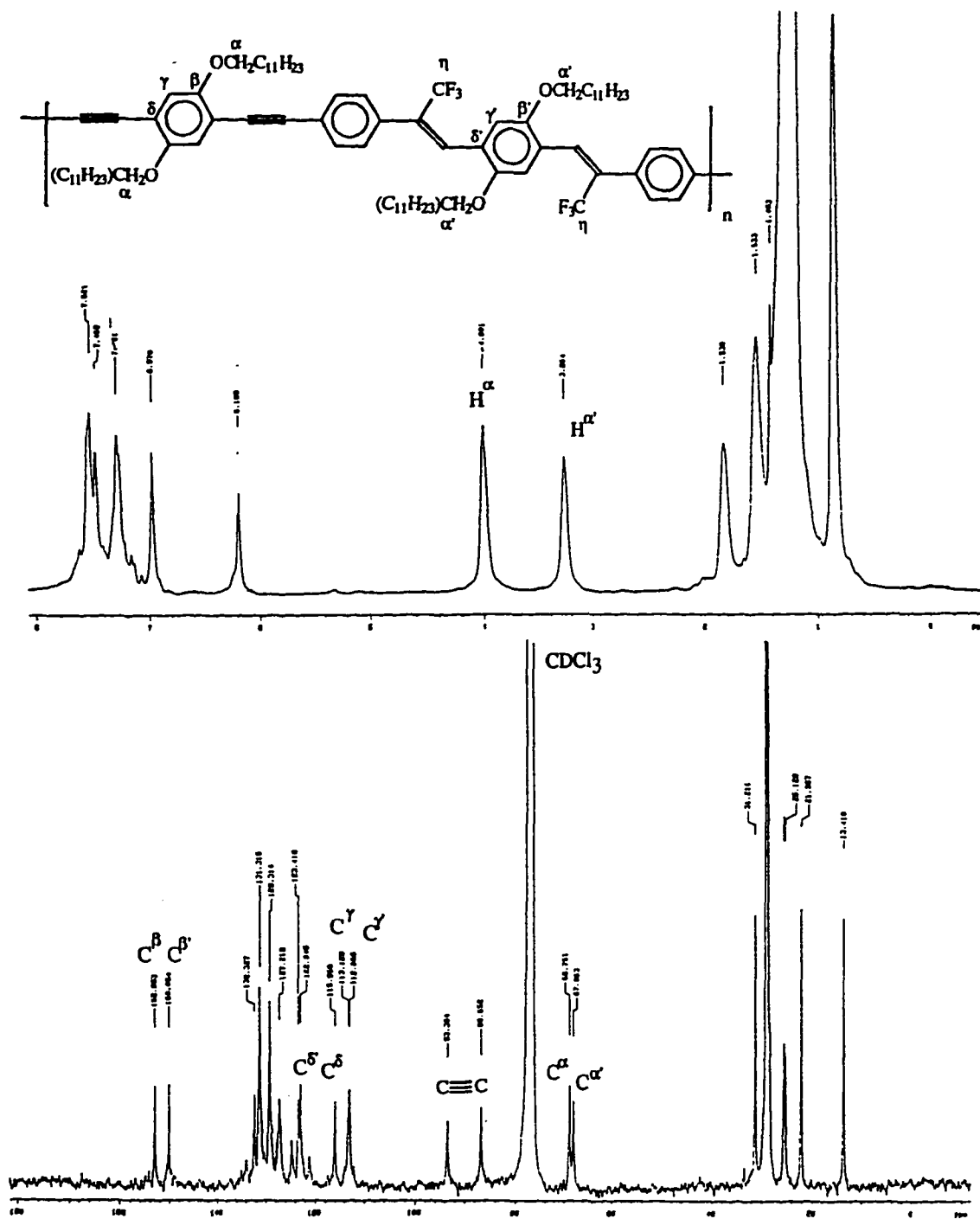


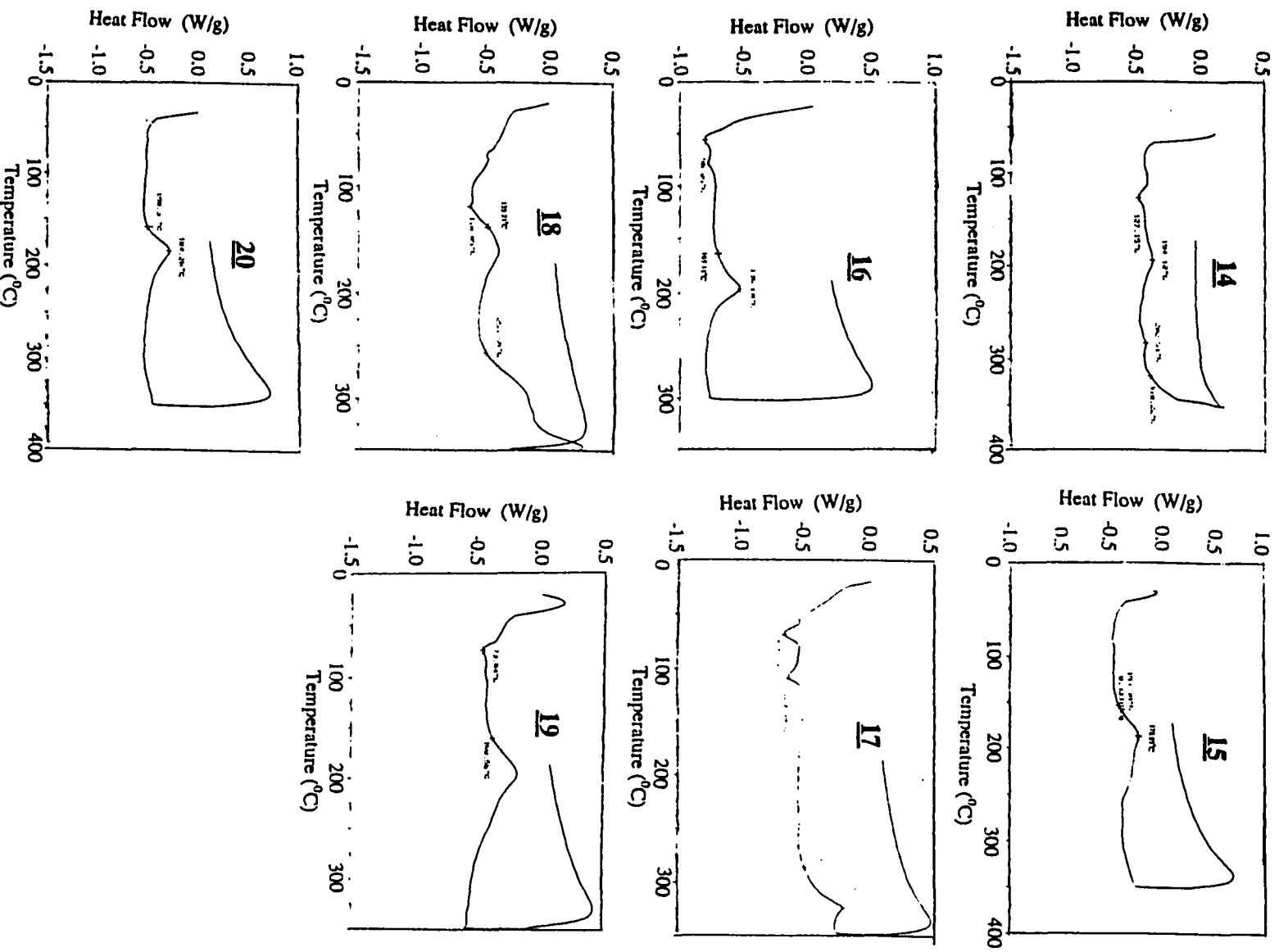
Figure 9: The $^1\text{H-NMR}$ and $^{13}\text{C-NMR}$ spectra of polymer **16**

Table 4: TGA and DSC results of the polymers

Polymer	TGA		DSC
	Temperature (°C) (% remained weight)	% remained weight at 600°C	Crosslinking temperature (°C)
14	395 (97)	48	194, 318
15	390 (93)	46	153
16	381 (95)	45	165
17	353 (95)	29	286
18	333 (94)	50	135, 256
19	352 (95)	42	160
20	373 (96)	49	158

weight loss) the weight loss is slow. At end (600°C), the weight loss is 52%. A summary of the TGA data is shown in Table 4.

The thermal transitions of these polymers were studied by DSC as shown in Figure 10. The endothermic peaks usually show the melting process (T_m) while exothermic peaks show crosslinking. All these polymers have an exothermic peak before they start to decompose except polymers **15** and **20**. DSC for polymer **14** shows melting at $\sim 127^\circ\text{C}$ and exothermic reactions starting at $\sim 194^\circ\text{C}$ and 283°C due to crosslinking. Polymer **15** has only one exothermic peak at $\sim 178^\circ\text{C}$ starting at 153°C , which shows crosslinking happens before polymer melting. There are two endothermic peaks at $\sim 56^\circ\text{C}$ and 77°C and a exothermic reaction at $\sim 197^\circ\text{C}$ for the polymer **16**. Polymer **17** has a small endothermic peak at 119°C and starts to crosslink at 135°C and 256°C . Polymer **18** has two endothermic peaks at 69°C and 109°C , and starts to crosslink at 286°C . Polymer **19** melts at about 74°C with a small endothermic peak and start to crosslink at 161°C . There is no melting peak before polymer **20** starts to crosslink at $\sim 158^\circ\text{C}$. After cooling to room temperature, the brown crystals were

Figure 10: DSC thermogram of polymers **14** - **20**

usually recovered. All these crystals were not soluble in normal organic solvents anymore, indicating crosslinking.

Conductivities. Conjugated polymers are capable of being doped, through chemical or electrochemical oxidation or reduction, to states of higher electrical conductivity. The conductivities of these polymers were measured by two in-line probes. All these polymers were insulators when undoped. After doping with I₂ vapor under vacuum, they became semi-conducting. Polymer **14** has a conductivity of $\sigma = 4-10 \times 10^{-4}$ S/cm, while polymer **15** with its -CN group has a conductivity of $\sigma = 2-4 \times 10^{-3}$ S/cm. Other polymers also have very low conductivities of σ about 1×10^{-4} - 10×10^{-4} S/cm, which are similar to those of PPE,^{25(b)} except polymer **17** with conductivity of 50-100 S/cm.

UV/Vis Absorption. The UV/Vis absorption spectra of these polymers were recorded and are shown in Figure 11. The absorption edges (λ_c) were estimated within ± 5 nm. All the polymers show strong absorptions in the visible range between 384 to 472 nm (Table 5). Polymer **14** was synthesized as comparison to PPE and PPV. The λ_{max} polymer **14** in THF solution is 414 nm, which is smaller than those of PPE (429 nm^{25(a,d)}) and PPV (459 nm⁵¹), probably due to the low molecular weight of polymer **14** compared with PPE and PPV. The absorption edge (λ_c) of polymer **14** is 464 nm, which could be used to estimate a bandgap of 2.67 eV. The -CN group was introduced into polymer **15** as a study of effects of the substituent on the electronic properties of the polymer. The λ_{max} of polymer **15** in THF is 14 nm red-shifted compared with that of polymer **14**, indicating the bandgap of polymer **15** is lower than that of polymer **14**. The effect of an electron-withdrawing group of CN was studied by Holmes et al in CN-PPV (Figure 5).²⁴ They reasoned that the electron withdrawing group -CN would make polymer more electronegative, lower the LUMO and HOMO levels, thus improving the electron injection to the polymer layer in LED devices. The CN-PPV-based LEDs had internal quantum efficiencies of 4-10%, the highest efficiencies reported. In 1994, Heeger et al. calculated the influence of donor and acceptor substituents on the electronic characteristics of PPV and PPP. It also showed that CN lowers the LUMO and HOMO energies. Figure 12 shows the bandgaps, HOMO and LUMO energies. The low LUMO level can match to the low workfunction metal like calcium, thus improving the efficiency of

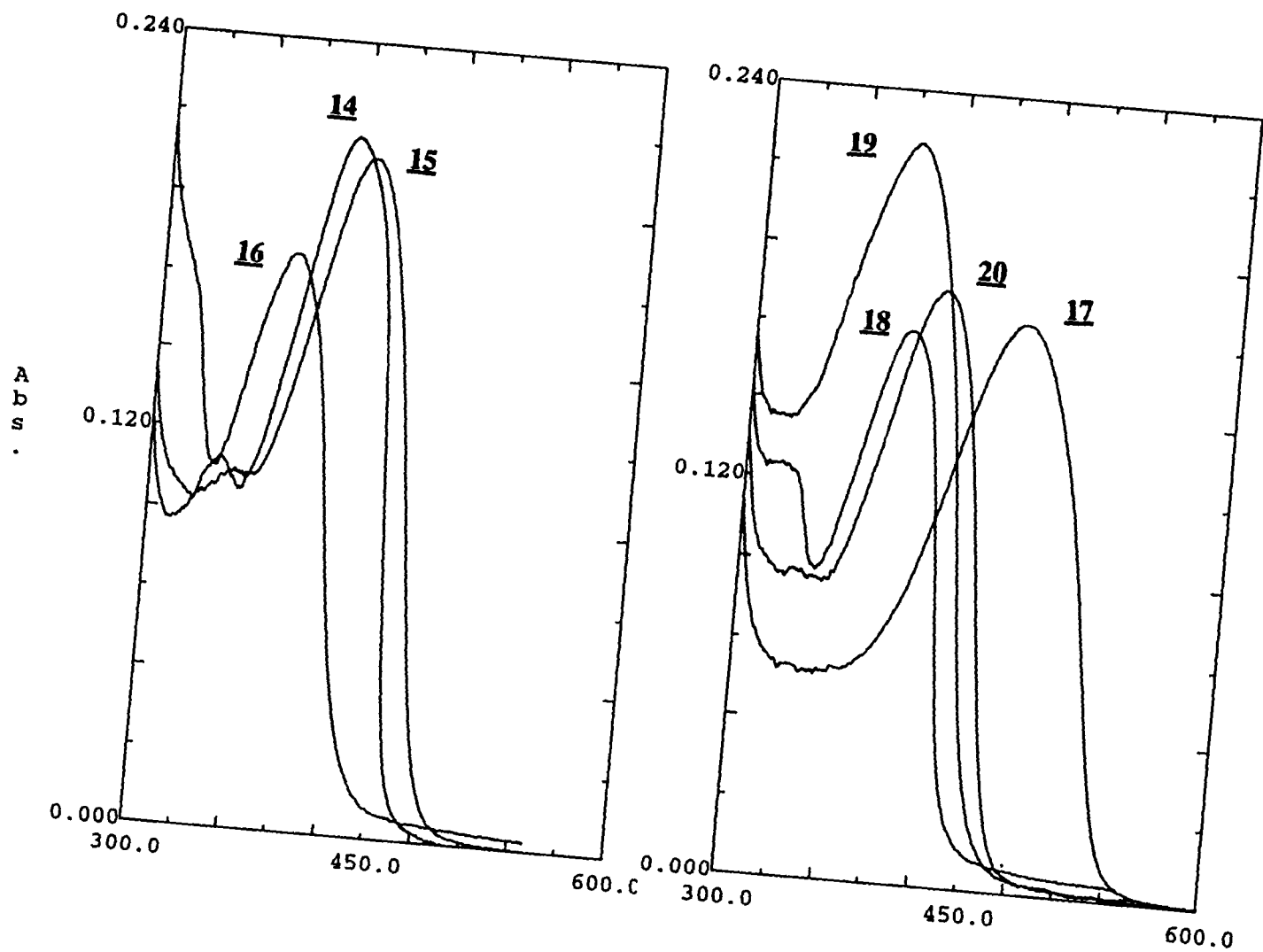


Figure 11: The UV spectra of the polymers in THF solution

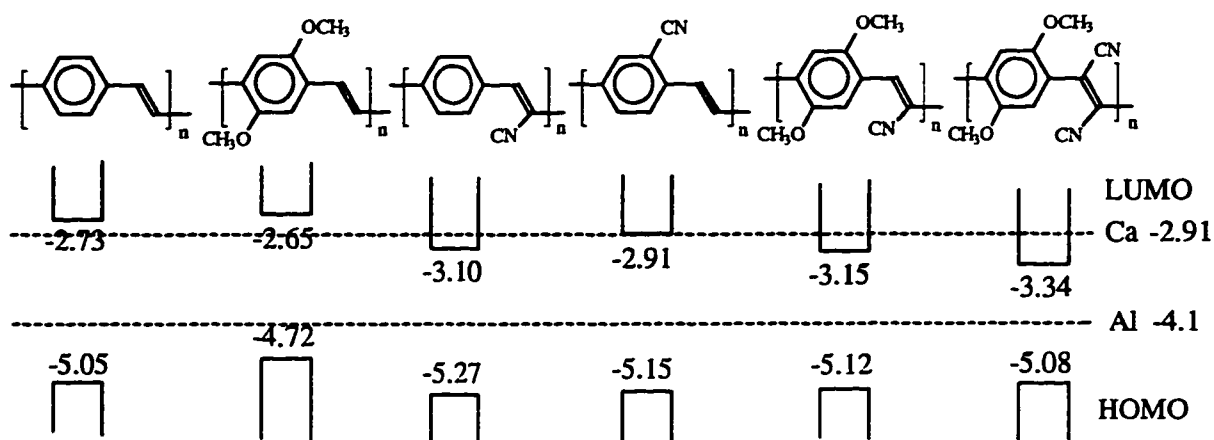


Figure 12: Sketch of the band structures of the polymers, relative to the workfunctions of Ca and Al

electron ejection. This effect of CN can also be seen in polymers **19** and **20** with λ_{\max} of 378 and 416 nm, and with λ_c of 467 and 458 nm, respectively.

Another electron withdrawing group $-\text{CF}_3$ was introduced into polymer **16** as a comparison with polymers **14** and **15**. Both $-\text{CF}_3$ and $-\text{CN}$ are electron withdrawing groups, but $-\text{CN}$ exhibits electron-withdrawing by resonance while $-\text{CF}_3$ exhibits electron-withdrawing by sigma induction. However, the λ_{\max} of polymer **16** is at a much shorter wavelength than that of polymer **15**, and even polymer **14**. The most likely rationalization is that the bulky trifluoromethyl group reduces conjugation by causing the phenyl to twist. In 1996, Holmes et al. also studied the effect of electron-withdrawing groups $-\text{CF}_3$ and CN on the model compounds of PPV (Figure 13).^{24(g)} It was found that CF_3 substituted derivatives have shorter wavelength of UV/Vis absorption than those CN substituted derivatives.

Replacement of the phenyl by thiophene in the polymer main chain greatly changes the UV absorption. Thus λ_{\max} of polymer **17** (472 nm) is considerable red-shifted from λ_{\max} of all of the other polymers. Conjugated polymers with thiophene rings usually allow a better delocalization of π -orbitals than the corresponding phenylene rings. It is because thiophene has less aromaticity than phenyl, thus allowing the π -electrons more mobility.^{25(d)} For example

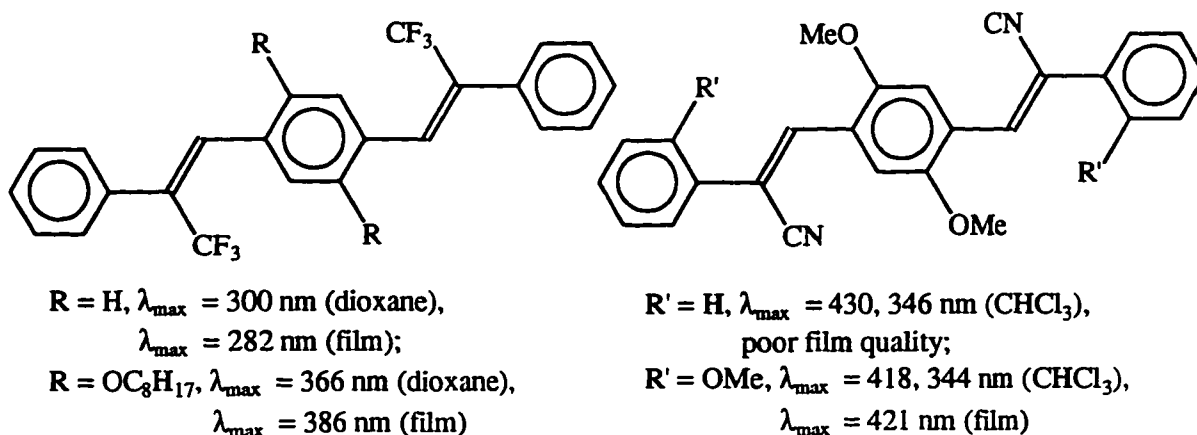


Figure 13: The UV/Vis absorption of CF_3 and CN substituted compounds

PPP has an electronic bandgap of 3.0 eV (413 nm) as compared with 2.1 eV (590 nm) for PT.⁴¹

Increasing PPP units in the polymer increases the bandgap energies. The UV/Vis absorption λ_{\max} of polymer **18** (396 nm in THF) is 33 nm longer than that of PPE (429 nm) even polymer **18** has only one more phenyl in the repeating units. Compared the UV/Vis absorption of polymer **19** with polymer **14** and polymer **20** with polymer **15**, polymer **19** is 26 nm longer than polymer **14** while polymer **20** is 12 nm longer than polymer **15**. As mentioned earlier, the more phenyl rings in the polymer main chain, the more aromaticity of the polymer, thus the more localization of the π -electrons in the phenyl region.

The UV/Vis absorption spectra of these polymer films were also measured and the absorption edges (λ_c) were estimated (Table 5). The films were made by dropping polymer THF solutions onto spinning quartz plates. After the solvent was evaporated, the films formed on the plates were directly measured. The films of polymers **14**, **16**, **18** and **20** have similar absorption peaks as their solutions, but with a red shift of the main peak of about 27 to 58 nm. Polymer **14** in the film has a 44 nm red-shift compared with in THF solution. Polymer **15** has the largest red-shift of 58 nm. Polymer **16** has a 43 nm red-shift. Polymer **16** has a red-shift of 43 nm. Polymer **17** has the smallest red-shift of 27 nm. Polymer **18** is about 36 nm red-shifted. Polymer **19** has a red-shift of 34 nm. Polymer **20** has a larger red-shift of 56 nm. The films of polymers **15**, **17** and **19** have quite different absorption peaks from their

solutions. Besides the main peaks red-shift, the peaks in film states are more broad and the tails of the peaks more extend. The tails of absorption of polymer **15** ($\Delta\lambda_{\max} = 58$ nm, $\Delta\lambda_e = 78$ nm) and **19** ($\Delta\lambda_{\max} = 34$ nm, $\Delta\lambda_e = 62$ nm) films extend about 20 nm ($\Delta\lambda_e - \Delta\lambda_{\max}$) longer than their main peaks. The tail of absorption of polymer **17** ($\Delta\lambda_{\max} = 27$ nm, $\Delta\lambda_e = 75$ nm) extends even 48 nm longer. This suggests the conformations in the film states allow much better conjugation.

Table 5: UV/Vis absorption maxima (λ_{\max}) and band edges (λ_e) of the polymers in THF solution and their films

Polymer	THF solution		Film	
	$\lambda_{\max}(\text{nm})$	$\lambda_e(\text{nm})$ (eV)	$\lambda_{\max}(\text{nm})$	$\lambda_e(\text{nm})$ (eV)
14	414	464 (2.67)	458	508 (2.45)
15	428	482 (2.58)	486	560 (2.22)
16	384	433 (2.87)	427	490 (2.54)
17	472	535 (2.32)	499	600 (2.07)
18	396	440 (2.82)	432	484 (2.56)
19	378	458 (2.71)	412	520 (2.39)
20	416	467 (2.66)	472	524 (2.37)

Fluorescence. All the polymers are photoluminescent in both solutions and the solid states. The photoluminescence (PL) spectra of these polymers in THF solutions have been obtained (Figure 14). The solutions were excited by the UV/Vis light with excitation wavelength (λ_{ex}) about 10 nm shorter than the corresponding absorption maximum

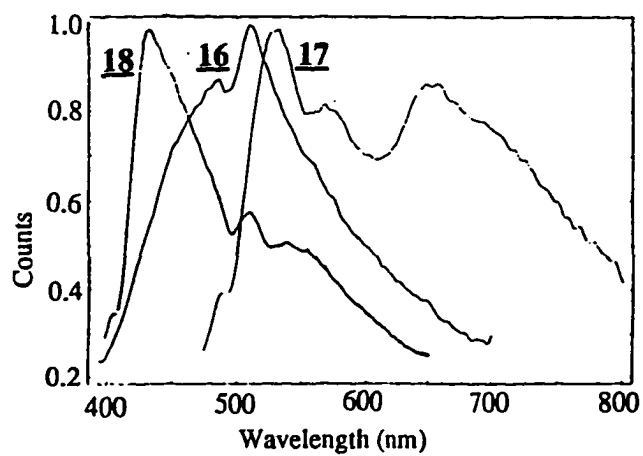
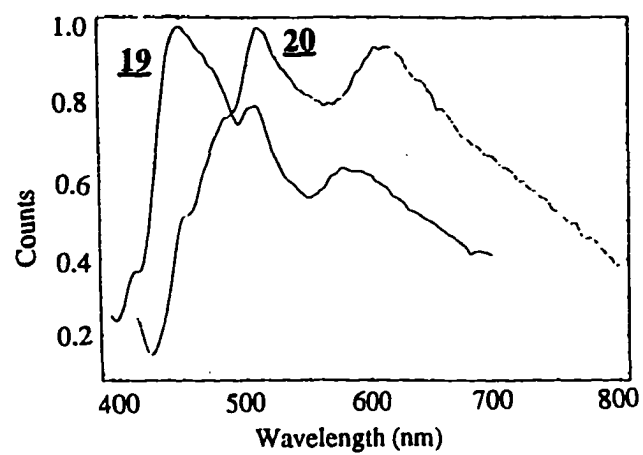
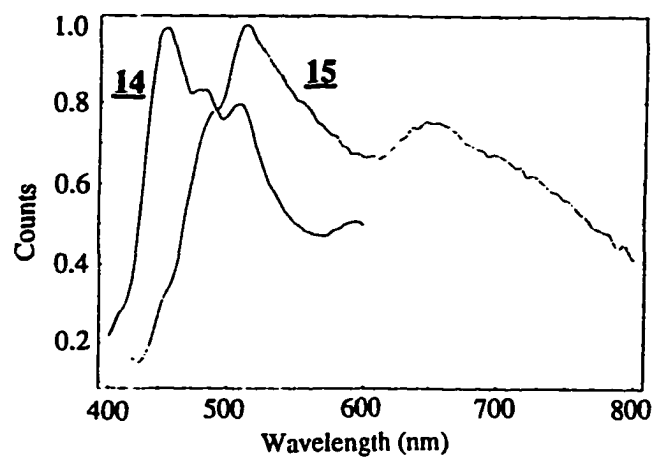


Figure 14: The photoluminescence (PL) spectra of the polymers

wavelength (λ_{\max}). The emission bands are sharper than the absorption bands, but with broad peaks at the long tail regions. The emission bands are usually largely red-shifted compared with their absorption bands. These broad emission bands can be associated with recombination processes between defect levels within the gap which may result from interruption of the conjugation of the chains. The emission of polymer **15** with a peak at 512 nm is dramatically shifted relative to the analogous polymer **14** with a peak at 456 nm. The emission of polymer **14** has two small, broad emission side bands at 485 nm and 509 nm while polymer **15** has only one broad side band at 646 nm. Polymer **16** has an emission band at 510 nm with a shoulder around 487 nm. The shoulder is due to recombination from the high vibration states of the excitation state to the ground state. Polymer **17** has the longest emission band at 532 nm with two broad side bands at 568 and 658 nm. This indicates polymer **17** has the lowest bandgap, which is also shown in its the longest UV/Vis absorption. Polymer **18** has only a sharp emission band at 434 nm and a small band at 510 nm. The emission of polymer **20** with a band at 510 nm is large red-shifted compared with that of polymer **19** with a band at 448 nm. Like polymer **15**, polymer **20** has a broad side band at 604 nm. The emission spectra of these polymers are summarized in Table 6.

Table 6: The summary of the photoluminescence (PL) spectra of the polymers

Polymer	λ_{ex} (nm)	λ_{max} (nm)
14	410	456, 485(br), 509(br)
15	420	512, 646(br)
16	375	510, 487
17	460	532, 568(br), 658(br)
18	380	434, 510
19	365	448, 510(br), 570(br)
20	405	510, 604(br)

The Polymer-Based LEDs

Because these polymers emit strong fluorescence upon excitation, the films of these polymers could be used as the emissive layer in LED devices. In a collaboration with Prof. J. Shinar (Department of Physics, Iowa State University), the polymer **14**-based LED device has been made and studied.⁴² The LED device structure is shown in Figure 2. The LED devices were fabricated by spin coating Standish LCD indium-tin-oxide (ITO)-coated glass with a 6 mg/ml polymer **14** solution in toluene or chloroform either in air or in a protective nitrogen atmosphere. The Standish ITO was partially stripped by the manufacturer. The ITO was normally 50 μm thick with a sheet resistance of $\sim 200 \Omega$. The polymer solutions were pumped through 0.2 or 0.5 μm syringe filters into clean glassware for storage until use. The polymer layer had typical thickness of 100-200 μm . Al contacts with an area of about 10 mm^2 was thermally or *e*-beam evaporated onto the polymer layer in vacuum.

I-V measurements was performed with the device submerged in liquid N_2 for heat-removal. Lifetimes under these conditions were indefinite. However, measurement at room temperature yielded lifetimes of only several hours. The electroluminescence (EL) and photoluminescence (PL) spectra were measured by directing the collected light from the device into a Jarrell-Ash monochromator with 7 nm resolution, followed by a Si photoiode. Figure 15 presents a typical *I-V* curve of a polymer **14**-based device at 77 K. As clearly seen, it is symmetric in both forward and reverse bias voltages with a turn-on voltage of about 12 V. This symmetric *I-V* curve is quite different from the non-symmetric curves reported for normal PPV-based^{43(a, b)} or PPE-based LEDs.^{25(c)} The electroluminescence intensity (I_{EL}) was also measured and the $I_{\text{EL}}-V$ curve is also presented in Figure 15. It closely follows the *I-V* curve, and the device clearly emits symmetrically with either polarity of the electrodes. In addition, the curve is similar to that of forward biased ITO/PPV/Al LEDs, suggesting a quantum efficiency of about 0.05%.

In order to study the nature of the reverse bias emission, the electroluminescence (EL) spectra was measured in both biasing directions under identical values of *V* and *I*, and are shown in Figure 16. The spectra are identical and very similar to the PL, which is also shown

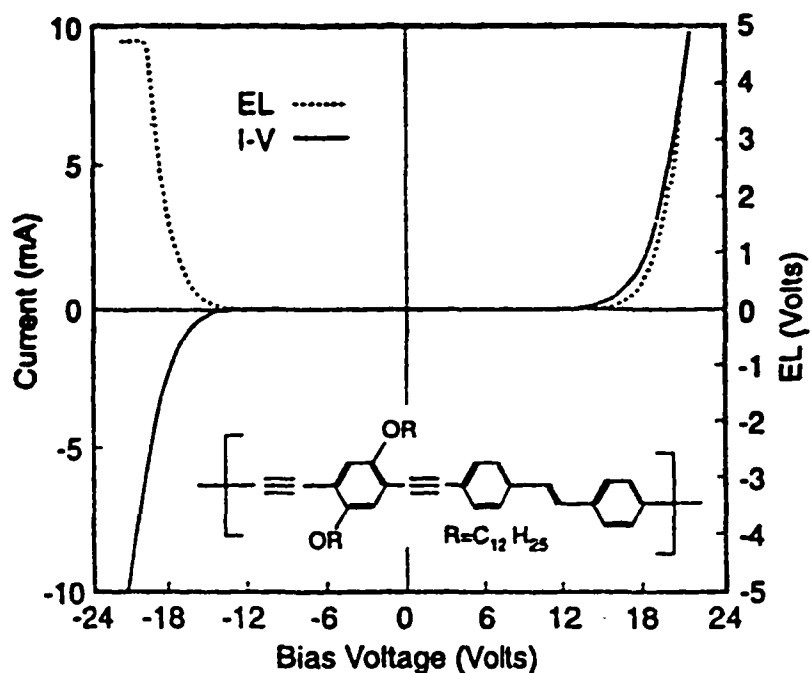


Figure 15: The *I-V* curve of polymer 14-based LED device (solid line) and the dependence of the integrated intensity of the EL on the applied bias voltage (dotted line)

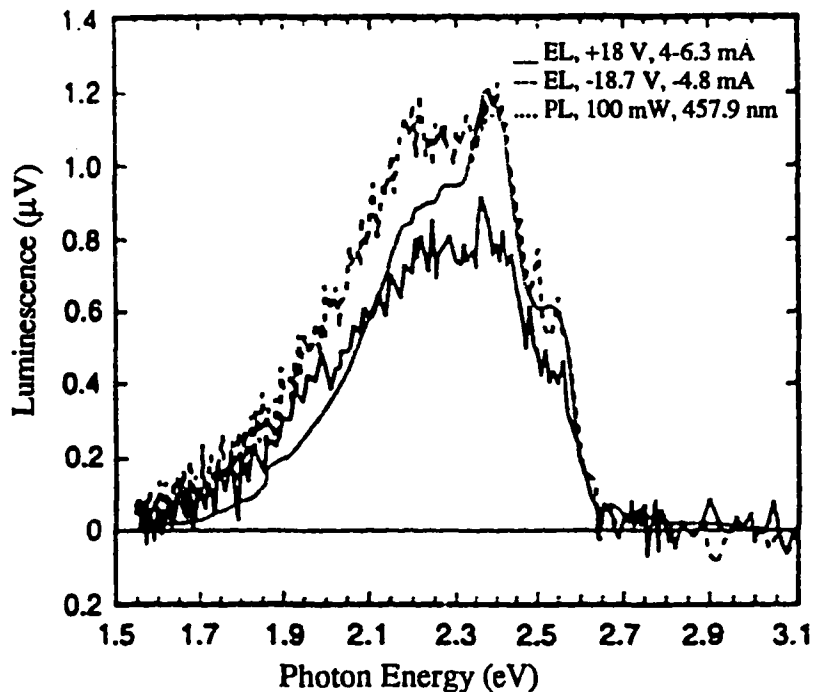


Figure 16: The EL spectra for positive and negative bias voltage of 18V of polymer 14-based LED device (solid line) compared to the PL spectrum (dotted line)

in Figure 16. This similarity shows that the mechanism leading to emission in both biasing directions is identical and probably due to exciton recombination. This is particularly significant for the reverse bias spectra, where avalanche emission could otherwise be suspected. The coincidence of the EL and PL is also similar to that observed in PPV-based devices^{43(c)} and distinct from that of PPE-based emitters.^{25(c), 43(c)}

In PPV-based LEDs, the I - V characteristics of diodes prepared with different metal electrodes have indicated that metal and ITO work functions determine the barrier heights for electron and hole injection, respectively, at their interfaces with the polymer.⁴⁴ This picture is invalid in the present case of polymer **14**-based structure. This behavior could be explained by Femi energy (E_F) pinning by a high density of deep defect states at interfaces. These defects can capture carriers from the bulk, creating barriers at the interfaces. Whereas contact of a clean surface with a metal usually results in charge exchange between the metal and the surface states, in the case of a high density of surface states the barrier height at the interface is not effected by presence of the metal, resulting in pinning of E_F at the defect states.

For polymer LEDs, basic tunneling theory predicts

$$I \propto V^2 \exp(-b/V), \quad \text{Eq. (1)}$$

where $b = 4(2m^*)^{1/2} \phi^3 / 2d / (3eh)$ for a triangular barrier of height ϕ and m^* is the effective mass of the carrier. A plot of $\ln(I/V^2)$ vs. I/V , based on Figure 15, is shown in Figure 17(a).⁴⁵ It indicates the Eq. (1) fits the observed behavior from 14 to 21 V, but substantially deviates from it at low bias voltages. One-step tunneling is not expected to be valid at low voltages, since the tunneling distance $x = d\phi/V$ is then too large. For example, $x > 10 \mu\text{m}$ at $V = 1 \text{ V}$ and $d = 100 \mu\text{m}$. It has, therefore, been suggested that the excess injection current at low V is due to sequential tunneling of carriers via localized states near E_F .⁴⁶ That model predicts the following relationship

$$\ln(I) = -\gamma(d/V)^{1/2}, \quad \text{Eq. (2)}$$

where $\gamma = 4(\Gamma/3)^{1/2} (2m^*/e^2\hbar^2)^{1/4} \phi^{3/4}$, $\Gamma = -\ln(p)$, and p is the probability that a carrier will find another localized state with an energy close to E_F . Figure 17(b) display $\ln(I)$ vs. $V^{-1/2}$ for the

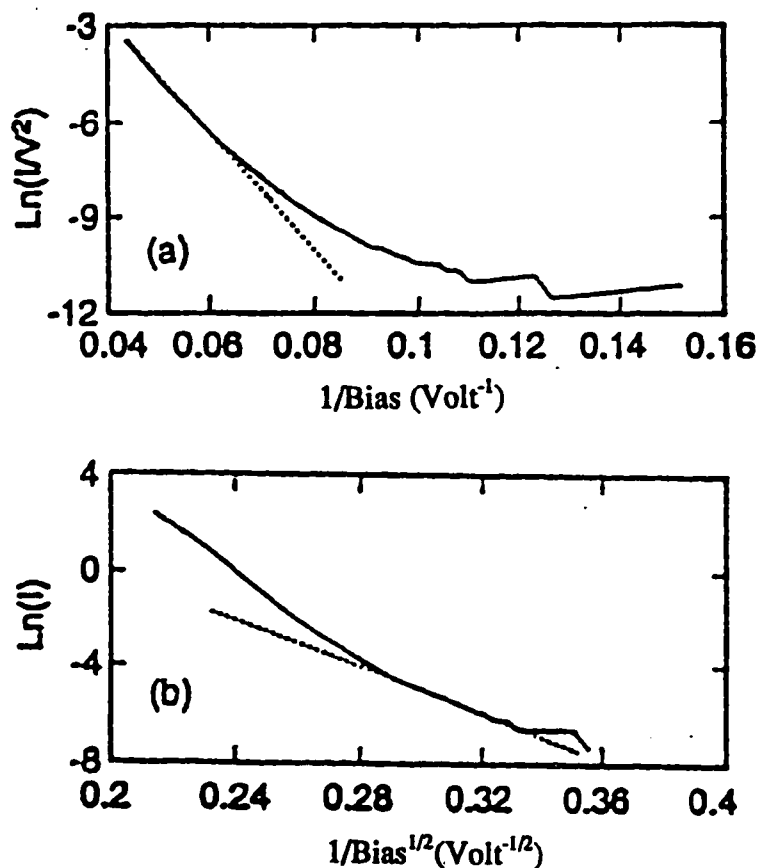


Figure 17: I - V plots of the polymer **14** device: (a) $\ln(I/V^2)$ vs. $1/V$; (b) $\ln(I)$ vs. $V^{1/2}$

polymer **14**-based diode. The curve is linear for $V < 13$ V, which is just below the bias range at which Eq. (1) fits the results.

Conclusions

A series of copolymers containing units of PPV, PPE and PPP were synthesized by polymerization of diethynylene arylenes and dibromo- (or diiodo-) arylenes in the palladium catalyst system. All the polymers were characterized by ^1H and ^{13}C NMR, GPC, UV/Vis, TGA and DSC.

The thermal stabilities and thermal behaviors of these polymers were studied. Most of these polymers start to decompose at above 350°C . They usually cross-link at about 300°C .

The conductivities were also studied. At undoped states, all these polymers are nonconductive. After doped by I₂ vapor in the vacuum, the polymers are semi-conductive with conductivities of about 1×10^{-4} - 10×10^{-4} S/cm.

The optical properties of these polymers were studied. The UV/Vis absorption and photoluminescence spectra were measured. The electron withdrawing group, -CN, can reduce the bandgap energy, thus increasing the λ_{max} values of UV/Vis absorption and emission. The replacement of phenyl with thiophene can enhance the delocalization of π -orbitals, thus dramatically increasing the λ_{max} of UV/Vis absorption. Increasing the number of PPP units into the repeating unit can increase the localization of π -orbitals, thus decreasing the λ_{max} of UV/Vis absorption. The photoluminescence spectra show there are several broad peaks at tail regions besides the major emission bands, indicating the defects in the polymer main chains. These defects are due to the interruption of the conjugation of the polymer main chains.

Polymer-based LEDs were studied. The polymer **14**-based device showed symmetric *I*-*V* curve, which is quite different from the non-symmetric curves reported for PPV-based devices. This behavior could be explained by the defects in intersurface of the polymer and the metal or ITO and defects in the polymer main chain. This property could broaden the application of polymer-based LEDs.

Experimental

¹H and ¹³C-NMR spectra were acquired on a Varian VXR-300 spectrometer. In order to assure the quantitative features of the ¹³C-NMR spectra, the relaxation agent chromium(III) acetylacetonate was used in CDCl₃ with a relaxation delay of 5 seconds.

Routine GC-MS spectra were obtained on a Hewlett Packard 5970 GC-IR-MS spectrometer at 70 eV. The exact masses were obtained from a Kratos MS 50 mass spectrometer with 10,000 resolution. The infrared spectra were recorded on a Bio-Rad Digilab FTS-7 spectrometer from neat sample. The UV/Vis spectra were obtained on a

Hewlett Packard 8452A diode array UV/VIS spectrometer and λ_{\max} were determined at optical densities of 0.2-0.5.

Polymer molecular weights were determined by gel permeation chromatography (GPC) with 6 Microstyrigel columns in series of 500 Å, 2×10^3 Å, 2×10^4 Å, 2×10^5 Å. THF was used as an eluent at a flow rate of 1 ml/min. The system was calibrated by polystyrene standards. GPC analyses were performed on a Perkin-Elmer series 601 LC equipped with Beckman solvent delivery system, a Walter Associate R401 refractive index detector and a Viscotek viscometer. Differential scanning calorimetry (DSC) analyses were performed on a Du Pont 910 Differential Scanning Calorimeter. The UV/Vis spectra were measured on a Hewlett Packard 8452A Diode Spectrophotometer. Photoluminescence spectra were measured on a FL 900 fluorometer made by Edinburgh.

Toluene and benzene were distilled over CaH_2 . THF was distilled from sodium/benzophenone before use. Other reagents were used as received from Aldrich Chemical Co. without further purification unless specified otherwise. Acetic acid, isopropanol and methanol were used as received from Fisher without further purification. All the reactions were performed under argon atmosphere. 1,4-Didodecyloxy-benzene was synthesized in good yield according to the literature.³⁰ 4-Bromo-2,2,2-trifluoroacetophenone³⁵ and *o*-formylphenylboronic acid⁴⁰ were synthesized according to the literature.

1,4-Didecyloxy-2,5-diiodobenzene 10: To a solution of 1,4-didecyloxybenzene 9³⁰ (15.557 g, 34.88 mmol) in acetic acid (300 ml) were added ZnCl_2 (11.860 g, 87.2 mmol) and BTMAICl_2 (30.345 g, 87.2 mmol). The mixture was stirred at 50-60°C for 1 day. The reaction was quenched by adding water (200 ml) and then a saturated sodium bisulfite aqueous solution (300 ml) was added to consume the unreacted BTMAICl_2 . The precipitate was collected by filtration and washed by water. The product was purified by precipitation from MeOH/THF twice to give a white solid (24.346 g, yield 53.5%). m.p. 59-61°C; Mass: m/z cal. for $\text{C}_{30}\text{H}_{52}\text{O}_2\text{I}_2$ = 698.20567, measured (HiRes EI) = 698.20548; $^1\text{H-NMR}$: δ 7.130 (s, 2H), 3.883 (t, 4H, J 6.3 Hz), 1.744 (m, 4H), 1.474-1.100 (br, 36H), 0.875 (t, 6H, J 6.9

Hz); $^{13}\text{C-NMR}$: δ 152.83, 122.76, 86.29, 70.34, 31.90, 29.55(2), 29.32, 29.14, 26.03, 22.69, 14.12

1,4-didecyloxy-2,5-bis[(trimethylsilyl)ethynyl]benzene: To a degassed solution of 1,4-didecyloxy-2,5-diiodobenzene **10** (3.00 g, 5.15 mmol) in a mixture of benzene (50 ml) and triethylamine (50 ml) were added trimethylsilylacetylene (1.35 g, 13.7 mmol) and a mixture of CuI (21 mg) and PdCl₂(PPh₃)₂ (85 mg). The solution was stirred for 12 hours at room temperature under an argon atmosphere. After the salt was removed by filtration, the solvent was evaporated to afford a yellow solid. Recrystallization of this solid from a mixture of methanol and isopropanol gave a yellow crystal (2.45 g, 90%). m.p. 73-74^oC; Mass: *m/z* cal. for C₄₀H₇₀O₂Si₂ = 639.16560, measured (HiRes EI) = 639.16478; $^1\text{H-NMR}$: δ 6.845 (s, 2H), 3.897 (t, 4H, *J* 3.3 Hz), 1.744 (m, 4H), 1.474-1.100 (br, 36H), 0.851 (t, 6H, *J* 6.9 Hz), 0.212 (s, 18H); $^{13}\text{C-NMR}$: δ 153.26, 116.4, 113.16, 100.33, 99.34, 68.71, 31.23, 28.94, 28.73, 28.66, 25.32, 22.02, 13.47, -0.72

1,4-Bis(bromomethyl)-2,5-didecyloxy-benzene **11³⁴:** To a 1000 ml three neck round bottom flask fitted with a mechanical stirrer, a thermometer, and an additional funnel was charged with 1,4-didecyloxybenzene **9** (26.76 g, 60 mmol), paraformaldehyde (11.65 g), NaBr (14.86 g, 144 mmol) and CH₃COOH (500 ml). A solution of H₂SO₄ in CH₃COOH (20 ml) was added dropwise over 20 minutes. The mixture was then heated to an internal temperature of 80^oC overnight. After the solution was allowed to cool to room temperature, the resulting white precipitate was collected by filtration and saved. The filtrate was then poured into ice water. The aqueous layer was extracted by CH₂Cl₂ (2 x 200 ml). After solvent was removed, the residue was precipitated from methanol. The combined white solid was further purified by precipitation from CH₂Cl₂/MeOH (29.000 g, yield 76.5%). m.p. 94-96^oC; Mass: cal. *m/z* for C₃₂H₅₆O₂⁷⁹Br⁸¹Br = 632.26278, C₃₂H₅₆O₂⁷⁹Br₂ = 630.26469, C₃₂H₅₆O₂⁸¹Br₂ = 634.26086, measured (HiRes EI) = 632.26230, 630.26418, 634.26101; $^1\text{H-NMR}$: δ 6.826 (s, 2H), 4.506 (s, 4H), 3.961 (t, 4H, *J* 6.3 Hz), 1.790 (m, 4H), 1.543-1.240

(br, 36H), 0.863 (t, 6H, J 6.9 Hz); $^{13}\text{C-NMR}$: δ 150.65, 127.49, 114.62, 68.99, 31.91, 29.66, 29.63, 29.59, 29.34, 29.32, 28.74, 26.06, 22.68, 14.11

[2,5-Bis(dodecyloxy)-1,4-phenylene]dimethylenebis(triphenylphosphonium-bromide) 12: To a solution of 1,4-bis(bromomethyl)-2,5-didecyloxy-benzene **11** (1.870 g, 2.96 mmol) in absolute CHCl_3 (40 ml) was added PPh_3 (1.552 g, 5.92 mmol). The solution was refluxed for 3 days. After the solution was cooled to room temperature, the solvent was removed under vacuum. The residue was dissolved in minimum THF and then was added to hexane, resulting a white precipitate. The solid was collected by filtration and then was dried under vacuum (2.912 g, 85.0%). m.p. 146°C ; $^1\text{H-NMR}$: δ 7.72 (br, 30H), 6.78(s, 2H), 5.30 (d, 4H, J 13 Hz), 3.05 (t, 4H, J 4.5 Hz), 1.543-1.240 (br, 36H), 0.863 (t, 6H, J 6.9 Hz)

1,4-didecyloxy-2,5-diethynyl-benzene 1: To a degassed solution of 1,4-didecoxy-2,5-bis[(trimethylsilyl)ethynyl]benzene (2.100 g, 4.74 mmol) in methanol (100 ml) was added a saturated NaOH aqueous solution (0.05 ml). The solution was stirred for 1 hour at 50°C . Then the solution was cooled to 0°C and a yellow solid was precipitated. The product was further purified by recrystallization of this solid from methanol to obtain a yellow crystal (1.200 g, 85%). m.p. $106\text{-}107.5^\circ\text{C}$; Mass: m/z cal. for $\text{C}_{34}\text{H}_{54}\text{O}_2 = 494.41237$, measured (HiRes EI) = 494.41165; $^1\text{H-NMR}$: δ 6.909 (s, 2H), 3.925 (t, 4H, J 6.6 Hz), 3.288 (s, 2H), 1.756 (m, 4H), 1.440-1.100 (br, 36H), 0.840 (t, 6H, J 6.9 Hz); $^{13}\text{C-NMR}$: δ 153.34, 117.10, 112.60, 82.08, 79.26, 69.07, 31.35, 29.10, 29.10, 28.79, 28.54, 25.34, 22.14, 13.60

4,4'-Dibromostilbene 2: (a) Wittig Reaction:³⁰ To a round bottom flask equipped with a condenser was charged with 4-bromophenylmethyltriphenylphosphonium bromide (3.072 g, 6 mmol), K_2CO_3 (0.828 g, 6 mmol) and dry THF (25 ml). Then 4-bromobenzaldehyde (0.925 g, 5 mmol) and 18-crown-6 (15 mg) were added. The solution then was refluxed for 2 days. After the solution was cooled to the room temperature, the inorganic salt was removed by filtration and solvent was removed under vacuum. The residue was purified by column chromatography to obtain a white solid (0.900 g, yield 53%).

(b) McMurry Reaction:³¹ To a flame-dried three-necked flask equipped with a magnetic stirring bar, an additional funnel and an argon outlet was added activated Zn (3.923 g, 60 mmol) and THF (80 ml). The mixture was cooled to -10°C , then TiCl_4 (5.7 g, 30 mmol) was added dropwise, resulting in a green-yellow clean solution. The solution was refluxed for 4 hours. The resulting black solution was allowed to cool to room temperature. Then 4-bromobenzaldehyde (3.700 g, 20 mmol) in THF (20 ml) was added. The solution was refluxed overnight, then was allowed to cool to room temperature. To the black mixture was added aqueous K_2CO_3 solution (10%, 160 ml). After stirring for 1 hour, the precipitate was removed by filtration. The filtrate was extracted with ether (300 ml x 2). The organic layer was dried with MgSO_4 . After removal of ether, the residue was purified by column chromatography to obtain a white solid (2.031 g, yield 60.1%).

The *cis*-isomer was transferred to the *trans*-isomer by refluxing the isomer mixture in absolute benzene with a catalytic amount of iodine for 8 hours.³³ Mass: cal. *m/z* for $\text{C}_{14}\text{H}_{10}^{79}\text{Br}^{81}\text{Br} = 337.91301$, $\text{C}_{14}\text{H}_{10}^{79}\text{Br}_2 = 335.91492$, $\text{C}_{14}\text{H}_{10}^{81}\text{Br}_2 = 339.91067$, measured (HiRes EI) = 337.91248, 335.91423, 339.91067, respectively; $^1\text{H-NMR}$: 7.461 (d, 4H, *J* 8.4 Hz), 7.342 (d, 4H, *J* 8.4 Hz), 6.997 (s, 2H)

1,2-di-(4-bromo-phenyl)-1-cyano-ethene 3: This compound was prepared by a Knoevenagel condensation.^{24(a)} To a solution of 4-bromobenzaldehyde (0.925 g, 5 mmol) and 4-bromophenylacetonitrile (0.980 g, 5 mmol) in *t*-BuOH (100 ml) was added a solution of KO-*t*-Bu (0.672 g, 6 mmol) in *t*-BuOH (25 ml) at 55°C . The mixture was stirred at 55°C for 3 hours. After the mixture was cooled, hydrochloric acid (1 M, 50 ml) and water (50 ml) were added. The aqueous layer was extracted with CH_2Cl_2 (100 ml x 2). The combined organic layer was washed with water (50 ml x 2), dried with MgSO_4 . After solvent removed, the product was purified by crystallization from hexane to get a white solid (1.230 g, yield 68%). m.p. $126-128^{\circ}\text{C}$; Mass: *m/z* cal. for $\text{C}_{15}\text{H}_9\text{N}^{79}\text{Br}^{81}\text{Br} = 362.90826$, $\text{C}_{15}\text{H}_9\text{N}^{79}\text{Br}_2 = 360.91017$, $\text{C}_{15}\text{H}_9\text{N}^{81}\text{Br}_2 = 364.90634$, measured (HiRes EI) = 362.90816, 360.91013, 364.90608; $^1\text{H-NMR}$: δ 7.708 (d, 2H, *J* 8.4 Hz), 7.561 (d, 2H, *J* 8.4 Hz), 7.536 (d, 2H, *J* 8.1

Hz), 7.488 (d, 2H, *J* 8.1 Hz), 7.408 (s, 1H); ¹³C-NMR: δ 141.0, 132.6, 131.9, 131.8, 130.4, 127.2, 124.8, 123.3, 117.0, 110.8

1,4-Bis[2-(4-halophenyl)-2-trifluoromethyl-vinyl]-2,5-bis(dodecyloxy)benzene 4:

The product was prepared by a similar procedure according to the literature.³⁶ The mixture of 4'-halo-2,2,2-trifluoroacetophenone³⁵ (2.024 g, 8 mmol), [2,5-bis(dodecyloxy)-1,4-phenylene]-dimethylene-bis(triphenylphosphoniumbromide) 12 (4.626 g, 4 mmol), KF (9.28 g, 160 mmol) and dibenzo-18-crown-6 (0.8 mmol, 0.31 mg) in CH₃CN (140 ml) was stirred at 70-80°C for 5 hours. Then after the solvent was removed, CH₂Cl₂ was added to dissolve product. KF was removed by filtration. After most of CH₂Cl₂ was removed, the product was precipitated out by adding CH₂Cl₂ solution into MeOH. 4(a): X = Br, a yellow solid (2.763 g, yield 74.0%). m.p. 85-87°C; Mass: *m/z* cal. for C₄₈H₆₂⁷⁹Br⁸¹BrF₆O₂ = 944.30015, measured (GC-MS): 944 (M⁺) (100%), 942 (M⁺ for C₄₈H₆₂⁷⁹Br₂F₆O₂) (39%), 496 (M⁺ for C₄₈H₆₂⁸¹Br₂F₆O₂) (30%); ¹H-NMR: δ 7.507 (d, 4H, *J* 8.1 Hz), 7.454 (d, 2H, *J* 1.5 Hz), 7.145 (d, 4H, *J* 8.1 Hz), 6.108 (s, 2H), 3.239 (t, 4H, *J* 6.6 Hz), 1.554 (m, 4H), 1.258 (br, 36H), 0.863 (t, 6H, *J* 6.6 Hz); ¹³C-NMR: δ 150.0, 131.6, 131.4, 131.0, 127.2, 122.8, 122.4, 112.8, 67.9, 31.2, 28.9(2), 28.8, 28.6, 28.5, 28.2, 25.1, 22.0, 13.4; 4(b): X = I, a yellow solid (4.152g, yield 74.4%). m.p. 91-93°C; Mass: *m/z* for C₄₈H₆₂F₆I₂O₂ = 1038.27434, measured (GC-MS): 1038 (M⁺) (100%), 912 (M⁺-I) (31%) 869 (18%), 702 (27%), 71 (22%), 69 (26%), 57 (72%); ¹H-NMR: δ 7.703 (d, 4H, *J* 8.1 Hz), 7.434 (d, 2H, *J* 1.5), 7.005 (d, 4H, *J* 8.1 Hz), 6.093 (s, 2H), 3.222 (t, 4H, *J* 6.6 Hz), 1.555 (m, 4H), 1.294 (br, 36H), 0.853 (t, 6H, *J* 6.6 Hz); ¹³C-NMR: δ 149.84, 137.38, 131.84, 130.60, 126.95, 122.66, 112.65, 93.89, 67.75, 31.03, 28.69(2), 28.46, 28.09, 25.09, 21.82, 13.27

2,5-Bis(dodecyloxy)-1,4-bis[2-(5-bromo-2-thienyl)vinyl]benzene 6: The product was synthesized by a similar procedure in the literature.³³ [2,5-Bis(dodecyloxy)-1,4-phenylene]dimethylene-bis(triphenylphosphoniumbromide) 12 (2.313 g, 2 mmol) and 4-bromo-2-thiophenecarbaldehyde were dissolved in benzene (50 ml). Then KO-t-Bu (0.749 g, 6.7 mmol) was added. The solution was refluxed for 24 hours. The solvent was removed,

and H₂O (30 ml) and CH₂Cl₂ (30 ml) were added. The aqueous layer was extracted with CH₂Cl₂ (30 ml x 2). The combined organic layer was washed with H₂O, dried with MgSO₄. After CH₂Cl₂ was removed, the product was purified by precipitation from THF/MeOH twice to obtain a yellow solid (0.710 g, yield 43%). m.p. 75-78⁰C; Mass: *m/z* for C₄₂H₆₀⁷⁹Br⁸¹BrO₂S₂ = 820.23822, measured (GC-MS): 820 (M⁺) (100%), 818 (M⁺ for C₄₂H₆₀⁸¹Br₂O₂S₂) (16%), 822 (M⁺ for C₄₂H₆₀⁷⁹Br₂O₂S₂) (18%), 742 (13%), 740 (13%), 322 (17%), 321 (66%), 320 (17%), 97 (18%), 82 (12%), 71 (37%), 69 (20%), 57 (100%); ¹H-NMR: δ 7.132 (s, 2H), 7.116 (s, 2H), 6.952 (s, 2H), 6.925 (d, 2H, *J* 3.8 Hz), 6.761 (d, 2H, *J* 3.8 Hz), 3.986 (t, 4H, *J* 6.3 Hz), 1.831 (m, 4H, *J* 6.9 Hz), 1.553-1.252 (br, 36H), 0.866 (t, 6H, *J* 6.6 Hz); ¹³C-NMR: δ 150.4, 144.8, 129.9, 125.5, 125.4, 123.1, 121.1, 110.4, 110.0, 68.9, 31.3, 29.0(2), 28.8, 28.7, 25.6, 22.1, 13.5

2',5'-Bis(dodecyloxy)-p-terphenyl-1,4''-dicarboxaldehyde 13: To an aqueous Na₂CO₃ solution (2 M, 75 ml) was added a solution of o-formylphenylboronic acid⁴⁰ (1.80 g, 12 mmol) and 2,5-bis(dodecyloxy)-1,4-diiodobenzene (2.30 g, 3 mmol) in DME (75 ml), followed by addition of Pd(PPh₃)₄ (346 mg). The mixture was refluxed for 2 days. After mixture was allowed to cool to room temperature, the aqueous layer was separated and was extracted by CH₂Cl₂ (100 ml x 2). The combined organic layer was washed with water, dried with MgSO₄. After the solvent was removed, the product was precipitated from THF/MeOH twice to obtain a yellow solid (1.00 g, yield 51%). m.p. 86-90⁰C; Mass: *m/z* cal. for C₄₄H₆₂O₄ = 654.97388, measured (HiRes EI) = 654,97346; ¹H-NMR: δ 10.049 (s, 2H), 7.240 (d, 4H, *J* 8.4 Hz) 7.600 (d, 4H, *J* 8.4 Hz), 6.993 (s, 2H), 3.929 (t, 4H, *J* 6.3 Hz), 1.677 (m, 4H, *J* 6.9 Hz), 1.413- 1.229 (br, 36H), 0.858 (t, 6H, *J* 6.3 Hz); ¹³C-NMR: δ 191.0, 149.1, 143.4, 133.8, 129.0(2), 128.3, 114.6, 68.4, 30.7, 28.5, 28.4, 28.2, 28.1, 24.9, 21.5, 13.0

1,4''-Bis[2-(4-bromophenyl)vinyl]-2',5'-bis(dodecyloxy)-p-terphenyl 7: KO-t-Bu (0.596 g, 5.32 mmol) was added a refluxing compound 13 solution (0.620 g, 0.95 mmol) and 4-bromophenylmethyltriphenylphosphonium bromide (1.460 g, 2.85 mmol) in benzene (25 ml). The mixture was refluxed for 1 day. After the solution was cooled to room temperature,

CH₂Cl₂ (25 ml) and a saturated NH₄Cl solution (25 ml) were added. The aqueous layer was extracted by CH₂Cl₂ (25 ml). The combined organic layer was washed with water and dried with MgSO₄. After the solvent was removed, the product was precipitated twice from THF/MeOH to obtain a yellow solid (0.50 g, yield 55%). m.p. 155-160^oC; Mass: *m/z* for C₅₈H₇₂⁷⁹Br⁸¹BrO₂ = 960.35887, measured (GC-MS): 960 (M⁺) (100%), 962 (M⁺ for C₅₈H₇₂⁸¹Br₂O₂) (16%), 958 (M⁺ for C₅₈H₇₂⁷⁹Br₂O₂) (18%); ¹H-NMR: δ 7.611 (d, 4H, *J* 8.1 Hz), 7.539 (d, 4H, *J* 8.1 Hz), 7.473 (d, 4H, *J* 8.7 Hz), 7.383 (d, 4H, *J* 8.7 Hz), 7.112 (s, 2H), 7.086 (s, 2H), 6.991 (s, 2H), 3.914 (t, 4H, *J* 6.3 Hz), 1.675 (m, 4H), 1.541-1.219 (br, 36H), 0.854 (t, 6H, *J* 6.9 Hz); ¹³C-NMR: δ 149.8, 137.4, 135.8, 135.0, 131.3, 129.7, 129.3, 128.7, 127.5, 126.7, 125.6, 120.7, 115.4, 69.1, 31.3, 29.0(2), 28.8, 25.5, 22.1, 13.6

1,4''-Bis[2-(4-bromophenyl)-2-cyano-vinyl]-2',5'-bis(dodecyloxy)-p-terphenyl 8:

To a solution of compound 13 (0.580 g, 0.89 mmol) and 4-bromophenyl-acetonitrile (0.452 g, 2.30 mmol) in t-BuOH (10 ml) and THF (10 ml) was added a KO-t-Bu solution in t-BuOH (10 ml) at room temperature dropwise. The mixture was stirred at 55^oC for 4 hours. Then solvent was removed by evaporation under vacuum. CH₂Cl₂ (50 ml) was added. The organic layer was washed with H₂O and dried with MgSO₄. After removal of CH₂Cl₂, the product was precipitated from THF/MeOH to obtain a light yellow solid (0.750 g, yield 84.3%). m.p. 126-127^oC; Yellow color luminescence in THF; Mass: *m/z* for C₆₀H₇₀⁷⁹Br⁸¹BrN₂O₂ = 1010.37847, measured (GC-MS): 1010 (M⁺) (9%), 1012 (M⁺ for C₆₀H₇₀⁸¹Br₂N₂O₂) (5%), 1008 (M⁺ for C₆₀H₇₀⁷⁹Br₂N₂O₂) (4%), 676 (13%), 675 (13%), 674 (26%), 673 (13%), 594 (4%), 321 (5%), 71 (31%), 69 (36%), 57 (83%), 44 (100%); ¹H-NMR: δ 7.950 (d, 4H, *J* 8.7 Hz), 7.722 (d, 4H, *J* 8.4 Hz), 7.566 (s, 8H), 7.552 (s, 2H), 7.011 (s, 2H), 3.944 (t, 4H, *J* 6.6 Hz), 1.705 (m, 4H), 1.358-1.216 (br, 36H), 0.841 (t, 6H, *J* 6.9 Hz); ¹³C-NMR: δ 149.72, 141.92, 140.28, 132.91, 132.51, 131.67, 131.36, 129.44, 128.51, 125.96, 122.72, 117.15, 115.14, 109.28, 86.02, 68.98, 31.26, 29.02, 28.93, 28.70, 28.62, 25.41, 22.04, 13.50

Polymer 14-20: Polymerization was performed by Heck coupling according to the literature.^{25(d)} The monomers (1 mmol of each), palladium chloride (19.4 mg), copper acetate

(3.3 mg) triphenylphosphine (117 mg), triethylamine (50 ml) and THF (20 ml), all dried and degassed, were put into a two-necked 150 ml flask equipped with a magnetic stirrer and a condenser. The reaction mixture was refluxed for 3 days. The precipitated ammonium salt was filtered off and washed with THF. The solvent was removed, the residue was dissolved in hot THF (3 ml), poured into cold methanol (200 ml) to precipitate. The product was collected by filtration. The polymer was further purified by precipitation from MeOH/THF twice or more and dried under vacuum.

Polymer 14: Yield 92.5%; A yellow solid; $^1\text{H-NMR}$: δ 7.507, 7.114, 7.054, 4.030, 1.085, 1.547-1.244, 0.857; $^{13}\text{C-NMR}$: δ 152.58, 135.95, 130.95, 127.64, 125.61, 121.69, 115.78, 112.93, 94.07, 86.15, 68.61, 30.92, 28.65, 28.40, 25.09, 21.70, 13.16; GPC: $M_n = 3.50 \times 10^3$, $M_w = 8.53 \times 10^3$, PD = 2.438; UV/Vis: $\lambda_{\text{max}} = 414$ nm (THF), 458 nm (film)

Polymer 15: Yield 89.0%; A yellow solid; $^1\text{H-NMR}$: δ 7.865-7.844, 7.638-7.495, 7.002, 6.965, 3.990, 1.813, 1.500, 1.208, 0.823; $^{13}\text{C-NMR}$: δ 153.21, 131.60, 128.92, 125.43, 117.11, 116.30, 113.38, 110.73, 94.22, 88.50, 87.80, 69.14, 31.49, 29.22, 25.63, 22.27, 13.72; GPC: $M_n = 4.05 \times 10^3$, $M_w = 8.70 \times 10^3$, PD = 2.145; UV/Vis: $\lambda_{\text{max}} = 428$ nm (THF), 486 nm (film)

Polymer 16: For X = Br, yield = 75.4%; A yellow solid; GPC: $M_n = 1.24 \times 10^4$, $M_w = 2.47 \times 10^4$, PD = 1.983; UV/Vis: $\lambda_{\text{max}} = 382$ nm (THF); For X = I, yield = 90.2%; A yellow solid; GPC: $M_n = 6.36 \times 10^3$, $M_w = 9.84 \times 10^3$, PD = 1.546; UV/Vis: $\lambda_{\text{max}} = 384$ nm (THF), 427 nm (film); $^1\text{H-NMR}$: δ 7.521, 7.468, 7.281, 6.970, 4.001, 3.264, 1.830, 1.533, 1.403-1.218, 0.842; $^{13}\text{C-NMR}$: δ 152.96, 150.06, 132.33, 131.32, 129.31, 123.42, 122.95, 115.95, 113.13, 112.87, 93.38, 86.65, 68.75, 67.95, 31.21, 28.95, 25.38, 25.13, 21.99, 13.41

Polymer 17: Yield 90.0%; A brown solid; $^1\text{H-NMR}$: δ 7.258, 7.248, 7.165, 7.019, 6.983, 6.961, 4.029, 1.861, 1.59-1.256, 0.873; $^{13}\text{C-NMR}$: δ 152.27, 149.81, 144.47, 124.95,

123.20, 120.65, 116.42, 115.22, 112.63, 109.43, 89.83, 87.74, 68.44, 30.76, 28.49, 28.26, 24.90, 24.91, 21.55, 13.02; GPC: $M_n = 6.48 \times 10^3$, $M_w = 8.92 \times 10^3$, DP = 1.377; UV/Vis: $\lambda_{max} = 472$ nm (THF), 499 nm (film)

Polymer 18: Yield 91.1%; A yellow solid; $^1\text{H-NMR}$: δ 7.60, 7.04, 4.05, 1.85, 1.56, 1.23, 0.85; $^{13}\text{C-NMR}$: δ 153.21, 139.5, 131.64, 126.35, 122.32, 116.43, 113.55, 94.33, 86.59, 69.20, 31.49, 29.23, 25.67, 22.26, 13.70; GPC: $M_n = 3.15 \times 10^3$, $M_w = 4.58 \times 10^3$, PD = 1.451; UV/Vis: $\lambda_{max} = 396$ nm (THF), 432 nm (film)

Polymer 19: Yield 65.5%; A yellow solid; $^1\text{H-NMR}$: δ 7.59, 7.13, 7.02, 4.04, 3.94, 1.85, 1.71, 1.58, 1.25, 0.87; $^{13}\text{C-NMR}$: δ 152.88, 149.89, 137.14, 135.59, 131.45, 130.92, 129.39, 127.51, 125.83, 116.07, 115.58, 95.74, 86.64, 69.19, 31.47, 25.61, 22.24, 13.68; GPC: $M_n = 4.05 \times 10^3$, $M_w = 8.7 \times 10^3$, DP = 2.145; UV/Vis: $\lambda_{max} = 378$ nm (THF), 412 nm (film)

Polymer 20: Yield 66.0%; A yellow solid; $^1\text{H-NMR}$: δ 7.961, 7.719, 7.607, 7.025, 4.031, 3.956, 1.846, 1.716, 1.596, 1.229, 0.847; $^{13}\text{C-NMR}$: δ 152.94, 149.65, 141.58, 140.21, 133.36, 131.47, 129.35, 128.47, 125.18, 123.80, 117.20, 116.10, 115.08, 113.24, 109.71, 93.60, 87.23, 68.922, 31.20, 28.93, 25.35, 21.98, 13.47; GPC: $M_n = 1.36 \times 10^4$, $M_w = 7.74 \times 10^4$, PD = 5.707; UV/Vis: $\lambda_{max} = 416$ nm (THF), 472 nm (film)

II: SYNTHESIS, CHARACTERIZATION AND STUDY OF CONJUGATED POLYMERS CONTAINING SILOLE UNIT IN THE MAIN CHAIN

Literature Survey

Since the discovery in 1977⁴⁹ that polyacetylene (PA) could be n- or p-doped, either chemically or electrochemically, to nearly the metallic state, the development of the field of conducting polymers has continued to accelerate at a rapid rate.⁹ This rapid growth has been stimulated not only by the field's synthetic novelty and multi-disciplinary importance but also by its actual and potential technological application.⁵⁰

One of the fundamental challenges of the field of conducting polymers is the design and synthesis of low bandgap polymer. These low bandgap polymers can have good intrinsic conductivity without doping, good nonlinear optical and photoelectric properties and amphoteric electrochemical characteristics. The electronic and optical properties of conjugated polymers originate mostly from their π -electrons. In the simplest case of a linear chain, the band gap is proportional to the bond length alternation due to the Peierls instability in 1D. The bond length alternation (δr) is defined as the average of the difference between neighboring long and short C-C bonds. Polyacetylenes, which have the lowest bond length alternation, are the most conductive polymers. However, due to their poor environmental stabilities, more attentions are paid to design and synthesis of environmentally stable conjugated polymers with band gap energy lower than 1 eV. Heterocyclic five-membered ring systems (Figure 18) such as polypyrroles, polythiophenes, are of most interest because of their high stability and conductivity. The band gaps (E_g) of heterocyclic five-membered ring systems are determined by both geometrical and heteroatomic effects.^{56,57} In polythiophene, for example, the sulfur changes the bond length by locking in planarity of the butadiene unit. At the same time, the lone pair of electrons on sulfur strongly participates in the aromaticity of the ring. In 1987, Kertesz et al. calculated the effect of the heteroatomic substitutions on the band gap of polyacetylene.^{56(a)} The bond length alternation (δr) of polythiophene was shown to actually be smaller than the δr of polyacetylene (see Table 7). However, due to the orbital

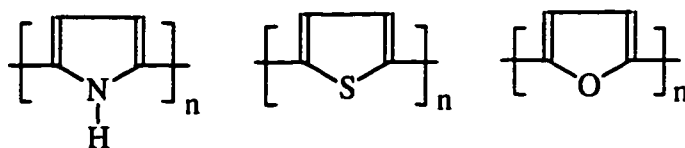


Figure 18: Heterocyclic five-membered ring systems

symmetry, only the LUMO of the backbone can interact with the $3p_z$ orbital of sulfur, which shifts the LUMO level upward by 0.89 eV, but leaves almost unchanged HOMO level. Thus, the main effect of sulfur in the aromatic ring is to enlarge E_g .^{56, 78}

In 1989, our group re-examined the thermal polymerization of diethynyldiphenylsilane and the catalytic polymerization of diethynylsilane with MoCl_5 or WCl_6 was studied, which gave a deep red polymer and a violet polymer respectively.⁵¹ The resulting polymer was first suggested by Shinar to be polysilole (PS) (Figure 19).⁵¹ However, one year later, the structure was described as polydiethynylsilane (PDS) having a four-membered backbone ring (Figure 19).^{52(a)} This four-membered structural model is supported by ^{13}C - and ^{29}Si -NMR and resonance Raman scattering measurements,^{52(b, c)} and by some ab initio Hartree-Fock calculations of the backbone structure.⁵³ The violet polymer, which has a very low bandgap energy value of 2.0 eV, is conductive upon doping with I_2 vapor with conductivity of 10^{-1} S/cm. The non-linear $\chi^{(3)}$ value at 625 nm was measured to be 3×10^{-9} esu, one of the largest measured in conjugated polymers.

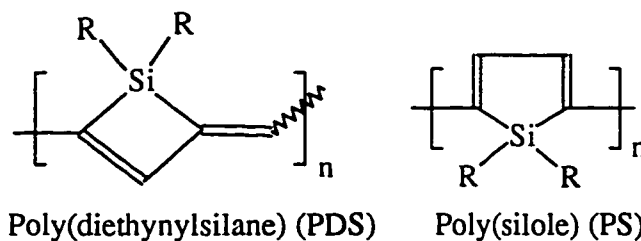


Figure 19: The structures of poly(diethynylsilane) and polysilole

In the course of elucidate the structure of PDS, several groups calculated both polysilole and poly(diethynylsilane)^{53, 54, 55} to compare with polyacetylene and other heterocyclic five-membered rings (see Figure 20).^{53, 54, 55, 56} In contrast to the heteroatoms in those heterocyclic five-membered ring systems which were studied, silicon (in PD and PDS) doesn't have a lone pair of electrons to interact with the conjugated π -orbitals of the systems.

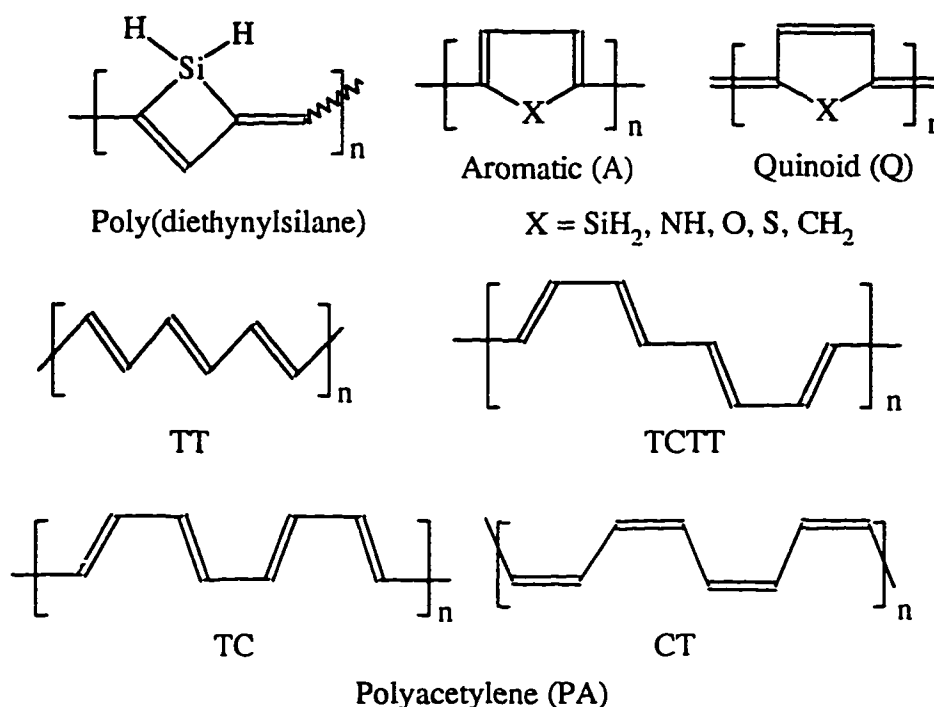


Figure 20: Conformation of PS, PDS, PA and other heterocyclic ring systems

In 1992, the calculations by Frapper et al. showed that 3p silicon orbitals do not participate in the conjugation because of their sp^3 hybrid states, and therefore the π -electron system is similar to that of polyacetylene.^{54(a)} Table 7 gives the calculated bond alternation and bandgap energies of acetylene isomers, poly(diethynylsilane) and polysilole. Both PS and PDS have very low bandgap energies, and are good candidates for high intrinsic conductive materials.

A surprising result, found by Grigoras et al.^{53, 54} and Frapper et al.,^{54(a, b)} indicated that while both aromatic and quinoid structures of polysilole are more stable by about 15-20

kcal/mol than that of poly(diethynylsilane) due to the four-membered ring strain, the quinoid structure of polysilole is only slightly more stable than its “aromatic” structure by 2 kcal/mol-ring (Figure 20). In 1995, Dr. Hong et al. calculated the conformation and electronic structures of poly(cyclopentadienylene) (PPD) (Figure 20, X = CH₂) and polysilole.⁵⁵ The calculation confirmed that the ground state geometries of polysilole (Figure 20, X = SiH₂, SiF₂) and poly(cyclopentadienylene) (Figure 20, X = CH₂, CF₂) are quinoid conformations. The bridging groups affect the band gaps in two principle ways: by decreasing the C1-C4 distance and by pure electronic effects. The large δr values of both PS, PPD and PDS compared to the δr values for PT, PPy and PF imply that the CH₂, SiH₂ bridging groups interact with the polymeric backbone less strongly than do the heteroatoms, S, N and O.

Recently, Bakhshi et al. designed novel donor-acceptor polymers which contained silole backbones, and calculated their bandgap energies.⁵⁷ They were found to have very low

Table 7: Bond alternation and bandgap energy

	Polyacetylene ^{54(a)}				Polythiophene ⁵⁶		Polypyrrole ⁵⁶	
	TT	TCTT	TC	CT	(A)	(Q)	(A)	(Q)
δr	0.105	0.102	0.100	0.106	0.062	0.114	0.030	0.105
E_g	1.80	1.52	1.29	2.18	2.51	0.47	3.18	1.31

	Polyfuran ⁵⁶		Polysilole ^{55(b)}		Poly(cyclopentadienylene) ^{55(b)}		Poly(diethynyl silane) ^{54(a)}
	(A)	(Q)	(A)	(Q)	(A)	(Q)	
δr	0.046	0.113	0.082	0.114	0.068	0.119	1.106
E_g	2.93		1.14	1.93	1.21	1.72	1.99

δr : Bond alternation, in angstroms; E_g : Bandgap energy, in eV

bandgap energies. The principal idea behind donor-acceptor polymers is that a regular alternation of conjugated donor- and acceptor-like moieties in a conjugated chain will induce a low bandgap. The designed polymers (Figure 21) can be viewed as analogues of *trans-cisoid* polyacetylene (*cis*-PA), but stabilized by different bridging groups (X as an electron donor and Y as an electron acceptor). Although these are not known polymers, they are calculated to have bandgaps lower than 1 eV.

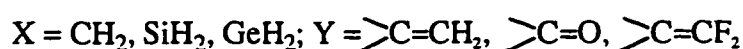
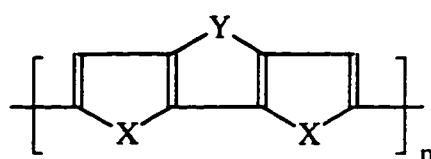


Figure 21: The structure of donor-acceptor polymers

Because PS and PDS are much similar to polyacetylene, they should exhibit higher second order hyperpolarizabilities like PA. In 1992, Grigoras et al. calculated the second-order hyperpolarization $\langle\gamma\rangle$ of model structures of PS, PDS, PA and PDA (Figure 22) and found that PS and PDS have comparative $\langle\gamma\rangle$ values to PA.⁵³

In 1995, Matsuzaki et al. calculated the longitudinal second hyperpolarizabilities (γ_{zzz}) of both aromatic and quinoid forms of PS and PDS, as well as PA (with polymerization degree n up to 8) by the finite field (FF) method, including electron correlation at the level of the Moller-Plesset second-order perturbation theory (MP2).⁵⁸ It is surprising that PS shows the largest γ_{zzz} value among the π -conjugated polymers and the strongest n -dependence (n is degree of polymerization) of γ_{zzz} .

Up to now polysilole have not been synthesized yet. The most straight forward route to polysilole would be the direct coupling of silole monomers at 2,5-position, which requires two functional groups such as Li, Br, SnR_3 at the 2,5-position. The synthesis and organic chemistry of silole have been recently reviewed.⁵⁹ The conventional methods to synthesize the siloles include direct or indirect dehydration of silacyclopent-4-en-3-ol (Scheme 10), a

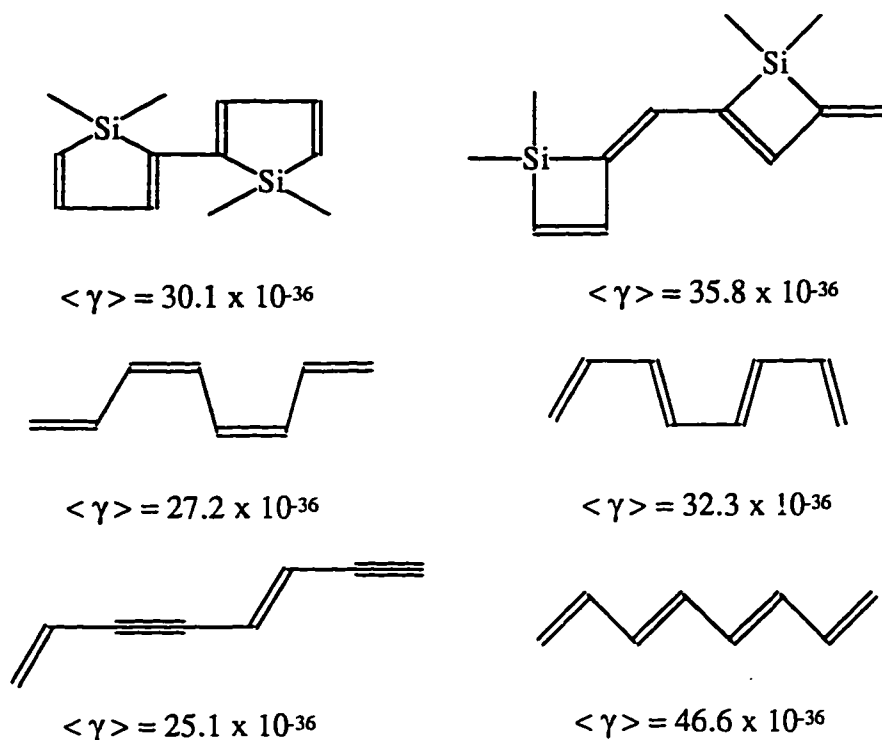
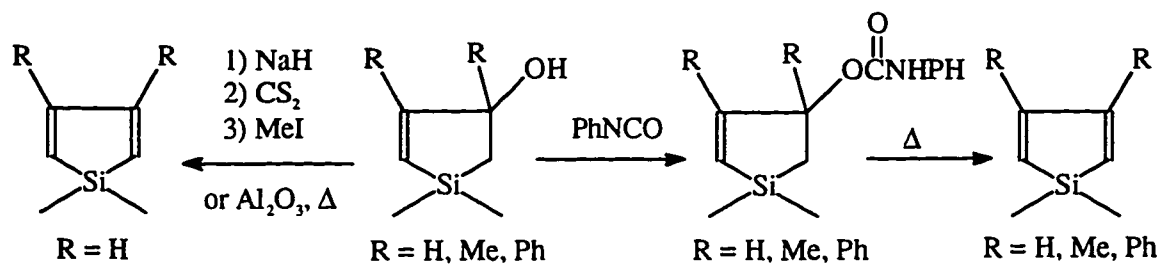
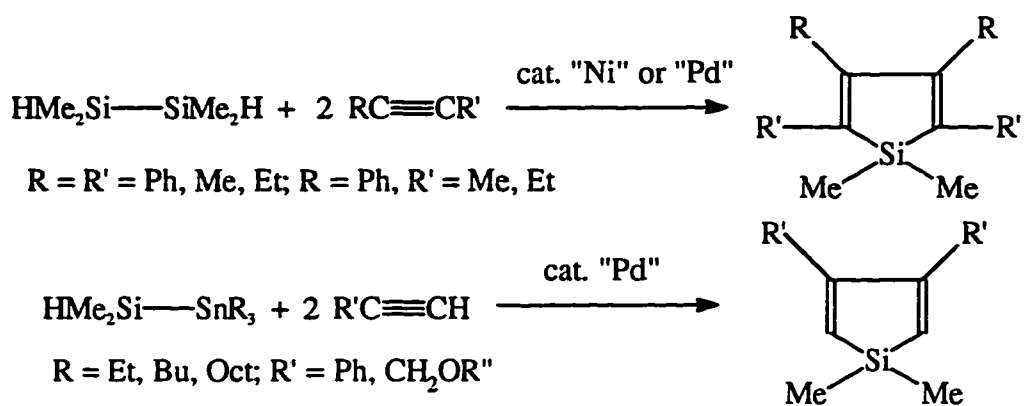
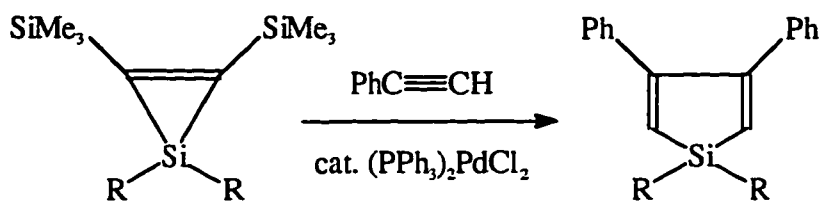
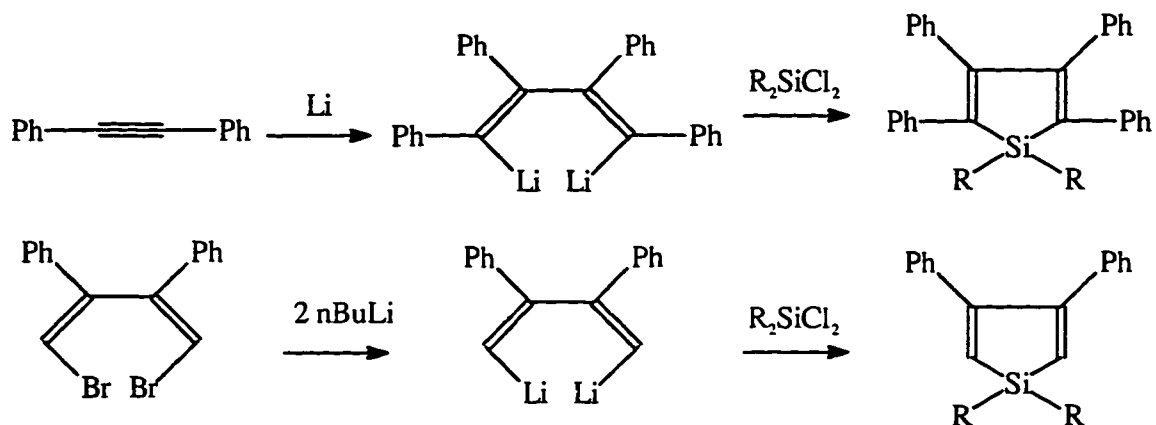


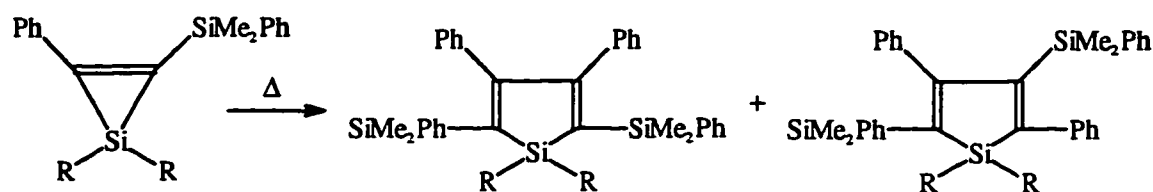
Figure 22: Structures considered for the estimation of second-order polarizability (e.s.u)

reaction between an alkyne and a disilane or a stannylsilane (Scheme 11), cyclization of 1,4-dilithio-1,3-butadienes with a polyfunctional compound R_nSiX_{4-n} ($n = 0-2$) (Scheme 12), a reaction of an alkyne and a silirene (Scheme 13), thermolysis of silirenes (Scheme 14), dehydrogenation of 1,1-dialkyl-2,5-diphenylsilacyclopentane (Scheme 15), dehydrohalogenation (Scheme 16), flash vacuum pyrolysis of 1-allylsilacyclopent-3-enes (Scheme 17), and other methods.⁵⁹ None of these methods gives a 2,5-difunctional silole.

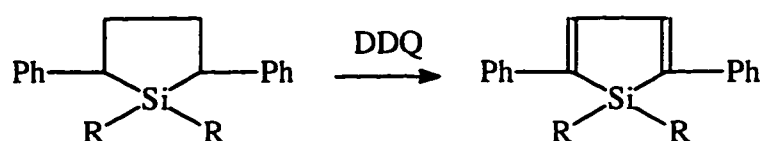


Scheme 10: Dehydration of silacyclopent-4-en-3-ol⁵⁹

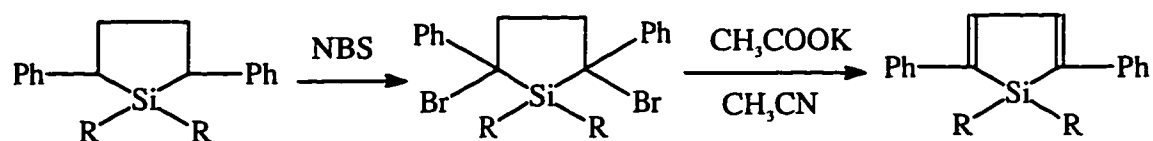
Scheme 11: Reaction between an alkyne and a disilane⁵⁹Scheme 12: Reaction between an alkyne and a silirene⁵⁹Scheme 13: Cyclization of 1,4-dilithio-1,3-butadienes⁵⁹



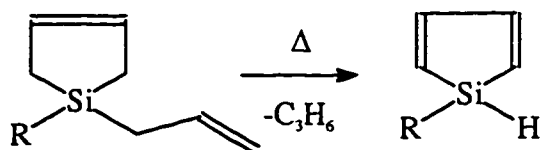
Scheme 14: Thermolysis of a silirene⁵⁹



Scheme 15: Dehydrogenation of 1,1-dialkyl-2,5-diphenylsilacyclopentane⁵⁹

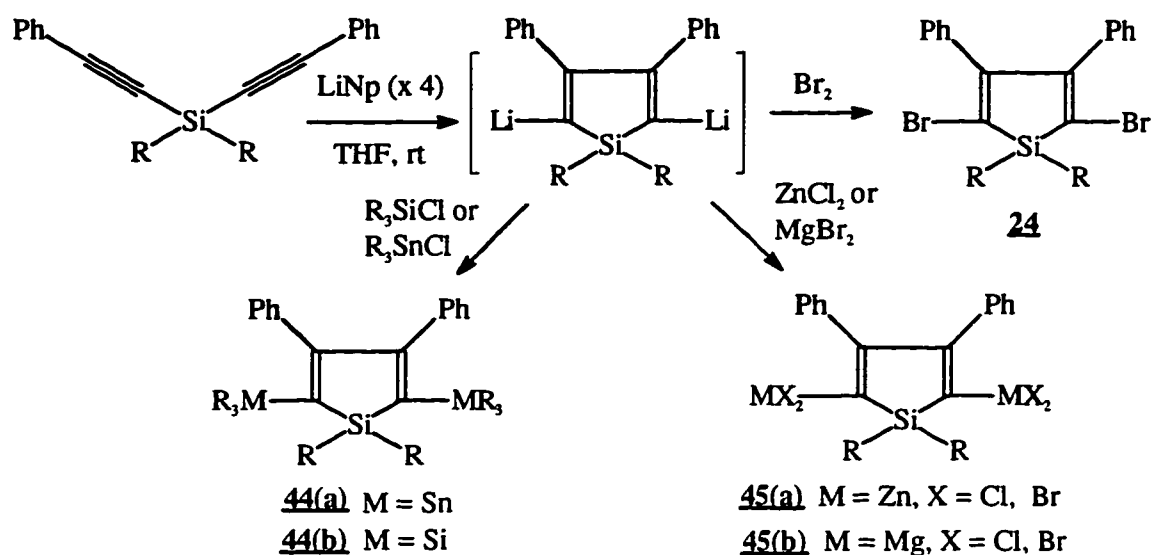


Scheme 16: Dehydrohalogenation⁵⁹



Scheme 17: Flash vacuum pyrolysis of 1-allylsilacyclopent-3-ene⁵⁹

In 1994, Tamao et al. first reported the synthesis of a 2,5-difunctional silole (Scheme 18).⁶⁰ They found that diethynylsilane undergo intramolecular reductive cyclization upon treatment with lithium naphthalenide to form 2,5-dilithiosilole, which could be quenched by electrophiles such as Br_2 , R_3SnCl or R_3SiCl . This first reported *endo-endo* mode of reductive cyclization could be rationalized by the crucial bis(anion radical) intermediate being stabilized by the phenyl and silicon (Figure 23).



Scheme 18: Synthesis of 2,5-difunctional silole^{60(a)}

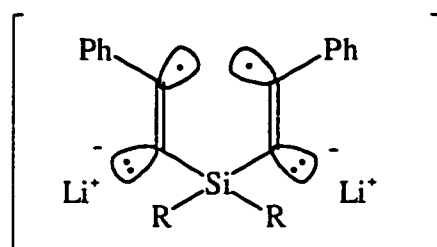
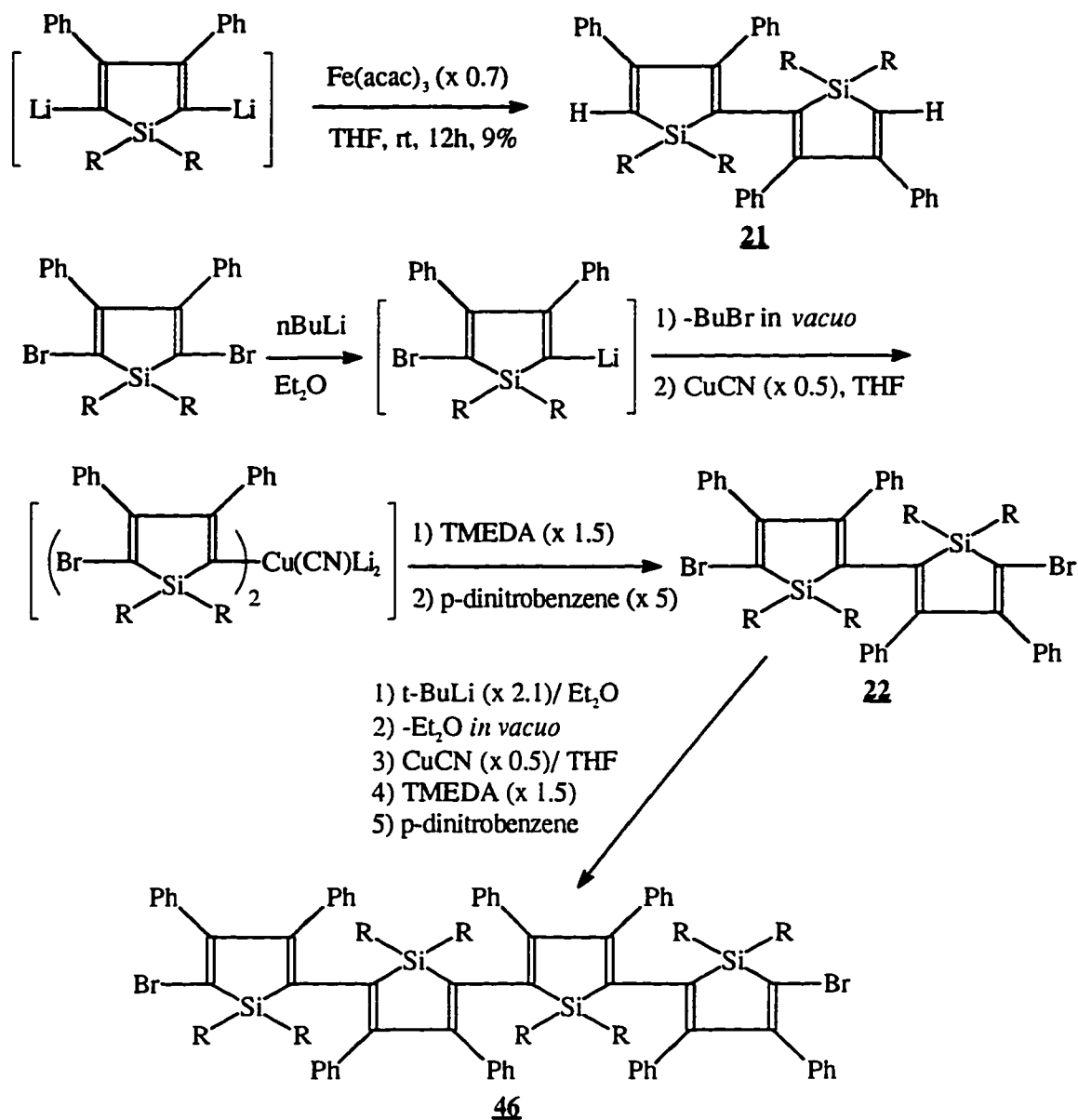


Figure 23: Bis(anion radical) species

However, the attempted polymerization of these 2,5-bifunctional siloles under a variety of conditions (including homocoupling of 2,5-dilithiosilole with Fe(III), Ni(II), Cu(II) etc., homocoupling of 2,5-dibromosilole **24** with 2,5-bisstannylsilole **44(a)**, magnesium reagent **45(b)** or zinc reagent **45(a)** in the presence of nickel or palladium catalyst), were unsuccessful. Large steric hindrance due to the phenyl group at 3,4-positions of silole and an inherent low reactivity at 2,5-positions of silole may be responsible for these failures. The low reactivity at 2,5-positions of silole may be exemplified by the fact that the silyl groups thereon could not be desilylated by a variety of electrophiles.⁶⁰ However, the dimer, 3,3',4,4'-tetraphenyl-2,2'-bisilole **21** or 5,5'-dibromo-3,3',4,4'-tetraphenyl-2,2'-bisilole **22**, and tetramer,

dibromoquatersilole **46**, of silole were synthesized by oxidative coupling of lithiosiloles via higher order cyanocuprate or with tris(acetylacetonato)iron(III) (Scheme 19).

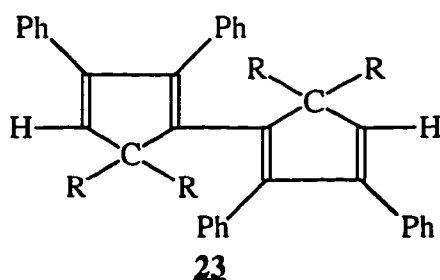


Scheme 19: Synthesis of dimer and tetramer of silole^{60(a)}

Bisilole **21** and dibromosilole **22** have unusually long UV/Vis absorption with λ_{max} of 398 nm and 417 nm (in chloroform), respectively. For comparison, a carbon analog,

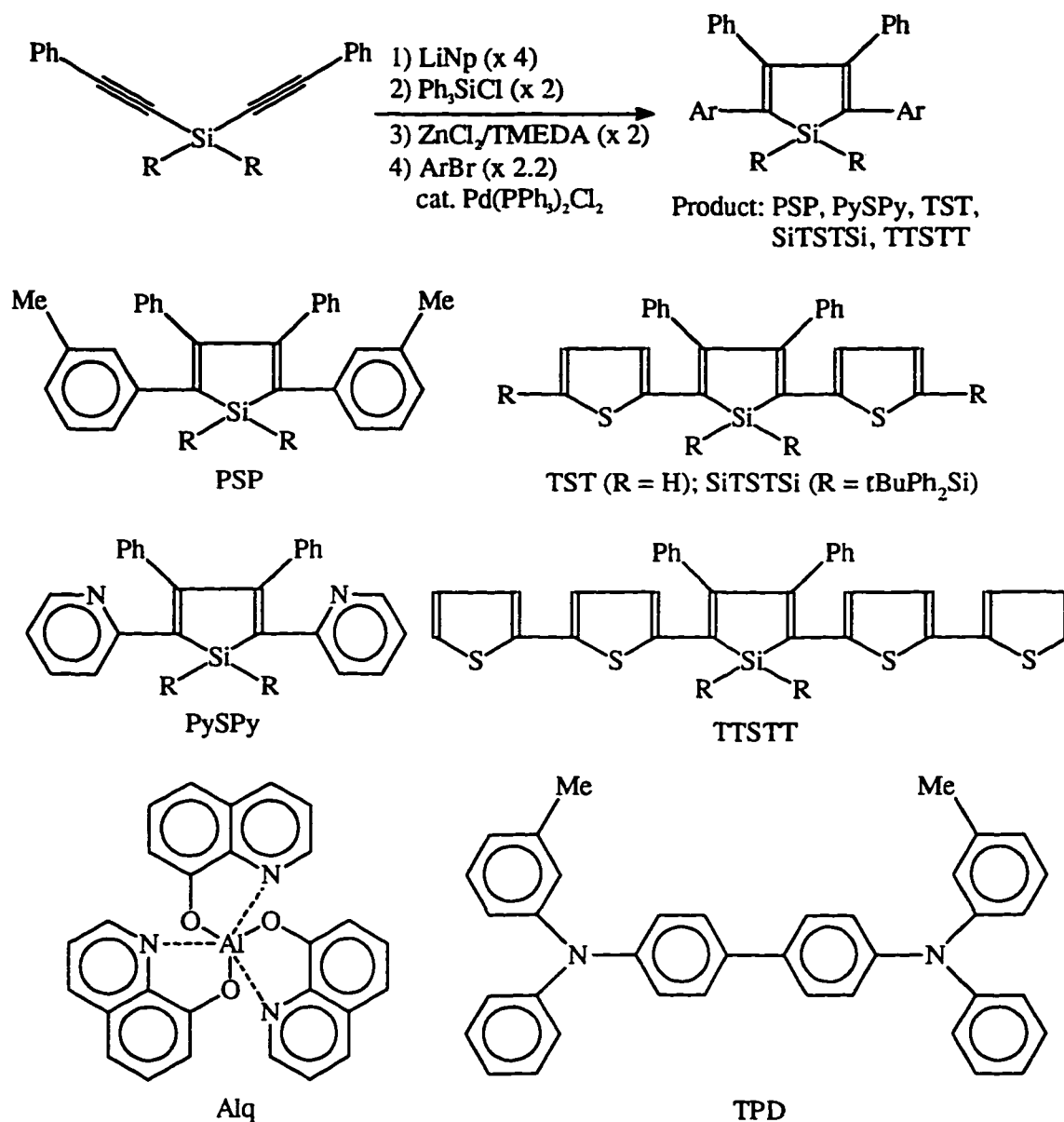
2,2',3,3'-tetraphenyl-1,1''-bicyclopentadiene **23** was synthesized by a similar route to bisilole by the same group two years later.^{61(a)} It is surprising, considering their twisted conformations, that values of λ_{\max} of bisiloles are the longest of those of nonfused two-ring π -conjugated compounds (Table 8). The difference in λ_{\max} between **21** and **23** is 58 nm. Recently, the theoretical calculations were carried out to explain this difference.⁶² It was found that the origin of the unusually optical properties was the low-lying LUMO level of the bisilole, arising from σ^* - π^* conjugation between a π -symmetry σ^* orbital of exocyclic σ bonds on silicon and a π^* orbital of the butadiene skeleton.

Table 8: The UV absorption maxima of two-ring π -conjugated compounds



Bisilole 21	Dibromobisilole 22	Bicyclopentadiene 23
398 nm	417 nm	340 nm
2, 2'-Bifuran	2, 2'-Bithiophene	2, 2'-Biselenophene
278 nm	302 nm	321 nm

Most recently, in 1996, Tamao et al. evaluated the performance of small molecules containing silole as electron transporting (ET) materials (Scheme 20).^{61(b)} The configuration of the devices is ITO/TPD/ET-material/Mg:Ag (see structures of TPD and ET materials in Scheme 20). Tamao et al. compared the performance of silole derivatives with that of tris(8-hydroxyquinoline)aluminum (Alq), one of the most efficient ET materials reported so far. It



Scheme 20: Synthesis and study of silole derivatives as ET materials^{61(b)}

was found that the device PySPy/Alq, consisting of PySPy as the ET material and Alq as the emissive material, exhibited nearly 3 times higher *I-V* efficiency than those obtained with the device using only Alq, and the device with TTSTT exhibited one order higher *I-V* efficiency

than that with only Alq. These findings demonstrated for the first time that the silole ring is a promising candidate as a core component for efficient ET materials.

Despite of unsuccess of synthesis of polysilole, the synthesis and study of silole-containing polymers has continued to attract the scientists. In 1991, Corriu et al. synthesized and studied polymers including silole ring in the polymer main chains (Figure 24).⁶³ However, the silole ring does not participate in the π -conjugation in the polymer main chain as it is insulated by the silicon atom.

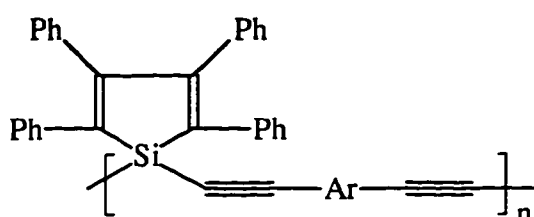
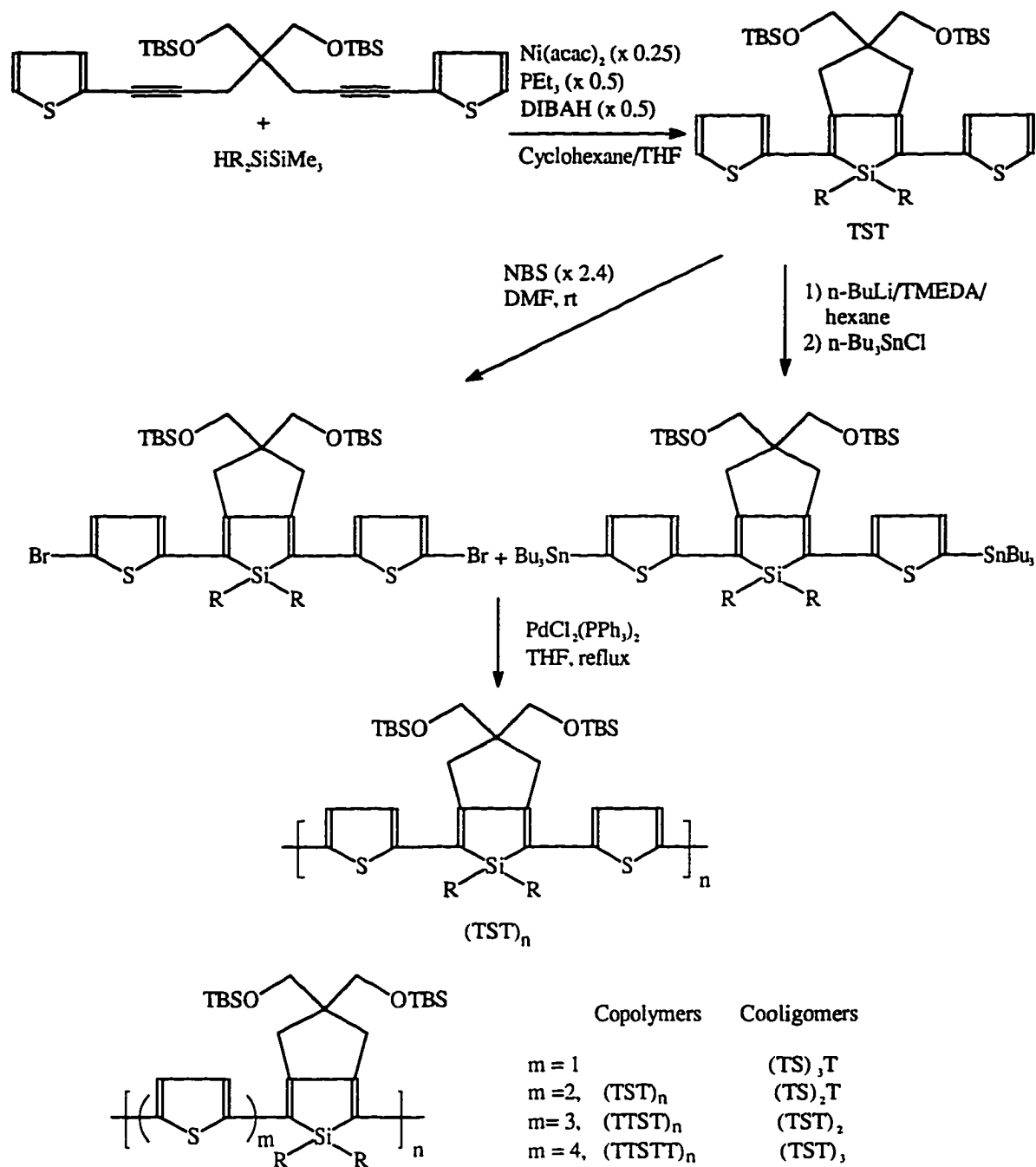


Figure 24: Silole-containing polymers

The only one example of silole-containing, fully π -conjugated polymers, are the thiophene-silole copolymers and cooligomers shown in Scheme 21.⁶⁴ The thiophene-silole-thiophene (TST) was prepared by the nickel-catalyzed intramolecular cyclization of a thiophene-containing 1,6-diyne with a hydrodisilane.^{64(a)} TST could be mono- and dibromination with NBS in DMF or mono- and dimetalation by *n*-BuLi/TMEDA. By the same method, the other silole-containing compounds such as TTST and TTSTT were synthesized.^{64(b)} By coupling reactions of their brominated monomers and stannylated monomers, a series of thiophene-silole copolymers and oligomers was synthesized. The silole-thiophene 1:1 copolymer could not be prepared by this method. However, its precursors, oligomers (TS)₂T (S:T = 2:3) and (TS)₃T (S:T = 3:4) were synthesized.

All these thiophene-silole cooligomers and polymers show much longer absorption in the visible region compared with thiophene homooligomers and homopolymers (Table 9). Significantly, there is a general tendency that a higher silole ratio causes a bathochromic shifts. Of particular interest are the broad absorptions of the copolymer (TST)_n at 594 and 615 nm,



Scheme 21: The synthesis of thiophene-silole cooligomers and copolymers⁶⁴

Table 9: UV/Vis absorption data for thiophene-silole cooligomers and copolymers and thiophene homooligomers and homopolymers⁶⁴

Compound	No. of thiophene and silole	UV absorption λ_{\max} (nm)
Terthiophene	T ₃	353
Quaterthiophene	T ₄	391
Quinquethiophene	T ₅	418
Bisilole 21	S ₂	398
Dibromosilole 22	S ₂	417
Dibromoquartersilole	S ₄	443
TST	T ₂ S	267, 416
TTSTT	T ₄ S	473
(TS) ₂ T	T ₃ S ₂	490, 524
(TS) ₃ T	T ₄ S ₃	544, 582
(TST) ₂	T ₄ S ₂	505
(TST) ₃	T ₆ S ₃	549
(TST) _n	T _{2n} S _n	594, 615
(TTST) _n	T _{3n} S _n	546
(TTSTT) _n	T _{4n} S _n	549
Poly(3-alkylthiophene)	T _n	435

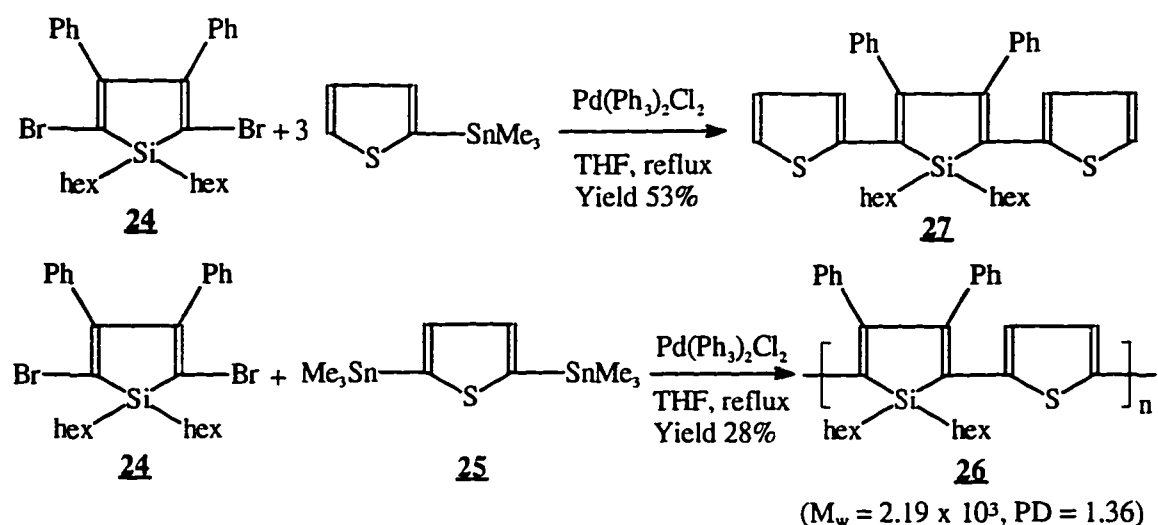
which are the longest wavelength ever found for thiophene-based polymers. The λ_{\max} value (582 nm) of the seven-ring system (TS)₃T (S:T = 3:4) exceeds the λ_{\max} value (549 nm) of the nine-ring system (TST)₃ (S:T = 1:2). However, the λ_{\max} values of dibromobisilole (S₂) **22** (417 nm) is about the same as that of TST (416 nm).

Because of the promising optical properties caused by unusual low bandgap of silole, further exploration of the field was conducted. A series of conjugated polymers containing silole was synthesized, and their optical properties were studied.

Results and Discussions

Synthesis and Study of Poly(2,5-thiophene-2,5-silole)

Synthesis. Despite the thiophene-silole copolymers had been synthesized, the copolymer with S:T = 1:1 had not.⁶⁴ This copolymer should exhibit the longest λ_{\max} of UV absorption among thiophene-silole copolymers. Given the availability of 2,5-difunctional silole,⁶⁰ the copolymer with S:T = 1:1, **26**, could be synthesized by direct coupling of 2,5-dibromosilole with 2,5-bis(trialkylstannyl)thiophene **25** as shown in Scheme 22.



Scheme 22: Synthesis of poly(2,5-thiophene-2,5-silole) **26** and model compound **27**

The polymerization was carried out by refluxing the reactants and the catalyst in THF for 7 days. The polymer was purified by precipitation from MeOH. The polymerization was very slow and the yield was low (about 28%). Polymer **26** is a deep purple solid which is very soluble in organic solvents such as THF and chloroform, giving bright reddish solutions. In

order to characterize polymer **26** by NMR, the model compound **27** was synthesized as the same method. After the reaction mixture was refluxed for 2 days, compound **27** was obtained in a moderate yield (53%) (Scheme 22). Compound **27** is a bright yellow solid and give bright green color luminescence in the solution state.

Characterization. The structure of polymer **26** was characterized by comparison with model compound **27**. The $^1\text{H-NMR}$ spectrum of polymer **26** shows two regions around 7.12 and 1.19 ppm representing the aromatic and the hexyl protons respectively. The $^{13}\text{C-NMR}$ spectra of polymer **26** and model compound **27** are shown in Figure 25. The chemical shifts of sp^2 carbons in silole unit of compound **27** are 153.79 and 143.13 ppm. The carbon of thiophene attaching to silole is at 139.37 ppm. Similarly, all these carbons can also be seen clearly in polymer **26** at 153.66, 143.33 and 139.35 ppm, respectively. The molecular weight of polymer **26** measured by GPC was relatively low ($M_w = 2.19 \times 10^3$, PD = 1.36). This can be explained by the steric hindrance due to the phenyl groups at 3,4-positions of silole and low reactivity of dibromosilole. This steric hindrance and low reactivity were also seen in the synthesis of model compound **27** with a moderate yield (53%) even at excess trimethylstannylthiophene. The average length of the polymer chain contains about four to five silole and thiophene units. TGA of polymer **26** shows the polymer start to decompose at 334°C . A DSC thermogram of polymer **26** is shown in Figure 24 where an endothermic peak is observed at $\sim 56^\circ\text{C}$ and an exothermic reaction starts at $\sim 165^\circ\text{C}$, probably due to the crosslinking.

UV/Vis Absorption. The UV/Vis absorption spectra of compound **27** and polymer **26** were measured and given in Figure 27. To our surprising, despite of its steric hindrance between phenyl and thiophene and its twisting structure, the UV/Vis maximum absorption λ_{max} (418 nm) of compound **27** is essentially the same as that of TST (416 nm),⁶⁴ which has a smaller steric effect. The λ_{max} value (590 nm) of polymer **26** is much red shifted compared with that of compound **27** (418 nm). However it is still shorter than that of $(\text{TST})_n$ polymer (594 nm, 615 nm) even S:T ratio is 1:1 instead of 1:2. The λ_{max} value of polymer **26** is very close to that of $(\text{TS})_3\text{T}$ (582 nm). It can be rationalized by the fact that the chain length of polymer **26** is similar to that of $(\text{TS})_3\text{T}$. Absorption edge (λ_c) was estimated as 740 nm, which

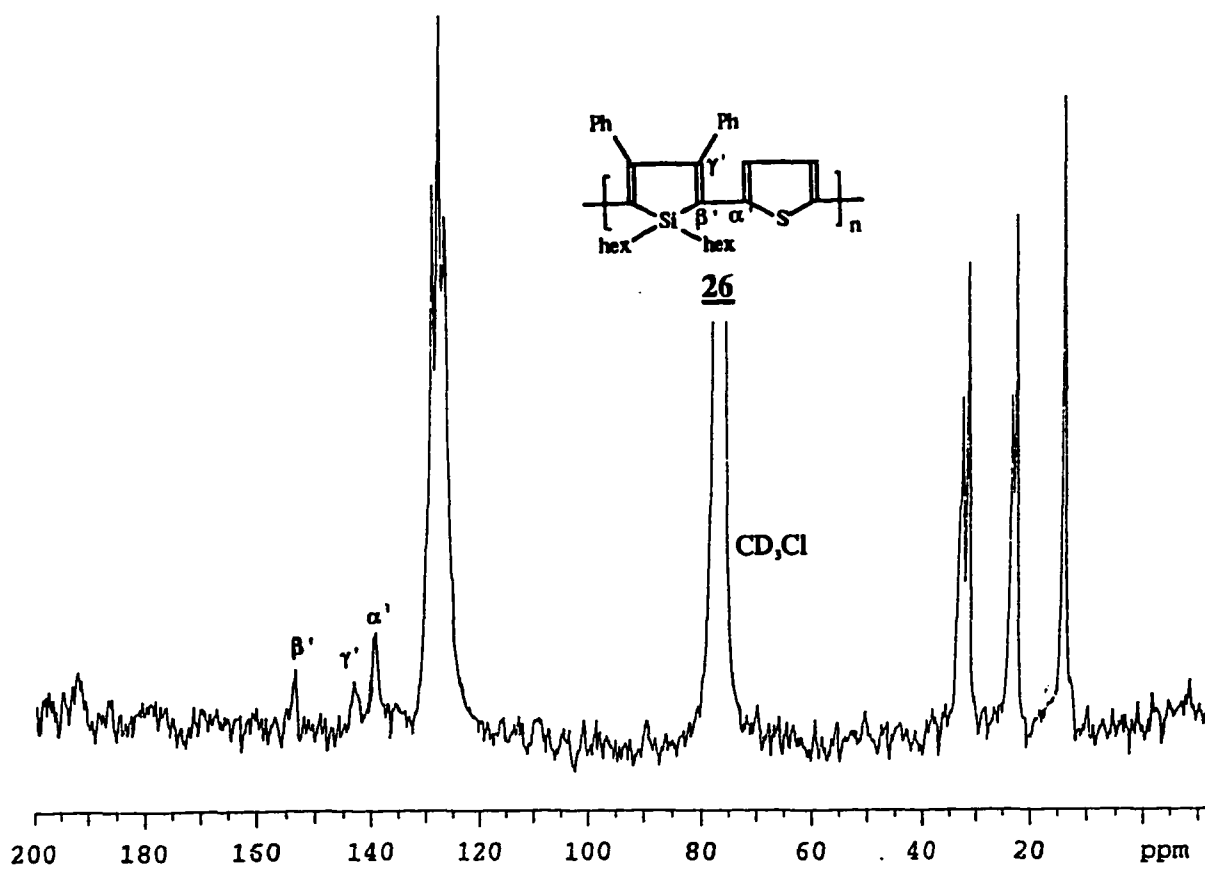
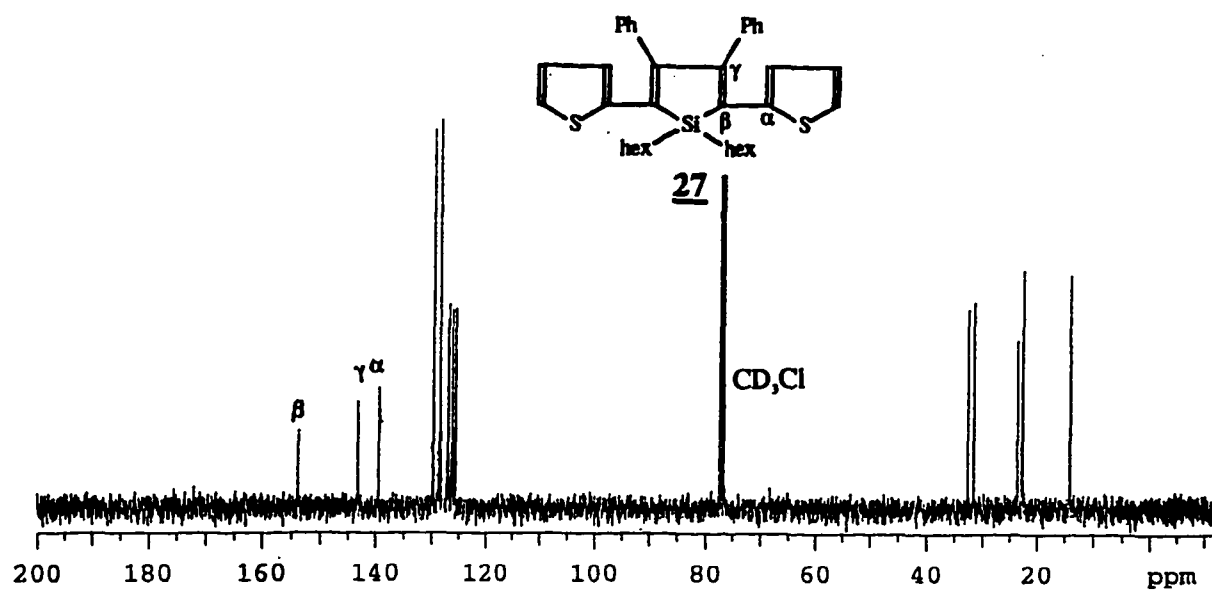


Figure 25: ^{13}C -NMR spectra of compound **27** and polymer **26**

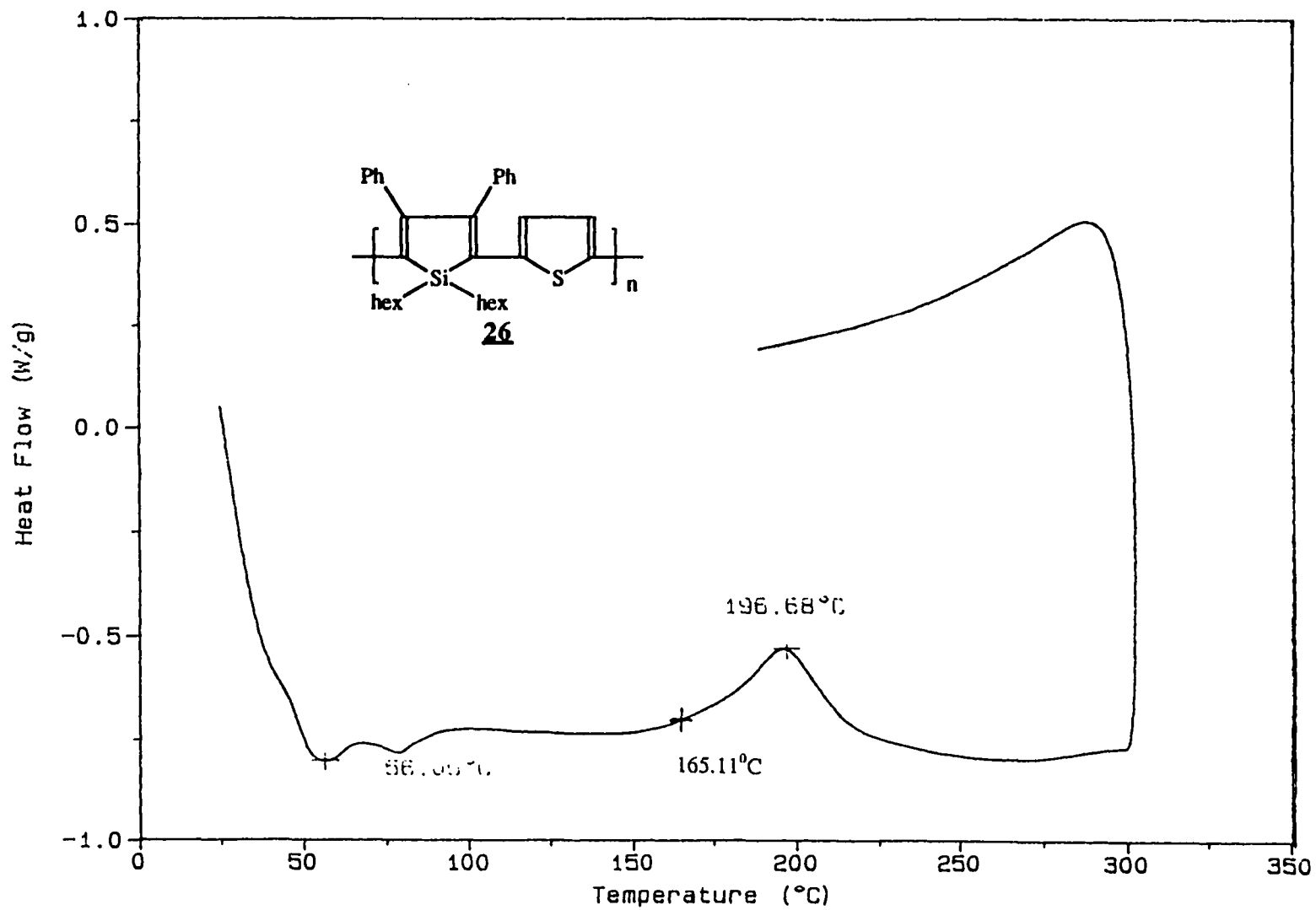


Figure 26: DSC thermogram of polymer **26**

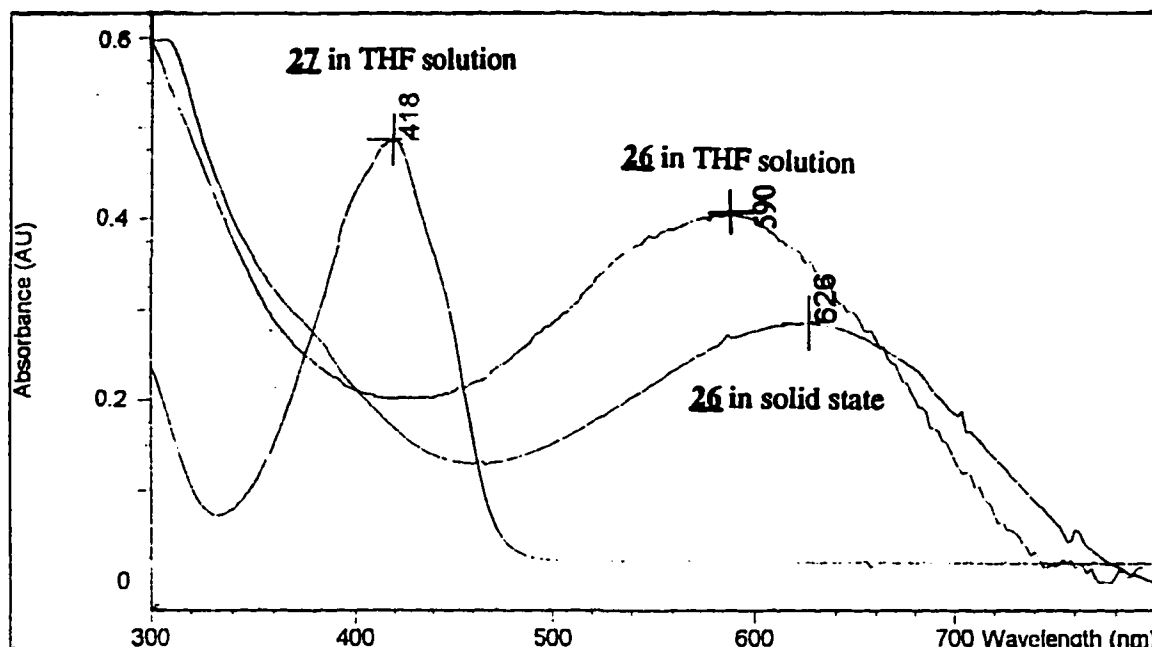


Figure 27: The UV/Vis absorption spectra of polymer 26 in THF solution and the solid state and compound 27 in THF solution

corresponds to a bandgap energy of 1.67 eV. The UV/Vis absorption of polymer film was also measured. The λ_{max} (626 nm) in the solid state is 36 nm longer than in solution, suggesting that the polymer in the solid state is better aligned than in solution.

Fluorescence. Polymer 26 has a red-colored luminescence in THF. The emission spectrum of polymer 26 was recorded and is shown in Figure 28. The deoxygenated THF solution was excited by a laser at 510 nm. The emission maximum is at 631 nm with two shoulders at 674 and 693 nm. The tail of emission band reaches beyond 800 nm.

Electrical Conductivity. Polymer 26 is an insulator at its neutral state. When doped by I_2 vapor under vacuum, its conductivity increased to 4.3×10^{-5} S/cm, which is close to the conductivity of $(\text{TS})_3\text{T}$ (3×10^{-5} S/cm), but much lower than that of $(\text{TST})_n$ (9×10^{-3} S/cm) and that of well-defined poly(3-alkylthiophene) (10^2 - 10^3 S/cm). The reason is probably its low molecular weight and its poor film-forming ability.

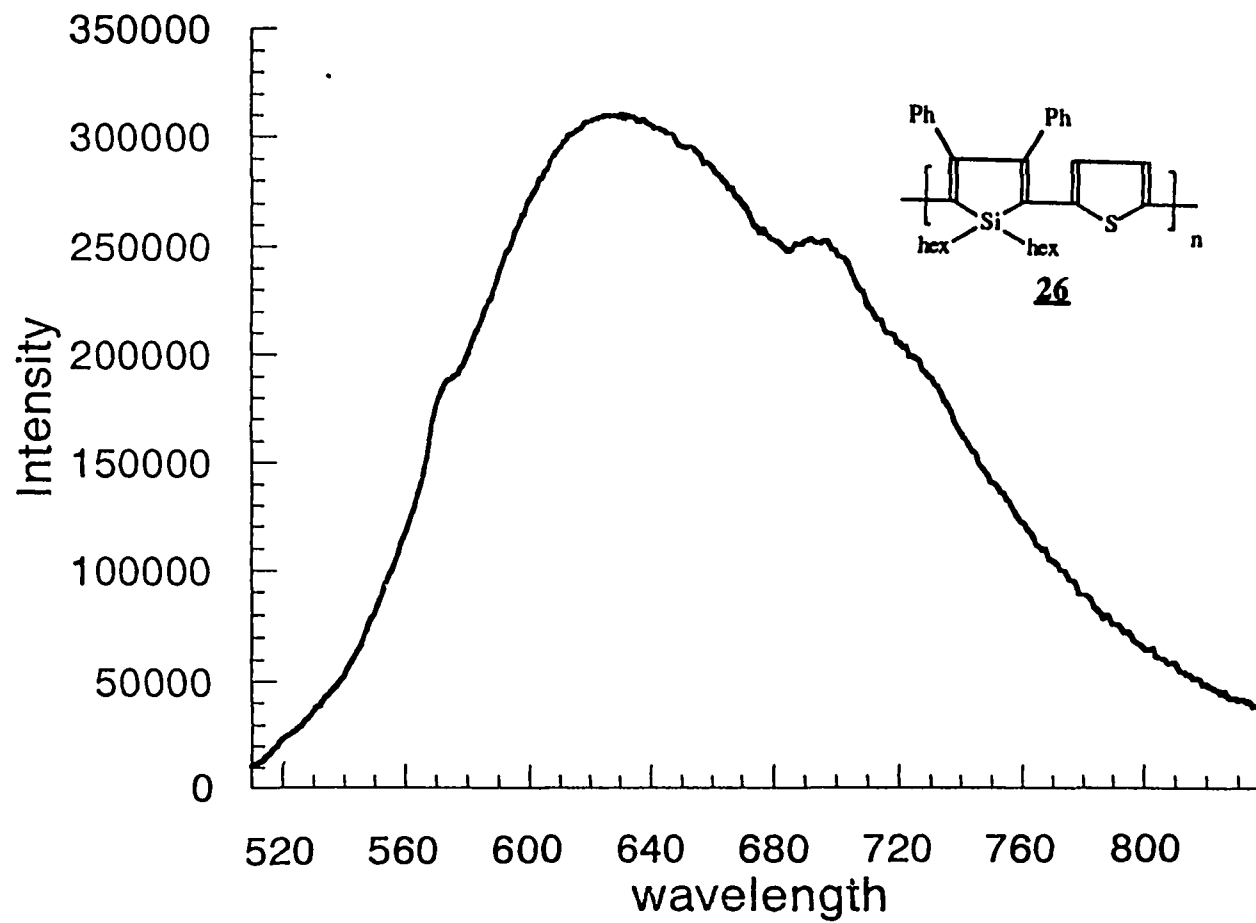
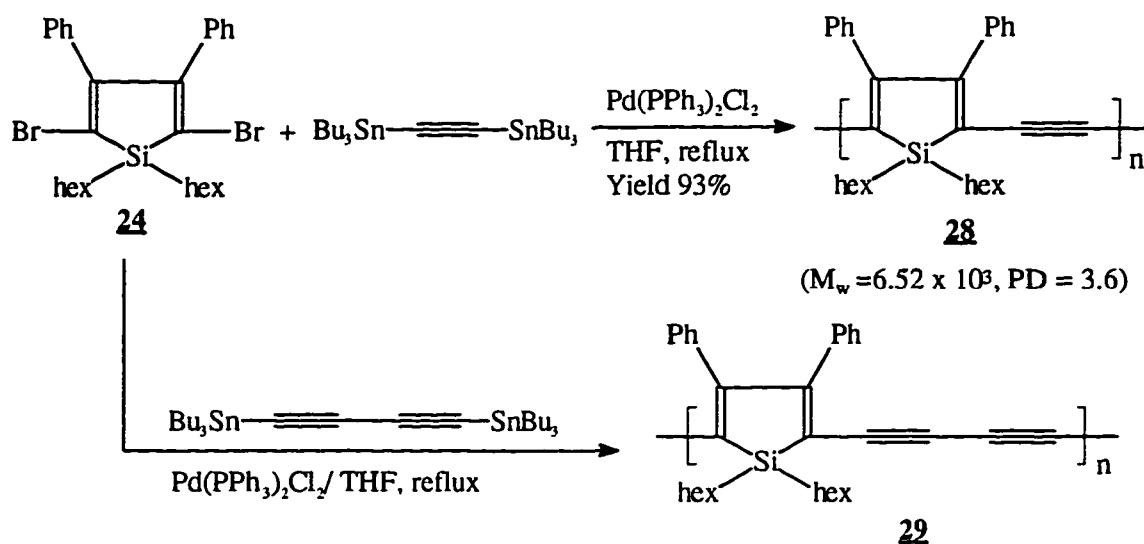


Figure 28: The emission spectrum of polymer **26** in THF solution

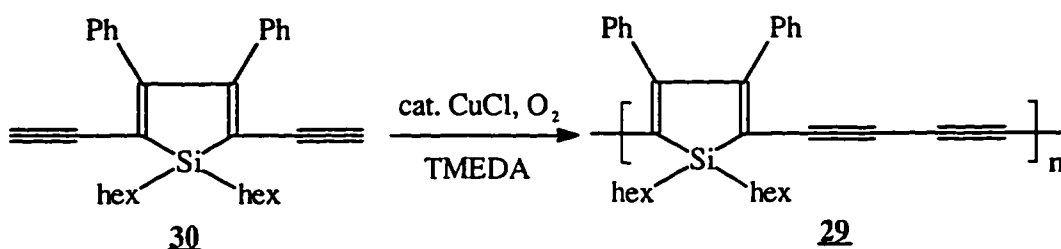
Synthesis and Study of Poly(2,5-silole-ethynylene) and Poly(2,5-silole-butadiynylene)

Synthesis. The electronic structure of a silole unit is much like that of a butadiene unit. The backbones of poly(silole-ethynyl) and poly(silole-butadiynylene), which have double bond and triple bond repeating units, are much like polydiacetylene. Since silicon can lower the LUMO level of the polymer, they should have even low bandgap energies than polydiacetylene. Poly(silole-ethynylene) or poly(silole-butadiynylene) can be easily synthesized by direct coupling between bis(trialkylstannyl)acetylene or bis(trialkylstannyl)butadiyne and 2,5-dibromosilole **24** (Scheme 23). Unlike thiophene, ethynylene is linear and shouldn't have any steric hindrance. Indeed, the reaction was much faster than coupling between dibromosilole **24** and 2,5-bis(trialkylstannyl)thiophene **25**. The polymerization was carried out by refluxing bis(tributylstannyl)acetylene and dibromosilole **24** in THF in the presence of palladium catalyst for 36 hours. Polymer **28** was precipitated from MeOH as a very deep blue (like black) solid in 93% yield. Polymer **28** is very soluble in organic solvents, exhibiting a deep blue color in THF.



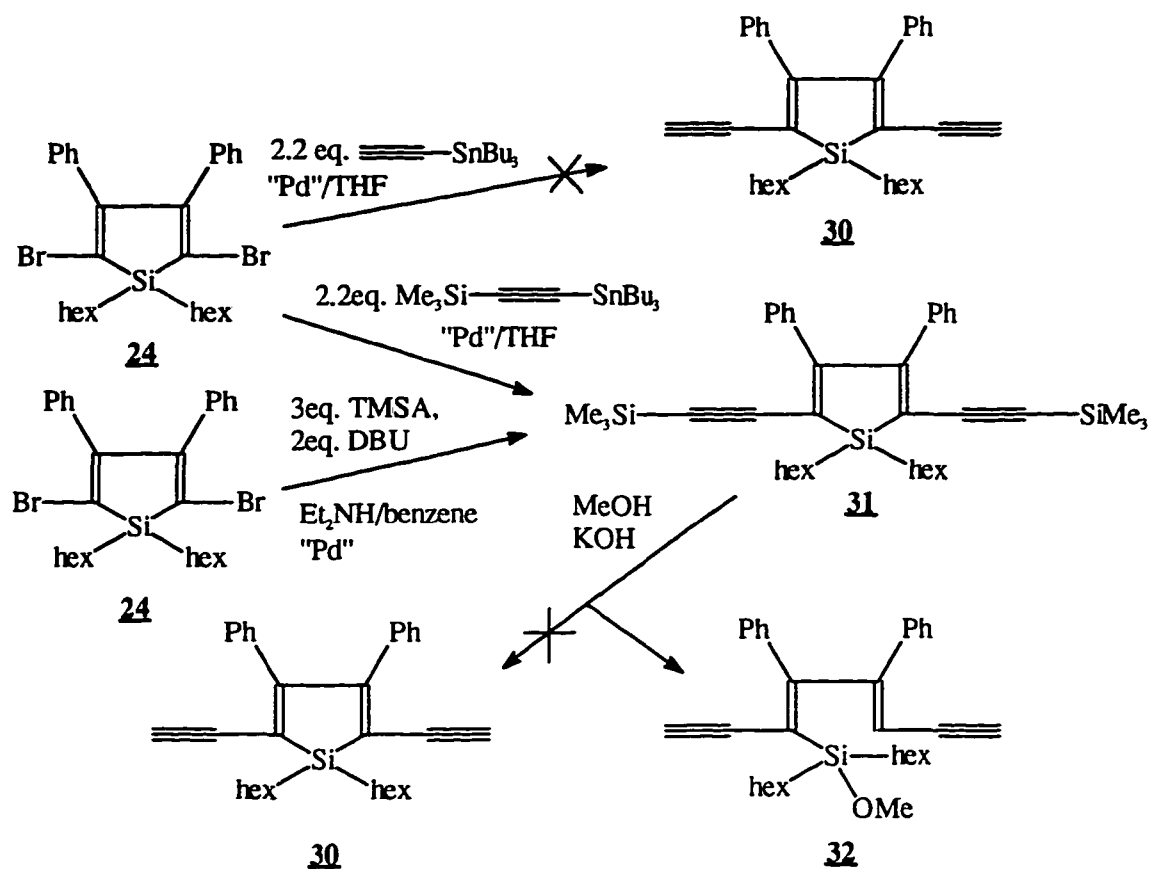
Scheme 23: Synthesis of poly(silole-ethynylene) **28** and poly(silole-butadiynylene) **29** by palladium-catalyzed coupling

However, refluxing of dibromosilole **24** and bis(tributylstannyl)butadiyne in THF solution in the presence of palladium catalyst for only 2 hours resulted in a very viscous, insoluble black gel, obviously the result of crosslinking. Reducing the temperature gave only either no polymer (which could be precipitated from MeOH) or insoluble black gel. The crosslinking could happen because polydiacetylene is not stable and easily crosslinked in the presence of palladium catalyst. In order to avoid crosslinking during the polymerization in the presence of palladium catalyst, synthesis of polymer **29** was attempted by oxidative coupling of 2,5-diethynylsilole **30** in the presence of Cu(I) as a catalyst (Scheme 24).



Scheme 24: Synthesis of poly(silole-butadiynylene) **29** by oxidative coupling

Attempted syntheses of monomer, 2,5-diethynyl-1,1-dihexyl-3,4-diphenylsilole **30**, are presented in Scheme 25. The reaction between dibromosilole **24** and tributylstannylacetylene in THF gave unidentified mixtures. By using an internal acetylene, 1-tributylstannyl-2-trimethylsilyl-ethyne, the coupling reaction went smoothly. The desired product **31** was obtained in high yield, but was contaminated with the byproduct tributylbromotin, which could not be separated from product **31** by column chromatography. The attempted reaction of dibromosilole **24** with trimethylsilylacetylene in Et₂NH/benzene in the presence of Pd(PPh₃)₄/CuI for 4 hours gave no precipitate. However, after 2.2 equivalent of a strong base, 1,8-diazabicyclo-[5,4,0]-undec-7-ene (DBU), was added to this mixture, a white precipitate formed immediately. After further stirring at room temperature for 6 hours, compound **31** was obtained in 57% yield. Detrimethylsilation of compound **31** in MeOH in the presence of a catalytic amount of KOH failed to give the desired product **30**, instead a ring-opening product **32** was obtained in 40% yield. No further attempts to prepare monomer **30** was made.



Scheme 25: Attempted synthesis of 2,5-diethynyl-3,4-diphenylsilole **30**

Characterization. Polymer **28** was characterized by NMR, GPC, TGA and DSC. The ^1H -NMR spectrum (Figure 27) shows only two regions of absorption between 7.3 and 6.9 ppm and between 1.3 and 0.7 ppm, representing the protons of the phenyl and hexyl groups, respectively. The ratio between these two regions is ~ 2.6 , indicating polymer **28** has high molecular weight. The ^{13}C -NMR spectrum has only two sp^2 carbons at ~ 168 and 138 ppm for silole, four carbons between 161 and 124 ppm for phenyl, only one sp carbon at ~ 102 ppm for ethynylene carbons and six sp^3 carbons for the hexyl groups. This spectrum fits the structure of polymer **28** perfectly. Because of the symmetry of the structure of the polymer, only one sp ethynylenic carbon is expected.

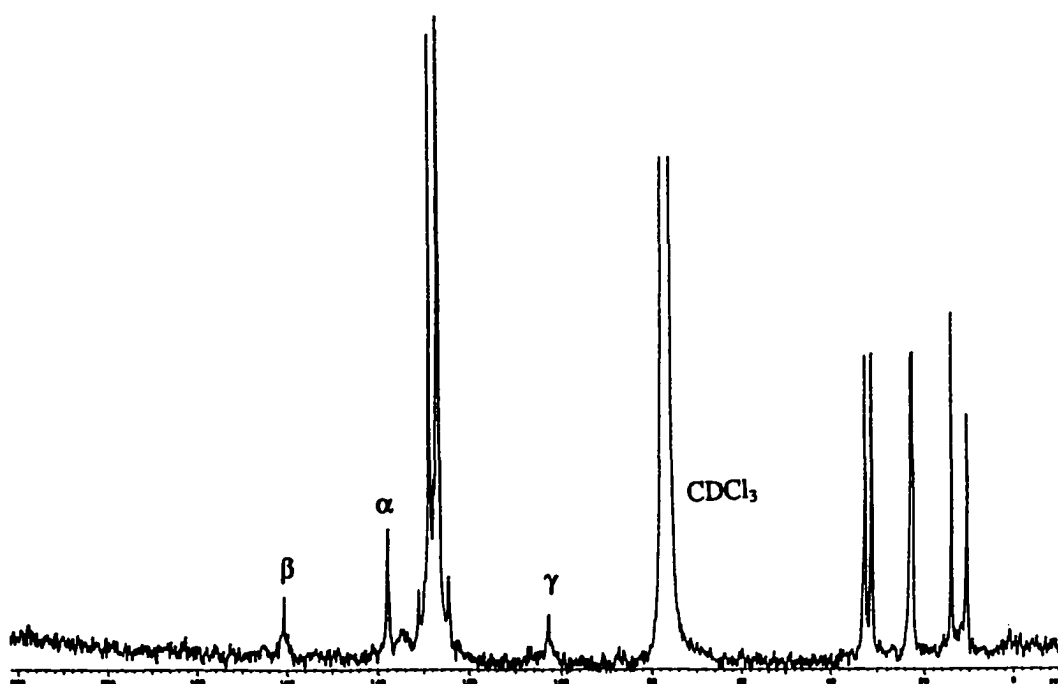
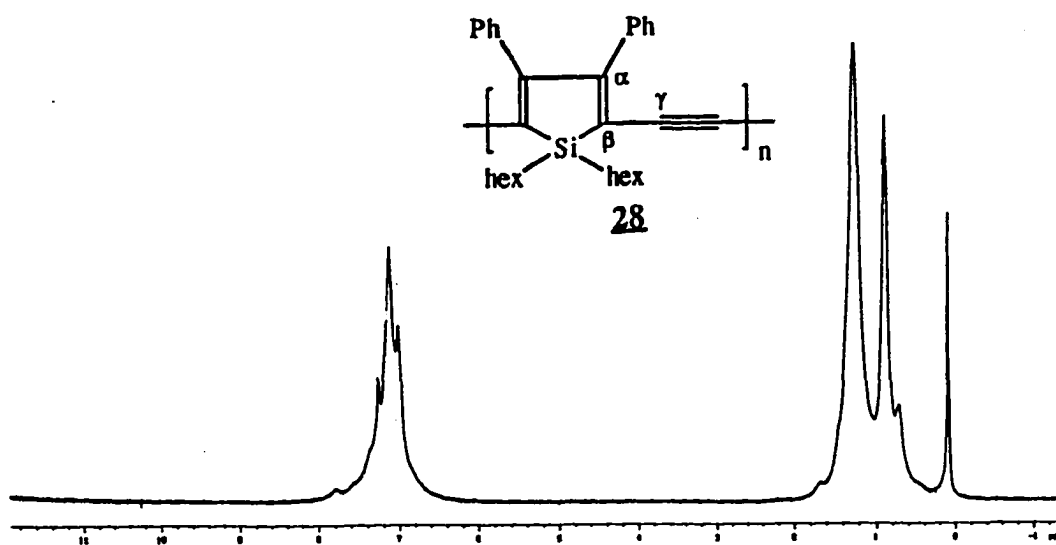


Figure 29: $^1\text{H-NMR}$ and $^{13}\text{C-NMR}$ spectra of polymer **28**

The molecular weight of polymer **28** was measured by GPC; $M_w = 6.52 \times 10^3$ with PD = 3.6. The average number of units in the polymer chain is ~16. The TGA spectrum of polymer **28** (Figure 30) shows there is a small endothermic peak at ~60°C, then the polymer starts to give off the heat slowly until ~170°C. An exothermic peak at ~240°C is probably due to the crosslinking at 202°C.

Due to the crosslinking during the polymerization and failure of synthesis by the other route, polymer **29** cannot be fully characterization by NMR and GPC. So its characterization and electronic properties won't be discussed in this thesis.

UV/Vis Absorption. The UV/Vis spectra of polymer **28** in THF and in the solid state are shown in Figure 29. The UV/Vis absorption λ_{max} in THF is 604 nm, which is the longest absorption wavelength among those of normal conjugated polymers having similar structure, such as poly(phenylene-ethynylene) ($\lambda_{max} = 425$ nm),^{25(d)} and poly(thiophene-ethynylene) ($\lambda_{max} = 438$ nm) (see Table 10 in page 80). The lack of the aromaticity of the silole unit and $\sigma^*-\pi^*$ conjugation between a π -symmetry σ^* orbital of exocyclic σ bonds on silicon, and a π^* orbital of the skeleton⁶² enhance overlap of π -electrons along the chain, thus dramatically lowering the bandgap energy. The absorption tail extends up to 740 nm. The bandgap energy can be estimated as low as 1.67 eV. Polymer **28** can form a shining smooth metallic film. The pattern of the UV/Vis absorption of the film is very close to that of its THF solution, red-shifted by 28 nm but otherwise very similar.

Fluorescence. Unlike PPV and PPE, polymer **28** has only a weak photoluminescence. Polymer **28** is much like polydiacetylene, which also has a very weak photoluminescence. Polymer **28** was excited at a fixed wavelength at 550 nm. Emission peaks were observed at 622 and 655 nm (Figure 32). The reason for the sharp peak at 655 nm is unclear. The small shoulder at 575 nm is possibly due to emission from the high vibration states in the excited state to the ground state.

Electrical Conductivity. The conductivity of undoped **28** is small (4.5×10^{-7} S/cm). The conductivity increased dramatically upon doping by I₂ vapor under vacuum. The maximum conductivity (2.3×10^{-1} S/cm) was essentially achieved in the first 5 minutes. Further doping did not increase the conductivity. Despite its low bandgap energy, the

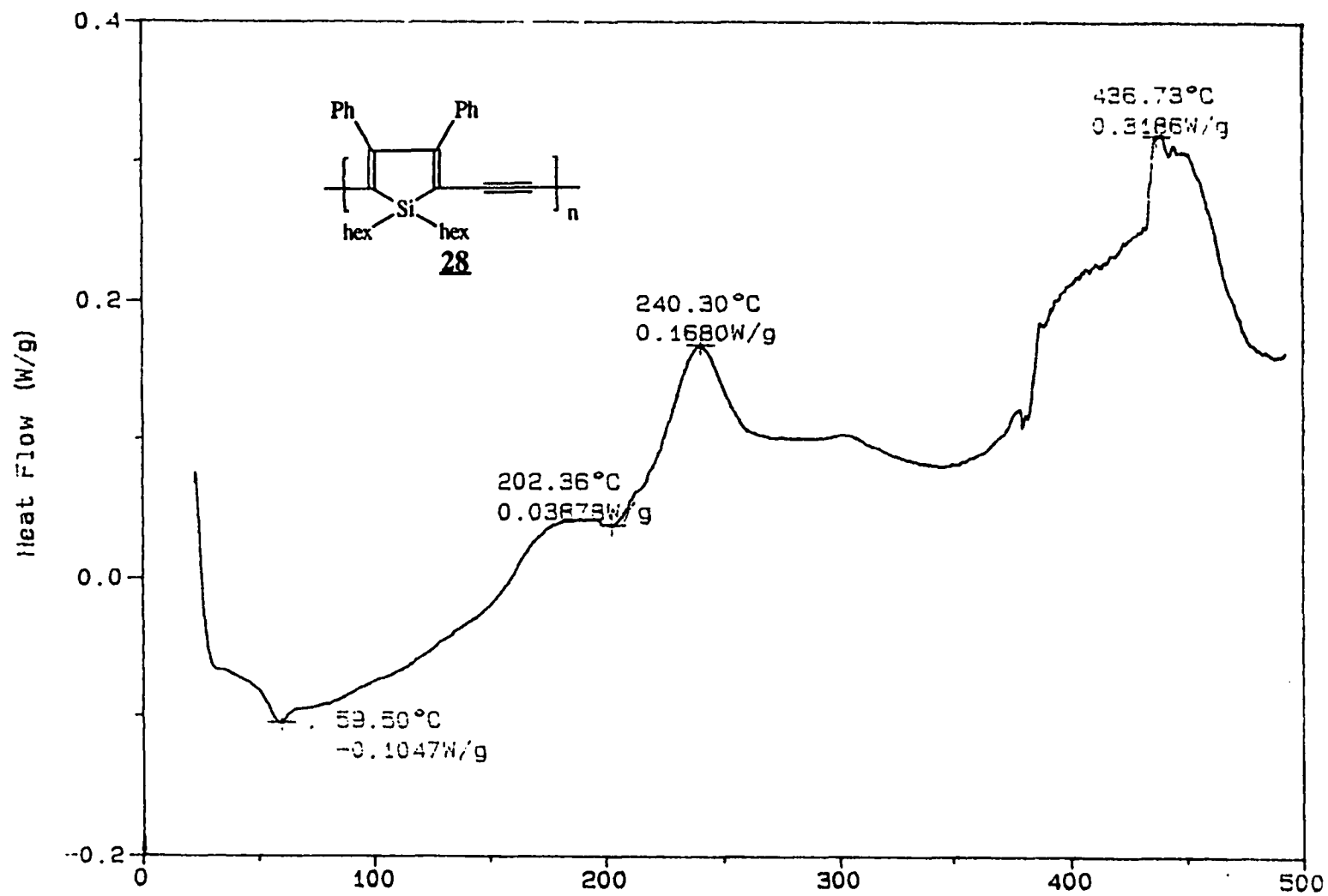


Figure 30: DSC thermogram of polymer **28**

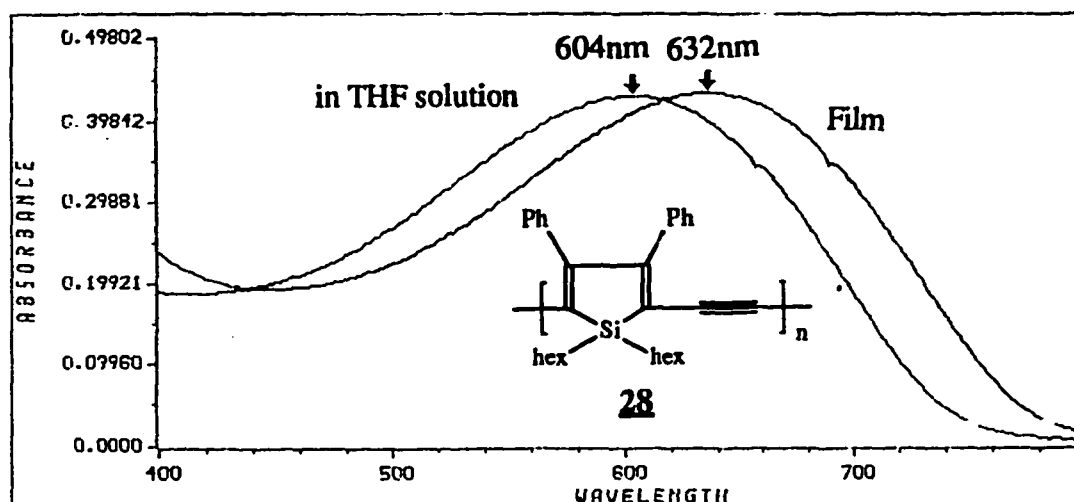


Figure 31: The UV/Vis absorption spectra of polymer **28** in THF solution and in the solid state

conductivity of polymer **28** is still much lower than those of polythiophene, polyacetylene and polydiacetylene.

Synthesis and Study of Poly(silole-ethynylene-paraphenylene-ethynylene)

Synthesis. As discussed in the first part of my thesis, there has been a wide variety of poly(arylene-ethynylene) derivatives synthesized and studied (see Figure 7). Since the silole unit has the electronic effect of lowering the LUMO level of the polymer main chain, the synthesis and study of poly(arylene-ethynylene) derivatives containing silole units are of much interest. The synthesis of poly(silole-ethynylene-paraphenylene-ethynylene) could be achieved via dibromosilole **24**. The polymerization was first carried out by reacting **24** with 1,4-diethynylbenzene and DBU in $\text{Et}_2\text{NH}/\text{THF}$ in the presence of $\text{Pd}(\text{PPh}_3)_2\text{Cl}_2/\text{CuI}$. The organic salt precipitated during the polymerization. However, during work up, no polymer precipitated from MeOH. This is presumably due to low molecular weight of the polymer which resulted from low reactivity between dibromosilole **24** and 1,4-diethynylbenzene. Reactivity of 1,4-bis(trialkylstannyl)benzene should be higher than that of 1,4-diethynylbenzene because the reductive elimination step during the polymerization does not need a base

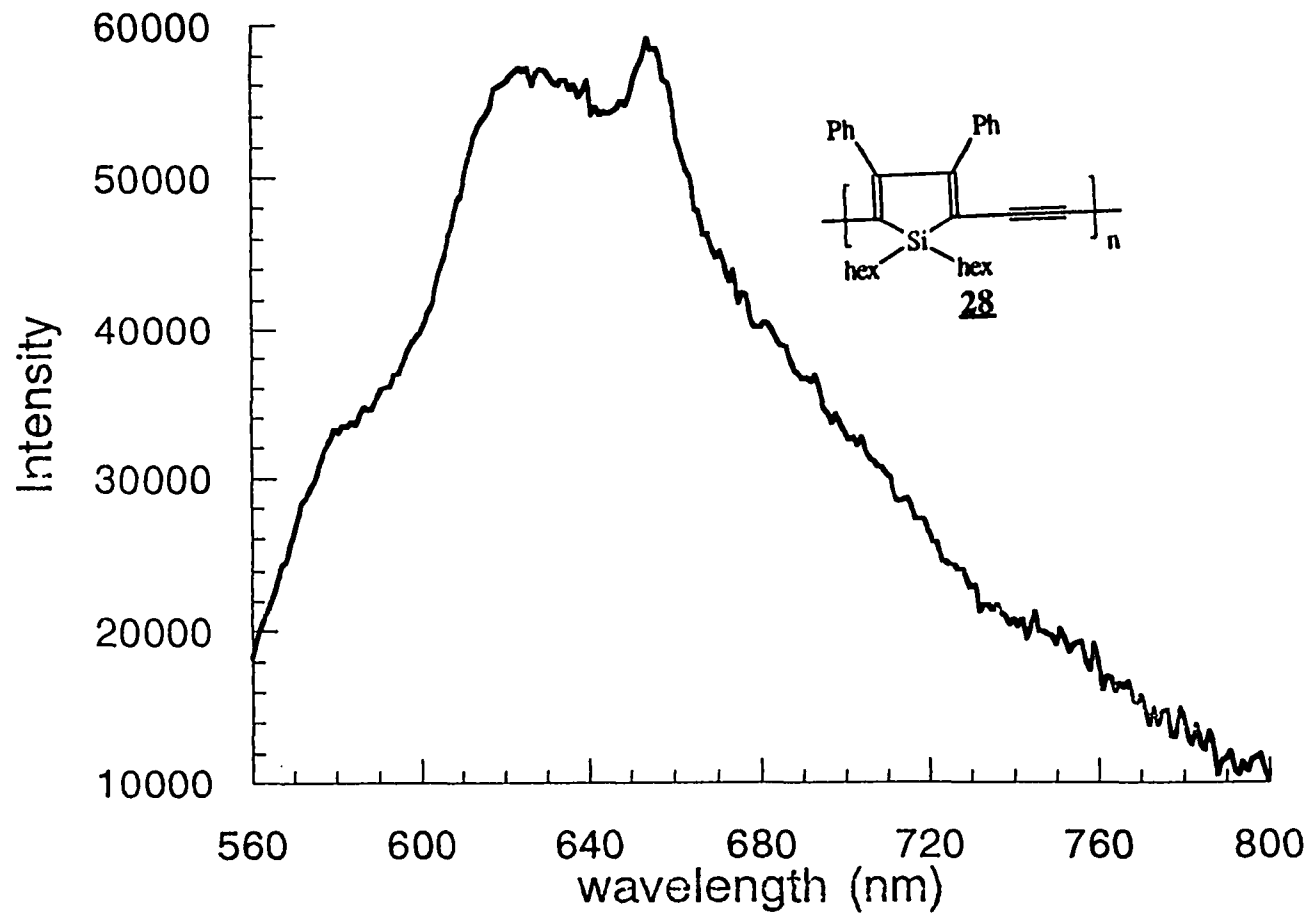
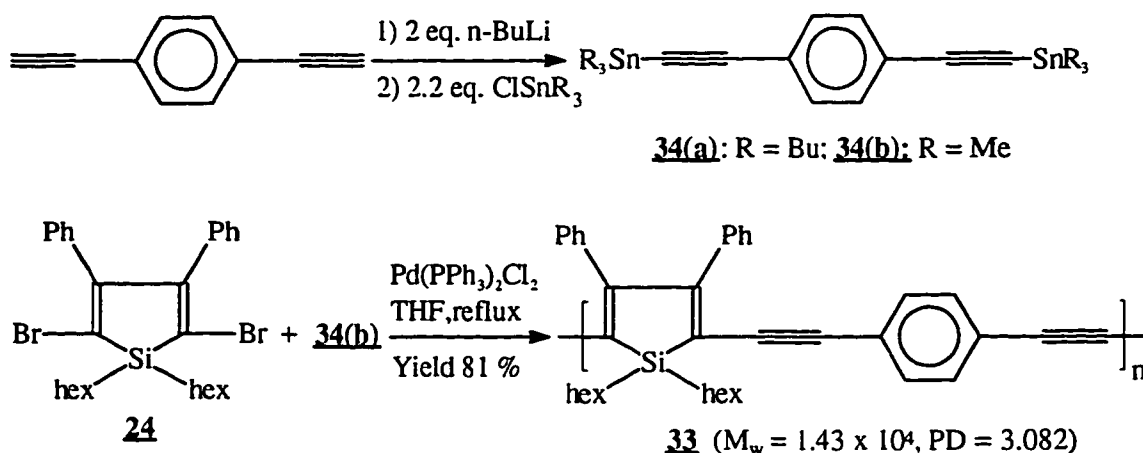


Figure 32: The emission spectrum of polymer **28**

to participate. The reaction of 1,4-diethynylbenzene with *n*-BuLi, followed by chlorotributyltin gave one major product 1,4-bis(tributylstannyl)benzene **34(a)** according to TLC. However, purification by column chromatography resulted in partial destannylation to give several mixtures which were difficult to separate. When 1,4-bis(tributylstannyl)benzene (Scheme 26) was assumed to be in 100% yield, and was allowed to react directly with dibromosilole **24** and catalytic Pd(PPh₃)₂Cl₂ without further purification, a very low molecular polymer was obtained. This is because the yield of 1,4-bis(tributylstannyl)benzene was not 100%. However, when diethynylbenzene reacted with *n*-BuLi, followed by quenching with chlorotrimethyltin, the resulting product 1,4-bis(trimethylstannyl)benzene **34(b)** (a white solid), could be purified by crystallization from hexane in 46% yield. Stirring 2,5-dibromo-3,4-diphenylsilole **24**, 1,4-bis(trimethylstannyl)benzene **34(b)** and catalytic Pd(PPh₃)₂Cl₂ in THF at 50°C for seven days gave polymer **33** in 81% yield (Scheme 26). Polymer **33** is very soluble in THF, CHCl₃, CH₂Cl₂. However, after storage in the atmosphere for several days, the polymer was not totally soluble in THF. This indicates polymer **33** is unstable in the atmosphere, possibly due to the crosslinking.



Scheme 26: Synthesis of poly(silole-ethynylene-paraphenylene-ethynylene) **33**

Characterization. The ¹H-NMR spectrum (Figure 33) of polymer **33** shows two groups of protons, one at between 7.41 and 6.97 ppm for the phenyl groups and the other at between 1.63 and 0.87 ppm for the hexyl groups. The ¹³C-NMR spectrum (Figure 33) shows

two sp^2 carbons of silole ring at ~ 162 and 137 ppm, three big peaks and one small peak between 131 to 123 ppm for the phenyl carbons, two sp ethynylene carbons at ~ 99 and 92 ppm, and six sp^3 hexyl carbons between ~ 32 and 10 ppm. The NMR spectra fit the structure of polymer **33** quite well. The molecular weight of **33** measured by GPC was 1.43×10^4 (PD = 3.082). The thermal stability of **33** was studied by TGA. The polymer starts to lose weight rapidly at $\sim 285^\circ\text{C}$ (4.5% weight loss) up at $\sim 593^\circ\text{C}$ (39% weight loss). After 593°C , the weight loss is very slow. At 800°C , the weight loss is $\sim 44\%$. The thermal behavior of **33** was also studied by DSC as shown in Figure 34. The polymer has an endothermic peak at $\sim 73^\circ\text{C}$ and starts an exothermic reaction slowly at $\sim 128^\circ\text{C}$ to give a broad exothermic peak. This probably is due to slow crosslinking

UV/Vis Absorption. The UV/Vis absorption spectra of polymer **33** in THF solution and in the solid state were measured and shown in Figure 35. The λ_{max} of polymer **33** is 494 nm in THF solution and 526 nm in the solid state. These numbers are the largest among those of poly(arylene-ethynylene) analogs, except poly(anthraceneethynylene). Table 10 shows λ_{max} values of these polymers. The λ_{max} of polymer **33** is 65 nm longer than that of poly(2,5-dialkoxy-1,4-phenyleneethynylene). By changing the thiophene unit of poly(thiophene-ethynylene-paraphenylene-ethynylene) to silole unit of polymer **33**, the λ_{max} can change 69 nm from 425 to 494 nm. However, compared with the λ_{max} (604 nm) of poly(silole-ethynylene) **28**, the λ_{max} (494 nm) of polymer **33** is 110 nm shorter. This is the further evidence that the silicon dramatically lowers the bandgaps in these systems.

Fluorescence. Polymer **33** has a weaker photoluminescence than PPV and PPE, but a stronger photoluminescence than polymer **28**. It seems apparently that increasing the ratio of phenyl rings to ethynylene enhances the photoluminescence. Polymer **33** was excited at a fixed wavelength at 430 nm. The emission peak was observed at 549 nm (Figure 36). The quantum yield was not measured.

Electrical Conductivity. Like other poly(aryleneethynylene) polymers, polymer **33** is an insulator when undoped. After exposure to I_2 vapor under vacuum, the conductivity increased to 4.3×10^{-3} S/cm.

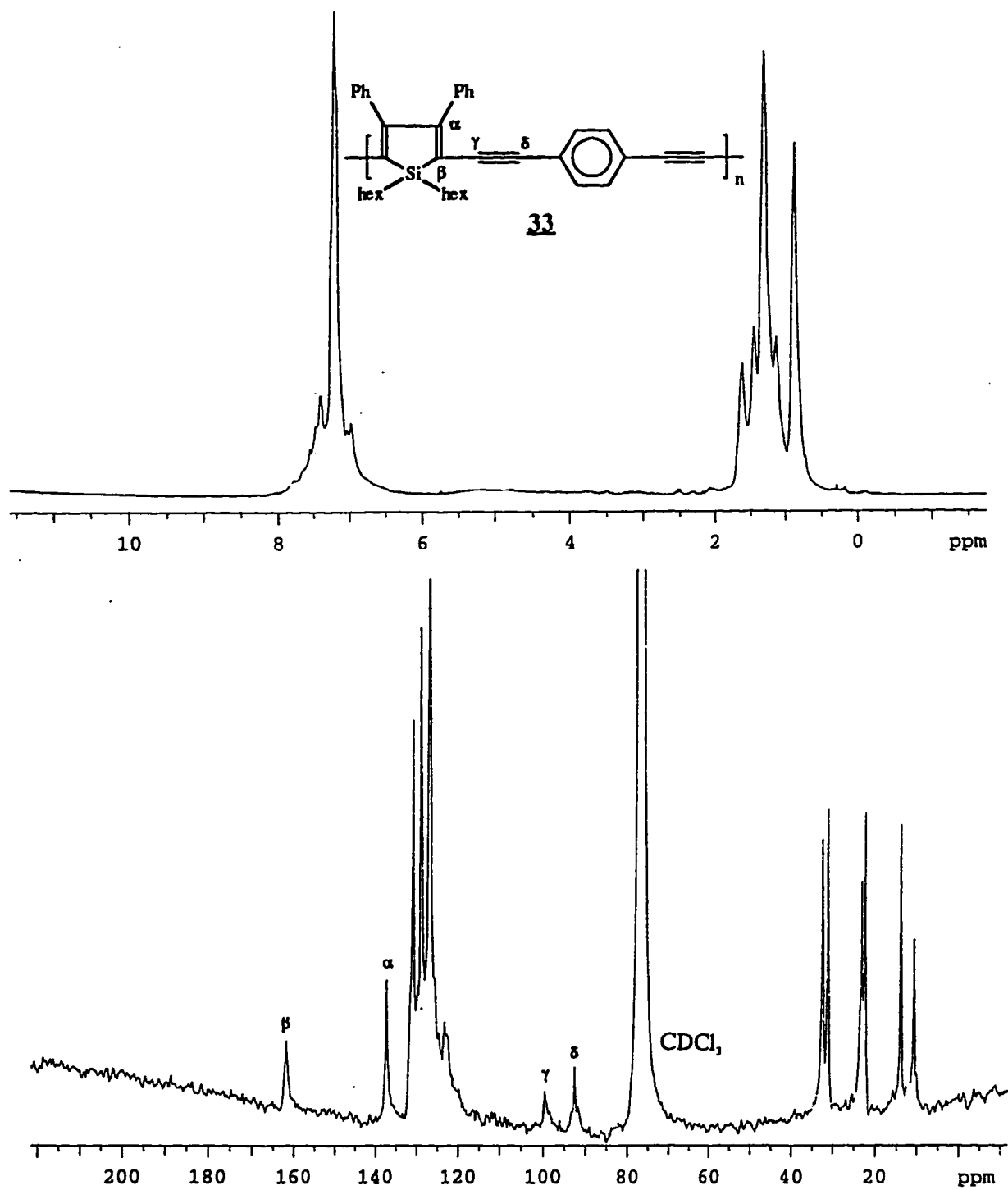


Figure 33: The $^1\text{H-NMR}$ and $^{13}\text{C-NMR}$ spectra of polymer **33**

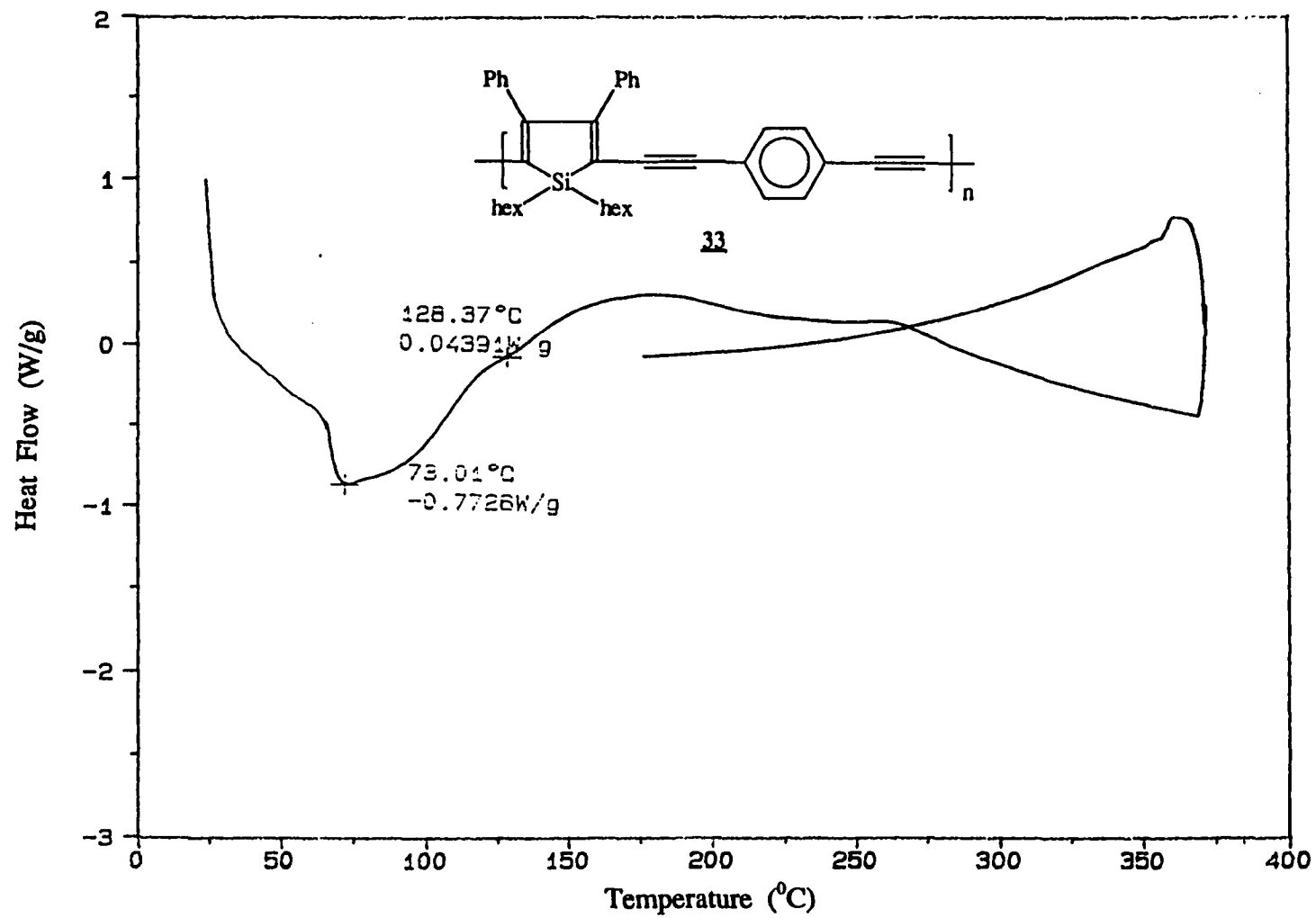


Figure 34: DSC thermogram of polymer 33

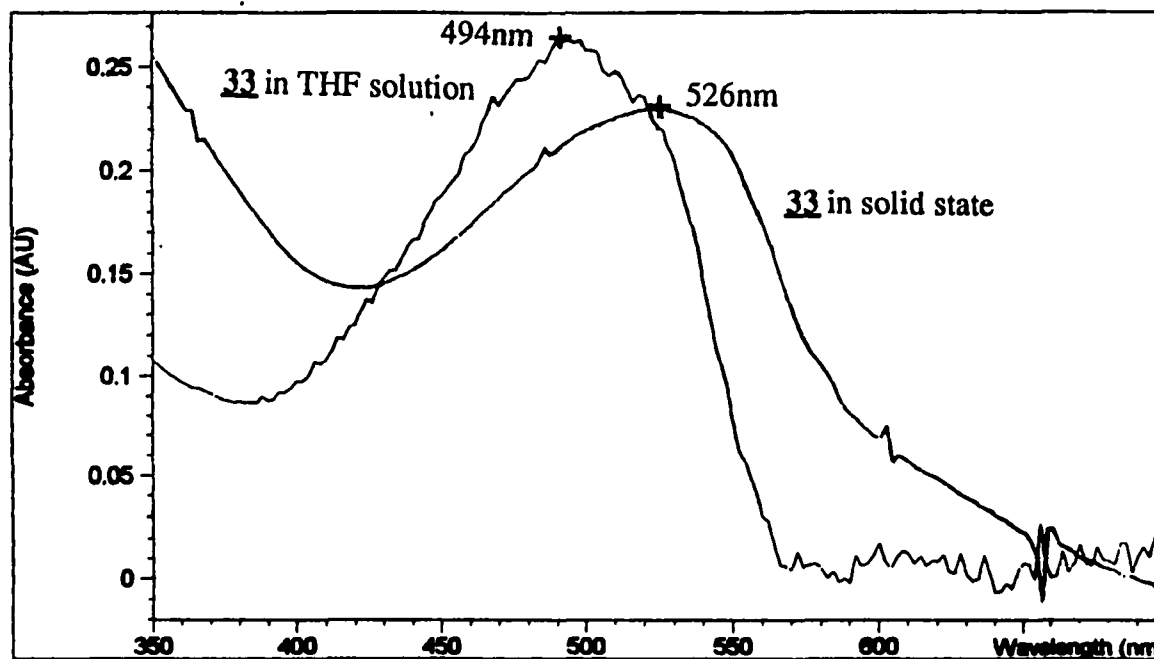
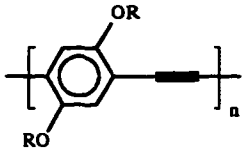
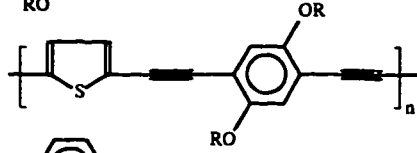
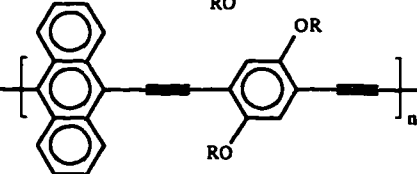
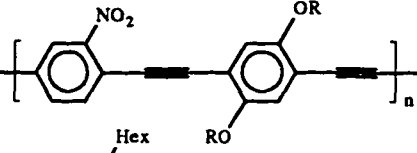
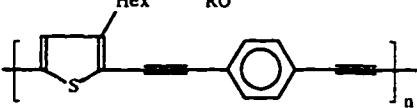
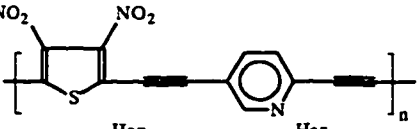
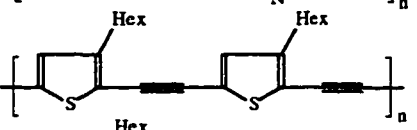
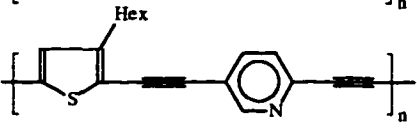
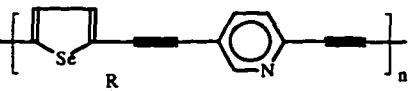
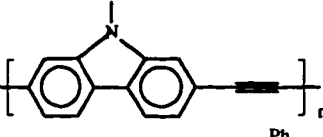
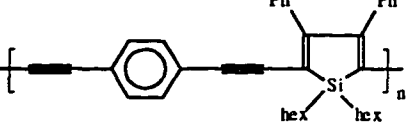


Figure 35: The UV/Vis spectra of polymer 33 in THF solution and the solid state

Table 10: The λ_{\max} of poly(aryleneethynylene) in solution and the solid state

Polymers	λ_{\max} (solution) (nm)	λ_{\max} (film) (nm)	Ref.
	429 (THF)	455	25(d)
	425 (THF)	453	25(d)
	508 (THF)	521	25(d, g)
	404 (THF)	412	25(a)
	403 (CH ₂ Cl)	410	25(a)
	360 (HCOOH)	350	25(a)
	438 (THF)		25(f)
	426 (CH ₂ Cl)	432	25(a)
	462 (CH ₂ Cl)	460	25(a)
	366 (THF)	366	27
	494 (THF)	526	this work

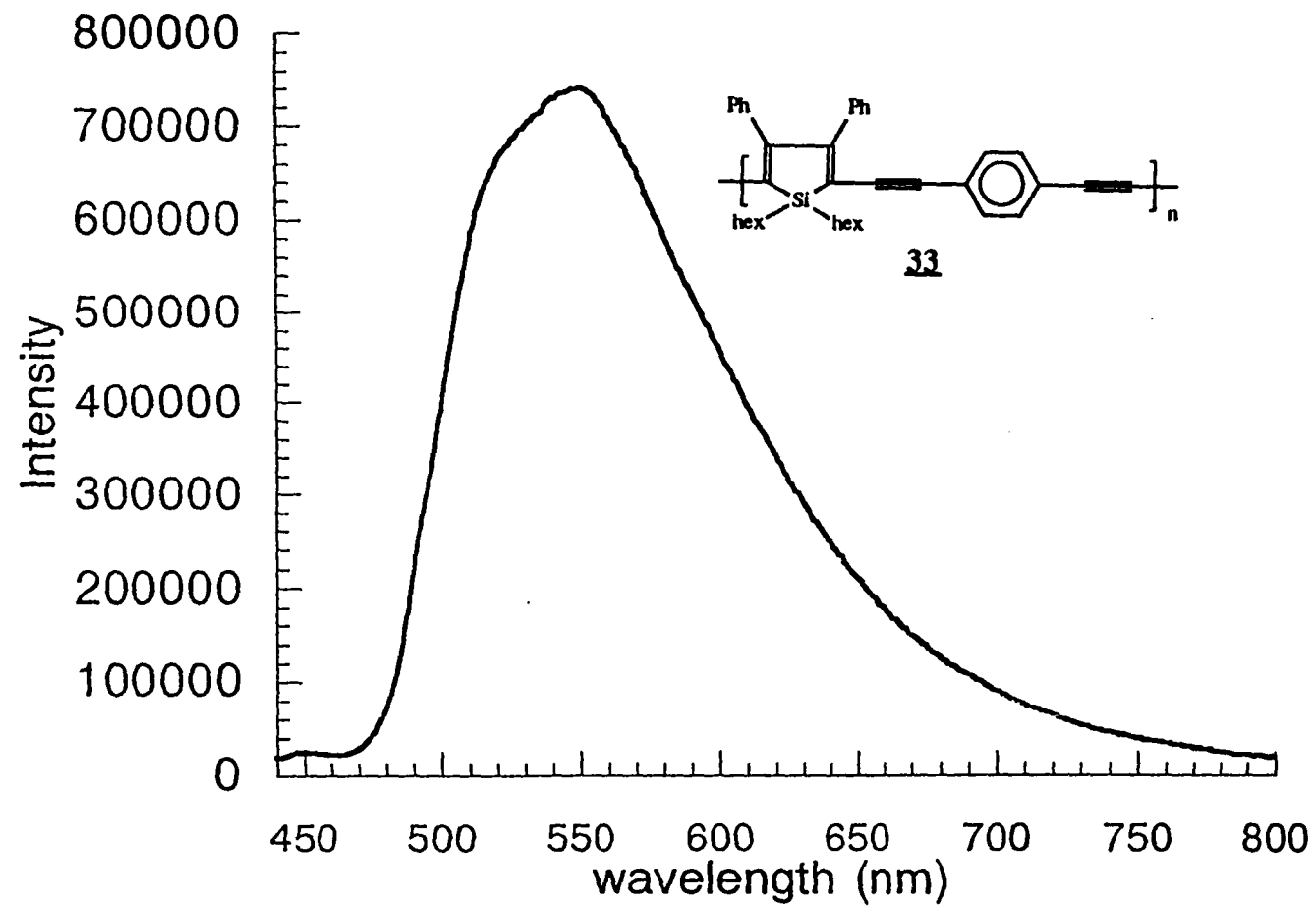
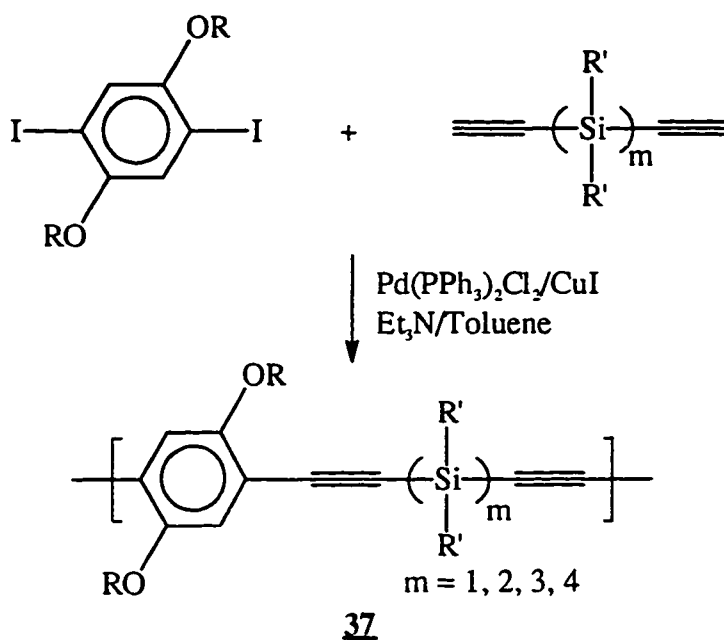


Figure 36: The emission spectrum of polymer 33

Synthesis and Study of Poly(2,5-silole-ethynylene-dimethylsilylene-ethynylene)

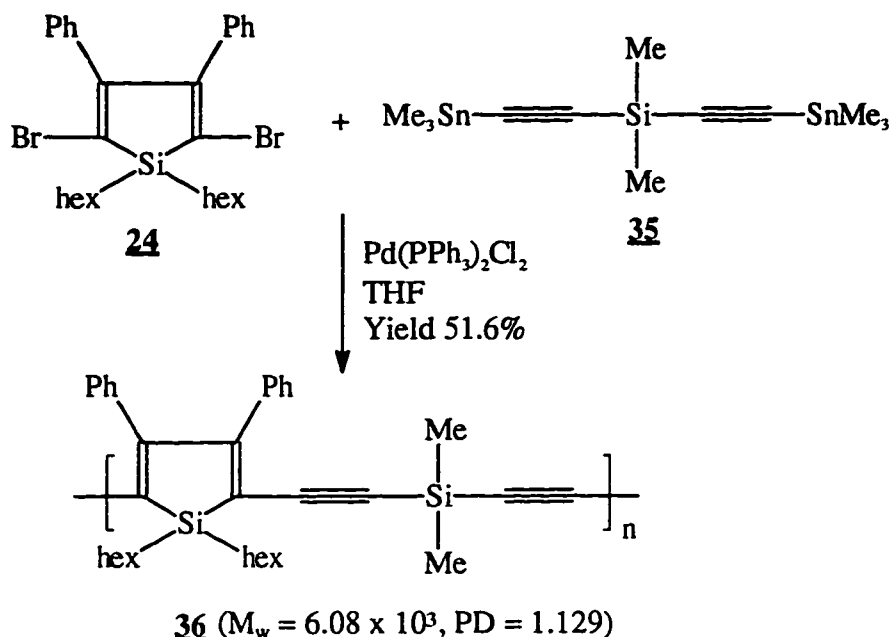
Conjugated polymers interrupted by a silylene unit have σ - π interaction along their main chains. The study of polymers having σ - π conjugated systems is an interesting subject, because of their potential utility as electronically conducting, semiconducting, and emitting polymers.⁶⁵ In 1994, our group synthesized and fully studied liquid crystalline properties of silylene-containing polymer, poly(ethynylene-dialkylsilylene-ethynylene-1,4-phenylene) (Scheme 27).^{25(b)} Like a phenyl, the silole unit has a rigid structure. Therefore, poly(2,5-silole-ethynylene-dialkylsilylene-ethynylene) has a rigid, rod-like backbone, and should have liquid crystalline properties. Silole, much like butadiene, lowers the bandgap energy, thus changing electronic properties of the polymer.



Scheme 27: Synthesis of poly(ethynylene-dialkylsilylene-ethynylene-1,4-phenylene) **37**

Synthesis. The synthesis of poly(2,5-silole-ethynylene-dimethylsilylene-ethynylene) **36** is similar to that of polymer **33** (Scheme 28). Bis(trimethylstannylethynyl)-dimethylsilane **35** reacted with dibromosilole **24** in THF in the presence of catalytic $\text{Pd}(\text{PPh}_3)_2\text{Cl}_2$ to give

polymer **36** in 52% yield. Polymer **36** is a brown solid and very soluble in organic solvents, the THF solution being reddish.



Scheme 28: Synthesis of poly(silole-ethynylene-dimethylsilylene-ethynylene) **36**

Characterization. The $^1\text{H-NMR}$ spectrum (Figure 37) of polymer **36** shows one broad peak at 7.09 ppm for the phenyl protons, four peaks between 1.55 and 0.87 ppm for the hexyl groups, one peak at 0.16 ppm for the protons of the dimethylsilyl group. The $^{13}\text{C-NMR}$ spectrum (Figure 37) shows two carbons at ~ 162 and 137 ppm for the silole unit, three peaks for the phenyl carbons, two ethynylenic carbons at ~ 105 and 102 ppm, six hexyl carbons between 32.32 and 10.29 ppm, and one dimethylsilyl carbon at 0.11 ppm. The molecular weight of polymer **36** is 6.06×10^3 (PD = 1.129) according to GPC. TGA shows the polymer starts to decompose at $\sim 366^\circ\text{C}$ (weight loss 4%). The weight loss is rapid between 366°C and 562°C (weight loss 38%). After 562°C , the weight loss is very slow. At 800°C , the weight loss is $\sim 43\%$. DSC thermogram (Figure 38) shows a strong endothermic peak at $\sim 74^\circ\text{C}$. This endothermic peak indicates polymer **36** starts to melt at 74°C . An exothermic reaction starts at $\sim 261^\circ\text{C}$ to give a peak at 337°C . This peak is probably due to the crosslinking.

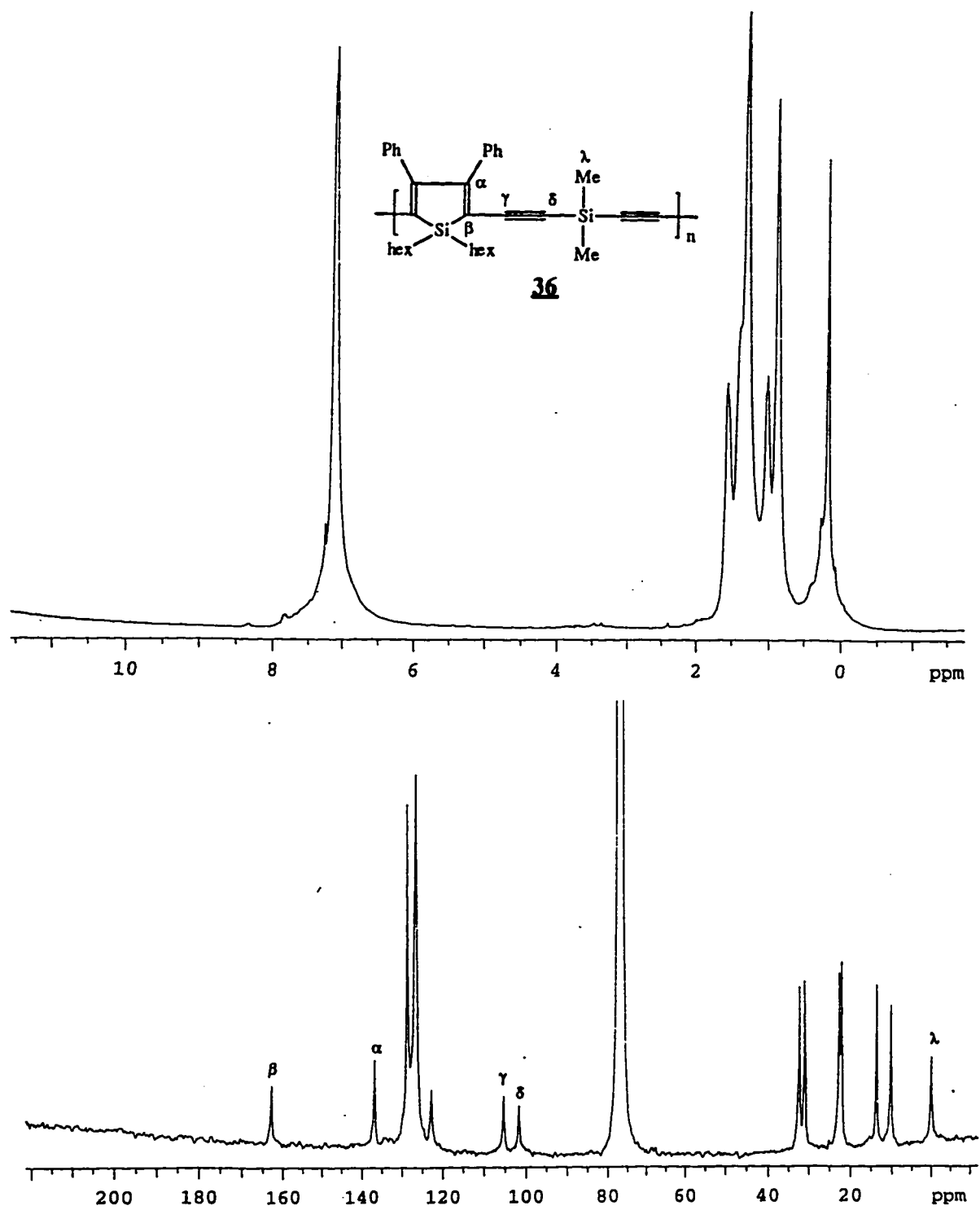


Figure 37: The ^1H and ^{13}C NMR spectra of polymer **36**

UV/Vis Absorption. The UV/Vis spectra of polymer **36** in THF solution and film were shown in Figure 39. The absorption maximum in THF solution is 400 nm. To fully study the σ - π interaction, the UV/Vis absorption of the model compound **31** was measured. The λ_{max} of **31** is 336 nm in THF, which is about 64 nm shorter than that of polymer **36**. It indicates extensive conjugation despite the interruption by the silylene unit. The silylene unit participates in the conjugation by the σ - π interaction. Compare with the λ_{max} value of poly(ethynylene-dialkylsilylene-ethynylene-1,4-phenylene) **37** (~364 nm),^{25(b)} the λ_{max} of polymer **36** is 36 nm red-shifted, which shows the silole unit decreases the bandgap. The peak shape of the film was also recorded and is similar to that in THF solution, but red-shifts 26 nm. The absorption edge in THF solution is ~460 nm.

Electrical Conductivity. The conductivity of polymer **36** in the neutral state is 4.49×10^{-6} S/cm. After doped by I₂ vapor, the conductivity didn't change much with $\sigma = 3.67 \times 10^{-5}$ S/cm.

All these polymers should exhibit high $\chi^{(3)}$ values. The study of third-nonlinear optical properties of these polymers should be very interesting.

Attempted Synthesis of Poly(2,5-silole-1,2,3-butatriene)

Organic polymeric materials with π -conjugated systems, which exhibit very large nonlinear optical response, are polyacetylene, poly(phenylenevinylene) (PPV), polythiophene, polydiacetylene and other conjugated polymers (see Table 2). Cumulenes such as butatriene and hexapentaene also have extended π -electrons and linear structures. However, conjugated polymers containing the cumulene unit have been paid little attention. Theoretical calculations of polyenes, polyenyne and cumulenes within the correlated Pariser-Parr-Pople (PPP) model (defined over the π -frame by Albert et al⁶⁶) showed that for the same chain length, cumulenes have the largest polarizability and third harmonic generator (THG) coefficients. The optical gaps for these systems were also calculated, with cumulenes possessing the smallest gap at 0.75 eV, polyenes at 2.86 eV, and polyenyne at 4.37 eV. Prasad reported the first experimental determination of the third-order nonlinear optical susceptibilities of some cumulenes in 1993.⁶⁷ The $\langle\gamma\rangle$ values increase dramatically with increasing of the numbers of

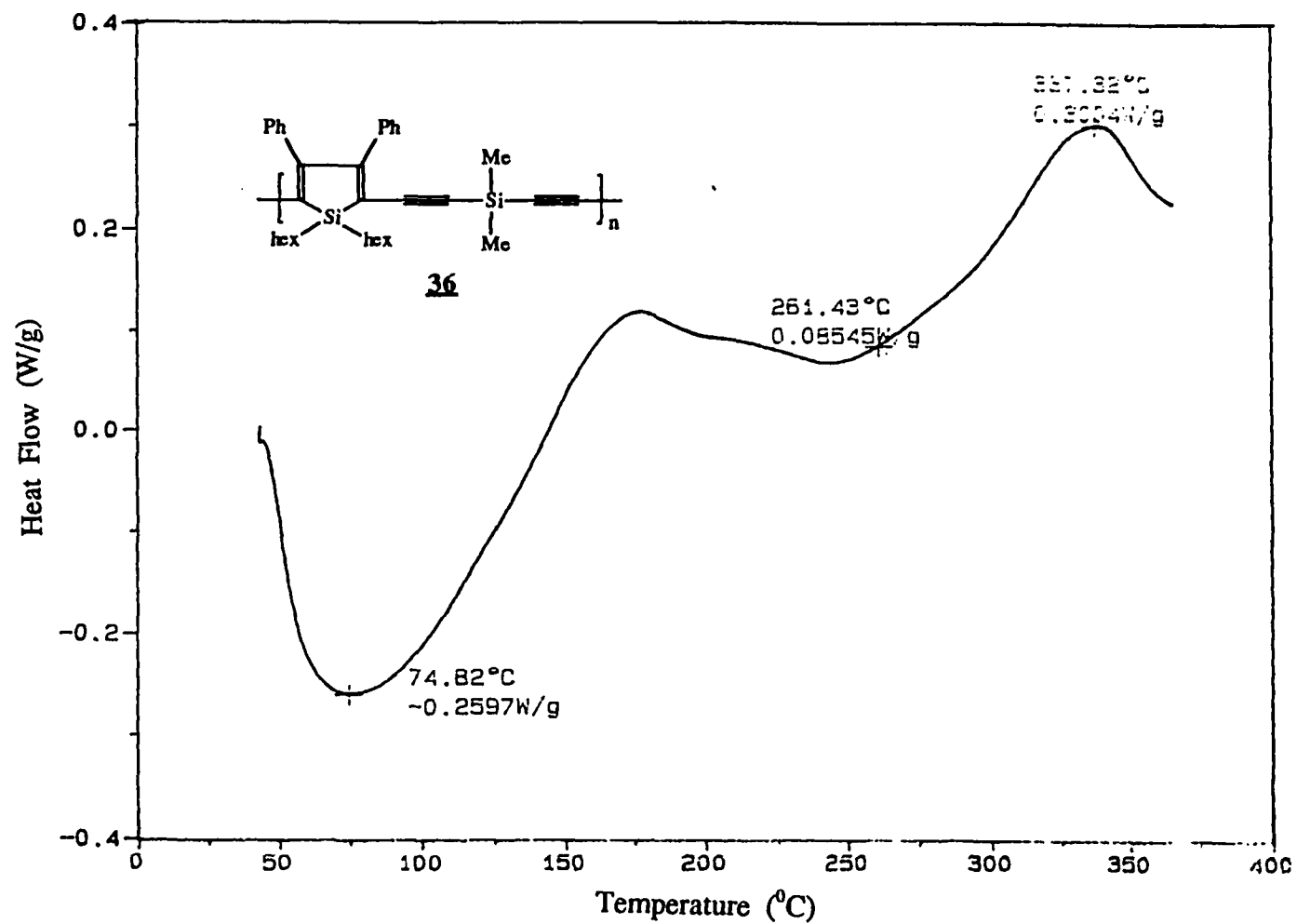


Figure 38: DSC thermogram of polymer **36**

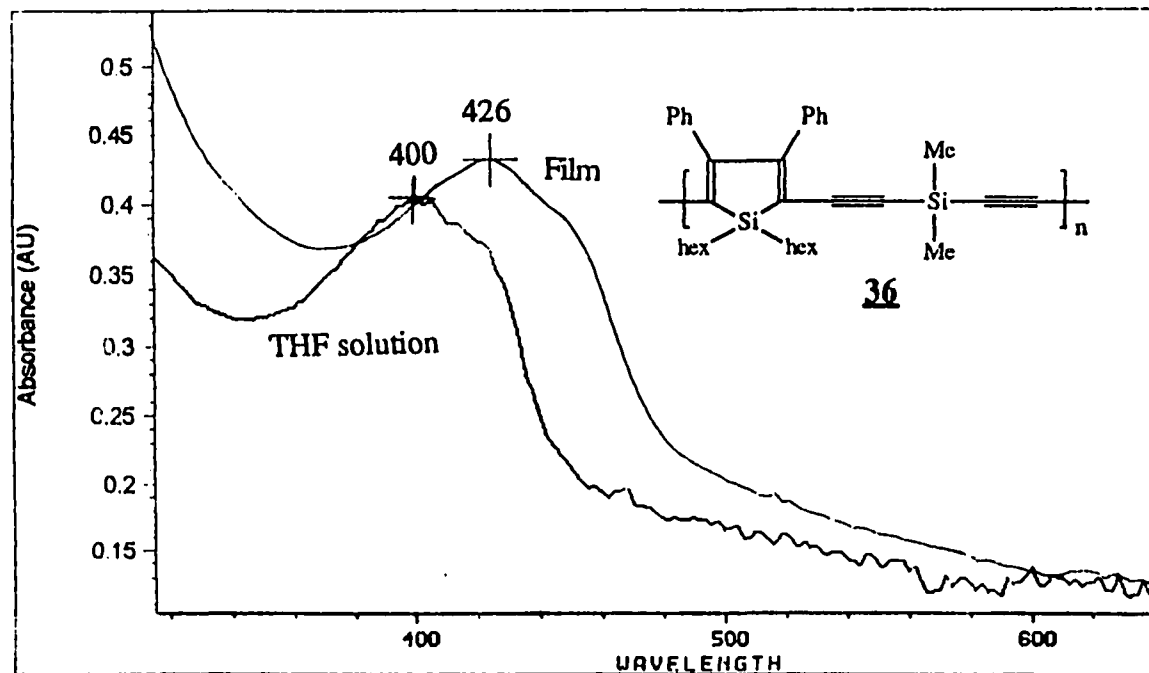
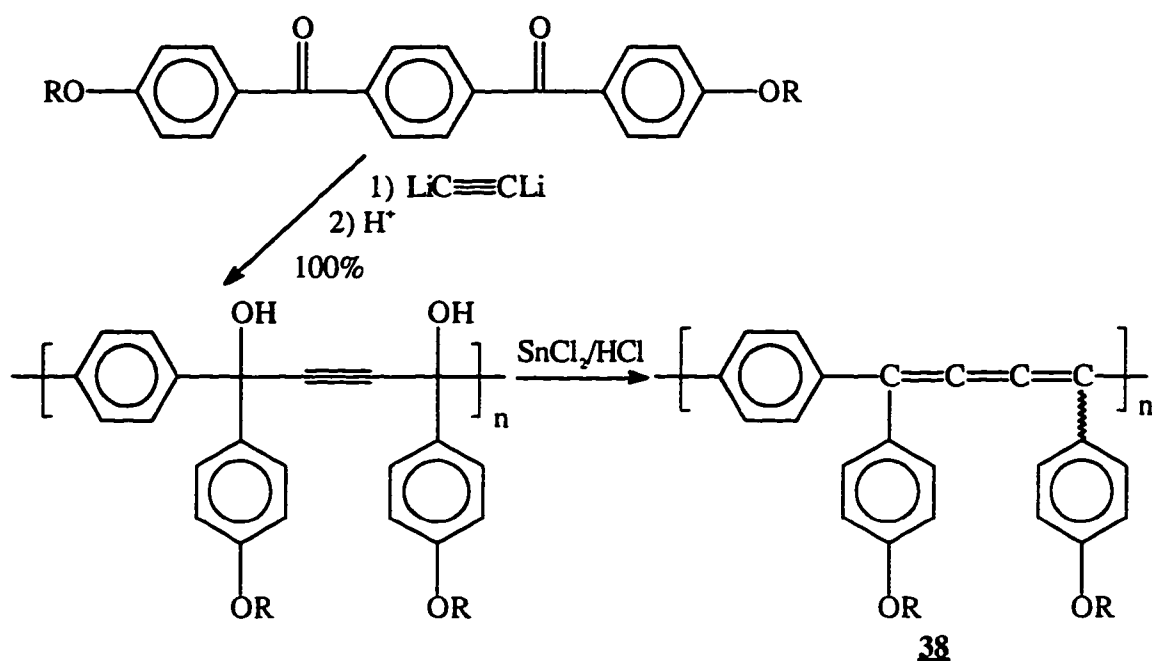


Figure 39: UV/Vis absorption spectra of polymer **36** in THF solution and in the solid state

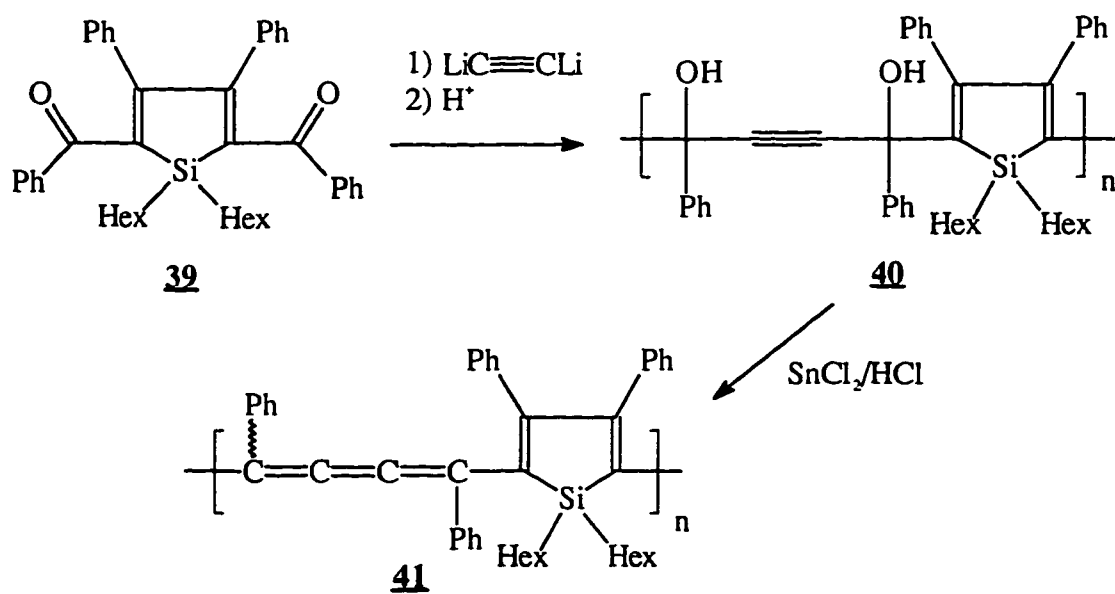
cumulene units. The $\langle\gamma\rangle$ values are comparative to those of polyacetylenes and polydiacetylenes. In 1995, our group first reported the synthesis and study of cumulene-containing polymers (Scheme 29).⁶⁸ It was found that the second hyperpolarizability $\langle\gamma\rangle$ measured for **38** is about two orders of magnitude higher than the cumulene molecule with the highest second hyperpolarizability ($\langle\gamma\rangle = 10^{-31}$ esu) reported by Prasad. Replacement of the phenyl in the main chain of polymer **38** with the silole unit should dramatically enhance nonlinear optical property because polysilole shows the largest $\langle\gamma\rangle$ value according to the calculation.^{53,58} The route (Scheme 30) to polymer **41**, containing silole and butatriene units, was similar to that for polymer **38**.

Several routes were tried to synthesize monomer **39** (Scheme 31). Direct coupling between 2,5-bis(tributylstannyl)silole **42** and benzoyl chloride in the presence of $\text{Pd}(\text{PhCH}_2)(\text{PPh}_3)_2\text{Cl}$ in THF⁶⁹ for 3 days gave no reaction. Steric hindrance may be responsible for this failure. When 2,5-dibromosilole **24** was treated with 2 equivalents of *n*-BuLi, then quenched by either benzonitrile or benzoyl chloride, none of the desired product was isolated in either case. The possible reason for the failure is that 2,5-dibromosilole **24** could not be completely converted into 2,5-dilithiosilole by treatment with 2 equivalents of *n*-BuLi. However, 2,5-dilithiosilole, generated directly from diethynylsilane and 4 equivalents of lithium naphthalenide according to the literature,⁶⁰ was quenched by benzoyl chloride to give the desired product **39** in 30% yield after purification by column chromatography several times.

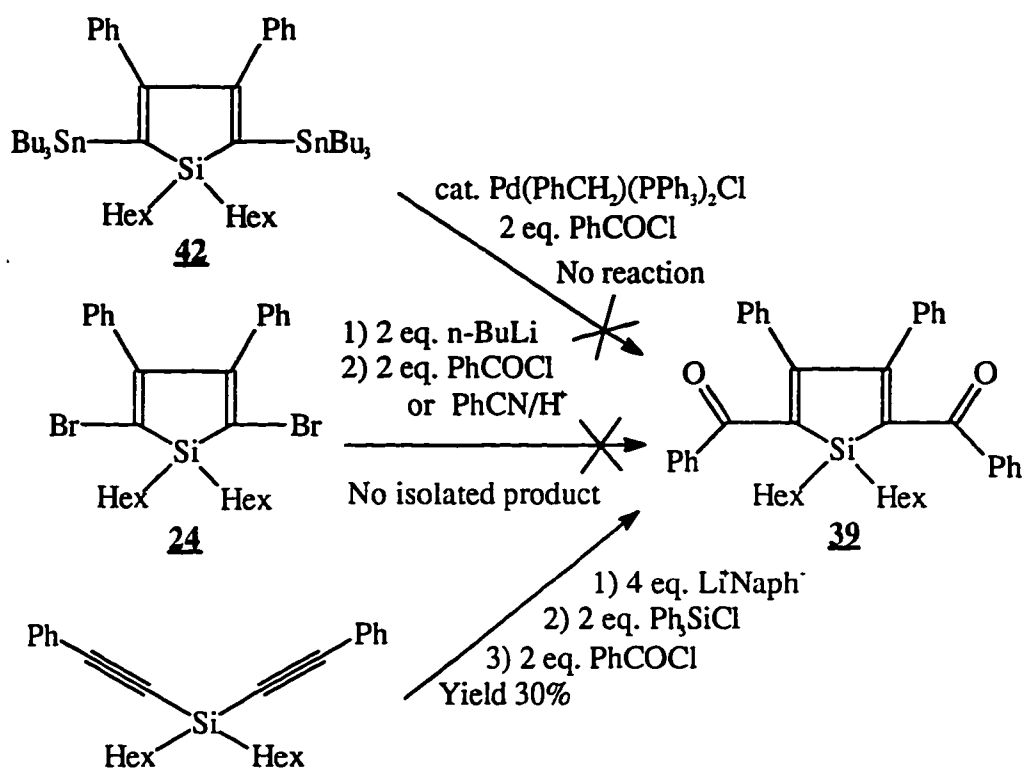
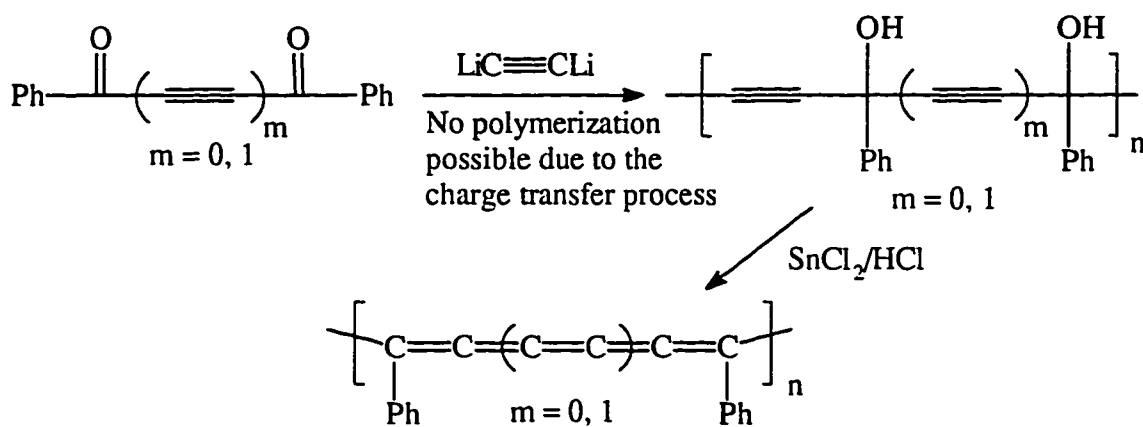
However, polymerization of **39** with dilithium acetylide failed. The reaction of monomer **39** and dilithium acetylene yielded a red/black solid with broad ¹³C-NMR peaks at 127-128 ppm. There is no peaks observed for acetylenic carbons. Further GPC analysis showed the molecular weight was less 1000, indicating no polymerization. A possible explanation is the charge transfer process where one electron was transferred from the dilithium acetylene to silole. This possible charge transfer process was also seen in the attempted preparation of polycumulene carried in our group by using benzil or diketone acetylene and dilithium acetylide (Scheme 32).^{68(b)}



Scheme 29: Synthesis of polymer containing butatriene unit^{68(b)}

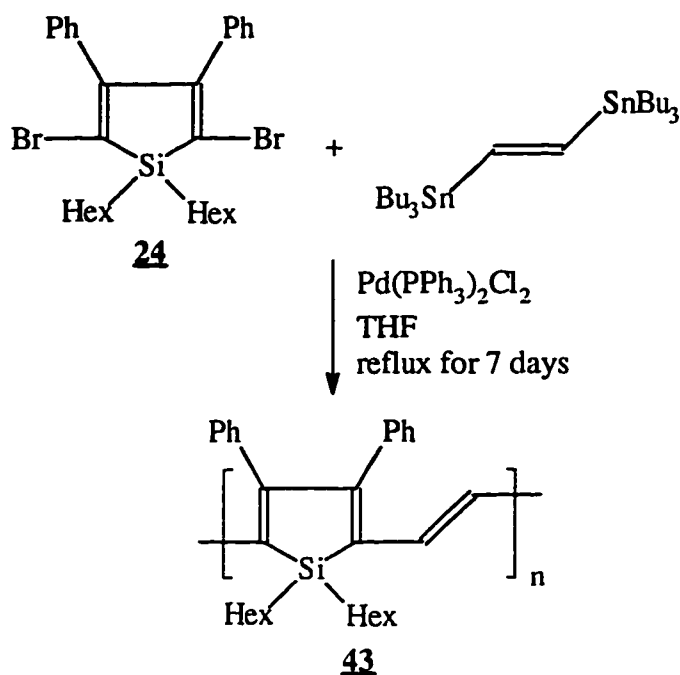


Scheme 30: Proposed route to poly(2,5-silole-1,2,3-butatriene) **41**

Scheme 31: Synthesis of monomer **39**Scheme 32: Attempted synthesis of polycumulene^{68(b)}

Attempted Synthesis of Poly(2,5-silole-1,2-vinylene)

Poly(3,4-diphenyl-1,1-dihexyl-2,5-silole-1,2-vinylene) **43**, which has alternate double bonds on the backbone, is a polyacetylene derivative. Recently, theoretical calculations have shown that σ^* - π^* conjugation, between a π -symmetry σ^* orbital of exocyclic σ bond on silicon and a π^* orbital of the butadiene skeleton, lowers the LUMO level, thus further decreasing the bandgap without decreasing the stability,⁶² and polysilole has the largest second hyperpolarizabilities.⁵⁸ Furthermore, the dialkylsilylene group can provide long side chains to increase the solubility of the polymer. Poly(3,4-diphenyl-1,1-dihexyl-2,5-silole-1,2-vinylene) **43** should exhibit high conductivity and high second order hyperpolarizability like polyacetylene. The synthesis and study of **43** should be of particular interest. The synthesis of polymer **43** was tried by direct coupling between 1,2-bis(tributylstannyl)ethylene⁷¹ and dibromosilole **24** in the presence of palladium catalyst. Thus, the mixture of catalytic Pd(PPh₃)₂Cl₂, bis(tributylstannyl)ethylene and dibromosilole **24** in THF was refluxed for more than 7 days, resulting in a black solution (Scheme 33). After the solvent was removed, the polymer could not be precipitated from MeOH. Only a sticky liquid, which was hard to dry and further purify and characterize, was isolated. The molecular weight of **43** was ~1000 measured by GPC. The number of repeating units is ~3-4. The low reactivity of 2,5-dibromosilole **24** and 1,2-bis(tributylstannyl)ethylene was the main reason. The UV/Vis absorption maximum of its THF solution was only at 420 nm, which is far below the UV/Vis absorption maximum of polyacetylene (495 nm),⁷² poly(3,4-dialkyl-2,5-thiophene-vinylene) (550 nm),⁷³ and even PPV (459 nm).⁵¹ Changing catalyst from Pd(PPh₃)₂Cl₂ to Pd(PPh₃)₄ or to bis[1,2-bis(diphenylphosphino)ethane]-palladium (0) gave similar result. The low reactivity of **24** is the main reason for the failure. Use of compound 2,5-diiodo-silole as a starting material should give polymer **43** with high molecular weight. However, the further attempts to polymer **43** were not carried out.



Scheme 33: Attempted synthesis of poly(2,5-silole-vinylene) **43**

Conclusions

Polysilole attract scientist recently because their theoretical calculations have shown their special electronic property and their attractive applications. Despite the fact that polysilole has not been synthesized, the silole-containing polymers were synthesized and exhibited unique properties. Silole unit can enhance the π -electron overlap along the main chain, lowering the LUMO energy. The values of the UV/Vis absorption maxima of these polymers are always much longer than those of their thiophene and phenyl analogues. The polymers were not significantly photoluminescent and did not dope to high electroconductivity.

Experimental

¹H and ¹³C-NMR spectra were acquired on a Varian VXR-300 spectrometer. In order to assure the quantitative features of the ¹³C-NMR spectra, the relaxation agent chromium(III) acetylacetonate was used in CDCl₃ with a relaxation delay of 5 seconds.

Routine GC-MS spectra were obtained on a Hewlett Packard 5970 GC-IR-MS spectrometer at 70 eV. The exact masses were obtained from a Kratos MS 50 mass spectrometer with 10,000 resolution. The infrared spectra were recorded on a Bio-Rad Digilab FTS-7 spectrometer from neat sample. The UV/Vis spectra were obtained on a Hewlett Packard 8452A diode array UV/VIS spectrometer and λ_{\max} were determined at optical densities of 0.2-0.5.

Polymer molecular weights were determined by gel permeation chromatography (GPC) with 6 Microstyrigel columns in series of 500 Å, 2×10^3 Å, 2×10^4 Å, 2×10^5 Å. THF was used as an eluent at a flow rate of 1 ml/min. The system was calibrated by polystyrene standards. GPC analyses were performed on a Perkin-Elmer series 601 LC equipped with Beckman solvent delivery system, a Walter Associate R401 refractive index detector and a Viscotek viscometer. Differential scanning calorimetry (DSC) analyses were performed on a Du Pont 910 Differential Scanning Calorimeter. The UV/Vis spectra were measured on a Hewlett Packard 8452A Diode Spectrophotometer. Photoluminescence spectra were measured on a FL 900 fluorometer made by Edinburgh.

Toluene and benzene were distilled over CaH_2 . THF was distilled from sodium/benzophenone before use. Other reagents were used as received from Aldrich Chemical Co. without further purification unless specified otherwise. Acetic acid, isopropanol and methanol were used as received from Fisher without further purification. All the reactions were performed under argon atmosphere. Diethynyldihexylsilane was synthesized by reaction of ethynylmagnesium bromide and dichlorodihexylsilane. 2-Trimethylstannylthiophene was synthesized by reaction of 2-bromothiophene with n-BuLi, followed by quenching with chlorotrimethyltin. Bis(tributylstannyl)acetylene or 1,4-bis(tributylstannyl)butadiyne was synthesized by reaction of bis(trimethylsilyl)acetylene or 1,4-bis(trimethylsilyl)butadiyne with (tributyltin) oxid in the presence of catalyst tetrabutylammonium fluoride (TBAF).⁷⁰ 1,2-Bis(tributylstannyl)ethylene was synthesized by hydrostannylation of tributylstannylacetylene with tributyl hydride.⁷¹ 1,4-Bis(trimethylstannylethynyl)benzene **34** was prepared according to the literature by using 1,4-diethynylbenzene, 2 equivalents of n-BuLi and trimethylchlorotin.⁷⁹

Bis(phenylethynyl)dihexylsilane: To a degassed solution of iodobenzene (20.4 g, 0.1 mol) and diethynyldihexylsilane (12.4 g, 50 mol) in Et₃N (30 ml) was added Pd(PPh₃)₂Cl₂ (350 mg) and CuI (140 mg) at room temperature. The mixture was stirred overnight. The salt was removed by filtration and was washed by hexane. After the solvent was removed, the product was purified by column chromatography (hexane as an eluent) (16.5g, yield 82.5%). Mass: cal. *m/z* for C₂₈H₆₀Si = 424.86999, measure (HiRes EI) = 424.86987; ¹H-NMR (300 MHz, CDCl₃): δ 7.539-7.500 (m, 6H), 7.346-7.293 (m, 4H), 1.636-1.278 (m, 16H), 0.950-0.870 (m, 10H); ¹³C-NMR (300 MHz, CDCl₃): δ 132.09, 132.03, 128.07, 128.13, 122.83, 106.53, 89.44, 32.69, 31.50, 23.66, 22.58, 14.81, 14.11

2,5-Bibromo-1,1-dihexyl-3,4-diphenylsilole 24: The procedure was performed according to the literature.⁶⁰ A solution of lithium naphthalenide was prepared by stirring a mixture of naphthalene (7.68 g, 60 mmol) and lithium powder (0.420 g, 60 mmol) in THF (100 ml) for 3 hours at room temperature under argon atmosphere. To the solution of lithium naphthalenide was added a solution of bis(phenylethynyl)dihexylsilane (6.000 g, 15 mmol) in THF (50 ml) dropwise at room temperature, and then the mixture was stirred for 15 minutes. The resulting 2, 5-dilithiosilole solution was cooled to -78⁰C, followed by dropwise addition of a solution of chlorotriphenylsilane (8.835 g, 30 mmol) in THF (50 ml) in order to quench the excess lithium naphthalenide. After stirring for 20 minutes, bromine (4.800 g, 30 mol) was added dropwise to the reaction mixture over 20 minutes at -78⁰C. The resulting yellow-white suspension was gradually warmed up to room temperature and was stirred at room temperature for overnight. After removal of salts and most part of the hexaphenyl disilane produced by filtration, the filtrate was concentrated, followed by addition of saturated aqueous Na₂S₂O₃. The mixture was extracted with ether (200 ml x 2). The combined extract was washed with brine, dried over MgSO₄, filtered and evaporated. The residue was heated to 55⁰C in vacuum (0.5 mmHg) to remove the most naphthalene by sublimation. The residue was purified by column chromatography (hexane as an eluent), followed by crystallization from hexane (5.000 g, yield 60%). m.p. 63⁰C (lit.⁶⁰ 64⁰C); Mass: cal. *m/z* for C₂₈H₆₀⁷⁹Br⁸¹BrSi

= 584.54951, $C_{28}H_{60}^{81}Br_2Si$ = 586.54760, $C_{28}H_{60}^{79}Br_2Si$ = 582.55142, measured (HiRes EI) = 584.467772, 586.54723, 582.55160, respectively; 1H -NMR: δ 7.200-7.100 (m, 10H), 6.963-6.932 (m, 16H), 1.600-1.320 (m, 16H), 1.015 (t, J = 8.4 Hz, 4H), 0.912 (m, J = 6.6 Hz, 6H); ^{13}C -NMR: δ 156.81, 137.17, 128.94, 127.50, 127.34, 121.83, 32.68, 31.41, 22.86, 22.57, 14.13, 9.70

1,1-Dihexyl-3,4-diphenyl-2,5-bis(thienyl)silole 27: To a mixture of 2,5-dibromo-1,1-dihexyl-3,4-diphenylsilole 24 (0.224 g, 0.4 mmol) and 2-trimethylstannyl-thiophene (0.296 g, 1.2 mmol) in THF (15 ml) was added the catalyst $Pd(PPh_3)_2Cl_2$ (28 mg, 0.04 mmol). The solution was refluxed for 2 days. After the solvent was removed, the residue was purified by column chromatography (hexane as an eluent) (0.102 g, yield 37%). Mass: cal. m/z for $C_{36}H_{44}S_2Si$ = 568.96296, measure (HiRes EI) = 568.96270; 1H -NMR: δ 7.05-7.21 (m, 6H), 7.03 (dd, J = 6.0 and 3.0 Hz, 2H), 6.97-7.00 (m, 4H), 6.90 (d, J = 6.0 Hz, 2H), 6.88 (d, J = 3.0 Hz, 2H), 1.19-1.55 (m, 20H), 0.85 (t, J = 6.0 Hz, 6H); ^{13}C -NMR: δ 153.79, 143.13, 139.37, 129.62, 128.39, 127.07, 126.85, 126.14, 125.50; UV/Vis: λ_{max} (THF) = 418 nm

Poly(2,5-thiophene-1,1-dihexyl-3,4-diphenyl-2,5-silole) 26: To a solution of 2,5-dibromo-1,1-dihexyl-3,4-diphenylsilole 24 (1.038 g, 1.854 mmol) and 2,5-bis(trimethylstannyl)thiophene 25 (0.760 g, 1.854 mmol) in THF (25 ml) was added $Pd(PPh_3)_2Cl_2$ (66 mg). The solution was refluxed for 7 days. After the solvent was removed, the polymer was precipitated by adding the polymer solution in THF into methanol (0.249 g, yield 27.8%). 1H -NMR: δ 6.90-7.36(br, 12H), 1.19 (br, 20H), 0.81 (br, 6H); ^{13}C -NMR: δ 153.66, 143.33, 141.39, 129.47, 128.34, 127.22, 32.57, 31.52, 23.53, 22.67, 14.16; GPC: M_w = 2.19×10^3 , M_n = 1.61×10^3 , PD = 1.360; UV/Vis: λ_{max} (THF) = 590 nm, λ_{max} (film) = 620 nm; Emission: λ_{max} = 631 nm, 674 nm, 693 nm (excitation at 510 nm); Electrical conductivity: 4.3×10^{-5} S/cm (doped by I_2)

Poly(1,1-dihexyl-3,4-diphenyl-2,5-silole-ethynylene) 28: To a solution of 2,5-dibromo-1,1-dihexyl-3,4-diphenylsilole 24 (0.527 g, 0.94 mmol) and bis(tributylstannyl)-

acetylene (0.569 g, 0.94 mmol) in THF (10 ml) was added Pd(PPh₃)₂Cl₂ (70 mg). The mixture was refluxed for 36 hours. After THF was removed, MeOH was added to precipitate the product. The precipitate was collected by filtration and then dissolved in small amount of THF. The polymer was precipitate again by adding MeOH (0.37g, yield 93%). The polymer is very deep blue with metallic sheer. ¹H-NMR: δ 7.259, 7.108, 6.997, 1.239, 0.872; ¹³C-NMR: δ 160.78, 138.11, 131.24, 128.93, 126.97, 124.63, 102.82, 32.58, 31.19, 22.87, 22.48, 14.00, 10.64; GPC: M_w = 6.52 x 10³, M_n = 1.81 x 10³, PD = 3.600; UV/Vis: λ_{max} (THF) = 604 nm; Emission: 640 nm and 655 nm (excitation at 550 nm); Electrical conductivity: 2.3 x 10² S/cm (doped by I₂)

2,5-Di(trimethylsilylethynyl)-3,4-diphenylsilole 31: To a degassed solution of 2,5-dibromo-1,1-dihexyl-3,4-diphenylsilole 24 (1.147 g, 2.05 mmol) and Pd(PPh₃)₂Cl₂ (0.230 g)/CuI (0.057 g) in Et₂NH (10 ml)/benzene (10 ml) was added trimethylsilylacetylene (0.602 g, 6.14 mmol). After the mixture was stirred for 4 hours at room temperature, no salt was precipitated. Therefore, 1,8-diazabicyclo-[5,4,0]-undec-7-ene (DBU) (0.685 g, 4.51 mmol) was added into the mixture. The white precipitate was formed immediately. The mixture was stirred for 6 hours. The resulting salt was removed by filtration. After the solvent was removed, the residue was purified by column chromatography (hexane/ethyl acetate = 10:1 as eluents) to afford 31 (0.700 g, yield 57.0%). m.p. 65^oC; Mass: cal. *m/z* for C₃₈H₇₈Si₃ = 619.29382, measure (HiRes EI) = 619.29476; ¹H-NMR: δ 7.24 (br, 8H), 1.74 (m, 4H), 1.57 (m, 4H), 1.48 (m, 8H), 1.18 (t, *J* = 6 Hz, 4H), 1.05 (t, *J* = 4 Hz, 6H), 0.25 (s, 18H); ¹³C-NMR: δ 162.82, 137.42, 129.25, 127.34, 127.04, 123.40, 105.64, 105.12, 32.82, 31.52, 23.21, 22.57, 14.19, 10.74, 0.00

3-Dihexylmethoxysilyl-4,5-diphenyl-octa-3,5-dien-1,7-diyne 32: To a solution of 2,5-bis(trimethylsilylethynyl)-1,1-dihexyl-3,4-diphenylsilole 24 (0.624 g, 1.05 mmol) in MeOH (15 ml)/THF (15 ml) was added a catalytic amount of KOH. The mixture was stirred for 3 hours at room temperature. The solvent was removed and the residue was purified by column chromatography to afford 32 (0.320 g, yield 63.2%). m.p. 60^oC; Mass: cal. *m/z* for C₃₃H₆₅OSi

= 505.96400, measure (HiRes EI) = 505.96320; $^1\text{H-NMR}$: δ 7.77 (dd, $J = 6$ and 2 Hz, 2H), 7.61 (dd, $J = 6$ and 2 Hz, 2H), 7.28 (m, 6H), 6.01 (d, $J = 3$ Hz, 1H), 3.57 (s, 3H), 3.25 (s, 1H), 3.23 (d, $J = 3$ Hz, 1H), 1.56 (m, 4H), 1.38 (m, 16H), 0.98 (t, $J = 18$ Hz, 6H); $^{13}\text{C-NMR}$: δ 164.00, 152.98, 139.71, 136.55, 129.28, 129.16, 128.36, 128.17, 127.66, 127.59, 122.15, 109.08, 85.69, 85.06, 82.90, 81.64, 51.22, 33.07, 31.42, 23.15, 22.54, 14.08, 13.94

Poly(1,1-dihexyl-3,4-diphenyl-2,5-silole-ethynylene-1, 4-phenylene-ethynylene)

33: To a degassed solution of 2,5-dibromo-1,1-dihexyl-3,4-diphenylsilole **24** (0.200 g, 0.443 mmol) and 1,4-bis(trimethylstannylethynyl)benzene **34** (0.248 g, 0.443 mmol) in THF (10 ml) was added $\text{Pd}(\text{PPh}_3)_2\text{Cl}_2$ (18 mg). The mixture was stirred at 50°C for 7 days. After removal of the solvent, the polymer was precipitated by adding the saturated THF solution of the polymer into MeOH (0.188 g, yield 81.0%). $^1\text{H-NMR}$: δ 7.41, 7.21, 6.97, 1.63, 1.45, 1.31, 0.87; $^{13}\text{C-NMR}$: δ 162.40, 137.40, 131.02, 129.06, 126.98, 123.88, 99.19, 92.62, 32.59, 31.28, 23.16, 22.35, 13.93, 10.66; GPC: $M_w = 7.15 \times 10^3$, $M_n = 2.32 \times 10^3$, PD = 3.082; UV/Vis: λ_{max} (THF) = 494 nm, λ_{max} (film) = 526 nm; Emission: 549 nm (excitation at 430 nm); Electrical conductivity: 4.3×10^{-3} S/cm (doped by I_2)

Bis(trimethylstannylethynyl)-dimethylsilane 35: To a solution of diethynyldimethylsilane (4.310 g, 40 mmol) in THF (80 ml) was added EtMgCl (87.7 mmol, 43.8 ml, 2.0 M in THF) at -78°C dropwise. The mixture was allowed to warm to room temperature, and then refluxed for 2 hours. The solution was again cooled to -78°C . A solution of chlorotrimethyltin (87.7 mmol, 87.7 ml, 1.0 M in hexane) was added dropwise. The mixture was allowed to warm to room temperature and stirred overnight. A saturated NH_4Cl aqueous solution (100 ml) was added. The aqueous layer was extracted by ether (100 ml x 2). The combined organic layer was washed with water, dried with MgSO_4 . After the solvent was removed, the product was purified by crystallization from hexane (10.600 g, yield 61.2%). Mass: cal. m/z for $\text{C}_{12}\text{H}_{24}\text{SiSn}_2 = 433.82806$, measure (GC-MS): 415.85 (41.47%) (M^+-15), 416.85 (36.60%) (M^+-15), 417.85 (86.09%) (M^+-15), 421.85 (80.29%) (M^+-15), 420.85 (46.95%) (M^+-15), 419.85 (95.45%) (M^+-15), 418.85 (58.56%) (M^+-15), 162.35

(24.25%), 163.35 (75.13%), 164.35 (28.24%), 165.35 (100%), 167.35 (15.62%); $^1\text{H-NMR}$: δ 0.28 (s, 6H), 0.25 (s, 18H); $^{13}\text{C-NMR}$: δ 114.97, 113.62, 0.89, -7.68

Poly(1,1-dihexyl-3,4-diphenyl-2,5-silole-ethynylene-dimethylsilylene-ethynylene)

36: To a degassed solution of 2,5-dibromo-1,1-dihexyl-3,4-diphenylsilole **24** (1.074 g, 1.917 mmol) and bis(tributylstannylethynyl)dimethylsilane **35** (0.831 g, 1.917 mmol) in THF (25 ml) was added $\text{Pd}(\text{PPh}_3)_2\text{Cl}_2$ (66 mg). The mixture was refluxed for 7 days. After the solvent was removed, the polymer was precipitated by adding the saturated THF solution of the polymer into MeOH to afford a deep brown solid (0.501 g, yield 51.6%). $^1\text{H-NMR}$: δ 7.09 (br, 10H), 1.55, 1.38, 1.01, 0.87, 0.16; $^{13}\text{C-NMR}$: δ 162.86, 136.78, 128.79, 126.66, 122.92, 105.43, 101.70, 32.39, 31.03, 22.75, 22.16, 13.75, 10.29, 0.10; GPC: $M_n = 5.39 \times 10^3$, $M_w = 4.77 \times 10^3$, PD = 1.129; UV/Vis: λ_{max} (THF) = 400 nm, λ_{max} (film) = 426 nm; Electrical conductivity: 4.6×10^{-6} S/cm (undoped), 5.4×10^{-5} S/cm (doped by I_2)

2,5-Bisbenzoyl-1,1-dihexyl-3,4-diphenylsilole 38: 1, 1-Dihexyl-3,4-diphenyl-2,5-dilithiosilole was prepared from bis(phenylethynyl)dihexylsilane (4.000 g, 10 mmol) and lithium naphthalenide (40 mmol) in THF (70 ml) after excess lithium naphthalenide was quenched by triphenylchloride (5.900 g, 20 mmol) as described in preparation of 2,5-dibromo-1,1-dihexyl-3,4-diphenylsilole **24**. Then the mixture was cooled to -78°C . Benzoyl chloride (2.810 g, 20 mmol) was added dropwise. The mixture was allowed to warm to room temperature and was stirred overnight. The resulting white precipitate was removed by filtration. A NH_4Cl aqueous solution was added. The aqueous layer was extracted by Et_2O (100 ml x 2). The combined organic layer was dried with MgSO_4 . After the solvent was removed, the naphthalene was removed by vacuum sublimation at 55°C . The residue was purified by column chromatography 4 times to afford a yellow solid (1.830 g, yield 30%). m.p. 67°C ; Mass: cal. m/z for $\text{C}_{47}\text{H}_{70}\text{OSi}$ = 635.10220, measure (HiRes EI) = 635.10271; $^1\text{H-NMR}$: δ 7.66 (dd, $J = 9$ and 3 Hz, 4H), 7.30 (m, 2H), 7.18 (m, 6H), 6.89 (d, $J = 1$, 4H), 6.85 (dd, $J = 15$ and 3 Hz, 4H), 1.40 (m, 4H), 1.26-1.07 (m, 16H), 0.81 (t, $J = 6$ Hz, 6H); ^{13}C -

NMR: δ 199.29, 156.74, 145.62, 137.08, 132.43, 129.03, 127.91, 127.49, 127.26, 32.90, 31.20, 23.63, 22.39, 4.01, 11.36

III: SYNTHESIS, CHARACTERIZATION AND STUDY OF SILICON-BRIDGED AND BUTADIENE-LINKED POLYTHIOPHENES

Literature Survey

Conducting polymers are at present intensively studied because of their potential technological application.^{1,2} The modern era of conducting polymers began at the end of the 1970s when Heeger and MacDiarmid discovered that polydiacetylene, synthesized by Shirakawa's method,⁸⁰ could increase a 12 order of magnitude of conductivity upon charge-transfer oxidative doping.⁸¹ However, polyacetylenes are environmental unstable, which constitutes a major obstacle to practical applications. Recent interest in conducting polymers have shifted to poly(heterocycles) because of their higher environmental stability and structure versatility which allows the modulation of their electronic and electrochemical properties by manipulation of the monomer structure.

An important step in the development of conjugated poly(heterocycles) occurred in 1979 when it was shown that highly conducting and homogeneous free-standing films of poly(pyrrole) could be produced by oxidative electropolymerization of pyrrole.⁸² Since then, the electrochemical polymerization has been rapidly extended to other aromatic compounds such as thiophene,^{83, 84} furan,⁸⁴ indole, carbazole, azulene, pyrene,⁸⁵ benzene,⁸⁶ fluorene,⁸⁷ and aniline. Among them, polythiophenes have rapidly become a "hot subject" for their potential applications. These applications include rechargeable battery electrodes, electrochromic devices,^{88(a, b)} chemical and optical sensors,^{88(c)} light-emitting diodes,^{24(c), 88(d)} molecular-based devices,^{88(e, f)} and nonlinear optical active materials.^{10, 88(g, h)}

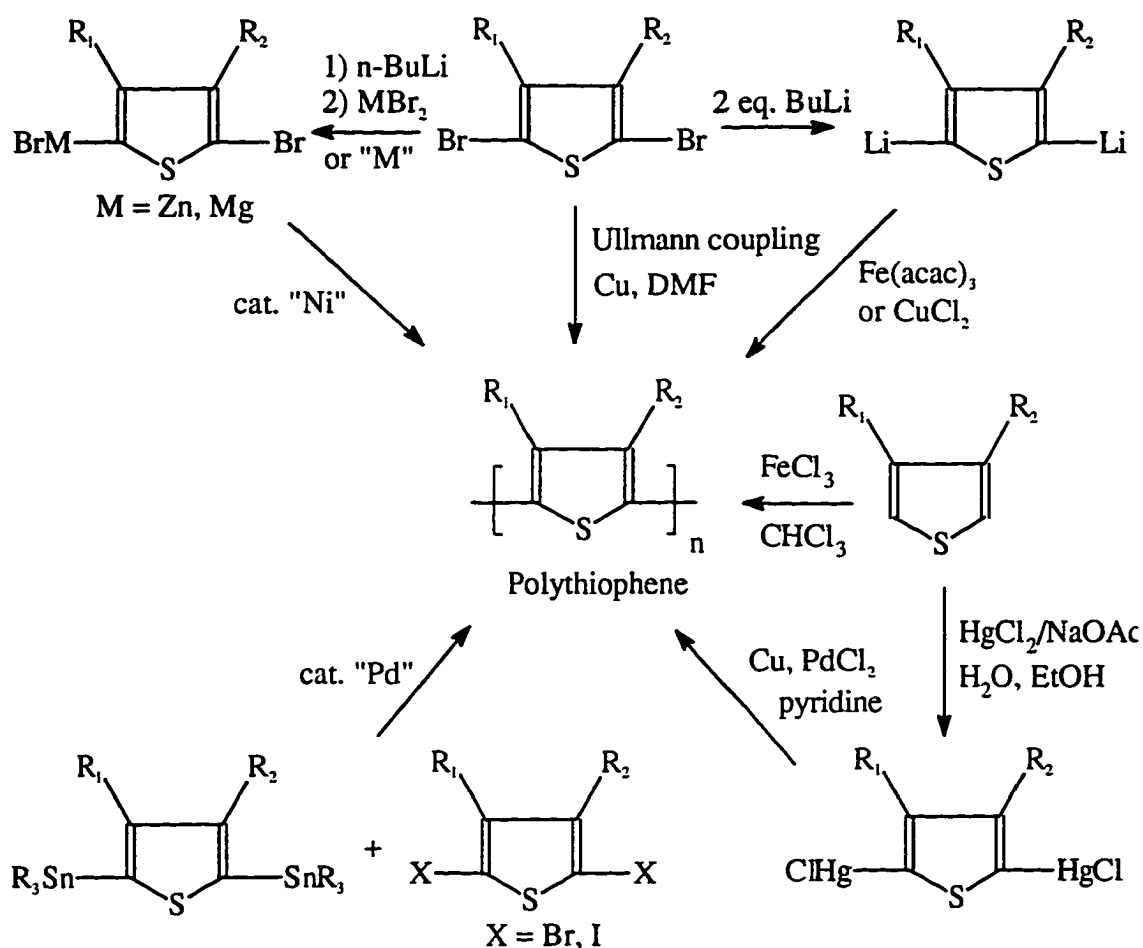
Polythiophenes have already been considered in several reviews devoted to conducting polymers in general or to some of their more specific aspects such as electropolymerization,⁸⁹ electrochemistry,⁹⁰ environmental stability,⁹¹ or optical properties.^{88(a)} There are two reviews which focused only on polythiophenes in 1986^{9(a)} and 1992.^{5(a)} However, considerable progress has been accomplished in their preparation and characterization of their structures

and electronic and electrochemical properties, and the essential part of the work on functional polythiophenes and their practical applications in the past several years.

Polythiophenes are usually prepared by either electrochemical polymerization or chemical polymerization. The chemical polymerization is usually carried out in an electric cell. Noble metals such as platinum and gold, and optically transparent tin oxide or indium-tin oxide (ITO) are used as electrodes. The solvents employed are anhydrous aprotic solvents of high dielectric constants and low nucleophilicities, such as acetonitrile, benzonitrile, nitrobenzene and propylene carbonate. These solvents lead to highest current efficiency of electropolymerization. The electrolytes are anions, derived from strong acids such as ClO_4^- , PF_6^- , BF_4^- and AsF_6^- , associated with lithium or tetraalkylammonium cations. The solution is prepared by dissolving the monomer and electrolyte in the solvent in about 0.1-0.5 M concentration in a three-electrode cell (third electrode as a reference) and degassed. Polythiophenes are generally grown on the electrode in potential static or galvanostatic conditions and by recurrent potential sweeps, or current pulses.

The chemical syntheses are the most adequate methods of preparation of oligomers of defined structures. Several methods have been developed for preparation of polythiophenes (Scheme 34). Ni-catalyzed polycondensation of 2-bromo-5-(bromozincio)-thiophene⁹² or 5-(2-bromo-thienyl)-magnesium bromide,⁹³ generated from either oxidative addition of Zn or Mg to 2,5-dibromothiophene or metathesis of the corresponding organolithium reagents with ZnBr_2 or MgBr_2 , and Pd-catalyzed polycondensation of 2,5-dihalothiophene with 2,5-distannylthiophene, are the most used methods. Oxidative coupling of 2,5-dilithiothiophene in the presence of $\text{Fe}(\text{acac})_3$ or CuCl_2 ⁹⁴ is much simpler than Ni or Pd-catalyzed coupling, but gives lower molecular polymers (Scheme 34). Oxidative coupling of 2,5-dilithiothiophene and Ni or Pd-catalyzed coupling can ensure the 2,5-linkage necessary for conjugation. However, all these methods require extremely pure monomers and can not tolerate electrophilic functional groups. Recently, direct slow oxidative polymerization of thiophene using FeCl_3 as an oxidant⁹⁵ was developed and widely used for preparation of polythiophenes because it doesn't need pure monomers, is easy and suitable for large scale production, and gives high molecular weight polymers (Scheme 34). But it also result in conjugation-breaking α - β '

links,⁹⁶ chloride substitution,⁹⁷ or iron impurities which enhance oxidative degradation.⁹⁸ In order to synthesize polythiophene with electron-withdrawing substituents directly attached to the thiophene and with substituents having electrophilic groups such as acids, esters and carbonyls, several novel methods were developed recently. In 1995, polythiophenes with a carbonyl group directly attached to the ring were prepared via an Ullman reaction by refluxing 2,5-dibromothiophene with activated Cu in DMF (Scheme 34).⁹⁹ The other method is oxidative coupling of 2,5-bis(chloromercurio)-3-alkylthiophene by Cu and PdCl₂.¹⁰⁰ These two methods, however, gave regiorandom polymers when 3-substituted thiophene was used as a monomer, which may result in an out-of-plane conformation for the units along the polymer chain.



Scheme 34: Chemical preparation of polythiophenes

A variety of polythiophenes with functionalized substituents have been synthesized. The functional groups can be introduced into the 3- or 4-position to increase the solubility of the polymer and provide special properties to polythiophene. The most studied polythiophenes are the 3-substituted polythiophenes (Figure 40). 3-Substituted polythiophenes display properties superior to those of 3,4-disubstituted polythiophenes because of their less steric effects between substituents grafted on adjacent thiophene. An ethereal or thioethereal side chain allows the fine-tuning of electrical and optical properties of polythiophene.¹⁰¹ A crown ether side chain results in ionochromic activity in the polythiophene.¹⁰² A chiral side chain yields an optically active polythiophene.¹⁰³ An alkanesulfonic acid side chain produces a water-soluble self-doping conducting polymer.¹⁰⁴

Fused ring systems (Figure 41) have also been prepared, mainly by electrochemical polymerization.^{5(a)} These ring systems, which have a bridge to enhance planar structures, have lower bandgaps than 3-substituted polythiophenes. Poly(isothianaphthene) has been shown to

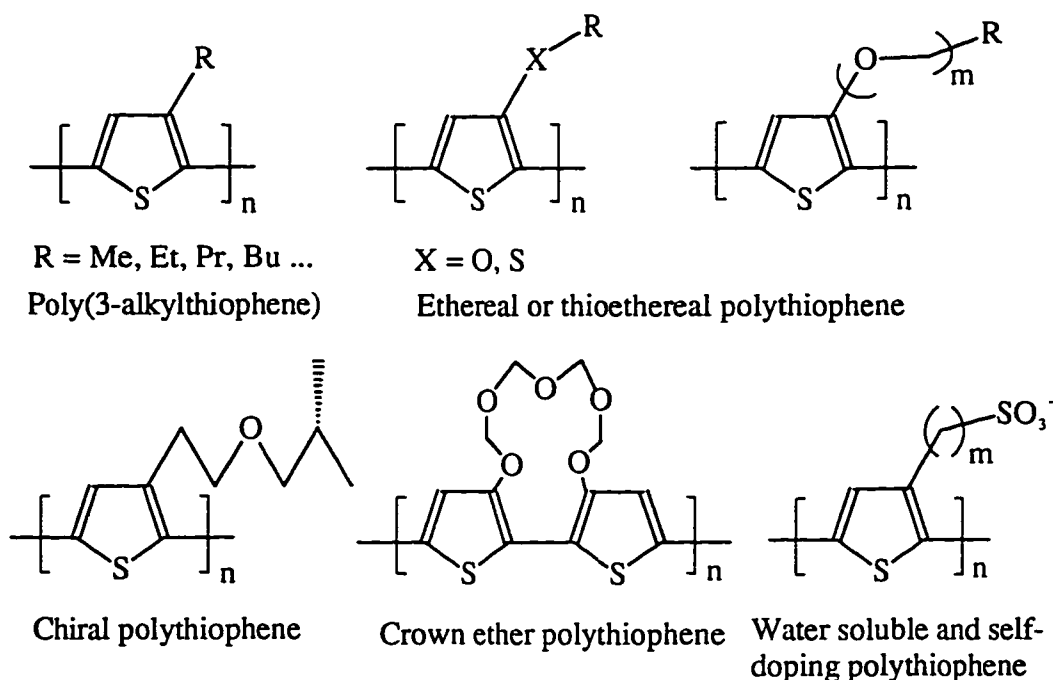


Figure 40: Examples of 3-substituted polythiophene

We designed polythiophene **51** having a bridging silicon unit (Figure 42). The bridge, dialkylsilylene, not only provides two big alkyl groups to increase the solubility, and enhances the planar structure of the polymer, but also fully interacts with the π -orbitals, decreasing the bandgap energy. The polymer structure can also be viewed as containing a silole unit. This silicon-bridged polythiophene should have a very low bandgap, and therefore high conductivity and other special properties.

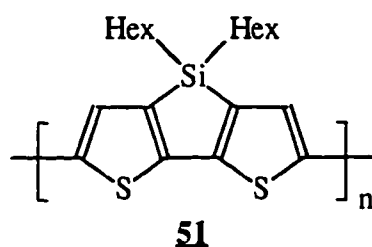
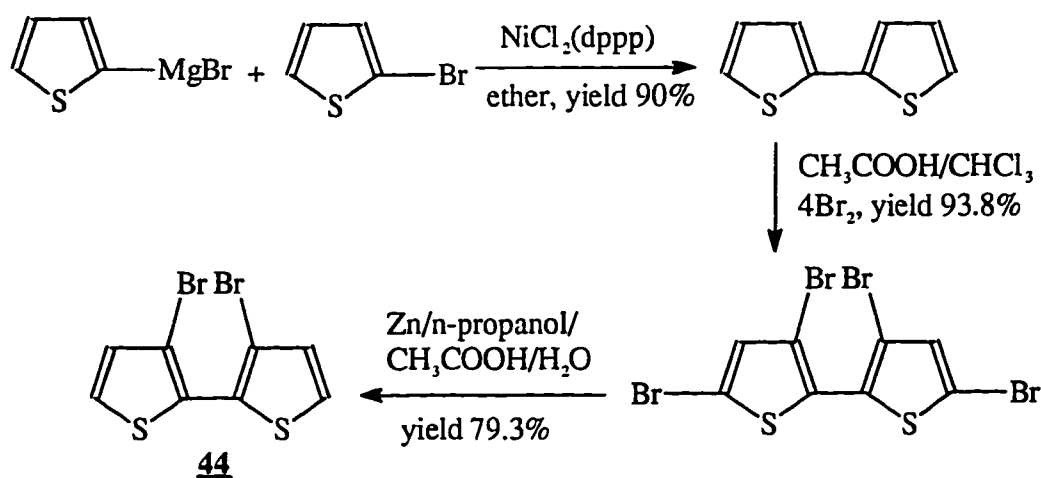


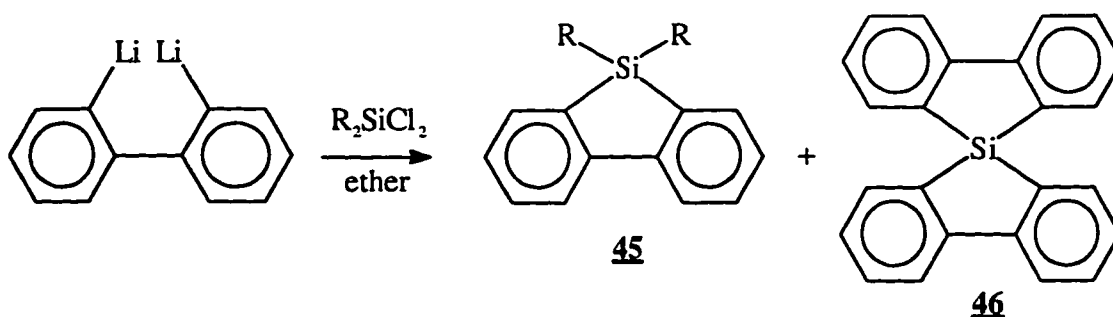
Figure 42: The design of silicon bridged polythiophene

Synthesis and Characterization. The key compound leading to the silicon-bridged polythiophene **51** was designed as silicon-fused bithiophene **48**. First, 3,3'-dibromo-2,2'-bithiophene **44** was synthesized starting with 2-bromothiophene (Scheme 35) according the literature.¹⁰⁵



Scheme 35: Synthesis of 3,3'-dibromo-2,2'-bithiophene **44**¹⁰⁵

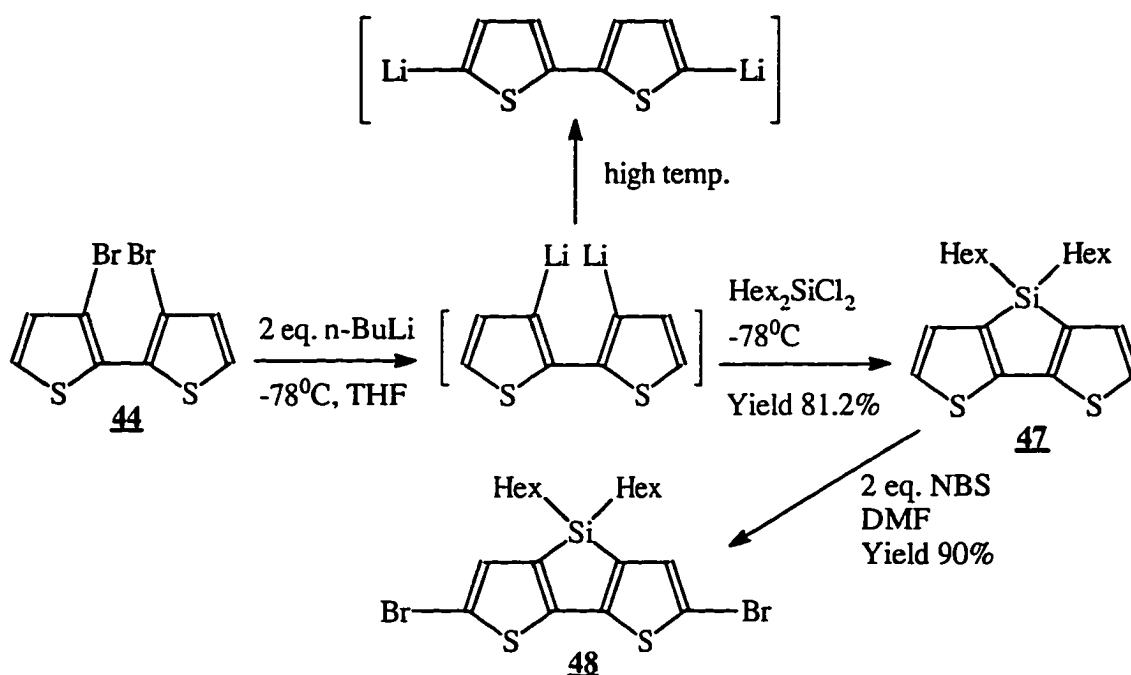
In 1955, Gilman developed a method to synthesize 9-silafluorenes **45** by a reaction of 2,2'-dilithiobiphenyl, generated from 2,2'-dibromobiphenyl and 2 equivalents of *n*-BuLi, with R_nSiCl_n ($n = 2-4$) (Scheme 36).¹⁰⁶ The reaction was carried out by slow addition of a 2,2'-dilithiobiphenyl solution into a refluxing R_nSiCl_n ether solution. When dialkyldichlorosilanes (R_2SiCl_2) were used, the yields were very low (18-25%) with byproduct **46** being formed. When $RSiCl_3$ or $SiCl_4$ was used, the yields were improved to higher than 70%, and the product 9-chloroalkyl- (or dichloro-)silafluorene could be transformed into 9-dialkylsilafluorene **45** by reacting it with alkyllithium or Grignard reagents.



Scheme 36: Synthesis of 9-silafluorene¹⁰⁶

The synthesis of 3,3'-dihexylsilylene-2,2'-bithiophene **47** was first tried by using Gilman's procedure. A 3,3'-dilithio-2,2'-bithiophene solution, generated from 3,3'-dibromo-2,2'-bithiophene **44** and 2 equivalents of *n*-BuLi at $-78^{\circ}C$, was added into a refluxing dichlorodihexylsilane solution. After work-up, the yield was only 10%. We rationalized that 3,3'-dilithio-2,2'-bithiophene was not stable at high temperature. It would easily undergo metal-hydrogen exchange to give more stable 5,5'-dilithio-2,2'-bithiophene.¹⁰⁷ The reaction condition was then modified by directly adding dichlorodihexylsilane into a 3,3'-dilithio-2,2'-bithiophene solution at $-78^{\circ}C$ and keeping the solution stirring at $-78^{\circ}C$ for 5 hours (Scheme 37). After then, the reaction mixture was allowed to warm to room temperature and stirred at room temperature overnight. The yield of **47** was improved up to 81.2%.

Compound **47** was then converted to 5,5'-dibromo-3,3'-dihexylsilylene-2,2'-bithiophene **48** by reacting it with 2 equivalents of NBS in DMF in 90% yield (Scheme 37). It was important that the solution was stirred at room temperature for less than 20 minutes. The longer stirring time resulted in the desilated product.



Scheme 37: Synthesis of 3,3'-dihexylsilylene-2,2'-bithiophene **47** and 5,5'-dibromo-3,3'-dihexylsilylene-2,2'-bithiophene **48**

Compounds **47** and **48** have blue luminescence in THF solution. The UV/Vis absorption maximum (λ_{max}) of **47** is 338 nm, which is much larger than those of bithiophenes, such as 2,2'-bithiophene (302 nm), 3,4'-dimethyl-2,2'-bithiophene (302 nm) and 3,3'-methylene-2,2'-bithiophene (312 nm), but still smaller than those of dithieno[3,2-b:2'3'-d]thiophene (346 nm) and cyclopenta[2,1-b:3',4'-b']dithiophene-4-one (474 nm) (Figure 43). The λ_{max} of **47** is 26 nm longer than that of its carbon analog 3,3'-methylene-2,2'-bithiophene. The UV/Vis absorption maximum of **48** was 358 nm, 20 nm longer than that of **47**. The λ_{max} values of **47** and **48** show that silicon has more effect on electronic structure than carbon by dramatically lowering the LUMO energy.

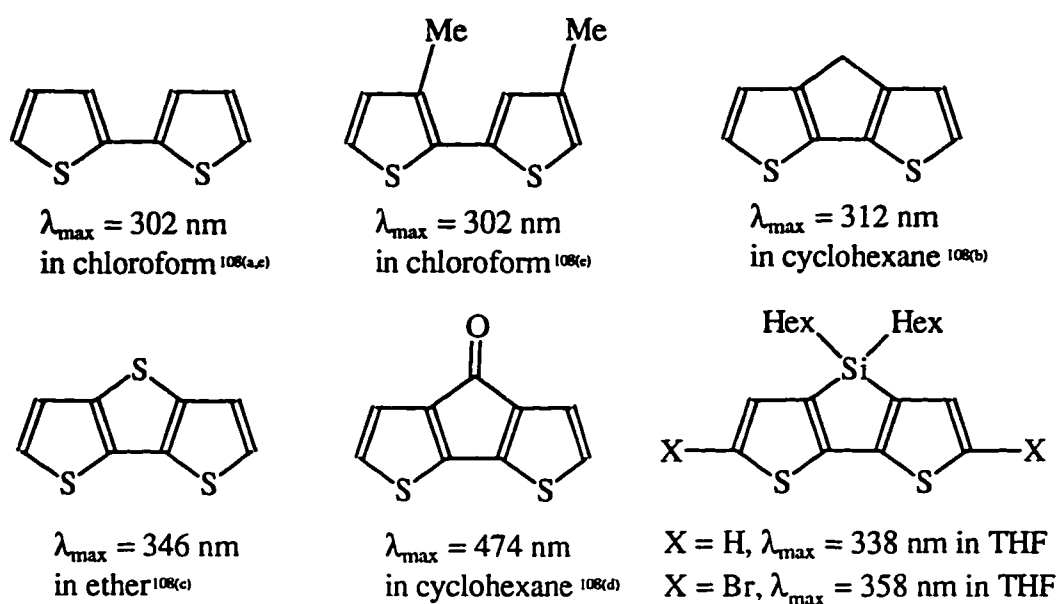


Figure 43: The bithiophenes and their UV/Vis absorption

Other evidence showing that a silicon group induces a bathochromic shift is found in a 1992 paper by Tour's group.¹⁰⁹ Tour et al. synthesized and studied a series of trimethylsilyl-capped α -oligothiophenes (Figure 44). It was found that the λ_{\max} values of trimethylsilyl-capped α -oligothiophenes were usually larger than those of non-capped α -oligothiophenes. They rationalized that $d\pi$ - $p\pi$ -conjugation contributed to these differences. It is surprising that the λ_{\max} (338 nm) of compound **47** is 18 nm longer than that of 5,5'-bis(trimethylsilyl)-2,2'-bithiophene (320 nm) because 5,5'-bis(trimethylsilyl)-2,2'-bithiophene has two silicon units while **47** has only one. This shows that the bridged silicon group enhances the planarity and participates in conjugation more effectively than a terminal silicon group.

Compound **48** was used as a monomer to couple with 2,5-bis(trimethylstannyl)-thiophene in the presence of catalytic $\text{Pd}(\text{PPh}_3)_2\text{Cl}_2$ to give a silicon-bridged polythiophene **49** (Scheme 38). The reaction was carried out in refluxing THF for 7 days. After the solvent was removed, polymer **49** was precipitated from MeOH to obtain a black metallic solid. Polymer **49** was very soluble in organic solvents such as CHCl_3 , CH_2Cl_2 , THF, and toluene,

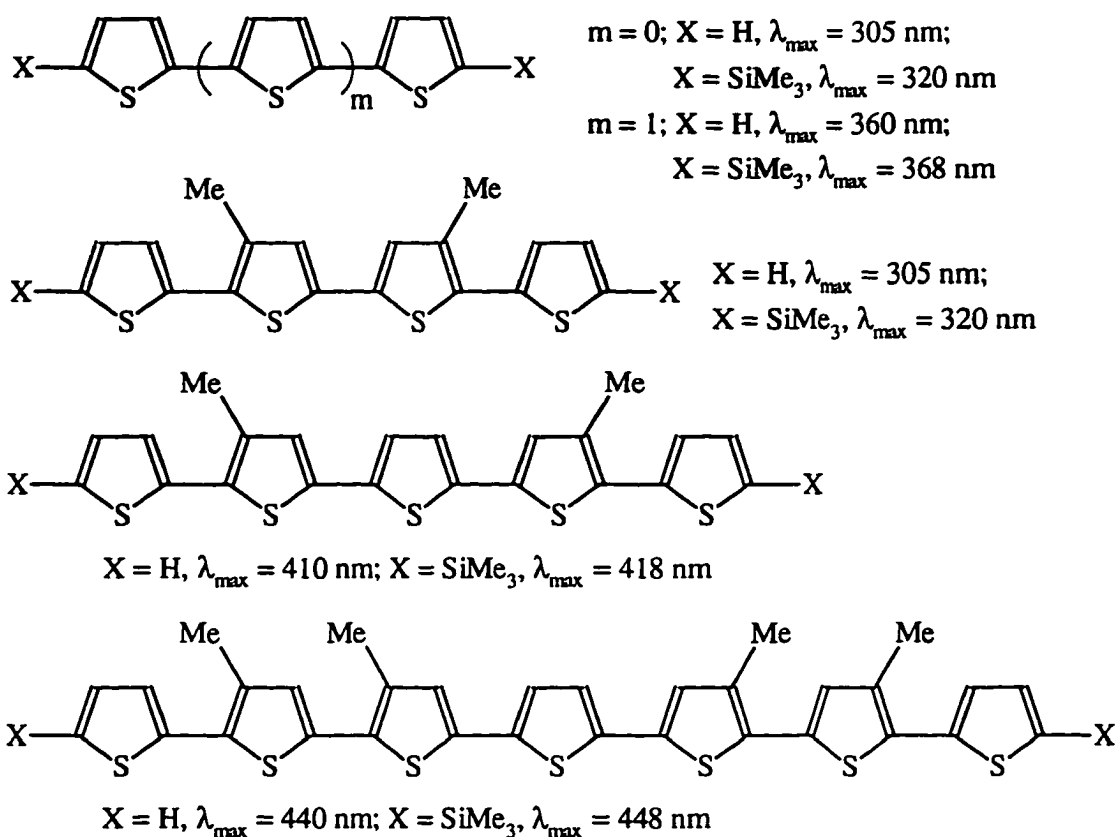
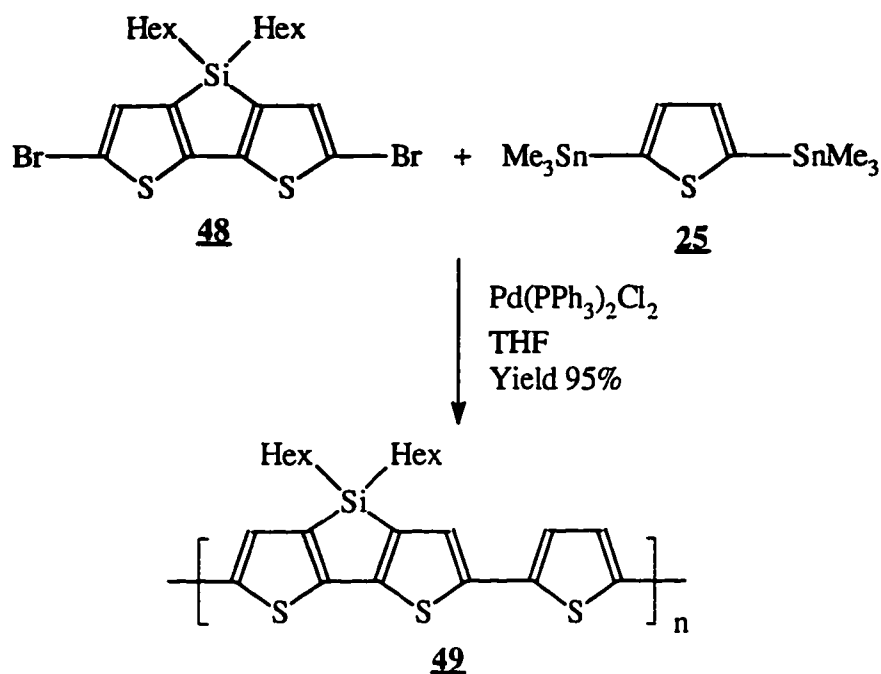


Figure 44: Trimethylsilyl-capped and non-capped oligothiophenes and their UV/Vis absorption¹⁰⁹

and gave a reddish solution in THF. The polymer film, made from a THF solution by evaporating the solvent slowly, was very smooth and deep red with a metallic luster.

Polymer **49** was characterized by ¹H- and ¹³C-NMR (Figure 45) and GPC. The ¹H-NMR spectrum shows a broad peak at ~7.10 ppm for the protons of thiophene and two broad peaks at ~1.29 and 0.89 ppm for the hexyl protons. The ¹³C-NMR spectrum shows exactly six peaks between 148 and 124 ppm corresponding to the six thiophene carbons (due to the symmetry of the polymer, only six thiophene carbons show the peaks in the repeating unit), and six hexyl carbons between 33 and 11 ppm. The six thiophene peaks are assigned to the six thiophene carbons as shown in Figure 45. The GPC chromatogram shows a main peak overlapping with a small shoulder, indicating that polymer **49** contains polymers of two different lengths. The weight molecular weight of polymer **49** is 3.16×10^4 and PD is 3.21.



Scheme 38: Synthesis of silicon-bridged polythiophene **49**

The synthesis of silicon-bridged polythiophene **51** was tried by different methods. Direct slow oxidative polymerization of 3,3'-dihexylsilylene-2,2'-bithiophene **47** with FeCl_3 in CHCl_3 (Scheme 33) gave a low molecular weight polymer in very low yield (10%). The ^1H - and ^{13}C -NMR spectra showed that the polymer lost the silicon bridge. It is believed that polymerization of thiophene with FeCl_3 in CHCl_3 involves a radical or a carbocation intermediate and produces HCl gas as a byproduct. Under these conditions, the desilylation could easily happen by either radicals (or carbocations) or HCl during the polymerization. Ullman reaction by refluxing **48** with activated Cu powder in DMF for 6 days (Scheme 34) also gave a low molecular weight polymer. Oxidative coupling of 5,5'-dilithio-3,3'-dihexylsilylene-2,2'-bithiophene, generated from either **48** and 2 equivalents of $n\text{-BuLi}$ or **47** and 2 equivalents of $n\text{-BuLi/TMEDA}$, with $\text{Fe}(\text{acac})_3$ also caused the desilylated product. The only good method is palladium-catalyzed coupling of monomer 5,5'-bis(trimethylstannyl)-3,3'-dihexylsilylene-2,2'-bithiophene **50** with 5,5'-dibromo-3,3'-dihexylsilylene-2,2'-bithiophene **48** (Scheme 35).

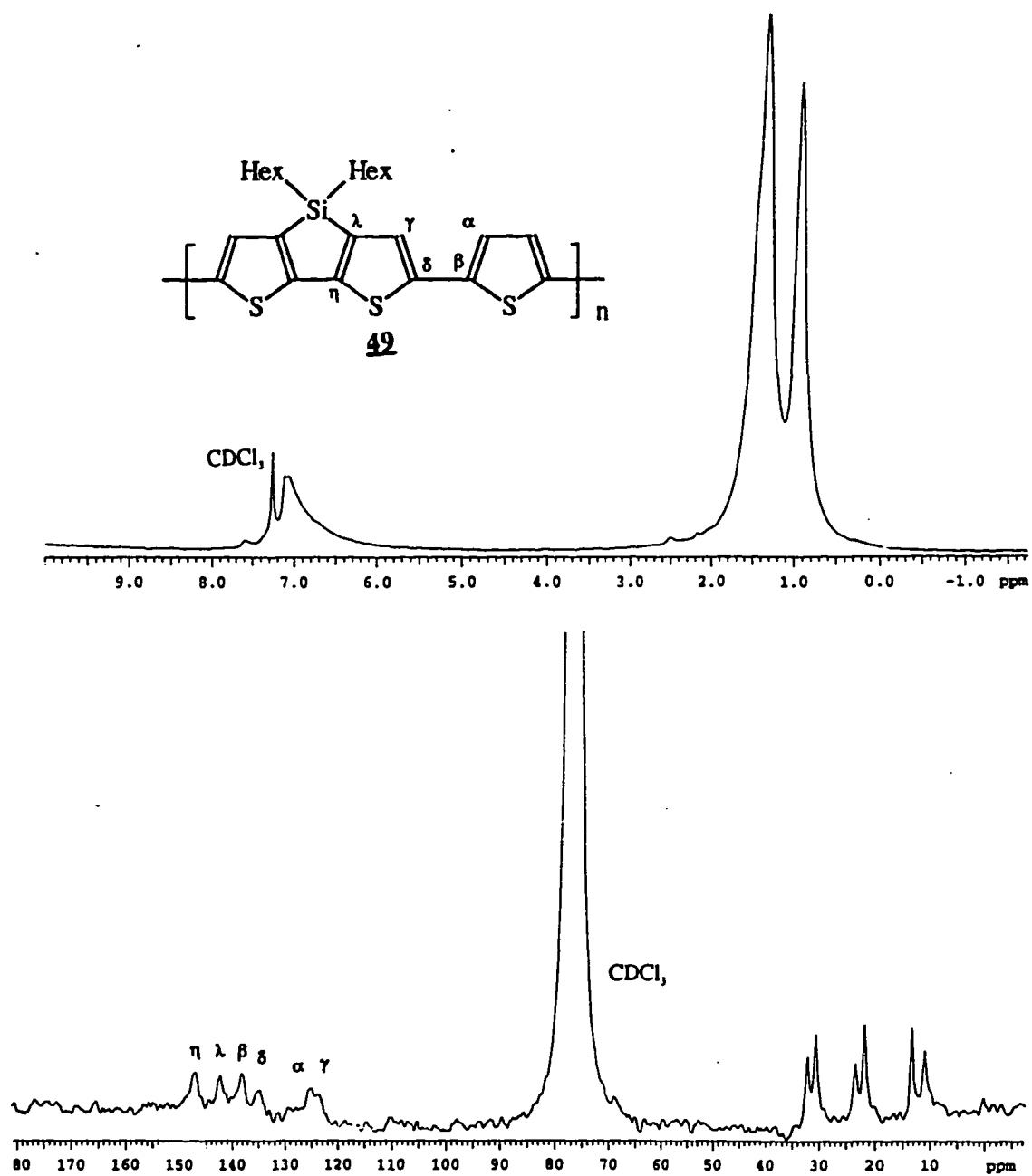


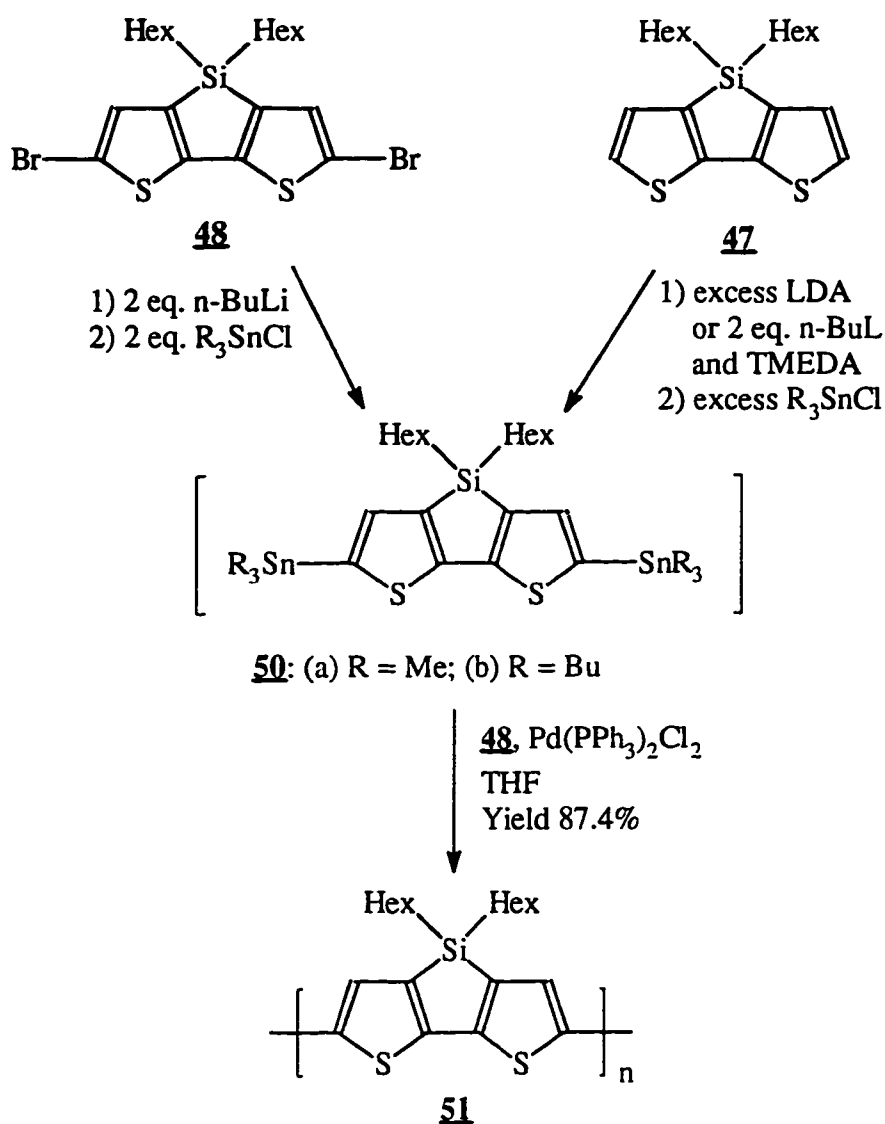
Figure 45: The ^1H - and ^{13}C -NMR spectra of polymer **49**

However, the synthesis of monomer 5,5'-bis(trialkylstannyl)-3,3'-dihexylsilylene-2,2'-bithiophene **50** was painful. First, 5,5'-dibromo-3,3'-dihexylsilylene-2,2'-bithiophene **48** was reacted with 2 equivalents of n-BuLi, followed by quenching with excess Bu₃SnCl. TLC showed only one spot, which had almost the same R_f as the debrominated compound **47**. The product, after purification by column chromatography, was confirmed as **47** by NMR. Second, direct metathesis of **47** with 2 equivalents of n-BuLi/TMEDA or excess LDA, followed by quenching with excess Bu₃SnCl, after purification by column chromatography, still failed to give the desired product **50** and gave the starting material **47** instead. Third, palladium-catalyzed reaction of **48** with excess hexabutylditin¹¹¹ also gave the product **47** after column chromatography. After all above failures, we realized that the product **50** had the same R_f as **47** and the destannylation could happen during the purification by column chromatography.

Thus compound **50** was assumed to be obtained in 100% yield by either direct metathesis of **47** with excess LDA or treatment of **48** with 2 equivalents of n-BuLi, followed by quenching with excess Me₃SnCl, and was used without further purification to couple with **48** in the presence of Pd(PPh₃)₂Cl₂ catalyst (Scheme 39). Indeed, after the mixture was refluxed in THF for 7 days, the desired polymer **51** was obtained in 87.4% yield. Polymer **51** is a black solid which is very soluble in common organic solvent such as THF, toluene, chloroform, and methylene chloride. The THF solution is purple with red luminescence.

Polymer **51** was characterized by ¹H- and ¹³C-NMR and GPC. The ¹H-NMR spectrum shows only one peak at 7.10 ppm for the thiophene protons, and the hexyl protons between 1.24 and 0.85 ppm. The ¹³C-NMR spectrum shows clearly only four sp² thiophene carbons between 147.16 and 125.68 ppm and six sp³ hexyl carbons between 32.65 and 11.56 ppm (Figure 46). The GPC shows the molecular weight of polymer **51** is 2.03 × 10⁴ (PD = 1.896).

Thermal Behavior. The thermal behavior of polymers **49** and **51** was studied by thermogravimetric analysis (TGA) and differential scanning calorimetric analysis (DSC) under argon atmosphere. The TGA was performed from room temperature to 800°C with a ramp of 15°C/min. From the TGA spectra (Figure 47), polymers **49** and **51** have similar thermal



Scheme 39: Synthesis of Silicon-bridged polythiophene **51**

stabilities. They starts to lose weight rapidly at about 430°C . Polymer **49** slowly loses weight after 600°C and has a 70% char yield at 800°C , while polymer **51** slowly loses weight after 532°C and has a 59% char yield at 800°C .

The thermal transitions of polymers **49** and **51** were studied by DSC. Polymer **49** has endothermic peaks at $\sim 278^\circ\text{C}$ and 497°C and an exothermic peak at $\sim 302^\circ\text{C}$ before it

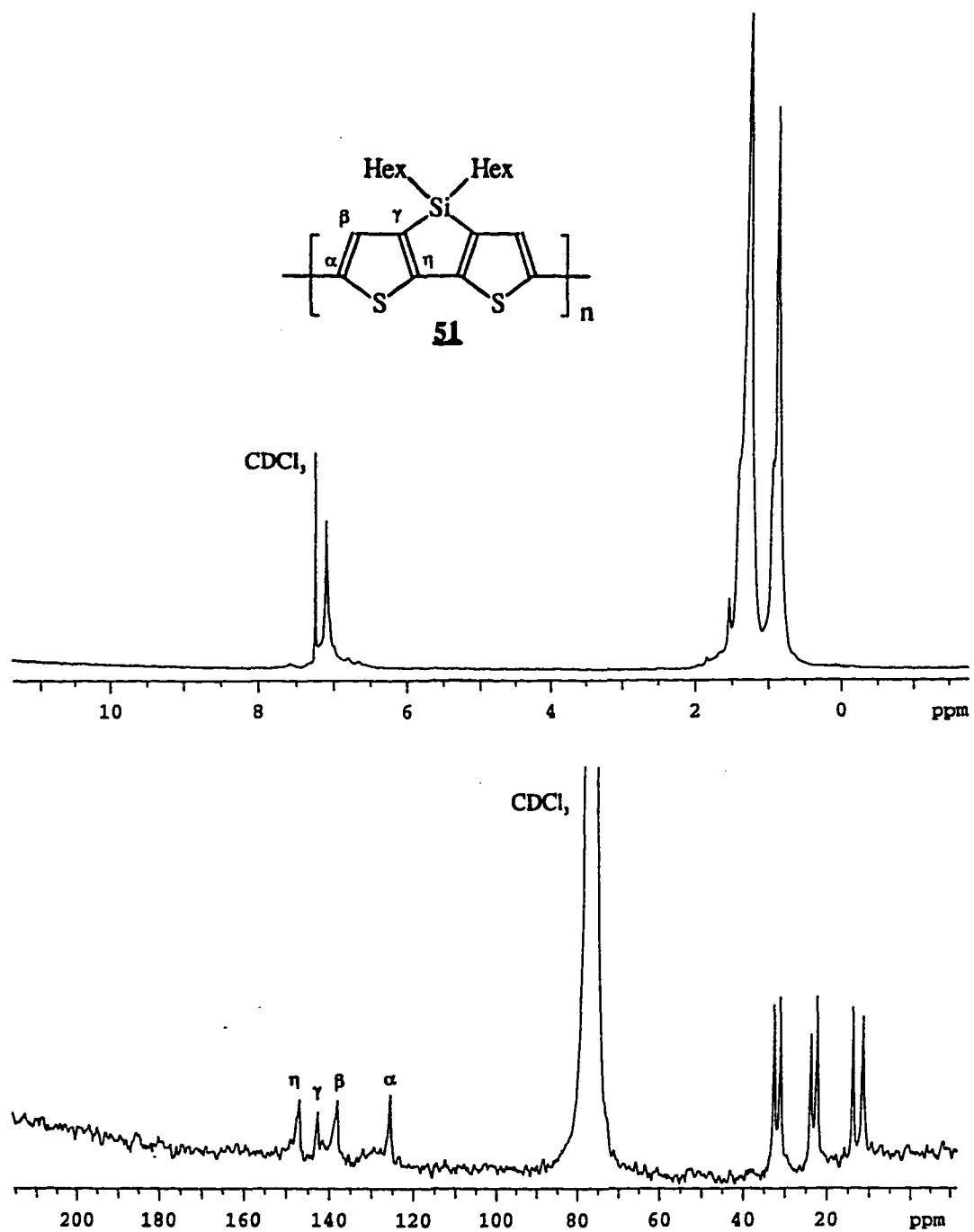


Figure 46: The ¹H- and ¹³C-NMR spectra of polymer **51**

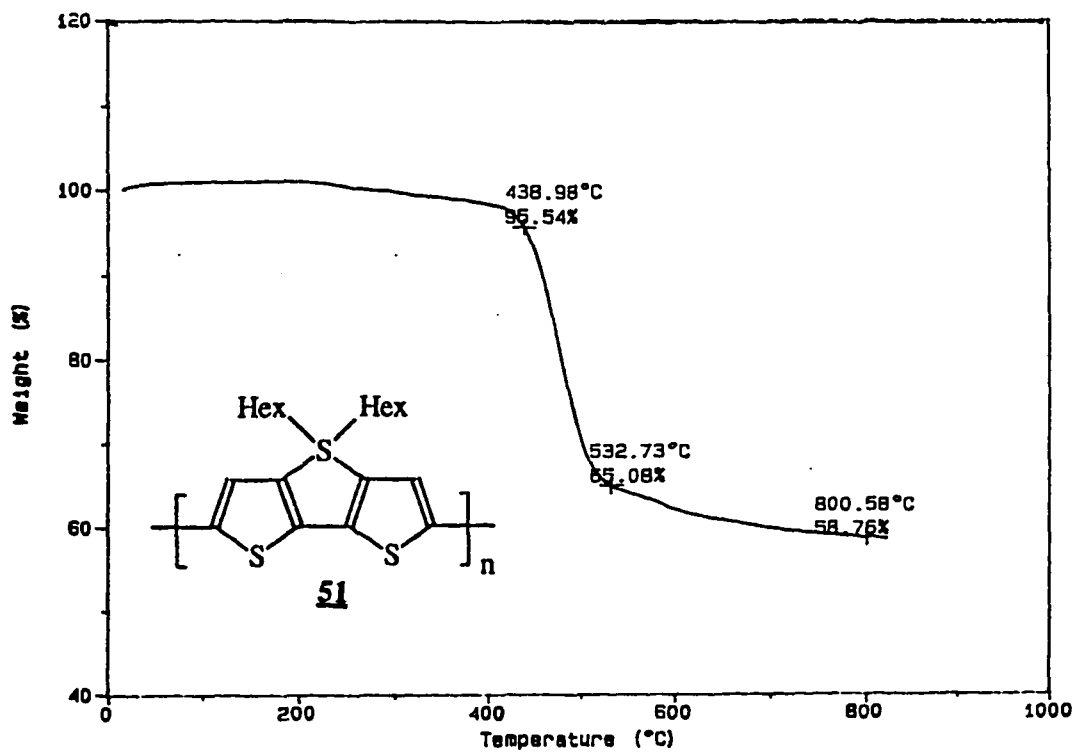
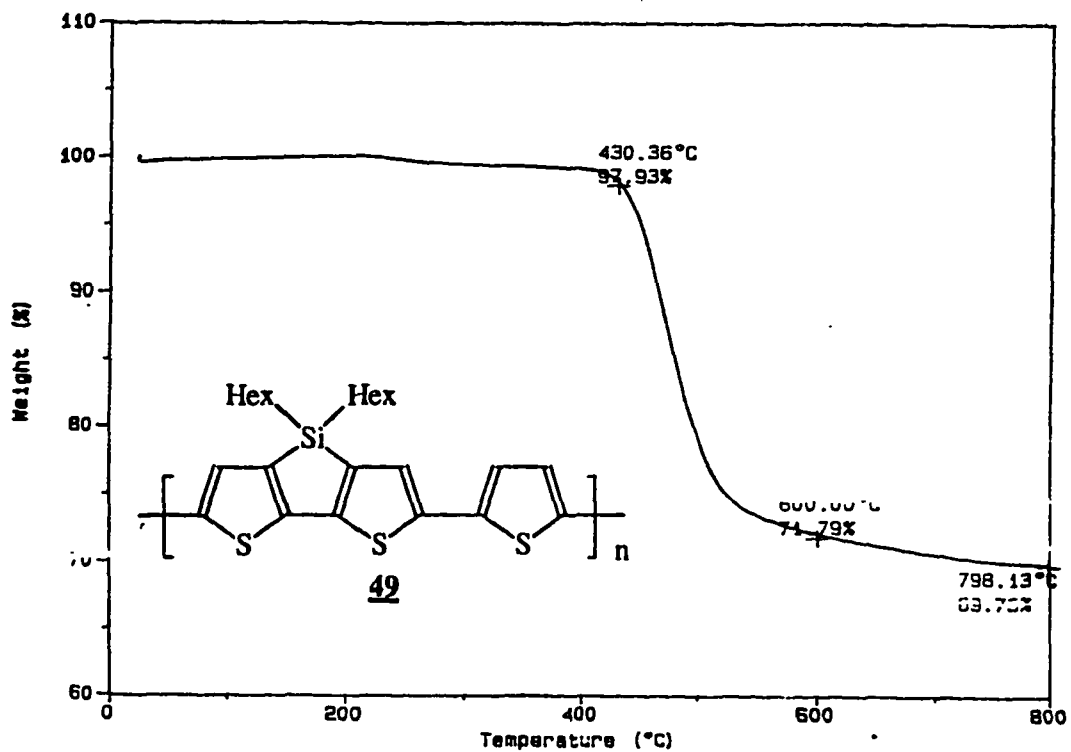


Figure 47: The TGA spectra of polymers **49** and **51**

Table 11: Thermal property analysis of polymers **49** and **51**

Polymer	TGA		DSC	
	T_d (°C) (4% weight lose)	Char Yield (at 800°C)	T_{endo} (°C)	T_{exo} (°C)
49	430	80%	278	302
51	439	59%		334

starts to decompose. Polymer **51** has an endothermic peak at 334°C. The thermal results are summarized in Table 11.

UV/Vis Absorption. The UV/Vis absorption spectra of polymers **49** and **51** in THF and the solid state were measured. Both polymers exhibit unusually long absorption maximum wavelengths. The λ_{max} values of polymers **49** and **51** in THF are 556 nm and 582 nm, respectively (Figure 48). These λ_{max} values are the longest among polythiophenes known to us. Compared with the λ_{max} of normal 3-substituted polythiophenes (448 nm⁹² for 3-octylpolythiophene, for example),⁵ the absorptions of polymers **49** and **51** are about 110 nm to 130 nm red-shifted. Compared with the λ_{max} of **49** (in which the silylene bridge to thiophene ratio is 1/3), the λ_{max} of **51** (in which the silylene bridge to thiophene ratio is 1/2) is 26 nm red-shifted. All these data show that the silicon on the main chain dramatically decreases the bandgap energy. A silicon unit can change the electronic structures of the polymers by interacting the σ^* orbital of silicon with π -conjugated orbitals, thus decreasing the LUMO energy.⁶² The absorption edges (λ_c) of polymers **49** and **51** were estimated in order to calculate the bandgap energy. Polymer **49** has a λ_c of 650 nm and the bandgap energy of polymer **49** can be estimated as 1.90 eV. Polymer **51** has a more extended absorption tail up to 720 nm compared with polymer **49** ($\lambda_c - \lambda_{\text{max}} = 92$ nm for polymer **49**, while $\lambda_c - \lambda_{\text{max}} = 138$ nm for polymer **51**). The bandgap of polymer **51** is estimated to be as low as 1.71 eV, one of the lowest bandgaps of polythiophenes ever reported.

The solid state UV/Vis absorptions of polymers **49** and **51** were also measured. These two polymers can form smooth “metallic” films. The UV/Vis absorptions of these films are similar to those of their THF solutions, but red-shifted. The film of polymer **49** has a λ_{\max} of 582 nm, 26 nm red-shifted compared with its THF solution. The film of polymer **51** has a λ_{\max} of 592 nm, only 10 nm red-shifted compared with that of its THF solution. The results of the UV/Vis absorptions of polymers **49** and **51** are summarized in Table 12.

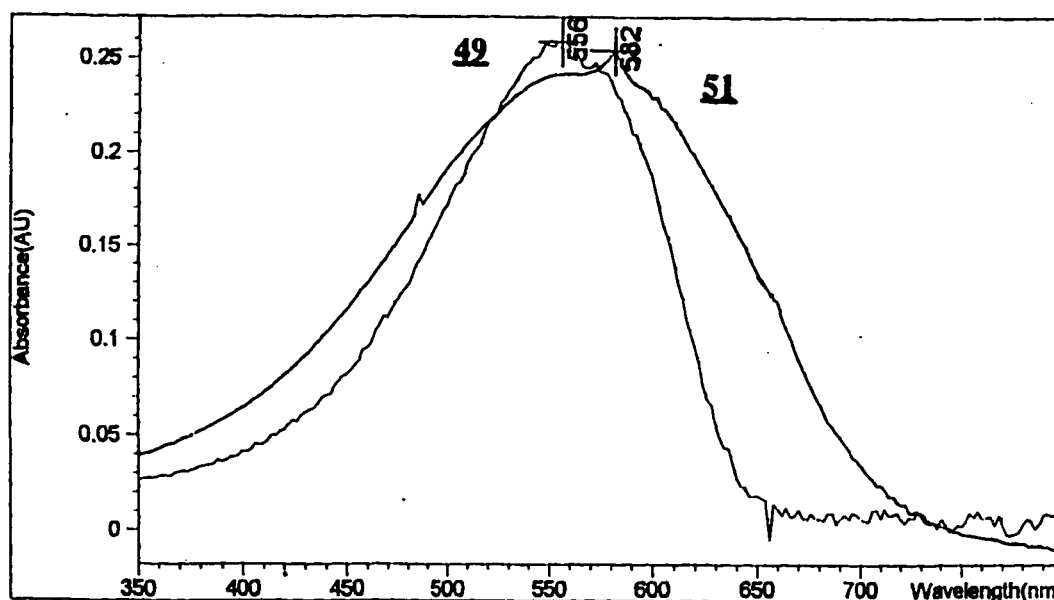


Figure 48: The UV/Vis absorptions of polymers **49** and **51**

Table 12: The results of UV/Vis absorptions of polymers **49** and **51**

Polymer	THF			Film
	λ_{\max}	λ_e	$\Delta\lambda (\lambda_e - \lambda_{\max})$	λ_{\max}
49	556 nm	650 nm (1.90 eV)	94 nm	582 nm
51	582 nm	720 nm (1.71 eV)	138 nm	592 nm

Fluorescence. Polymers **49** and **51** have weak reddish photoluminescence in THF. The fluorescence spectra of the polymers in THF were measured (Figure 49). Polymer **49** has two emission peaks at 627 and 662 nm when excited at 510 nm. These two emission peaks are probably due to two different lengths of polymers as shown in GPC (a main peak overlapping with a small shoulder). Polymer **51** has a weaker emission peak at 680 nm when excited at 540 nm.

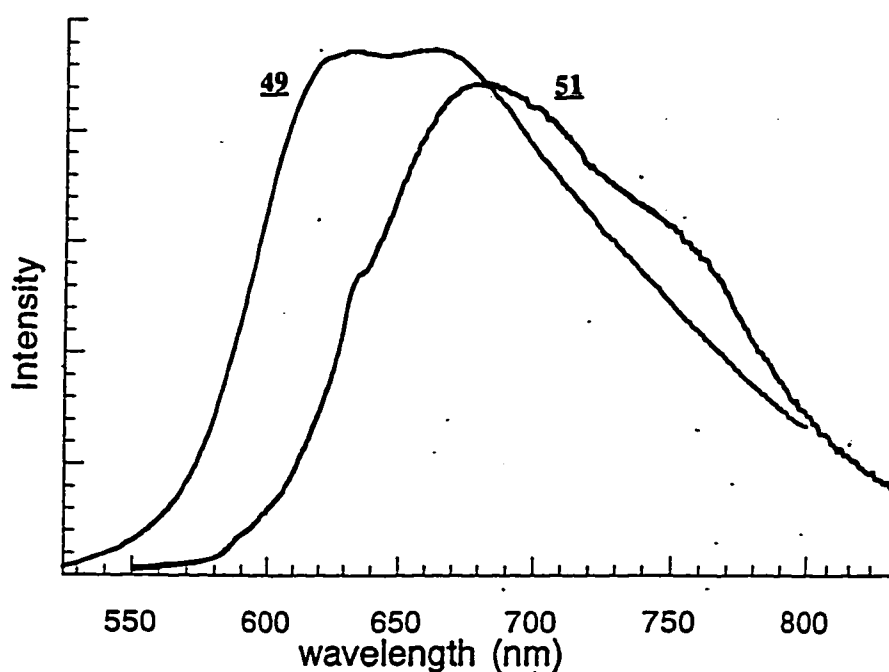


Figure 49: The fluorescence spectra of polymers **49** (excited at 510 nm) and **51** (excited at 540 nm)

Electrical Conductivity. Polythiophenes are most often used as conducting polymers. The narrow bandgaps of the silicon-bridged polythiophenes suggest that they might be highly conductive upon doping. The shiny, deep purple films of polymers **49** and **51** were nonconductive in their neutral states. But exposure to I_2 vapor under vacuum changed the conductivities of the films dramatically with a few seconds, and turned them into black shiny films. The I_2 -doped polymers exhibited a conductivity of $4-6 \times 10^2$ S/cm (determined by the

Table 13: Conductivities of I₂-doped polymers **49 and **51****

Polymer	I ₂ -doped conductivity (S/cm)
49	~400
51	~600

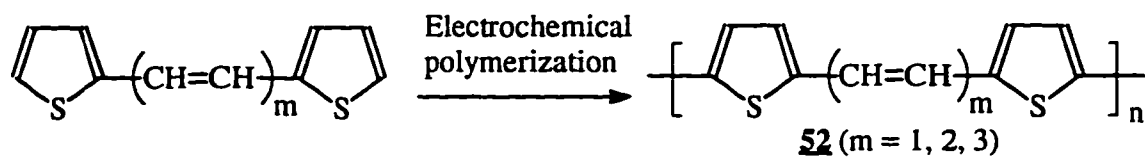
two-probe method) as listed in Table 13, one of the highest conductivities of polythiophenes (the highest conductivity is up to > 1,000 S/cm).⁵

Synthesis and Study of Butadiene-Linked Polythiophenes

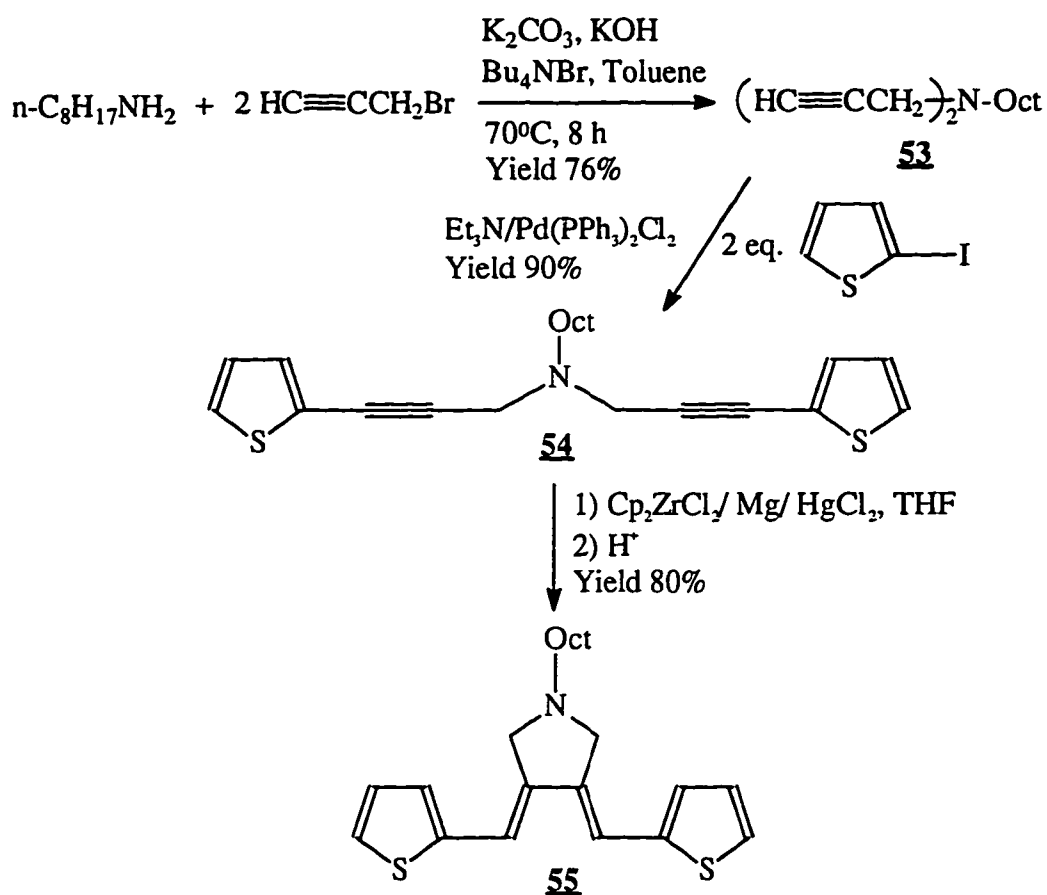
Polyacetylenes are the most conductive but environmentally unstable polymers. Polythiophenes, which increase the aromaticity along the main chains and the environmental stabilities, decrease the conductivity. We rationalized that decreasing the aromaticity of polythiophene by putting butadiene units into the polythiophene main chains will increase the mobility of π -electrons over the main chain, lowering the bandgap energy without significantly decreasing the environmental stability. Butadiene-linked polythiophenes, which are more like hybrids of polyacetylenes and polythiophenes, should exhibit special properties.

In 1985, Tanaka et al. synthesized polyene-linked polythiophenes **52** by electrochemical polymerization (Scheme 40), and studied their UV/Vis absorptions and conductivities.¹¹⁶ However, the polymers they synthesized were insoluble and were only characterized by IR spectroscopy. The conductivity of these polymers were very low ($\sigma = 2-8 \times 10^{-2}$ S/cm).

Synthesis and Characterization. One of the monomers for butadiene-linked polythiophenes is monomer **55**, which was synthesized, starting from n-octylamine, as shown in Scheme 41. Phase transfer N-alkylation¹¹² of n-octylamine with propargyl bromide yielded N,N-di(3-propynyl)-N-octylamine **53** in 76% yield. Palladium-catalyzed coupling of **53** with 2-iodothiophene in Et₃N gave product **54** in 90% yield. The zirconocene-mediated



Scheme 40: Synthesis of polyene-linked polythiophenes
by electrochemical polymerization¹¹⁶

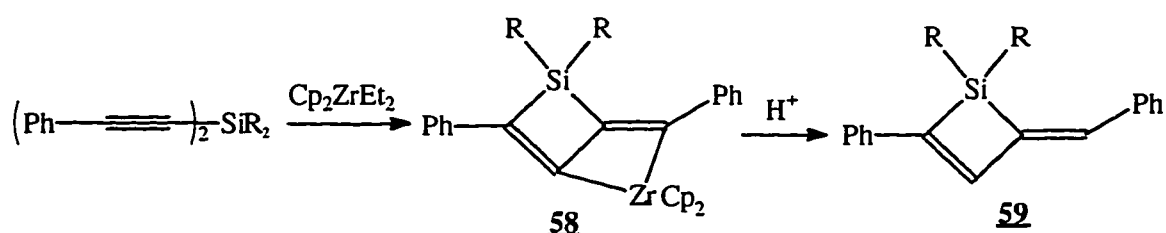
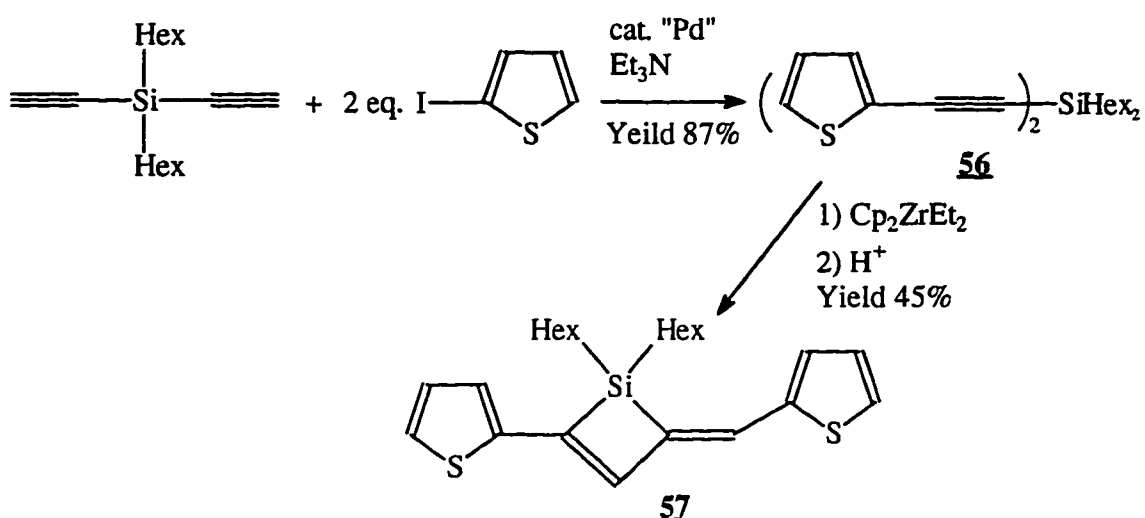


Scheme 41: Synthesis of monomer **55**

intramolecular cyclization¹¹³ of **54**, followed by quenching with acid, gave the desired monomer **55** in 80% yield.

The other monomer **57** has a butadiene linkage, but the silicon unit was introduced into the monomer in order to decrease the LUMO energy (Scheme 42). The Pd-catalyzed

coupling of diethynyldihexylsilane with two equivalents of 2-iodothiophene gave compound **56** in 87% yield. Treatment of **56** with Cp_2ZrEt_2 , generated from Cp_2ZrCl_2 and 2 equivalents of EtMgBr , followed by quenching with acid, gave a silacyclobutene derivative **57** in 45% yield.¹¹⁴ This reaction was discovered by the Takahashi's group in 1995.¹¹⁴ The intermediate from a reaction of di(phenylethynyl)dialkylsilane and Cp_2ZrEt_2 was the fused ring compound **58**, which was then quenched with acid to give silacyclobutene **59** (Scheme 43).¹¹⁴



Compared with the UV/Vis absorption of terthiophene ($\lambda_{\text{max}} = 353 \text{ nm}$ in benzene),^{64(a)} the UV/Vis absorption maxima of **55** and **57** are about 17 nm ($\lambda_{\text{max}} = 370 \text{ nm}$ in THF with two shoulders at 354 nm and 390 nm for **55**) and 19 nm ($\lambda_{\text{max}} = 372 \text{ nm}$ in THF with two shoulders at 356 nm and 388 nm for **57**) red-shifted, respectively, indicating that the energies

between the LUMO and the HOMO of **55** and **57** are smaller than that of terthiophene. The λ_{\max} of **57** is almost the same as that of **55** (only 2 nm red-shifted) even **57** has a silicon unit in the structure. The ring strain in **57** might offset the silicon effect. However, the silole-linked derivative of **57**, TST (which has less ring strain), has a UV/Vis absorption maximum of 416 nm, much longer than those of other compounds (Figure 50).

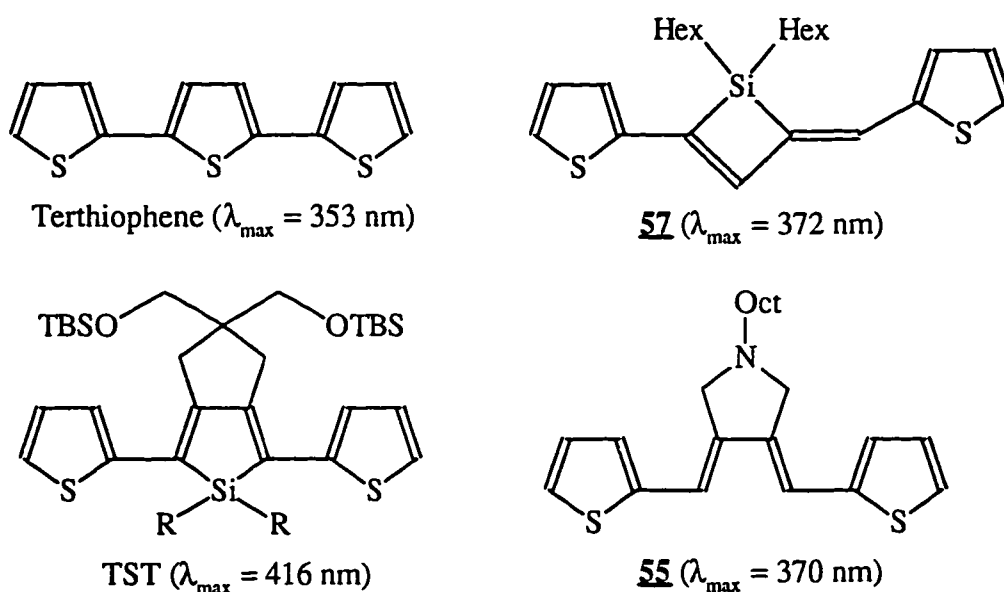
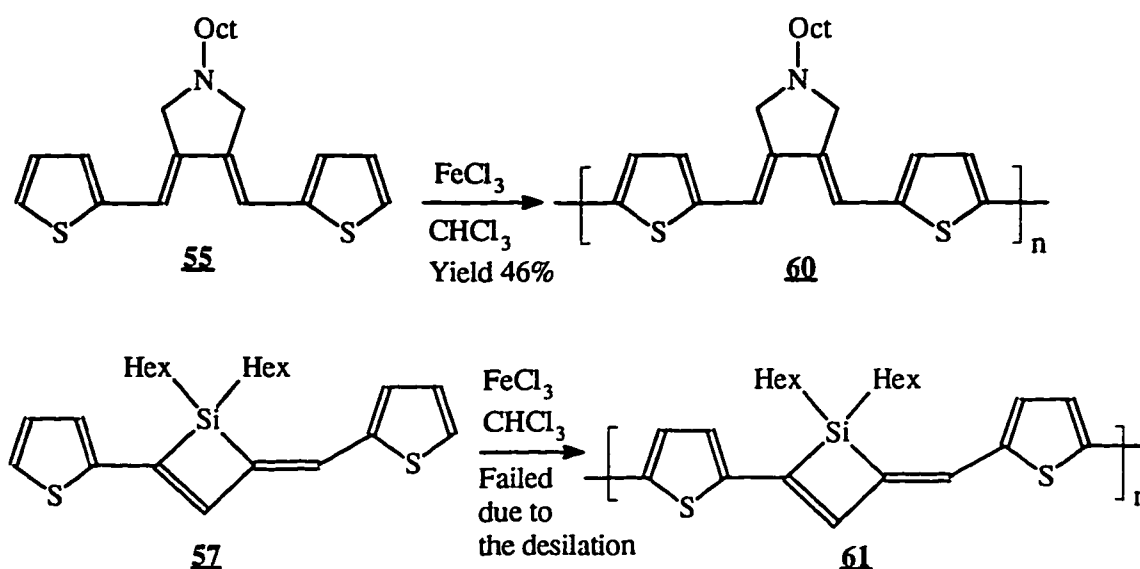


Figure 50: The comparison of the UV/Vis absorptions

Polymerization of monomers **55** and **57** was carried out by several methods. Bromination of **55** and **57** at the 5,5'-positions failed to give the desired 5,5'-dibromo-products. The direct metathesis of **55** and **57** at the 5,5'-positions with n-BuLi or LDA also failed. Due to the difficulties of introducing functional groups at the 5,5'-positions, the polymerization was carried out by direct oxidative coupling of the corresponding monomer using FeCl₃ in chloroform (Scheme 44). Polymer **60** was obtained in 46% yield. Polymer **60** was a deep red solid and very soluble in organic solvents. However, monomer **57** failed to give the desired polymer **61**, as the desilylation happened during the polymerization.



Scheme 44: Oxidative polymerization of **60** and **61**

Polymer **60** was characterized by ^1H - and ^{13}C -NMR (Figure 51) and GPC. The ^1H -NMR spectrum shows two peaks at 7.70 and 7.52 ppm for the protons on thiophene, one peak at 7.01 ppm for the vinyl protons, one peak at 4.21 ppm for the protons of cyclic methylene, one peak at 3.74 ppm for the protons of the acyclic methylene attached to nitrogen, and several peaks for the alkyl protons between 1.67 and 0.88 ppm. The ^{13}C -NMR spectrum shows clearly six sp^2 carbons between 140.00 and 111.78 ppm, two sp^3 carbons attached to nitrogen at 58.50 and 56.66 ppm, and seven sp^3 carbons between 38.73 and 10.97 ppm for octyl group. GPC shows polymer **60** has M_w of 1.39×10^4 with PD of 1.84.

Thermal Behaviors. The thermal behavior of polymer **60** was studied by thermogravimetric analysis (TGA) and differential scanning calorimetric analysis (DSC) under argon atmosphere. Polymer **60** started to lose weight (decompose) at $\sim 348^\circ\text{C}$ (3% weight loss) slowly up to 448°C (11% weight loss). After 448°C , the polymer lost weight dramatically. At 531°C , the weight loss was $\sim 58\%$. At 800°C , the char yield was 37% (Figure 52). DSC shows the polymer melted at $\sim 130^\circ\text{C}$ and crosslinking started at $\sim 243^\circ\text{C}$ to give a large exothermic peak at 306°C (Figure 53).

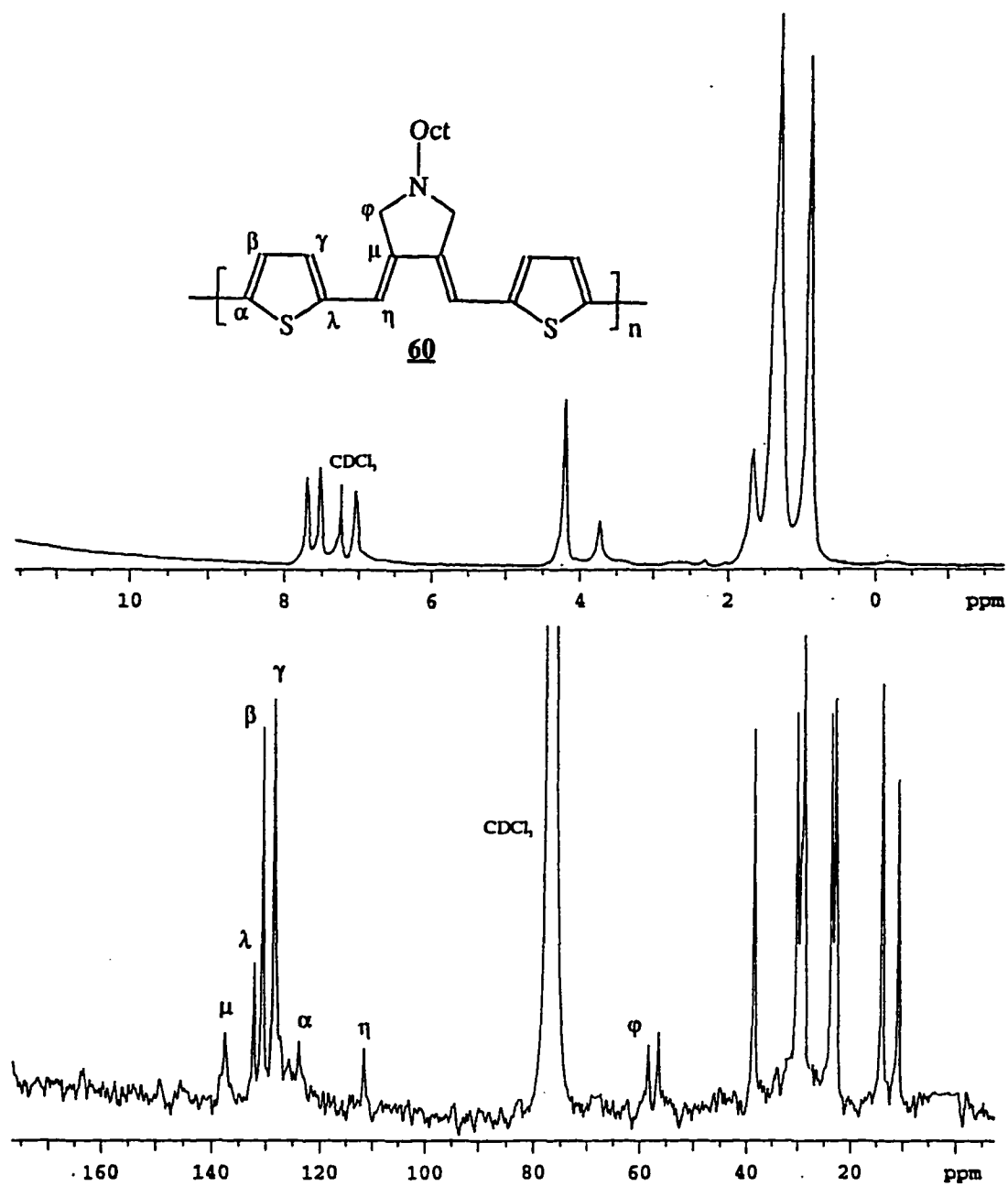


Figure 51: The ^1H - and ^{13}C -NMR spectra of polymer **60**

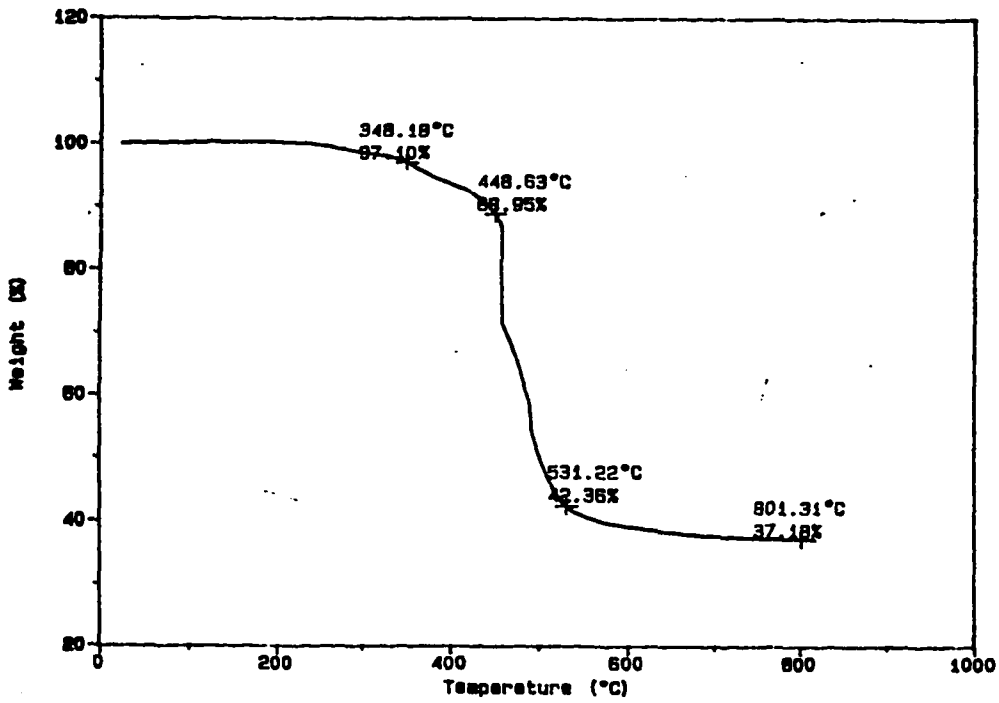


Figure 52: The TGA spectrum of polymer 60

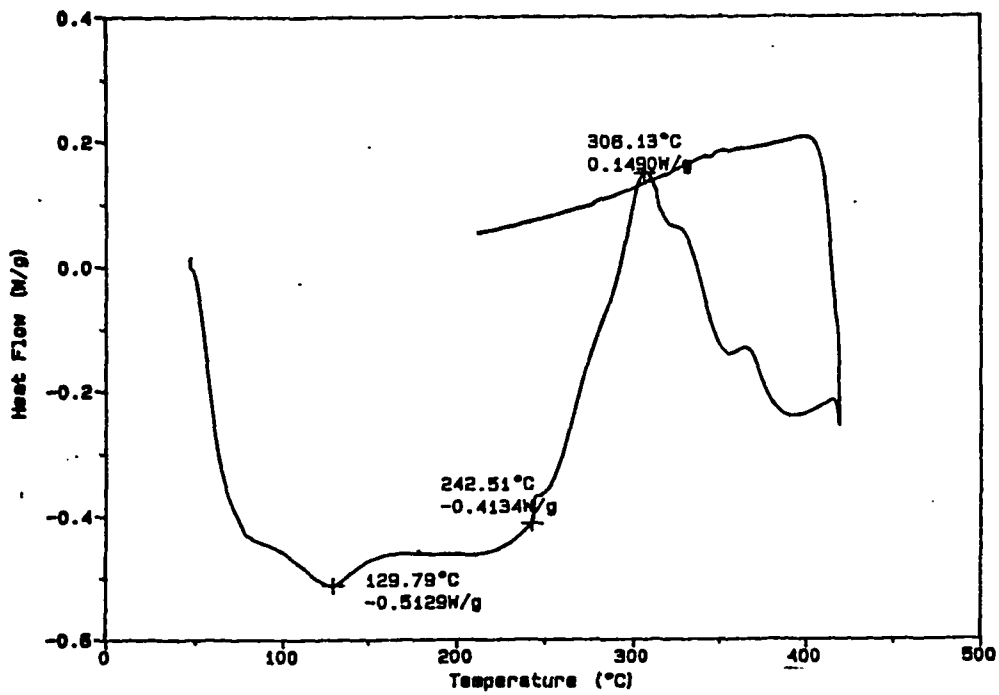


Figure 53: The DSC thermogram of polymer 60

UV/Vis absorption. The UV/Vis absorption of polymer **60** was measured (Figure 54). The λ_{\max} of polymer **60** in THF solution is 514 nm, which is larger than that of usual 3-substituted polythiophene (448 nm⁹² for 3-octylpolythiophene, for example),⁵ but much smaller than those of silicon-bridged polythiophenes (see Table 10). The absorption edge (λ_c) of polymer **60** was estimated as 630 ± 5 nm. The bandgap can be estimated as about 1.96 eV.

In 1985, the butadiene-linked polythiophene **52** ($m = 2$) (Scheme 39) film was prepared by electrochemical polymerization.¹¹⁶ The neutral polymer **52** ($m = 2$) film was red with a λ_{\max} of only 390 nm. Polymer **60** can form a smooth reddish film by spin-coating technique. The UV/Vis absorption of the polymer **60** film was also measured. The λ_{\max} of the polymer **60** film is 534 nm, about 20 nm longer than that of its THF solution. Compared with the λ_{\max} of the polymer **52** ($m = 2$) film, the λ_{\max} of polymer **60** film is 144 nm longer.

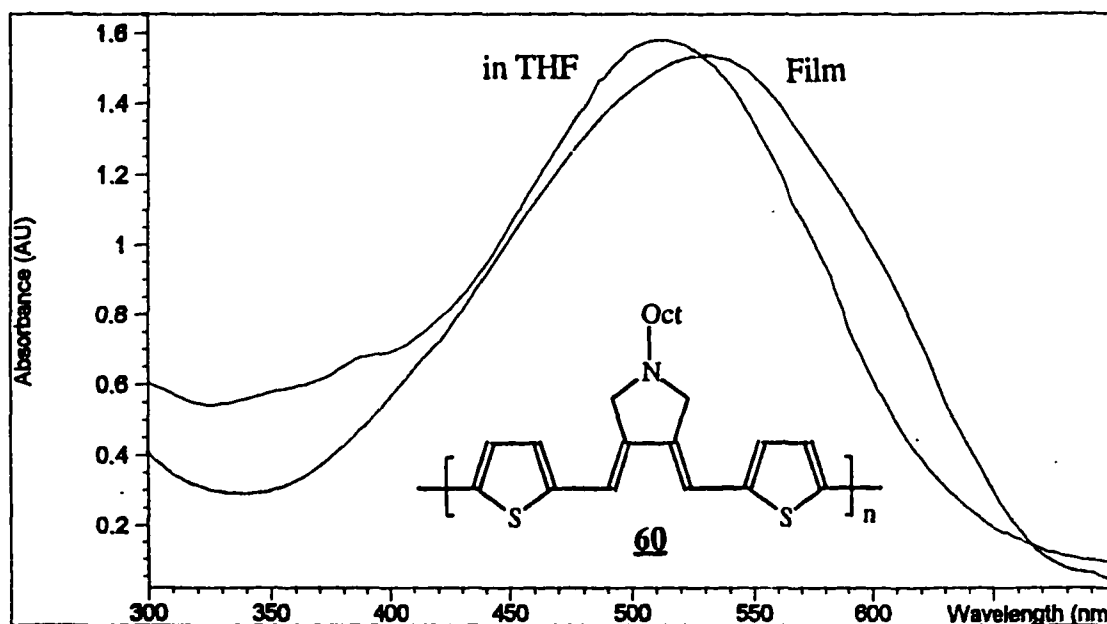


Figure 54: The UV/Vis absorption of polymer **60** in THF and the solid state

Fluorescence. Polymer **60** has weak luminescence in THF solution. The fluorescence spectrum of its THF solution was measured as shown in Figure 55. Polymer **60** has an emission peak at 554 nm with a small shoulder at ~470 nm when excited at 440 nm.

Electrical Conductivity. The conductivity of polymer **60** was studied as comparison with that of the butadiene-linked polythiophene **52** ($m = 2$), prepared by electrochemical polymerization.¹¹⁶ The dark green film of polymer **52** ($m = 2$) had the highest conductivity of 0.5 S/cm when oxidized by Bu_3NClO_4 . The polymer **60** film is nonconductive at its neutral state. After exposure to I_2 vapor under vacuum, the conductivity of the polymer **60** film increased dramatically up to σ of ~2 S/cm, which is 4 fold larger than that of polymer **52** ($m = 2$). However, it is still low considering its low bandgap energy.

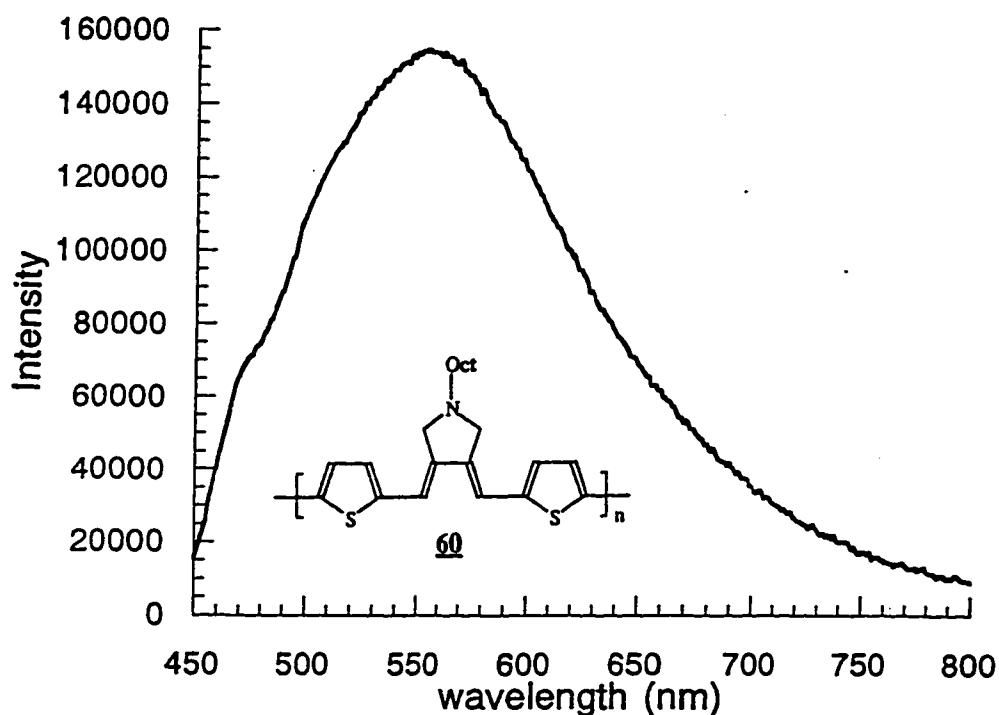


Figure 55: The emission spectrum of polymer **60** in THF solution

Conclusions

Novel silicon-bridged and butadiene-linked polythiophenes were synthesized. Their thermal and optical properties were studied. The silicon-bridged polythiophenes exhibited very unusual optical properties. They have the longest UV/Vis absorption maximum wavelengths among the polythiophenes ever reported, which indicates they have the lowest bandgap energies. The bridged silicon can not only enhance the planarity of the polymers, but also participate in the conjugation along the main chains by interacting σ^* orbital of silicon with π -conjugated orbitals of the backbones, thus decreasing the bandgap energies dramatically. The conductivities of the silicon-bridged polythiophenes were measured as high as ~400-600 S/cm, one of the highest conductivities among polythiophenes. The butadiene-linked polythiophene also showed that its UV/Vis absorption maximum wavelength was longer than that of normal 3-substituted polythiophene. However, the butadiene-linked polythiophene didn't exhibit high conductivity as expected.

Experimental

^1H and ^{13}C -NMR spectra were acquired on a Varian VXR-300 spectrometer. In order to assure the quantitative features of the ^{13}C -NMR spectra, the relaxation agent chromium(III) acetylacetonate was used in CDCl_3 with a relaxation delay of 5 seconds.

Routine GC-MS spectra were obtained on a Hewlett Packard 5970 GC-IR-MS spectrometer at 70 eV. The exact masses were obtained from a Kratos MS 50 mass spectrometer with 10,000 resolution. The infrared spectra were recorded on a Bio-Rad Digilab FTS-7 spectrometer from neat sample. The UV/Vis spectra were obtained on a Hewlett Packard 8452A diode array UV/VIS spectrometer and λ_{max} were determined at optical densities of 0.2-0.5.

Polymer molecular weights were determined by gel permeation chromatography (GPC) with 6 Microstyrigel columns in series of 500 A, 2×10^3 A, 2×10^4 A, 2×10^5 A. THF was used as an eluent at a flow rate of 1 ml/min. The system was calibrated by polystyrene

standards. GPC analyses were performed on a Perkin-Elmer series 601 LC equipped with Beckman solvent delivery system, a Walter Associate R401 refractive index detector and a Viscotek viscometer. Differential scanning calorimetry (DSC) analyses were performed on a Du Pont 910 Differential Scanning Calorimeter. The UV/Vis spectra were measured on a Hewlett Packard 8452A Diode Spectrophotometer. Photoluminescence spectra were measured on a FL 900 fluorometer made by Edinburgh.

Toluene and benzene were distilled over CaH₂. THF was distilled from sodium/benzophenone before use. Other reagents were used as received from Aldrich Chemical Co. without further purification unless specified otherwise. Acetic acid, isopropanol and methanol were used as received from Fisher without further purification. All the reactions were performed under argon atmosphere. Diethynyldihexylsilane was synthesized by reaction of ethynylmagnesium bromide with dichlorodihexylsilane. 2,5-Bis(trimethylstannyl)thiophene was synthesized by reaction of 2,5-dibromothiophene with 2 equivalents of n-BuLi, followed by quenching with chlorotrimethyltin. 3,3'-Dibromo-2,2'-bithiophene **44** was synthesized according to the literature, starting from 2-bromothiophene.¹⁰⁵

3,3-Dihexylsilylene-2,2'-bithiophene 47: A flask was charged with n-BuLi (60 mmol, 24 ml, 2.5 M in hexane) and THF (500 ml). The solution was cooled to -78^oC and a solution of 3,3'-dibromo-2,2'-bithiophene (30 mmol, 9.720 g) in THF (100 ml) was added dropwise. The solution was stirred at -78^oC for 1 hour, resulting in a white precipitate. Then a solution of dichlorodihexylsilane (30 mmol, 8.070 g) in THF (100 ml) was added. The solution was stirred at -78^oC for 5 hours, and then was allowed to warm to room temperature and was stirred overnight. A saturated NH₄Cl solution (300 ml) was added. The aqueous solution was extracted with Et₂O (300 ml). The combined organic layer was washed with water and dried (MgSO₄). After the solvents were removed, the product was purified by column chromatography to yield a bright green-yellow liquid (8.812 g, yield 81.2%). Mass: cal. *m/z* for C₂₀H₃₀S₂Si = 362.67570, measured (HiRes EI): 362.67532; IR: ν (cm⁻¹) 3070, 2950, 2918, 2844, 1462; ¹H-NMR: δ 7.20 (d, 2H, *J* = 6 Hz), 7.06 (d, 2H, *J* = 6 Hz), 1.27 (br, 16H), 0.92 (t, 6H, *J* = 9 Hz), 0.63 (d, 4H, *J* = 6 Hz); ¹³C-NMR: δ 149.17, 141.53, 129.58,

124.91, 32.83, 31.43, 24.15, 22.54, 14.08, 11.88; Element analysis: cal. for $C_{20}H_{30}S_2Si$, C 66.24; H 8.34; S 17.68; Si 7.74, found C 66.10; H 8.40

5,5'-Dibromo-3,3'-dihexylsilylene-2,2'-bithiophene 48: To a solution of 3,3'-dihexylsilylene-2,2'-bithiophene 47 (5 mmol, 1.810 g) in DMF (40 ml) was added NBS (11 mmol, 1.958 g). After the mixture was stirred at room temperature for 20 minutes only (don't exceed 20 minutes), water (50 ml) was added. The solution was extracted with Et_2O (50 ml x 3). The combined organic layer was washed with water (50 ml) and dried ($MgSO_4$). After ether was removed, the product was purified by column chromatography (hexane as eluent) to yield a green-yellow liquid (2.374 g, yield 91.3%). Mass: cal. m/z for $C_{20}H_{28}^{79}Br^{81}BrS_2Si$ = 519.97493, $C_{20}H_{28}^{79}Br_2S_2Si$ = 517.97786, $C_{20}H_{28}^{81}Br_2S_2Si$ = 521.97301, measured (HiRes ED) = 519.97466, 517.97655, 521.97301, respectively; IR: ν (cm^{-1}) 3074, 2952, 2918, 2850, 1667, 1462; 1H -NMR: δ 7.00 (s, 2H), 1.32-1.22 (m, 16H), 0.88 (t, 4H, $J = 6$ Hz), 0.86 (t, 6H, $J = 3$ Hz); ^{13}C -NMR: δ 148.90, 140.96, 132.12, 111.40, 32.77, 31.35, 23.96, 22.52, 14.05, 11.62; Element analysis: for $C_{20}H_{28}Br_2S_2Si$, C 64.62; H 5.42; Br 30.70; S 12.32; Si 5.40, found C 64.13; H 5.52

Polymer 49: The monomers, 2,5-bis(trimethylstannyl)thiophene 25 (1.5 mmol, 0.614 g) and 5,5'-dibromo-3,3'-dihexylsilylene-2,2'-bithiophene 48 (1.5 mmol, 0.780 g), and the catalyst $Pd(PPh_3)_2Cl_2$ (55 mg) were dissolved in THF (50 ml) and the solution was refluxed for 7 days. After the solvent was removed, the polymer was purified by precipitation from MeOH/THF twice to yield a black shining solid (0.630 g, yield 95%). GPC: $M_w = 3.16 \times 10^4$, PD = 3.21, $n = 67.7$; IR: ν (cm^{-1}) 3056, 2956, 2923, 2853, 1546; 1H -NMR: δ 7.11 (br, 4H), 1.29 (br, 20H), 0.89 (br, 6H); ^{13}C -NMR: δ 147.29, 142.50, 138.37, 135.00, 125.40, 124.59, 32.41, 30.92, 23.60, 22.06, 13.57, 11.24; Element analysis: cal. for $(C_{24}H_{30}S_3Si)_n$, C 65.10; H 6.83; S 21.72; Si 6.34, found C 64.84, H 6.85; UV/Vis: λ_{max} (THF) = 556, 574 nm, λ_{max} (film) = 582 nm; Emission: $\lambda_{max} = 627, 662$ nm ($\lambda_{excit.} = 510$ nm); Electrical conductivity: ~ 400 S/cm (doped by I_2 vapor)

Polymer 51: To a solution of 5,5'-dibromo-3,3'-dihexylsilylene-2,2'-bithiophene 48 (0.773 mmol, 0.402 g) in THF (20 ml) was added n-BuLi (1.85 mmol, 0.74 ml, 2.5 M in hexane) dropwise at -78°C . After addition, the mixture was stirred at -78°C for one half hour, resulting in a white-yellow precipitate. Then chlorotrimethyltin (2.411 mmol, 2.411 ml, 1.0 M in hexane) was added. The mixture was allowed to warm to room temperature and stirred for 2 hours. Then the solvent and BuBr were removed under vacuum. A solution of 5,5'-dibromo-3,3'-dihexylsilylene-2,2'-bithiophene 48 (0.773 mmol, 0.402 g) and the catalyst $\text{Pd}(\text{PPh}_3)_2\text{Cl}_2$ (56 mg) in THF (20 ml) was added. The mixture was refluxed for 7 days, resulting in a deep purple solution. After the solution was cooled down, water (30 ml) was added. The aqueous layer was extracted by CH_2Cl_2 (30 ml x 2). The combined organic layer was washed with water (40 ml) and dried with MgSO_4 . After the solvent was removed, the residue was dissolved in a minimum amount of THF and was added into methanol (200 ml). A deep purple (like black) solid was precipitate and collected by vacuum filtration. The polymer was purified by precipitation one more time from THF/MEOH (0.486 g, yield 87.4%). GPC: $M_w = 2.03 \times 10^4$, PD = 1.896, n = 56.29; IR: ν (cm^{-1}) 3054, 2957, 2923, 2854, 1549, 1464; $^1\text{H-NMR}$: δ 7.10 (br, 2H), 1.24 (br, 20H), 0.93-0.85 (br, 6H); $^{13}\text{C-NMR}$: δ 147.16, 142.75, 138.23, 125.68, 32.65, 31.16, 23.85, 22.33, 13.85, 11.56; Element analysis: cal. for $(\text{C}_{20}\text{H}_{28}\text{S}_2\text{Si})_n$, C 66.61; H 7.83; S 17.78; Si 7.78, found C 66.34, H 7.50; UV/Vis: λ_{max} (THF) = 582 nm, λ_{max} (film) = 592 nm; Emission: $\lambda_{\text{max}} = 680$ nm ($\lambda_{\text{excit.}} = 540$ nm); Electrical conductivity: ~ 600 S/cm (doped by I_2 vapor)

Di(3-propynyl)-octylamine 53: To a solution of n-octylamine (0.20 mol, 25.850 g) and propargyl bromide (0.42 mol, 49.980 g) in toluene (600 ml) was added K_2CO_3 (0.80 mmol, 110.400 g) and tetrabutylammonium bromide (0.20 mol, 6.440 g). The mixture was stirred at 70°C for 8 hours. Then KOH (0.20 mol, 11.200 g) was added and the mixture was kept stirring at 70°C overnight. The resulting white solid was removed by filtration. The solvent was distilled off and the product was distilled off under vacuum (b.p. $87-90^{\circ}\text{C}/0.15$ mmHg) to yield a colorless liquid (31.063 g, yield 75.8%). Mass: cal. m/z for $\text{C}_{14}\text{H}_{23}\text{N} = 205.18305$, measured (HiRes EI) = 205.18256; IR: ν (cm^{-1}) 3305, 2951, 2924, 2819, 1711,

1464; $^1\text{H-NMR}$: δ 3.404 (d, 4H, $J = 2.4$ Hz), 2.477 (t, 2H, $J = 7.5$ Hz), 2.184 (t, 2H, $J = 2.4$ Hz), 1.451-1.386 (m, 2H), 1.247 (br, 10H), 0.845 (t, 3H, $J = 6.9$ Hz); $^{13}\text{C-NMR}$: δ 78.795, 72.783, 52.973, 42.003, 31.788, 29.416, 29.1888, 27.286, 22.613, 14.058

Di-[1-(2-thienyl)-3-propynyl]-octylamine 54: To a degassed solution of di-(3-propynyl)-octylamine 53 (20 mmol, 4.100 g) and 2-halothiophene (42 mmol) in triethylamine (200 ml) was added the catalysts $\text{Pd}(\text{PPh}_3)_2\text{Cl}_2$ (0.140 g)/ CuI (0.076 g). The solution was stirred at room temperature for 36 hours. The resulting salt was removed by filtration. After the solvent was removed, the residue was directly purified by column chromatography to yield a liquid (for bromothiophene: 3.246 g, yield 44%; for iodothiophene: 6.639 g, yield 90%).

Mass: cal. m/z for $\text{C}_{22}\text{H}_{27}\text{NS}_2 = 369.15850$, measured (HiRes EI) = 369.15622; IR: ν (cm^{-1}) 3100, 2908, 2842, 2224, 1410; $^1\text{H-NMR}$: δ 7.21 (dd, 2H, $J = 3$ Hz), 7.19 (s, 2H), 6.95 (dd, 2H, $J = 3$ and 3 Hz), 3.72 (s, 4H), 2.64 (t, 2H, $J = 6$ Hz), 1.56 (m, 2H), 1.34-1.26 (m, 10H), 0.91 (t, 3H, $J = 9$ Hz); $^{13}\text{C-NMR}$: δ 131.67, 126.63, 126.50, 122.98, 88.73, 78.11, 53.03, 43.30, 31.68, 29.30, 29.09, 27.35, 27.21, 22.51, 13.98

Compound 55: A suspension of magnesium turnings (166.6 mmol, 4.000 g) and mercuric chloride (16.810 mmol, 4.566 g) in THF (200 ml) was stirred for 15 minutes. A solution of bis(cyclopentadienyl)zirconium dichloride (30.649 mmol, 8.950 g) and di-[1-(2-thienyl)-3-propynyl]-octylamine 54 (25.626 mmol, 9.456 g) in THF (200 ml) was added rapidly dropwise, and the mixture was stirred overnight at room temperature. The reaction solution was decanted from the unreacted magnesium, then rapidly quenched with HCl (3 M, 100 ml), and extracted with CH_2Cl_2 (150 ml x 3). The organic layer was washed with water (300 ml) and a saturated NaHCO_3 (300 ml) solution, and dried with MgSO_4 . After the solvent was removed, the residue was dissolved in a small amount of CH_2Cl_2 , and MeOH was added to precipitate a yellow solid (7.14 g, yield 80%). m.p. 65-68 $^\circ\text{C}$; Mass: cal. m/z for $\text{C}_{22}\text{H}_{29}\text{NS}_2 = 371.17415$, measured (HiRes EI) = 371.17507; IR: ν (cm^{-1}) 3006, 2917, 2750, 1617, 1495; $^1\text{H-NMR}$: δ 7.31 (d, 2H, $J = 3$ Hz), 7.09 (s, 2H), 7.07-7.03 (m, 4H), 3.75 (s, 4H), 2.69 (t, 2H, $J = 6$ Hz), 1.64 (m, 2H), 1.34 (m, 10H), 0.90 (t, 3H, $J = 6$ Hz); $^{13}\text{C-NMR}$:

δ 141.49, 136.89, 127.46, 127.13, 125.77, 111.66, 58.52, 56.57, 31.79, 29.48, 29.21, 28.43, 27.42, 22.61, 14.06; UV/Vis: λ_{\max} (THF) = 370 nm, 354 nm (shoulder), 390 nm (shoulder)

Bis(2-thienylethynyl)-dihexylsilane 56: To a degassed solution of diethynyldihexylsilane (3.92 mmol, 0.973 g) and 2-iodothiophene (8.28 mmol, 1.950 g) in triethylamine (30 ml) was added the catalysts Pd(PPh₃)₂Cl₂ (56 mg)/CuI (18 mg). The mixture was stirred at room temperature for 18 hours. The resulting white precipitate was removed by filtration. After the solvent was removed, the residue was purified by column chromatography (hexane/ethyl acetate = 10:1 as eluents) to yield a colorless liquid (1.400 g, 86.7%). Mass: cal. m/z for C₂₄H₃₂S₂Si = 412.17148, measured (HiRes EI) = 412.17084; IR: ν (cm⁻¹) 3110, 2964, 2857, 2148, 1510, 1468; ¹H-NMR: δ 7.31 (dd, 2H, J = 3 and 1 Hz), 7.28 (dd, 2H, J = 6 and 1 Hz), 6.99 (dd, 2H, J = 6 and 3 Hz), 1.60 (m, 4H), 1.49-1.36 (m, 16H), 0.95 (t, 5H, J = 6 Hz); ¹³C-NMR: δ 133.13, 127.72, 126.82, 122.80, 99.24, 93.81, 32.62, 31.45, 23.57, 14.59, 14.12

Compound 57: To a solution of bis(cyclopentadienyl)zirconium dichloride (4.11 mmol, 1.200 g) in THF (30 ml) was added EtMgBr (8.22 mmol, 8.22 ml, 1.0 M in THF) dropwise at -78^oC. The solution was stirred at -78^oC for 1 hour. A solution of dihexyl-di(2-thienylethynyl)silane 56 (3.29 mmol, 1.358 g) in THF (20 ml) was added dropwise. The mixture was allowed to warm to room temperature and was stirred for 1 hour. The reaction mixture was then quenched with 3N HCl, extracted with diethyl ether, and washed with water, NaHCO₃, and water. The extract was dried over MgSO₄. After the solvent was removed, the residue was purified by column chromatography to afford a yellow-green liquid (0.605 g, yield 44.4%). Mass: cal. m/z for C₂₄H₃₄S₂Si = 424.18713, measured (HiRes EI) = 414.18656; IR: ν (cm⁻¹) 3110, 2954, 2920, 2852, 1611, 1461; ¹H-NMR: δ 7.62 (s, 1H), 7.31 (d, 2H, J = 6 Hz), 7.14 (d, 2H, J = 3 Hz), 7.09-6.95 (m, 5H), 1.57 (m, 4H), 1.42-1.28 (m, 16H), 0.90 (t, 6H, J = 6 Hz); ¹³C-NMR: δ 148.04, 147.47, 145.76, 144.27, 142.21, 127.66, 127.60, 126.51, 125.76, 125.11, 122.86, 121.39, 32.77, 31.34, 23.75, 22.52, 14.22, 14.02; UV/Vis: λ_{\max} (THF) = 372 nm, 356 nm (shoulder), 388 nm (shoulder)

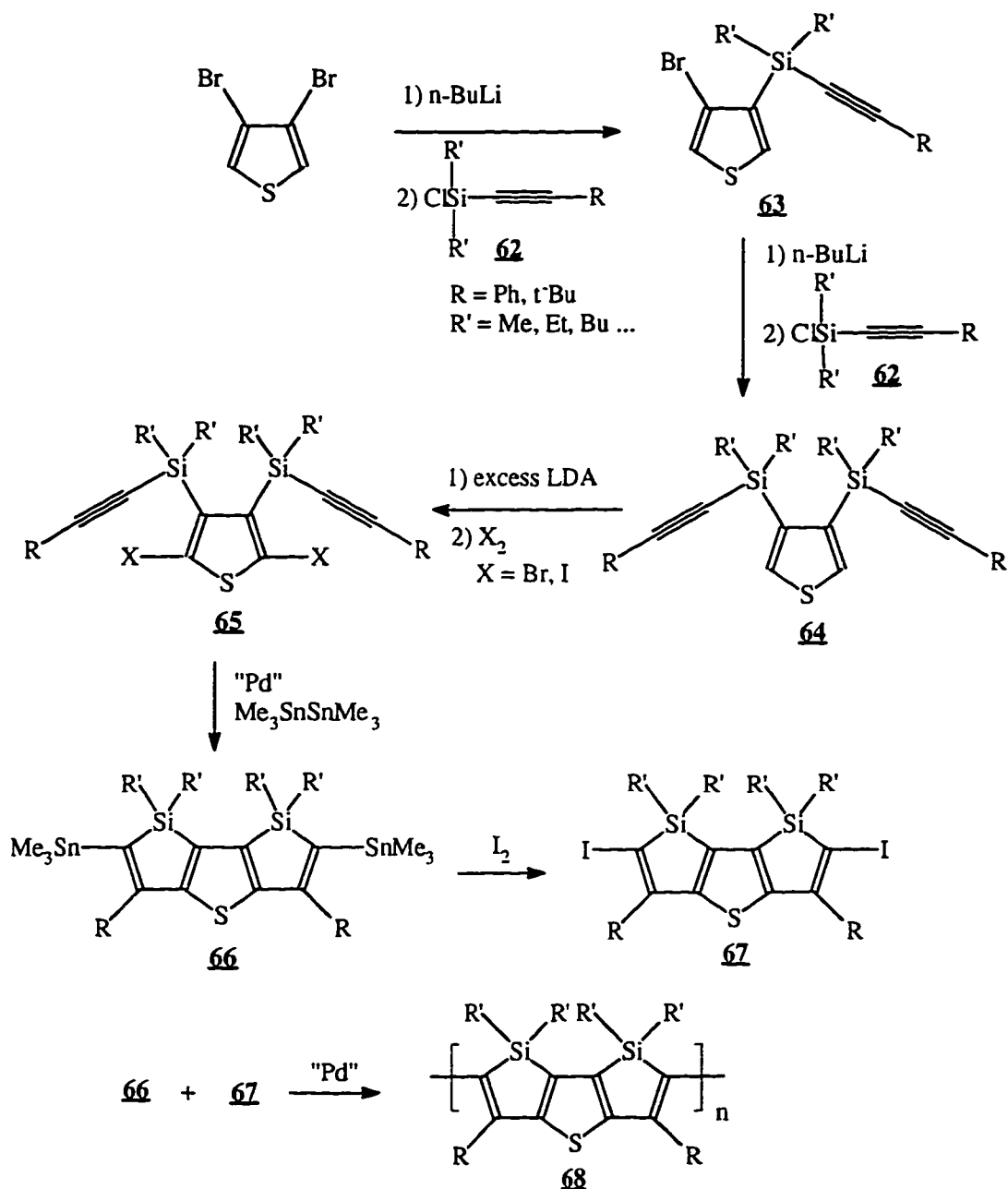
Polymer 60: To a degassed solution of FeCl₃ (2.06 mmol, 0.336 g) in CHCl₃ (12 ml) was added monomer **55** (0.516 mmol, 0.191 g). Argon was purged through the solution during the reaction. The solution was stirred at room temperature for 4 hours. The resulting blue-black solid was collected by filtration and washed with MeOH. The polymer was undoped by stirred the solid in hydrazine/CH₂Cl₂ solution for 2 hours. Then water was added. The organic layer was washed with water and dried (MgSO₄). After the solvent was removed, the polymer was precipitated from MeOH to yield a dark red solid (0.086 g, 46.0%). GPC: M_w = 1.39 × 10⁴, M_z = 2.37 × 10⁴, PD = 1.84; IR: ν (cm⁻¹) 3005, 2915, 2754, 1615, 1495; ¹H-NMR: δ 7.70, 7.52, 7.02, 4.21, 3.74, 1.67, 1.30, 0.90; ¹³C-NMR: δ 137.70, 132.44, 130.88, 124.08, 111.78, 68.16, 58.50, 56.66, 38.37, 30.37, 28.94, 23.75, 22.99, 14.09, 10.97; UV/Vis: λ_{max} (THF) = 514 nm, λ_{max} (film) = 534 nm; Emission: λ_{max} = 554 nm (λ_{excit.} = 440 nm); Electrical conductivity: ~2 S/cm (doped by I₂)

FUTURE WORK

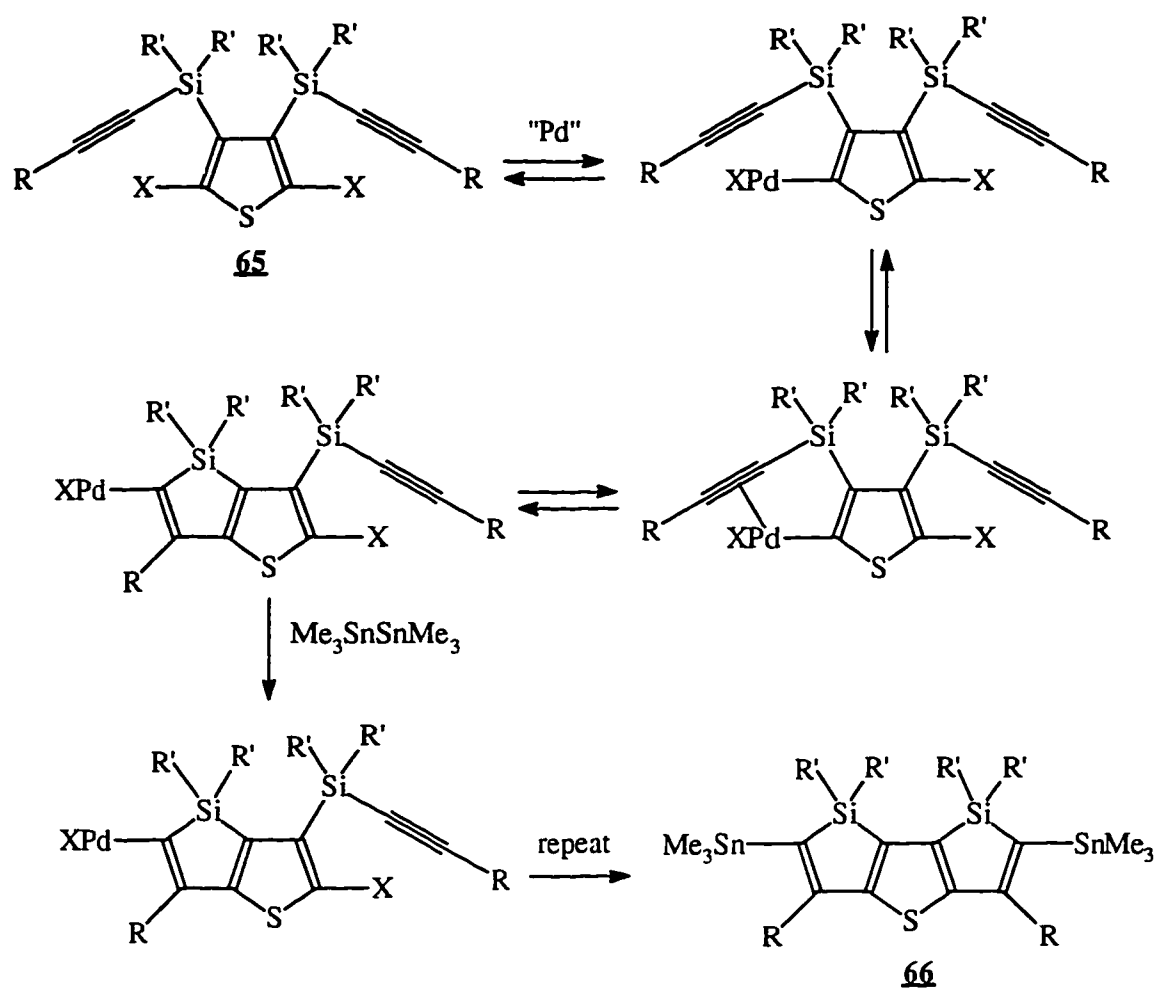
From our study of the above polymers, we learned that the silicon unit on the main chain decreases the bandgap energy. Polysilole, which was predicted as a promising polymer for high conductivity and third-order nonlinearity,^{57,58} is still a synthetic challenge for chemists. It was found by calculations that the silicon unit decreases the LUMO by σ^* - π^* conjugation.⁶² The introduction of an electron donating group, such as O or S, into polymer side chain was presumed to be able to decrease the bandgap by raising the energy of the HOMO.¹¹⁵ We thus designed the sulfur-bridged polysilole (Scheme 45). The combination of sulfur and silicon in the main chain should provide a polymer having high environmental stability and a very low bandgap.

The synthesis of sulfur-bridged silole was designed as shown in Scheme 45. We have already synthesized compound **64** (R = Ph, R' = Me), starting from 3,4-dibromothiophene. 3,4-Dibromothiophene was treated with 1 equivalent of n-BuLi, followed by quenching with 1-chlorodimethylsilyl-2-phenylethyne **62** (R = Ph, R' = Me) to give compound **63**. Repeat this step on **63** gave compound **64** (R = Ph, R' = Me) in ~80% overall yield. Direct treatment of 3,4-dibromothiophene with 2 equivalents or excess n-BuLi, followed by quenching with **62** in one step failed to give **64**, but instead gave a mixture. Compound **64** (R = Ph, R' = Me) was treated with excess LDA, followed by quenching with chlorotrimethylsilane to give compound **65** (R = Ph, R' = Me, X = SiMe₃) in ~76% yield. Based on this result, compound **65** (X = Br or I) should be obtainable when the reaction is quenched by Br₂ or I₂. The key step is intramolecular cyclization of **65** (X = Br, I) by palladium catalyst. We rationalize that palladium inserts into the thiophene-halogen bond, complexes with the triple bond, and then isomerizes to a cyclic intermediate, which could be quenched with Me₃SnSnMe₃ to give the cyclic product **66** (Scheme 46). Once **66** is obtained, it can be easily transformed into **67** by reacting with I₂. **67** can be used to couple with **66** in the presence of a palladium catalyst to give the desired polymer **68**. Polymer **68** is a promising polymer having a very low bandgap and high conductivity and third nonlinearity. Furthermore, desulfurization of **68** will give polysilole.

The other promising polymer is a ladder polymer containing sulfur and silicon as shown in Figure 56. The planar structure can be enhanced by the sulfur and silicon bridges. The long alkyl groups on the silicon can provide good solubility of the polymer. Polymer **69** should exhibit better properties than **68**.



Scheme 45: Design of synthesis of sulfur-bridged polysilole



Scheme 46: Proposed mechanism for intramolecular cyclization of **65**

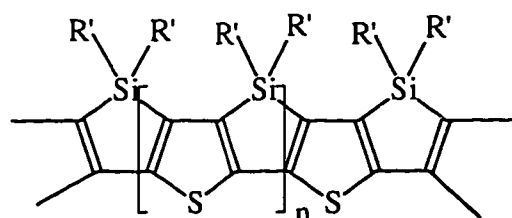


Figure 56: Design of a ladder polymer

REFERENCES

- 1) For recent reviews and developments see (a) Salaneck, W. R.; Lundstrom, L.; Ranby, B. *Conjugated Polymers and Related Materials*, Oxford, New York, **1993**. (b) Billingham, N. C. and Calvert, P. D. *Advances in Polymer Science: Conducting Polymers Molecular Recognition*, Springer-Verlag, New York **1989**, 1-104. (c) Aldissi, M. (ed.) *Intrinsically Conducting Polymers: An Emerging Technology*, Kluwer Academic Publishers, Norwell, MA, USA. **1993**, 125. (d) Garito, A. F.; Jen, A. K-Y.; Lee, C. and Dalton, L. R. (ed.) *Materials Research Society Symposium Proceedings: Electrical, Optical and Magnetic Properties of Organic Solid State Materials* **1994**, 328
- 2) For reviews see (a) Chien, J. C. W. *Polyacetylene: Chemistry, Physics and Materials Science*, Academic, New York **1984**. (b) Shirakawa, H.; Yamabe, T. and Yoshino, K. *Proceedings of the International Conference on Science and Technology of Synthetic Metals in Synth. Met.* **1987**, 17
- 3) For reviews see (a) Hann, R. A. and Bloor, D. (eds.) *Organic Materials for Non-linear Optics: The Royal Society of Chemistry*, London **1989**. (b) Cantow, H.-J. *Advances in Polymer Science: Polydiacetylenes*, Springer-Verlag, New York **1984**, 63
- 4) For reviews see (a) Speight, J. G.; Kovacic, P.; Koch and F. W. J. *Macromol. Sci.: Revs C* **1971**, 5, 295. (b) Kovacic, P. and Jones, M. B. *Chem. Rev.* **1987**, 87, 357
- 5) For recent reviews and developments see (a) Jean, R. *Chem. Rev.* **1992**, 92, 711. (b) McCullough, R. D.; Lowe, R. D.; Jayaraman, M. and Anderson, D. L. *J. Org. Chem.* **1993**, 58, 904. (c) Bauerle, P.; Fischer, T.; Bidlingmeier, B.; Stabel, A and Rabe, J. P. *Angew. Chem. Int. Ed. Engl.* **1995**, 34, 303
- 6) For review see Bradley, D. D. C. *Synth. Met.* **1993**, 54, 401
- 7) Giesa, R. and Schulz, R. C. *Macromol. Chem.* **1990**, 191, 857
- 8) For reviews on synthesis toward this polymer and related polymers see (a) Schlüter A.-D. *Adv. Mater.* **1991**, 3, 282. (b) Goldfinger, M. B. and Swager, T. M. *J. Am. Chem. Soc.* **1994**, 116, 7895. (c) Scherf, U. and Mullen, K. *Synthesis* **1992**, 23
- 9) For reviews see (a) Tourillon, G. *Handbook of Conducting Polymers*; Skotheim, T. A., Ed.;

- Marcel Dekker: New York, 1986. (b) Reynolds, J. R. *Chemtech*. **1988** (July), 440. (c) Kanatzidis, M. G. *C&EN*, **1990** (Dec. 3), 36. (d) Kiess, H. (ed.) *Springer Series in Solid-State Sciences 102: Conjugated Conducting Polymers*, Springer-Verlag, New York, **1992**
- 10) For principles and reviews see (a) Prasad, P. N. and Williams, D. J. *Introduction to Nonlinear Optical Effects in Molecules and Polymers*, John Wiley & Sons, New York, **1990**. (b) *Chem. Rev.* **1994**, No. 1
- 11) Burroughes, J. H.; Bradley, D. D. C.; Brown, A. R.; Marks, R. N.; MacKay, K.; Friend, R. H.; Burn, P. L. and Holmes, A. B. *Nature* (London) **1990**, 347, 539
- 12) For reviews see (a) Service, R. F. *Science* **1996**, 273, 878. (b) Sheats, J. R.; Antoniadis, H.; Hueschen, M.; Leonard, W.; Miller, J.; Moon, R.; Roitman, D. and Stocking, A. *Science* **1996**, 273, 884. (c) Kido, J. *Trends in Poly. Sci.* **1994**, 2(10), 350
- 13) (a) Ohmori, Y.; Uchida, M.; Muro, K. and Yoshino, K. *Jpn. J. Appl. Phys.* **1991**, 30, L1938. (b) Ohmori, Y.; Uchida, M.; Muro, K. and Yoshino, K. *Solid State Commun.* **1991**, 80, 605. (c) Braun, D.; Gustafsson, G.; McBranch, D. and Heeger, A. J. *J. Appl. Phys.* **1992**, 72, 564
- 14) Ohmori, Y.; Uchida, M.; Muro, K. and Yoshino, K. *Jpn. J. Appl. Phys.* **1991**, 30, L1941
- 15) Grem, G.; Leditzky, G.; Ullrich, B. and Leising, G. *Adv. Mater.* **1992**, 4, 36
- 16) Onoda, M.; Uchida, M.; Ohmori, Y. and Yoshino, K. *Jpn. J. Appl. Phys.* **1993**, 32, 3895
- 17) (a) Williams, D. J. (ed.) *Nonlinear Optical Effect in Organic Systems: ACS Symposium Series 233*, American Chemical Society, Washington, D. C., **1983**. (b) Reinhardt, B. A. *Trends in Poly. Sci.* **1993**, 1, 5
- 18) Kajzar, F.; Etemad, S.; Baker, G. L. and Messier, J. *Solid State Commun.* **1987**, 63, 1113
- 19) Singh, B. P.; Prasad, P. N. and Karasz, F. E. *Polymer* **1988**, 29, 1940
- 20) Prasad, P. N.; Swiatkiewicz, J. and Pflieger, J. *Mol. Cryst. Liq. Cryst.* **1988**, 160, 53
- 21) Rao, D. N.; Chopra, P.; Ghosal, S. K.; Swiatkiewicz, J. and Prasad, P. N. *J. Chem. Phys.* **1986**, 84, 7049
- 22) Most recent review on third-order nonlinear optical effects in organic systems: Bredas, J. L.; Adant, C.; Tackx, P.; Persoons, A. and Pierce, B. M. *Chem. Rev.* **1994**, 94, 243
- 23) Braun, D and Heeger, A. J. *J. Appl. Phys. Lett.* **1991**, 58, 1982

- 24) (a) Moratti, S. C.; Bradley, D. C.; Friend, R. H.; Greenham N. C. and Holmes, A. B. *Polymer Preprints* **1994**, 35(1), 214. (b) Moratti, S. C.; Cervini, R.; Holmes, A. B.; Baigent, D. R.; Friend, R. H.; Greenham, N. C.; Gruner, J. and Hamer, P. J. *Synth. Met.* **1995**, 71, 2117. (c) Greenham N. C.; Moratti, S. C.; Bradley, D. C.; Friend, R. H. and Holmes, A. B. *Nature* **1993**, 365, 628. (d) Brown, A. R.; Bradley, D. D. C.; Burn, P. L.; Burroughes, J. H.; Friend, R. H.; Greenham, N. C.; Holmes, A. B. and Kraft, A. M. *Appl. Phys. Lett.* **1992**, 61, 2793. (e) Burn, P. L.; Holmes, A. B.; Kraft, A.; Bradley, D. D. C.; Brown, A. R.; Friend, R. H. and Gymer, R. W. *Nature* **1992**, 356, 47. (f) Bredas, J. L. and Heeger, A. J. *Chem. Phys. Lett.* **1994**, 217, 507. (g) Lux, A.; Moratti, S. C.; Li, X-C.; Grimsdale, A. C.; Davies, J. E.; Raithby, P. R.; Gruner, J.; Cacialli, F.; Friend, R. H. and Holmes, A. B. *Polymer Preprints* **1996**, 37(1), 202
- 25) (a) Yamamoto, T.; Yamada, W.; Takagi, M.; Kizu, K.; Maruyama, T.; Ooba, N.; Tomaru, S.; Kurihara, T. and Kaino, T. and Kubota, K. *Macromolecules* **1994**, 27(22), 6620 and references cited therein. (b) Ding, Y. "Synthesis and Study of Acetylenic Polymers" Ph.D. thesis, Iowa State University, Ames, IA **1994**. (c) Swanson, L. S.; Shinar, J.; Ding, Y. and Barton, T. J. *Synth. Met.* **1993**, 55-57, 1. (d) Moroni, M.; Moigne, J. L. and Luzzati, S. *Macromolecules* **1994**, 27 (2), 562. (e) Chen, W.; Ijadi-Maghsoodi, S. and Barton, T. *Polymer Preprints* **1995**, 36(1), 495. (f) Pang, Y.; Wang, Z. and Barton, T. *Polymer Preprints* **1996**, 37(2), 333. (g) Swager, T. M.; Gil, C. J. and Wrighton, M. S. *J. Phys. Chem.* **1995**, 99, 4886
- 26) For the review of synthesis of PPV see: Meier, H. *Angew. Chem. Int. Ed. Engl.* **1992**, 31, 1399
- 27) (a) Sukwattanasinitt, M.; Ijadi-Maghsoodi, S. and Barton, T. J. *Polymer Preprints*, **1995**, 36(1), 497. (b) Sukwattanasinitt, M. "Synthesis, Characterization and Electronic Properties of N-interrupted Conjugated Polymers" Ph.D. thesis, Iowa State University, Ames, IA **1996**
- 28) (a) Nakatsuji, S.; Matsuda, K.; Uesugi, Y.; Nakashima, K.; Akiyama, S. and Fabian, W. J. *Chem. Soc. Perkin Trans. 1* **1992**, 755. (b) Nakatsuji, S.; Matsuda, K.; Uesugi, Y.;

- Nakashima, K.; Akiyama, S.; Katzer, G. and Fabian, W. J. *J. Chem. Soc. Perkin Trans. 2* **1991**, 861
- 29) Davey, A. P.; Elliott, S.; O'Connor, O. and Blau, W. *J. Chem. Soc., Chem. Commun.* **1995**, 1433
- 30) For a review see: Martin, A. R. and Yang, Y. *Acta Chemica Scandinavica* **1993**, 47, 221
- 31) Boden, R. *Synthesis* **1975**, 784
- 32) For review see: McMurry, J. E. *Chem. Rev.* **1989**, 89, 1513
- 33) Koßmehl, C. and Samandri, M. *Makromol. Chem.* **1983**, 184, 2437
- 34) Reinhardt, B. R. and Unroe, M. R. *Polymer Preprint* **1990**, 31(1), 620
- 35) Ansong, O.; Antoine, M. D. and Nwokogu, G. *J. Org. Chem.* **1994**, 59, 2506
- 36) Holzmann, D.; Koßmehl, C. and Nuck, R. *Makromol. Chem.* **1982**, 183, 1711
- 37) (a) Percec, V.; Okita, S. and Weiss, R. *Macromolecules* **1992**, 25, 1816. (b) Wang, Y. and Quirk, R. P. *Macromolecules* **1995**, 28, 3495. (c) Kaeriyama, K.; Mehta, M. A. and Masuda, H. *Synth. Met.* **1995**, 507
- 38) Percec, V.; Bae, J.-K.; Zhao, M. and Hill, D. H. *Macromolecules* **1995**, 28, 4415
- 39) For review on Suzuki coupling see Martin, A. R. and Yang, Y. *Acta Chem. Scand.* **1993**, 47, 221
- 40) Dewar, M. J. S. and Dougherty, R. C. *J. Am. Chem. Soc.* **1964**, 86, 433
- 41) Bradley, D. D. *Chem. Brit.* **1991**, 719
- 42) Jeglinski, S. A.; Amir, O.; Wei, X.; Vardeny, Z. V.; Wei, X.; Shinar, J.; Cerkvenik, T.; Chen, W. and Barton, T. J. *Appl. Phys. Lett.* **1995**, 67(26), 3960
- 43) (a) Zhang, C.; Seggern, H.; Pakbaz, K.; Kraabel, B.; Schmidt, H. W. and Heeger, A. J. *Polymer Preprints* **1993**, 34(2), 817. (b) Braun, D. and Heeger, A. J. *Appl. Phys. Lett.* **1991**, 18, 58. (c) Swanson, L. S.; Lu, F.; Shinar, J.; Ding, Y. W. and Barton, T. J., in *Electroluminescent Materials, Devices, and Large-Screen Displays*, SPIE Proc. 1910, edited by E. M. Conwell, M. Stolka and M. R. Miller (SPIE, Bellingham, WA, 1993) p. 101
- 44) I. D. Parker, *J. Appl. Phys.* **1994**, 75, 1656
- 45) Ohmori, Y.; Uchida, M.; Muro, K. and Yoshino, K. *Jpn. J. Appl. Phys.* **1991**, 30, L1941

- 46) Raikh, M. and Wei, X. *Mol. Cryst. Liq. Cryst.* **1994**, 256, 563
- 47) (a) Gailberger, M.; Greiner, A. and Bassler, H. *Synth. Met.* **1991**, 42-43, 1269. (b) Obrzut, M. J. and Karasz, F. E. *Synth. Met.* **1989**, 29, E103. (c) Guillet, J. *Polymer Photophysics and Photochemistry*: Cambridge University: Cambridge, U. K., **1985**: pp 328-335. (d) Mylnikov, V. S. *Usp. Khim.* **1974**, 43(10), 1821
- 48) Bradley, D. D. C. and Friend, R. H. *J. Molec. Electron.* **1989**, 5, 19
- 49) (a) Shirakawa, H.; Louis, E. J.; MacDiarmid, A. G.; Chiang, C. K. and Heeger, A. J. *J. Chem. Soc. Commun.* **1977**, 578. (b) Chiang, C. K.; Funcher, C. R. Jr.; Park, Y. W.; Shirakawa, H.; Louis, E. J.; Gan, S. C. and MacDiarmid, A. G. *Phys. Rev. Lett.* **1977**, 39, 1098. (c) Chiang, C. K.; Drury, M.A.; Gan, S. C.; Heeger, A. J.; Louis, E. J.; MacDiarmid, A. G.; Park, Y. W. and Shirakawa, H. *J. Am. Chem. Soc.* **1978**, 100, 1013
- 50) See, for instance: Aldissi M. (ed.) *Intrinsically Conducting Polymers: An Emerging Technology*, Kluwer, Dordrecht, **1993**
- 51) Shinar J.; Ijadi-Maghsoodi, S.; Ni, Q.-X.; Pang, Y. and Barton, T. J. *Synth. Met.* **1989**, 28, C593
- 52) (a) Wong, K. S.; Han, S. G.; Vardeny, Z. V.; Shinar, J.; Pang, Y.; Ijadi-Maghsoodi, S.; Barton, T. J.; Grigoras, S. and Parbhoo, B. *Appl. Phys. Lett.* **1991**, 58, 1695. (b) Wei, X.; Han, S. G.; Wong, K. S.; Hess, B. C.; Zheng, L. X.; Vardeny, Z. V.; Ni, Q.-X.; Shinar, J.; Pang, Y.; Ijadi-Maghsoodi, S.; Barton, T. J. and Grigoras, S. *Synth. Met.* **1991**, 41-43, 1583. (c) Ni, Q.-X.; Shinar, J.; Vardeny, Z. V.; Grigoras, S.; Pang, Y.; Ijadi-Maghsoodi, S.; Barton, T.J. *Phys. Rev. B* **1991**, 44, 5939
- 53) Grigoras, S.; Lie, G. C.; Barton, T. J.; Ijadi-Maghsoodi, S; Pang, Y.; Shinar, J.; Vardeny, Z. V.; Wong, K. S. and Han, S. G. *Synth. Met.* **1992**, 49-50, 293
- 54) (a) Frapper, G.; Kertesz, M. *Organometallics* **1992**, 11, 3178. (b) Frapper, G.; Kertesz, M. *Synth. Met.* **1993**, 55-57, 4255. (c) Kurti, J.; Surjan, P. R.; Kertesz, M. and Frapper, G. *Synth. Met.* **1993**, 55-57, 4338
- 55) (a) Hong, S. Y. and Marynick, D. S. *Macromolecules* **1992**, 25, 4652. (b) Hong, S. Y. and Marynick, D. S. *Macromolecules* **1995**, 28, 4991. (c) Hong, S. Y.; Kwon, S. J. and Kim, S. C. *J. Chem. Phys.* **1995**, 103(5), 1871

- 56) (a) Lee, Y. and Kertesz, M. *J. Chem. Phys.* **1988**, 88(4), 2609. (b) Hong, S. Y. and Marynick, D. S. *J. Chem. Phys.* **1992**, 96(7) 5497
- 57) Bakhshi, A. K.; Yamaguchi, Y.; Ago, H. and Yamabe, T. *Synth. Met.* **1996**, 79, 115
- 58) Matsuzaki, Y.; Nakano, M.; Tanaka, K. and Yamabe, T. *Synth. Met.* **1995**, 71, 1737
- 59) Dubac, J.; Laporterie, A and Manuel, G. *Chem. Rev.* **1990**, 90, 215
- 60) (a) Tamao, K; Yamaguchi, S. and Shiro, M. *J. Am. Chem. Soc.* **1994**, 116, 11715. (b) Kurita, J.; Ishii, M.; Yasuike, S. and Tsuchiya, T. *J. Chem. Soc., Chem. Commun.* **1993**, 1309
- 61) (a) Yamaguchi, S. and Tamao, K. *Tetrahedron Letters*, **1996**, 37(17), 2983. (b) Tamao, K.; Uchida, M.; Izumizawa, T.; Furukawa, K; and Yamaguchi, S. *J. Am. Chem. Soc.* **1996**, 118, 11974
- 62) Yamaguchi, S. and Tamao, K. *Bull. Chem. Soc. Jpn.* **1996**, 69, 2327
- 63) (a) Corriu, R. J.-P.; Douglas, W. E. and Yang, Z. *J. Organomet. Chem.* **1991**, 417, C50. (b) Corriu, R. J.-P.; Douglas, W. E. and Yang, Z. *J. Organomet. Chem.* **1993**, 456, 35
- 64) (a) Tamao, K.; Yamaguchi, S.; Shiozaki, M.; Nakagawa, Y. and Ito, Y. *J. Am. Chem. Soc.* **1992**, 114, 5867. (b) Tamao, K.; Yamaguchi, Ito, Y.; Matsuzaki, M.; Yamabe, T.; Fukushima, M. and Shigeru, M. *Macromolecules*, **1995**, 28, 8668
- 65) Fang, M; Watnabe, A. and Matsuda, M. *Macromolecules* **1996**, 29, 6807, and references cited there.
- 66) Albert, I. D. L.; Pugh, D.; Morley, J. O. and Ramasesha, S. *J. Phys. Chem.* **1992**, 96, 10160
- 67) Kminek, I.; Klimovic, J. and Orasad, P. N. *Chem. Mater.* **1993**, 5, 357
- 68) (a) Lin, J.; Ijadi-Maghsood, S. and Barton, T. *Polymer Preprints* **1995**, 36(1), 499. (b) Lin, J. "Synthesis and study of novel silicon-based unsaturated polymers" Ph.D. thesis, Iowa State University, Ames, IA **1995**
- 69) Milstein, D. and Stille, J. K. *J. Org. Chem.* **1979**, 44(10), 1613
- 70) Warner, B. P. and Buchwald, S. L. *J. O. Chem.* **1994**, 59, 5822
- 71) Bottaro, J. C.; Hansan, R. H. and Seitz, D. E. *J. Org. Chem.* **1981**, 46, 5221
- 72) Tamura, H.; Kanamaru, H.; Hirose, O. and Yamamoto, S. *Polymer Preprints* **1996**,

37(2), 284

- 73) Bolognesi, A; Catellani, M.; Porzio, W. and Speroni, F. *Polymers*, **1993**, 34 (19), 4150
- 74) Steinkopf, Rosler, and Setzer, *Ann.*, **1936**, 522, 35
- 75) Neenan, T. X. and Whitesides, G. M. *J.Org.Chem.*, **1988**, 53, 2488
- 76) Barton, T, J. and Groh, B. L. *Organometallics* **1985**, 4, 575
- 77) (a) Kafafi, S. A. and Lowe, J. P. *J. Am. Chem. Soc.* **1984**, 106, 5837. (b) Kafafi, S. A.; Lowe, J. P. and LaFemina, P. *J. Phys. Chem.* **1986**, 80, 6602. (c) Grant, P. M. and Batra, I. P. *Solid State Commun.* **1979**, 29, 225. (d) Paldus, J. and Chin, E. *Int. J. Quantum Chem.* **1983**, 24, 373
- 78) (a) Bredas, J. L.; Themans, B.; Fripiat, J. G.; Andre, J. M. and Chance, R. R. *Phys. Rev. B* **1984**, 29, 6761. (b) Mintmire, J. W.; White, C. T. and Elert, M. L. *Synth. Metals* **1987**, 16, 235
- 79) Wright, M. E. *Macromolecules* **1989**, 22(8), 3256
- 80) Ito, T.; Shirakawa, H. and Ikeda, S. *J. Polym. Sci., Polym. Chem. Ed.* **1974**, 12, 11
- 81) Chiang, C. K.; Park, Y. W.; Heeger, A. J.; Shirakawa, H.; Louis, E. J. and MacDiarmid, A. G. *Phys. Rev. Lett.* **1977**, 39, 1093
- 82) Diaz, A. F.; Kanazawa, K. K. and Gardini, G. P. *J. Chem. Soc., Chem. Commun.* **1979**, 635
- 83) Diaz, A. F. *Chem. Scr.* **1981**, 17, 142
- 84) Tourillon, G. and Garnier, F. *J. Electroanal. chem.* **1982**, 135, 173
- 85) Bargon, J.; Mohamand, S. and Waltman, R. J. *IBM J. Res. Develop.* **1983**, 27, 330
- 86) Delamar, M.; Lacaze, p. C.; Dumousseau, J. Y. and Dubois, J. E. *Electrochim. Acta* **1982**, 27, 61
- 87) Rault-Berthelot, J. and Simonet, J. *J. Electroanal. Chem.* **1985**, 182, 187
- 88) (a) Patil, A. O.; Heeger, A. J.; and Wudl, F. *Chem. Rev.* **1988**, 88, 183. (b) Mastragostino, M.; Arbizzani, C.; Bongigi, A. and Barbarella, Z. M. *Electrochim Acta.* **1993**, 38, 135. (c) Scrosati, B. *Applications of Electroactive Polymers*; Chapman & Hall: London, **1994**. (d) Gustafsson, G.; Cao, Y.; Treacy, G. M.; Klavetter, F.; Colaneri, N. and Heeger, A. J. *Nature* **1992**, 357, 477. (e) McCoy, C. H. and Wrighton, M. S. *Chem.*

- Mater.* **1993**, *5*, 914. (f) Garnier, F.; Yassar, A.; Hajlaoui, R.; Horowitz, G.; Deloffre, F.; Servet, B.; Rues, S. and Alnot, P. *J. Am. Chem. Soc.* **1993**, *115*, 8716. (g) Robitaille, L.; Leclerc, M. and Callender, C. L. *Chem. Mater.* **1993**, *5*, 1755. (h) Chittibabu, K. G.; Li, L.; Kamath, M.; Kumar, J. and Tripathy, S. K. *Chem. Mater.* **1994**, *6*, 475
- 89) (a) Waltman, R. J. and Bargon, J. *Can. J. Chem.* **1986**, *64*, 76. (b) Diaz, A. F. and Lacroix, J. C. *New J. Chem.* **1988**, *12*, 171. (c) Adamcova, Z. and Dempirova, L. *Prog. Org. Coat.* **1989**, *16*, 295
- 90) (a) Chandler, G. K. and Pletecher, D. *Spec. Period. Rep. Electrochem.* **1985**, *10*, 117. (b) Heinze, J. *Topics in Current Chemistry*; Springer-Verlag: Berlin, **1990**: Vol. 152, p 1
- 91) Baker, G. L. *Electronic and Photonic Applications of Polymers*; Bowden, M. J., turner, S. R., Eds.; ACS Advances in Chemistry Series 210; American Chemical Society: Washington, DC, **1988**: p 271
- 92) Wu, X.; Chen, T. and Rieke, R. D. *Macromolecules*, **1996**, *29*, 7671 and reference cited therein
- 93) (a) McCullough, R. D.; Lowe, R. D.; *J. Chem. Soc. Chem. Commun.* **1992**, 70. (b) McCullough, R. D.; Lowe, R. D.; Jayaraman, M. and Anderson, D. L. *J Org. Chem.* **1993**, *58*, 904. (c) McCullough, R. D. and Williams, S. P. *J. Am. Chem. Soc.* **1993**, *115*, 22608
- 94) Marsella, M. and Swager, T. M. *J Am. Chem. Soc.* **1993**, *115*, 12214
- 95) (a) Yang, C.; Orfino, F. P. and Holdcroft, S. *Macromolecules* **1996**, *29*, 6510. (b) Anderson, M. R.; Berggren, M.; Inganas, O.; Gustafsson, G.; Gustafsson-Carlberg, J. C.; Selse, D.; Hjertberg, T. and Wennerstrom, O. *Macromolecules* **1995**, *28*, 7525. (c) Anderson, M. R.; Selse, D.; Berggren, M.; Jarvinen, H.; Hjertberg, T.; Wennerstrom, O.; and Osterholm, J.-E. *Macromolecules* **1994**, *27*, 6503
- 96) Chen, S. A. and Tsai, C. C. *Macromolecules* **1993**, *26*, 2234
- 97) Della Casa, C.; Salatelli, E.; Andreani, F. and Costa Bizzarri, P. *Makromol. Chem., Macromol. Symp.* **1992**, *59*, 233
- 98) Abdou, M. S. A. and Holdcroft, S. *Macromolecules* **1993**, *26*, 2954
- 99) Pomerantz, M.; Yang, H. and Cheng Y. *Macromolecules* **1995**, *28*, 5706

- 100) McClain, M. D.; Whittington, D. A.; Mitchell, D. J. and Curtis, M. D. *J Am. Chem. Soc.* **1995**, 117, 3887
- 101) (a) Ruiz, J. P.; Gieselman, M. B.; Nayak, K.; Marynick, D. S. and Reynold, J. R. *Synth. Met.* **1989**, 28, C481-C486. (b) McCullough, R. D. and Williams, S. P. *J. Am. Chem. Soc.* **1993**, 115, 11608
- 102) (a) Swager, T. M.; Marsella, M. J.; Bicknell, L. K. and Zhou, Q. *Polym. Prepr.* **1994**, 35, 206. (b) Marsella, M.; Carroll, P. J. and Swager, T. M. *J. Am. Chem. Soc.* **1994**, 116, 9347
- 103) Bouman, M. M. and Meijer, E. W. *Polym. Prepr.* **1994**, 35, 309
- 104) (a) Ikenoue, Y.; Votani, N.; Patil, A. O.; Wudl, F. and Heeger, A. J. *Synth. Met.* **1989**, 30, 305. (b) Patil, A. O.; Ikenoue, Y.; Wudl, F. and Heeger, A. J. *J. Am. Chem. Soc.* **1987**, 109, 1858
- 105) Khor, E.; Ng, S. C.; Li, H. C. and Chai, S. *Heterocycles*, **1991**, 32(8), 1305
- 106) (a) Gilman, H. and Gorsich, R. D. *J. Am. Chem. Soc.* **1955**, 77, 6380. (b) Gilman, H and Gorsich, R. D. *J. Am. Chem. Soc.* **1958**, 80, 1883. (c) Wittenberg, D. and Gilman, H J. *Am. Chem. Soc.* **1958**, 80, 2677. (d) Gilman, H and Gorsich, R. D. *J. Am. Chem. Soc.* **1958**, 80, 3243
- 107) (a) Frohlich, H. and Kalt, W. *J. Org. Chem.* **1990**, 55, 2993. (b) Hawkins, D. W.; Iddon, B.; Longthorne, D. and Rosyk, P. *J. Chem. Soc. Perkin Trans. I* **1994**, 2735
- 108) (a) Shabana, R.; Galal, A.; Mark, H. B, Jr.; Zimmer. H.; Gronowitz, S. and Hornfeldt, A.-B. *Phosphorus, Sulfur, Silicon* **1990**, 48, 239. (b) Krk, A.; Weirsema, A.K.; Jordens, P. and Wynberg, H. *Tetrahedron*, **1968**, 24, 3381. (c) Chen, T. I. and Morris, M. D. *J. Phys. Chem.* **1983**, 87, 2317. (d) Jordens, P.; Rawson, G. and Wynberg, H. *J. Chem. Soc. (C)* **1970**, 273. (e) Cunningham, D. D.; Laguren-Davidson, L.; Mark, H. B. Jr.; Pham, C. V. and Zimmer, H. *J. Chem. Soc. Chem. Commun.* **1987**, 13, 1021
- 109) Tour, J. M. and Wu, R. *Macromolecules* **1992**, 25, 1901
- 110) Niemi, V. M.; Knuuttila, P.; Osterholm, J.-E. and Korvola, J. *Polymer* **1992**, 33, 1559
- 111) Kosugi, M.; Shimizu, K.; Ohtani, A. and Migita, T. *Chem. Lett.* **1981**, 829
- 112) Murray, R. E. and Zweifel, G. *Synthesis* **1980**, 150

- 113) (a) Nugent, W. A. and Calabrese, J. C. *J. Am. Chem. Soc.* **1984**, 106, 6422. (b) Nugent, W. A.; Thom, D. L. and Harlow, R. L. *J. Am. Chem. Soc.* **1987**, 109, 2788. (c) Negishi, E. In *Comprehensive Organic Synthesis*; Trost, B. M., Ed.; Pergamon Press: Oxford, **1991**,; Vol. 5. p 1163
- 114) Takahashi, T.; Xi, Z.; Obora, Y. and Suzuki, N. *J. Am. Chem. Soc.* **1995**, 117, 2665
- 115) (a) Blohm, M. L.; Pikett, J. E. and Van Dort, P. C. *Macromolecules* **1993**, 26, 2704. (b) Chen, S.-A. and Tsai, C.-C. *Macromolecules* **1993**, 26, 2234
- 116) Tanaka, S.; Sato, M. and Haeriyama, K. *Makromol. Chem.* **1985**, 186, 1685

ACKNOWLEDGMENTS

This dissertation could not have been completed without the inspiration and assistance of many people. First, I would like to thank Professor Thomas J. Barton for the great four years and eight months I have spent in his research group. His style of teaching and philosophy has always kept me looking forward to the group meeting. With his encouragement, support, acquaintance and humor, working with him has been one of the best parts in my life.

I would like to express my appreciation to the members of Barton research group, both past and present. Especially, I would like to thank Dr. Sina Ijadi-Maghsoodi for his technical advice and daily help; Mrs. Kathie Hawbaker, for her kind help on many occasions; Dr. Jibing Lin and Dr. Mongkel Sukwattanasinitt for their hand-on help when I joined the group; Mr. Nathan Classen and Mr. Andrew Chubb for correcting the English of this thesis.

In addition, professor Joseph Shinar have conducted the light emitting diode (LED) devices studies for the polymers. I would like to thank Mr. Woo Jae Lee for luminescence measurement; Dr. Dave Scott and Dr. Karen Ann Smith for their assistance in NMR spectroscopy; and Kamel Harrata and Mr. Charles Baker for mass spectroscopic data.

I would also like to use this work to express my deep gratitude to my parents. Their love, support and sacrifices throughout my education have been a main inspiration for me. I would also like to thank my two sisters and their husbands for encouragement, and taking care of my parents.

Moreover, I would like to thank my best friend Dr. Xu Li for his friendship during these five years. His support, understanding and advice will be always be greatly appreciated.

Finally, I want to express my greatest appreciation to my wife, Hongling Li, especially for her love and encouragement during my depression time. It would been impossible to finish this work without her support and caring.

This work was performed at Ames Laboratory under Contact No. W-7405-Eng-82 with the U.S. Department of Energy. The United State Government has assigned the DOE Report number IS-T 1808 to this thesis.